Technical Report

Plans for Testing the NREL Unsteady Aerodynamics Experiment 10-m Diameter HAWT in the NASA Ames Wind Tunnel

D. Simms, S. Schreck, M. Hand, L. Fingersh, J. Cotrell, K. Pierce, and M. Robinson

NREL

National Renewable Energy Laboratory

Plans for Testing the NREL Unsteady Aerodynamics Experiment 10-m Diameter HAWT in the NASA Ames Wind Tunnel

D. Simms, S. Schreck, M. Hand, L. Fingersh, J. Cotrell, K. Pierce, and M. Robinson

National Renewable Energy Laboratory

NOTICE

Contents

Attendees

Technical Oversight Committee:
Larry Carr, NASA Ames
Roddy Galbraith, University of Glasgow
Gordon Leishman, University of Maryland
Jim McCroskey, NASA Ames

European Partners:
Anders Björck, FFA – The Aeronautical Research Institute of Sweden
Helge Madsen, RISØ National Laboratory, Denmark
Flemming Rasmussen, RISØ National Laboratory, Denmark
Robert Rawlinson-Smith, Garrad-Hassan and Partners Limited, UK
Herman Snel, ECN – Netherlands Energy Research Foundation
Nando Timmer, Delft University of Technology, The Netherlands

Subcontractors:
Earl Duque, NASA Ames
Craig Hansen, University of Utah
Philippe Giguere, University of Illinois
Bill Holley, RANN Inc.
Case Van Dam, University of California, Davis
Lakshmi Sankar, Georgia Institute of Technology
Kyle Wetzel, Zond Energy Systems, Inc.
Jonathan Whale, University of Illinois
Bob Wilson, Oregon State University

Laboratory:
Dale Berg, Sandia
Gunjit Bir, NREL
Marshall Buhl, NREL
Sandy Butterfield, NREL
Jason Cotrell, NREL
Lee Fingersh, NREL
Maureen Hand, NREL
Sue Hock, NREL
Neil Kelley, NREL
Bob Kufeld, NASA Ames
Scott Larwood, NREL
Kirk Pierce, NREL
Mike Robinson, NREL
Scott Schreck, NREL
Dave Simms, NREL
Jim Tangler, NREL
Bob Thresher ,NREL
Walt Wolfe, Sandia
Alan Wright, NREL

Abbreviations

AIAA	American Institute of Aeronautics and Astronautics
AOA	Angle of Attack
ASME	American Society of Mechanical Engineers
CER	Combined Experiment Rotor
CFD	Computational Fluid Dynamics
CMM	Coordinate Measuring Machine
ECN	Netherlands Energy Research Foundation, Petten, The Netherlands
FFA	Aeronautical Research Institute of Sweden, Bromma, Sweden
EU	European Union
GH	Garrad Hassan and Partners Limited, Bristol, UK
IEA	International Energy Agency
IEC	International Electrotechnical Commission
HAWT	Horizontal Axis Wind Turbine
LDV	Laser Doppler Velocimetry
LFA	Local Flow Angle
NASA/	National Aeronautical & Space Administration
Ames	Ames Research Center, Moffett Field, CA. USA
NREL	National Renewable Energy Laboratory, Golden, CO. USA
NWTC	National Wind Technology Center, Boulder CO. USA
OSU	Ohio State University
RANN	Research Applied to National Needs, Inc., Palo Alto, CA. USA
RISØ	RISØ National Laboratory, Roskilde, Denmark
Sandia	Sandia National Laboratories, Albuquerque, NM. USA
TUD	Technical University of Delft, Delft, The Netherlands
TSR	Tip Speed Ratio
UAE	Unsteady Aerodynamics Experiment
VG	Vortex Generator

1. Summary

The first Science Panel meeting, "NREL-NASA Ames Unsteady Rotor Aerodynamics 10-m HAWT Wind Tunnel Test," was held at the National Wind Technology Center (NWTC) of the National Renewable Energy Laboratory (NREL) on October 5 and 6, 1998. The purpose of the meeting was to solicit recommendations and resolve technical issues related to testing the NREL 10-meter (m)-diameter instrumented research wind turbine in the National Aeronautical & Space Administration Ames Research Center's (NASA Ames) 24.4-m (80') by 36.6-m (120') wind tunnel. At the time of the meeting, the wind tunnel test was scheduled for a three-week period beginning September 20, 1999. The test dates were later postponed until early 2000.

The meeting focused on identifying and prioritizing test activities to produce the information needed to answer specific research questions. We were surprised at the high level of interest and positive response to the meeting and our planned test activities. Approximately 35 individuals experienced in wind turbine aerodynamics attended the meeting. Also in attendance were International Energy Agency (IEA) collaborative research partners representing the United Kingdom (UK), Denmark, Sweden, and The Netherlands.

This meeting focused specifically on semi-empirical models used to simulate the effects of dynamic stall and three-dimensional (3-D) responses, and on obtaining results from the wind tunnel test needed to validate these models. NREL and various European organizations rely heavily on the Beddoes-Leishman and other similar semi-empirical dynamic stall models. The models are incorporated into aeroelastic codes, which are used to design and simulate the structural dynamic responses of wind turbine configurations. The models reproduce the aerodynamic responses of airfoils subjected to varying degrees of atmospheric wind turbulence, inflow shear, off-axis operating yaw, and other dynamic effects. The Beddoes-Leishman model was originally developed for helicopter aerodynamic response simulation, but has been modified and adapted by various users for wind turbine applications.

During the meeting, the Science Panel and representatives from the wind energy community provided numerous detailed recommendations regarding test activities and priorities. The Unsteady Aerodynamics team of the NWTC condensed this guidance and drafted a detailed test plan. This test plan represents an attempt to balance diverse recommendations received from the Science Panel meeting, while still taking into account multiple constraints imposed by the UAE research turbine, the NASA Ames 80' X 120' wind tunnel, and other sources.

The NREL/NASA Ames wind tunnel tests will primarily focus on obtaining rotating blade pressure data. NREL has been making these types of measurements since 1987 and has considerable experience in doing so. In our first full-scale wind tunnel venture, we feel it is not wise to deviate significantly from what we are currently accustomed to doing – a sentiment clearly voiced by many members of the Science Panel.

The purpose of this wind tunnel test is to acquire accurate quantitative aerodynamic and structural measurements on a wind turbine that is geometrically and dynamically representative of full-scale machines in an environment free from pronounced inflow anomalies. These data will be exploited to develop and validate enhanced engineering models for designing and analyzing advanced wind energy machines.

Previous atmospheric turbine testing demonstrated the extremely complex dynamic nature of a typical wind-turbine-operating environment. Highly turbulent wind and sheared inflow conditions are major factors that contribute to the complexity. Testing in a controlled wind tunnel environment will eliminate

these factors. The resulting data will provide information from which a significant portion of the complex inflow-induced operating environment is removed. This will enable researchers to isolate and characterize specific dynamic-stall responses and 3-D rotational effects under benign steady-state operating conditions. Selected publications are listed in Appendix V.

2.   NREL Unsteady Aerodynamics Experiment (UAE) Background

The UAE research turbine is extensively instrumented for structural loads and aerodynamic response measurements. It includes a pressure-tapped blade with five radial stations of aerodynamic pressure profile characterization, local angle-of-attack (AOA), and spanwise flow angle measurements [see Huyer, et. al. "Unsteady Aerodynamics Associated with a Horizontal-Axis Wind Turbine", AIAA Journal, Volume 34, No. 7, July 1996]. Turbine inflow conditions and power output are also measured. The turbine has been field-tested in many different configurations since 1989. We are currently running a two-bladed damped-teeter rotor. We have a large repertoire of other equipment for the turbine that could be used in a variety of potential configurations for wind tunnel testing. All use active blade-pitch control. The possibilities include a two-bladed rigid hub; a two-bladed independent-blade flapping hub (damped or controlled); a three-bladed rigid hub; upwind; downwind; a tapered/twisted blade set; a twisted blade set; a rectangular blade set; and free yaw, fixed yaw, and variable revolutions per minutes (RPM).

The NREL UAE is capable of measuring several time-varying aerodynamic and structural quantities of interest to wind machine modelers and designers. Paramount among these is the capability to measure unsteady blade-surface pressures, angle of attack, and air speed at five blade span locations. In addition, blade pitch and yaw can be quickly set and held, or driven as a function of time, with a high degree of accuracy. Blade-root-bending moments are recorded, as are blade-tip and nacelle accelerations. Nacelle yaw angle and yaw moment are also measured, as well as hub rotation rate and generator power output. Finally, inflow parameters, including wind speed and direction, are constantly monitored.

The NASA Ames 80' x 120' wind tunnel will provide inflow conditions characterized by temporal stability and spatial uniformity not obtainable in a field test environment. Test section velocities from 5 m/s to 25 m/s will be used during the test, corresponding to representative turbine cut-in and cut-out wind speeds. Blockage and boundary effects will exercise minimal influence on the measurements being performed due to the large cross-sectional area of the test section. The wind tunnel balance system will provide six DOF force and moment measurements.

Since the meeting, the turbine suffered a catastrophic failure. On November 18, 1998, the instrumentation boom broke off the turbine rotor. As the boom broke loose and fell, it smashed into the instrumented blade. The blade sheared off at the 60% span location. The turbine was running in normal operating mode and collecting data at the time. The wind speed was approximately 20 m/s from the west. The 2-m outboard section of blade landed approximately 100 m downwind of the turbine. The instrumentation boom landed 15 m downwind. The failure was due to fatigue damage caused by stress concentrations on an aluminum section of the instrumentation boom near a joint. A preceding period of extremely high wind conditions most likely exacerbated the failure.

Because of the turbine failure, we took the following actions:
- The instrumented, untapered twisted blade was a total loss and could not be repaired. However, we had a new tapered and twisted blade set under construction. We had not planned to use these new blades in the wind tunnel for this particular test. Therefore, we restructured the planned activities and accelerated the construction and instrumentation of the new tapered twisted-blade set.

- We eliminated extensive pre-tunnel field tests of various rotor configurations (for example, free-flapping rotor) and redirected our efforts to rebuilding the damaged rotor systems and incorporating minor redesigns into test apparatus to increase robustness and expedite data acquisition and processing.
- We will only have time to run a short field test (one month) to verify operation of new systems and the new tapered and twisted blades prior to entering the wind tunnel.
- We subsequently delayed the wind tunnel entry by one month (October 18, 1999).
- Accommodating the recovery impacted our ability to prepare for the more diverse testing activities originally envisioned. The current test program, detailed in Section 12 below, focuses on collecting critical aerodynamic performance data for upwind and downwind turbine configurations that are necessary to validate current aerodynamics models. More detailed examinations of other high priority research issues melding tower/ blade interactions, wake flow, and 3-D boundary layer transition, etc., will be planned for a future test opportunity.

In late August 1999, we were informed by NASA Ames that the October 18 date might be delayed due to longer-than-anticipated testing by current tunnel occupants. We agreed to move the test to early 2000. This would give NASA Ames additional time to finish current tests, run a tunnel calibration test, and rebuild a fan motor. The delay provided NREL with the opportunity to build and test a yaw drive for the turbine and to evaluate and prepare for other wind tunnel tests.

3.   Meeting Objectives

The first meeting focused on defining a test matrix that would produce the wind tunnel test data sets needed to facilitate a better understanding of the following three wind turbine applied research topics:

1. <u>"Engineering" dynamic-stall model verification</u>. We typically call the semi-empirical dynamic stall models "engineering models" because they can be run quickly and are easily incorporated into other wind turbine structural dynamics and engineering design codes. The engineering dynamic-stall models are based on experimental data analyzed in conjunction with unsteady theory and enable empirical predictions in the stall regime. All U.S. wind turbine design codes use a version of the Beddoes-Leishman dynamic-stall model with pitching airfoil behavior algorithms implemented. This version, called "AeroDyn," was developed at the University of Utah and tuned with 2-D oscillating airfoil data from Ohio State University (OSU) [see Pierce, K., Hansen, A. C., "Prediction of Wind Turbine Rotor Loads Using the Beddoes-Leishman Model for Dynamic Stall", Journal of Solar Energy Engineering, Transactions of the ASME, v. 117, n. 3, Aug 1995].

    In addition, European wind-turbine designers conducted extensive research in developing and evaluating different engineering dynamic-stall models, including various other implementations of the Beddoes-Leishman model. Recent European experience identifies some serious limitations based on the way these models are implemented [see Rasmussen, et. al, "Dynamic Stall and Aerodynamic Damping", AIAA-98-0024]. As European turbine designers continue to optimize and refine large stall-controlled configurations, stall-induced blade vibrations, and the resulting reduction in blade fatigue life, are emerging as a major problem. Plunging and lead-lag motion algorithms that simulate the aerodynamic responses that drive these blade motions are not implemented or validated in the current U.S. or European engineering dynamic-stall models.

    The test objective for this research topic is to run the turbine under conditions designed to produce benign, controlled 3-D cyclic pitch and possibly plunging data. This will allow better implementation, tuning, and evaluation of the engineering dynamic-stall-model algorithms. A

potential topic of discussion is the relevance and necessity of obtaining lead-lag data and the difficulty associated with configuring an experiment to make these types of measurements.

2. <u>Computational Fluid Dynamics (CFD) model verification.</u> Ongoing advancements in computer technology are enabling U.S. and European researchers to develop complex numerical simulations of full-scale wind turbine 3-D rotor behavior using Navier-Stokes-based CFD computer codes. CFD results are used to produce data needed to further tune the semi-empirical dynamic-stall models. Basic 3-D rotor performance data are needed to enable initial comparison with CFD model results. The complex dynamic nature of typical wind turbine operation in a field environment makes it difficult to isolate baseline steady-state aerodynamic performance.

    The test objective for this research topic is to produce baseline 3-D rotating aerodynamic performance data under the most benign steady-state conditions possible. A potential topic of discussion is characterizing tunnel turbulence and defining its impact on model results. It may also be necessary to trip the boundary layer at a known location on the blade to further eliminate uncertainty and produce an initially comparable data set.

3. <u>Quantification of 3-D rotational effects.</u> Quite a bit of work in both the U.S. and European wind energy communities has gone into trying to develop models to characterize 3-D rotational effects. [see Snel, H., Houwink, R., and Bosschers, J., "Sectional Prediction of Lift Coefficients of Rotating Wind Turbine Blades in Stall" ECN Report ECN-C-93-052, Dec. 1994]. The main consequence of these effects are delayed stall and increased lift inboard, non-2-D post-stall behavior along the span, and tip-vortex-induced lift effects outboard. These effects are usually implemented by altering 2-D aerodynamic performance data used as input in engineering dynamic-stall models.

    The test objective for this research topic is to produce data needed to properly quantify the 3-D effects under various operating conditions so that existing or resulting models can be validated. A potential topic of discussion is to define the range of operating conditions that are likely to influence 3-D effects.

The need for subsequent Science Panel meetings will be decided later. It may be necessary to reassemble the full Science Panel prior to entering the wind tunnel to discuss and resolve issues related to the final proposed test matrix. However, it may suffice to meet only with the technical oversight committee or resolve issues via e-mail. Scheduling subsequent meetings will depend primarily on comments received after Science Panel members review the final test matrix. Follow-up meetings to summarize resulting data sets and to review analysis activities after wind tunnel testing has been completed are also a possibility.

4.   European Research Partner Participation

Since the late 1980s, many European Union (EU)-funded Joule research projects have taken an in-depth look at issues related to wind turbine dynamic stall and 3-D effects. Recent European research has identified shortcomings in the dynamic stall models resulting in significant blade design problems. As European wind turbine blade builders refine their designs to optimize weight and performance, stall-related issues, such as stall-induced vibrations, have surfaced. The aerodynamic mechanisms that drive these phenomena are not well understood and were not incorporated into the earlier dynamic-stall models. The resulting unsteady aerodynamic forces, coupled with blade structural responses, cause premature blade fatigue failure. Attempts were made to add algorithms to models to account for these forces, but data to validate the models are difficult to obtain. European researchers who attended the Science Panel

meeting were therefore asked to summarize the results of these EU Joule projects. These presentations are shown in Appendix G. European attendees were also asked to provide recommendations to NREL as to what data the wind tunnel test could provide to enable better validation of the models. These presentations were conducted during Session 3, and are shown in Appendices I-M. Based on the outcome of the Science Panel meeting, as summarized in this report, European research partners will submit proposals to NREL describing proposed research studies, with the resulting validated algorithms or methods being supplied to NREL in exchange for specified test data. These proposals will form the basis of the collaborative research and may be formalized under an International Energy Agency (IEA) agreement.

5.   NREL- NASA Ames Test Agreement

NREL had originally arranged to go into the NASA Ames wind tunnel through an informal non-paying agreement, possibly squeezing in for a short duration between other large-scale tests by paying customers. In that scenario, NREL would have provided all test apparatus and labor and conducted the tests in a similar fashion to those at the NWTC field test site. This meant that we would use our existing pressure measurement, structural instrumentation, and flow visualization systems, and would not require significant assistance or resources from NASA Ames staff. On August 14, 1998, this scenario changed to an official test date (originally October 18, 1999, now early 2000). In addition, we will be paying ($254,000) for a three-week test slot. The main advantage is that, in addition to our existing measurement capabilities, this also buys us the assistance and expertise of the NASA Ames staff to enhance the resulting test information. We are now attempting to re-calibrate our thinking and change the test plans to take advantage of this assistance. We are learning about the many various capabilities available to us at NASA Ames, especially in the areas of flow visualization, that can be used to provide information far beyond our field capabilities. This is fortunate because there was a strong sentiment at the Science Panel Meeting that, for example, transition location and wake characterization measurements need to be additionally undertaken during the wind tunnel test. We continue to work closely with NASA Ames to provide a means to supply these types of data during the wind tunnel test.

6.   Agenda

A preliminary meeting agenda was included with the meeting invitation information that was e-mailed to all potential participants. To keep the meeting objectives focused on the science issues described in Section 3, presenters were selected based on their work in the area of developing and using engineering methods to simulate wind turbine dynamic stall and 3-D effects. The meeting was also open to anyone interested in wind turbine unsteady aerodynamics wind tunnel testing. The final agenda was prepared after consulting with confirmed attendees about presentation topics; it is shown in Appendix A. The meeting followed the agenda closely until the final session, "Session 6 Conclusion and Wrap-up". The group discussion during this session went on until 5:30 p.m., and many attendees had to leave prior to this time. Consequently, there was never an opportunity for attendees to provide summary comments. We solicited comments from attendees after the meeting, and they are summarized in Section 10.

7.   Presentations

There were five sessions of presentations during the course of the two-day meeting. Session 1 provided an overview of the basic science issues of wind turbine aerodynamics, International Electrotechnical

Commission (IEC) design requirements and procedures for wind turbines, and turbulent wind inflow characteristics. These presentations are found in Appendices C, D, and E.

Session 2 presented an overview of wind turbine aerodynamics engineering methods as used by U.S. and European wind-turbine designers and modelers. In this session, various methods used to estimate wind turbine aerodynamic responses for engineering purposes (e.g. for inclusion into full-turbine structural dynamics models) were identified and briefly described. In addition to including models that account for the effects of dynamic stall, these methods also typically incorporate models of 3-D responses (e.g. delayed stall and tip loss effects). Presenters summarized method objectives, including, for example, who developed the method, what models are included in it, how it was tuned and validated, and modifications made to fix problems and improve performance. These presentations are found in Appendices F and G.

Session 3 provided a forum for users of the Beddoes-Leishman and other similar models to focus on issues specific to semi-empirical dynamic-stall models. The session began with a presentation by G. Leishman, who described the original model development and intent. Model users then described the use of their methods that incorporated models of both dynamic stall and 3-D effects. Each presenter was asked to present the following: 1) a brief description of modeling needs and efforts, including typical applications; 2) identification of model shortcomings, perceived limitations, and problems encountered; 3) a summary chart depicting model strengths and weaknesses; 4) a summary of needed improvements; and 5) specific information that the NREL wind tunnel test could provide to enable better model utilization and/or validation. These presentations are found in Appendices H through M.

Session 4 was similar to Session 3 except the emphasis was on 3-D effects and CFD modeling. These presentations are found in Appendices N through R.

Session 5 included a test site tour and described the NREL turbine experimental facility, reviewed the turbine systems, described planned test activities, discussed data processing methods, and introduced wind tunnel test logistic plans. A strawman of the initial test matrix and summary of research issues to be addressed was also presented. These presentations are found in Appendices S, T, and U.

8.   Minutes of the Group Discussion

These minutes summarize group discussions held during Session 6.

Parked-Blade Test

- This part of the test is designed to ascertain 3-D effects when the rotor is parked with the blade vertical. This will help identify issues regarding the five-hole probes in the flow field in relation to the blade. This will also help us define an upwash correction for the five-hole probes similar to that derived from the flag 2-D wind tunnel test.
- McCroskey suggested that the probes are possibly not measuring what we think they are measuring. Panel code methods could be used to estimate the induced velocity.
- Bjorck commented that the parked blade pitch oscillations should mimic those used during the OSU 2-D wind tunnel test in order to validate models currently based on this data.
- Hansen suggested that the pitch angles vary from ±180 degrees and that the amplitude of oscillation be reduced from that proposed.
- Rasmussen suggested that the mean pitch and oscillation amplitudes used during a parked-rotor test be duplicated in the rotating environment. There was discussion as to synchronizing the

oscillation with rotational speed. If the oscillation frequency is not synchronized with the rotational frequency, the average induction over the rotor would be affected.

- Larwood commented that the parked-blade test should include maximum blade loads for a pitch angle of 90 degrees to simulate parked-rotor maximum-load conditions under high wind speeds.
- The panel suggested that prioritizing the test was very important. Parked-rotor conditions should probably be run last because the most valuable aspect of the test is the opportunity to collect rotating data in the wind tunnel.
- Hansen suggested that very slow pitch rates would permit determining Cl max.

Rotating Blade Test

- Because all of the tests include both clean and tufted blades, the panel suggested that several points be selected to insure reproducibility of the measurements. The oil test should be used to determine transition locations on the blades.
- Participants suggested that finer resolution in wind speed should be obtained in regions where stall begins, such as around 30 degrees.
- Snel suggested that tip-speed ratios higher than eight (which is the maximum currently planned) would be desirable.
- Participants raised questions about the flow quality of the tunnel at low wind speeds. The option of variable-speed operation was proposed. Sonic anemometers will be used to measure the tunnel speed instead of the tunnel instrumentation. Because of the potential of horizontal wind shear in the tunnel, two sonics will probably be required. Based on graphs shown by Kufeld, a ±5% dynamic pressure fluctuation is expected due to the outside conditions. These conditions will be monitored carefully, and the experiment will probably be run on either the second or third shift to alleviate these problems.
- Holley suggested that the pitch angle corresponding to maximum power production be included in the test matrix. Currently, the chosen pitch angle for maximum gross annual energy production is three degrees.
- Holley also suggested a step change in pitch angle. This should be done under rotating conditions. The issue of synchronizing with the rotor speed was raised again, but was not completely resolved.
- A coning angle variation was suggested by Rasmussen. However, the discussion that followed suggested this could be the addition of another parameter that complicates the entire test.
- Buhl asked if the priority was to compare with field data or with CFD simulations. There is an interest in validating current engineering models through comparison with field data as well as using CFD.
- Participants raised the issue of delineating between pitch and plunge motion. Independent blade motion could cause interference with the wake. Hansen suggested that allowing the rotor to teeter at a 30-degree yaw angle would naturally create the plunge motion. Simms pointed out that design loads under these conditions cause concern. The panel determined that the flapping rotor option is not as important as the teeter option.
- As suggested, some of the rigid cases will be duplicated with the teeter degree-of-freedom (DOF).
- McCrosky suggested that a controlled flow disturbance upwind might provide valuable insight. A fixed-wing tip would produce a longitudinal vortex that could be directed to a known location on the rotor. Smoke released from the wing tip would provide flow visualization of the vortex contacting the rotor. NASA expertise could be used to implement the smoke and wing tip portion of the experiment.
- Hansen did not believe that the simple disturbance was of interest because of the complex disturbances found in the field environment. The tower shadow itself is an interesting disturbance. Berg believed that this sort of simple, quantifiable disturbance would be of great

help in validating models. Carr emphasized that this type of information would be invaluable to CFD modelers. Even if there was no current capability to model this, the next generation of CFD models most likely would have this capability. Both McCroskey and Carr commented that in the helicopter field, this type of experiment has proven desirable.

- Holley suggested that a jet disturbance normal to the rotor plane would be more interesting. A comparison with engineering models should be made immediately after the experiment for validation. Galbraith suggested that yawing the turbine in some sort of disturbance field would create an oblique path between the disturbance and the rotor. Rasmussen commented that, with and without the disturbance, the operation would provide the opportunity to examine superposition issues. Robinson confirmed that Duque would need a coherent vorticity impinging on the rotor for future CFD model validation.

- The issue of flow visualization of the wake as well as the blade surface was raised. Galbraith presented some of his work regarding another wind tunnel experiment that used a scale model of a wind turbine. To quantify tunnel wall effects, a prescribed wake method was used with the wall constrictions. It is possible that the wake and wall effects could be quantified using this type of prescribed wake model in conjunction with flow visualization in the form of smoke released from the blade tips. Only the tip vortices would be required. Marks on the tunnel wall could be used to provide dimensions, and the smoke release would be video taped. The wake expansion issue could be resolved in this manner.

- To focus the discussion, McCroskey suggested that each participant state what would be the single most important data point for their purposes. Hansen would like a teetered rotor at 30 degrees yaw and a wind speed that would produce maximum power, and Bjorck agreed. Snel requested operation in stall, low tip-speed ratio, and yawed conditions such that cyclic stall would occur. Rasmussen preferred zero yaw with dynamic stall due to cyclic flap motion. Robinson envisioned stall oscillation caused by yaw and by pitch.

- The list of suggestions that had been compiled throughout the meeting was presented. Those suggestions that could be met with the strawman matrix were checked. Those not checked were then discussed in the order in which they appeared on the list.

- Hansen's suggestion for multiple rotational speeds in order to broaden the K and Re range was discussed first. Cyclic AOA due to yaw errors at the same radius and different frequencies would be required. The suggestion received a low priority.

- Participants proposed conducting dynamic inflow tests that consist of abrupt pitch change over ranges of pitch angles and tip-speed ratios. Holley reiterated his support of this type of test. Robinson also indicated high priority for this test. Rawlinson-Smith, however, pointed out that during the Joule Dynamic Inflow studies, pitch variation caused little change in the inflow. Only high tip-speed ratio indicated a significant effect due to pitch variation. Robinson indicated that this type of known disturbance would be necessary to test models and control designs. Hansen suggested that abrupt pitch changes could be used to simulate emergency shutdown procedures.

- Another proposed test was tip-loss load differences between two- and three-bladed machines. However, the time required to change the rotor is completely impractical for the three-week duration of the test. Because three-bladed rotors are more commonly used in the industry, Holley and Wetzel suggested that this type of rotor would be most beneficial. However, Hansen strongly supported the teetered rotor, and Robinson indicated the political issues behind the use of the two-bladed rotor. He pointed out that the science issues would not differ significantly between the two rotors. The suggestion received a low priority rating.

- Boundary layer alterations resulting from vortex generators had been proposed by Snel. Again, the time constraint issue was raised. Issues regarding the necessary mixing as a result of the size of the disturbance were discussed. Kelley suggested that the conclusion reached by NASA during the MOD-2 tests should be reviewed. Panel members gave it a low priority rating.

- Periodic pitch motions had been included in the strawman matrix, but the panel discussed periodic plunge motions. Teeter may be used to create plunge motion by constraining the rotor, inducing high yaw angles, and releasing the rotor. Leishman indicated that the differences between pitch and plunge motions are very subtle effects and are difficult to measure in a 2-D environment. Holley suggested that plunge motion would be required to compare with pitch motion in order to delineate between the two types of motion. The consensus was that pitch motions are high priority and plunge motions are lower priority.
- In discussing wake measurements, McCroskey and Carr pointed out that the helicopter industry has expended tremendous resources to obtain wake information from several tests. Currently, an expensive test is being repeated for this purpose alone. Leishman also endorsed some type of wake measurement. The wake information would be required to validate models. The panel's consensus was that this type of information would almost certainly be desired at some point after the test.
- The panel again stressed the importance of wake measurements, as well as the difficulty of obtaining those measurements. NASA Ames expertise could be used to obtain these measurements; however, sophisticated measurements are unrealistic.
- Earlier, Holley suggested measurement of all six net forces and moments. When the yaw brake is applied, the yaw moment is measured using strain gages. Blade root flap and edge bending moments measure thrust and sideways moments. The thrust force can be inferred from the pressure measurement. The thrust and sideways moments can be measured with the instrumentation below the turntable in the wind tunnel. The panel assigned this suggestion a medium priority.
- The panel had another discussion about the issue of varied tip-speed ratios and the questionable nature of the tunnel inflow for low wind speeds. It reiterated the need to measure the inflow and observed that the dynamic pressure measurements on the blade would alleviate some of these concerns.
- In the area of tunnel wall effects and wake expansion, the panel suggested reviewing the Aeronautical Research Institute of Sweden (FFA) experience in the Chinese wind tunnel.
- The use of tip plates would be fairly easy to implement. Fingersh requested specific information for the type plate to be used. This test would assist in quantifying tip loss. However, the resolution of pressure measurements at the tip cannot be improved due to time constraints. Thus this test was given low priority.
- Whale suggested improving the resolution of pressure measurements inboard, but it was deemed impractical due to time constraints. However, during the parked-blade test, the intermediate taps inboard may be used to infer angles of attack.
- To accurately model the blades with CFD, participants suggested profiling the blade. An acceptable tolerance will be provided by Duque, and NREL will complete this task. It could possibly be delayed until after the test due to timing issues.

Tower Wake Characterization

- At zero degree yaw error, the blade cuts through the wake of the tower. At small yaw angles (5-10 degrees), the blade cuts through the wake obliquely. The current instrumentation could be used to characterize the tower wake. An additional option would be to park the blade in the tower wake or slowly rotate the turbine through the wake to provide better resolution. However, the tower wake alone is important. The elimination of the tower-blade interaction would be helpful for CFD analysis. Snel suggested that a pressure ring around the tower could be added.
- Because the Reynolds number is in the transition region, the panel suggested that the boundary layer be tripped. However, this creates a situation that has not been duplicated in the field, and it is not certain that the boundary layer will behave as expected. Also, if the turbine yaws, the

roughness would need to be attached to the entire circumference of the tower. The panel decided to attach roughness to fix transition as well as to test without roughness.

- In order to address acoustic concerns, Robinson would like to correlate the wind tunnel experiment with the field data. Thus, the tower should resemble the field tower as closely as possible. The coupling between the blade passing and the Strouhal number must be examined.
- The panel discussed placing the tower alone in a different tunnel with a rake to measure the wake. Again, flow visualization using smoke could help identify the wake structure.
- It would be helpful to distinguish between organized vorticity shed from the tower and blade passage through the velocity deficit in order to tune dynamic stall models.
- The pressure ring would pick up pulses in front of the tower that result from vortex shedding off the back of the tower.
- Some measurement of the tower wake conditions would permit sorting of the test data on various wake conditions.
- Will the tower vortex shedding in the wind tunnel differ with the field conditions?

Random Discussion

- The panel determined that that blade transition must be fixed in order to validate current CFD models, but in the future, fixed transition may not be necessary. Timmer suggested that placing a trip around 5% chord would cause transition within a couple of percent. The matrix should be studied to determine which sets of data would use the trip. It would be helpful to see what the trip does in conjunction with the tufts. The tufts could ascertain that the boundary layer is sufficiently tripped. Most of the wind tunnel test should be done with clean blades. Then a subset of tests could be run with fixed transition. The oil flow visualization experiment could also validate that the trip is working properly if it is done for both fixed and clean blades.
- The panel decided that varying the coning angle was relatively easy to implement. Rasmussen indicated that only two angles (3 degrees and 10 degrees) would be sufficient. This test could be done at the end of the experiment if time permits. This should be done in a downwind configuration.
- The small amplitude pitch oscillations are of higher importance than the duplication of the OSU experiment.
- Teeter is of very high priority to Hansen. He would very much like to see fixed yaw with a release.
- The rotating blade experiments are of the highest priority.
- The panel agreed that simulations of the various experiments would be completed ahead of time in order to provide a benchmark.

9. Summary of Attendee-Recommended Tests

Recommendations for various wind tunnel tests made throughout the course of the meeting sessions are summarized in Table A. The proposed tests (marked Y) were already planned and included in the original NREL proposed test matrix (shown in Appendix U) and are not discussed further. The items marked N were discussed and prioritized by the group as documented above in Section 8. Also shown in the table is the relative difficulty of performing the proposed test (1=easy, 10=impossible) during the allotted test period, taking into account NREL's previous test experience and the existing turbine hardware configuration. A rating of the technical priority of the test resulting from Science Panel group discussions of the underlying basic science rationale are shown in the next column. (high, medium, low). NREL's concerns and concluding responses to the recommendations are further discussed in Section 11.

Other proposed tests listed in Table A that NREL will not undertake during this test represent a significant deviation in what NREL is currently doing or is capable of doing. The fact that these tests are not included in the planned tunnel entry does not imply that they are unimportant from the perspective of understanding rotating blade aerodynamics. Some are certainly more important than obtaining pressure distributions. The concern is that we are not experienced in this area, or that we do not have sufficient time to prepare and make such measurements. With only a three-week tunnel test slot, we felt it would not be wise to undertake these tests. These are likely candidate tests for future wind tunnel experiments after first working out measurement methodology details in the field.

#	Recommended Turbine Test Condition	In Original Matrix?	Test Diffi-culty	Science Panel Priority	In New Test Matrix?
a	Steady state operation over yaw angles 0 through ±180 degrees over the maximum possible range of wind speeds and pitch angles	Y	1	H	Y
b	**Operate at multiple RPM's to broaden K and Re range**	**N**	**4**	**L**	**Y**
c	**Dynamic inflow tests where abrupt pitch angle changes are made over a wide range of mean pitch angles and tip speed ratios**	**N**	**2**	**H**	**Y**
d	Yaw releases made over a wide range of wind velocities	Y	1	H	Y
e	**Tests to determine tip loss and loading for two- and three-bladed rotors**	**N**	**9**	**L**	**N**
f	Fast cyclic periodic pitching on a rotating and non-rotating hub	Y	1	H	Y
g	**Boundary layer alterations such as vortex generators (VGs), stall strips, and transition trips**	**N**	**5**	**M**	**Y***
h	**Periodic plunge motions**	**N**	**8**	**L**	**N**
i	**Rotor wake flow visualization (qualitative), including measuring rotor wake skew angle**	**N**	**6**	**H**	**Y**
j	**Rotor wake field measurements, hotwire, Laser Doppler Velocimetry (LDV) etc. (quantitative) including measuring induced velocity in the wake, and taking measurements at high and low tip-speed ratios**	**N**	**9**	**L**	**N**
k	**Measure all six net forces and moments on turbine rotor**	**N**	**10**	**M**	**N**
l	**Quantify effects of tunnel walls on wake angle and expansion**	**N**	**5**	**H**	**P**
m	Steady state power curves for two pitch angles and clean blades	Y	1	H	Y
n	Blade tip and root pressure distributions	Y	1	H	Y
o	**Pressure distributions with tip plates**	**N**	**3**	**L**	**Y**
p	**Improve span-wise resolution between 25%–50% span**	**N**	**10**	**L**	**N**
q	Controlled environment over a greater range of local flow angles	Y	1	H	Y
r	Characterize inflow velocity and angularity distributions	Y	2	H	Y
s	**Wake profiles to characterize tower flow characteristics**	**N**	**9**	**H**	**N**
t	**Fix separation to characterize tower flow characteristics**	**N**	**9**	**H**	**N**
u	**Blade transition; fixed vs. free**	**N**	**7**	**H**	**Y**
v	**Different coning angles**	**N**	**3**	**L**	**Y**
w	**Duplicate OSU 2-D oscillating conditions**	**N**	**2**	**H**	**Y**
x	**Small amplitude oscillating conditions**	**N**	**2**	**H**	**Y**
y	**Higher resolution around stalled conditions (parked rotor)**	**N**	**2**	**H**	**Y**
z	**Higher resolution around max Cp**	**N**	**2**	**H**	**Y**
aa	Teetering rotor data	Y	1	H	Y
bb	**Flapping rotor data**	**N**	**8**	**L**	**N**
cc	**Prescribed disturbance through rotor plane**	**N**	**8**	**L**	**N**

*Transition strip tests only

The final determination of where the proposed test fits into the test plan is shown in the last column. This reflects NREL's conclusions, taking into consideration the Science Panel priority and weighing it against the difficulty of performing the test within the available time. NREL will schedule and attempt to conduct all tests marked "Y" in the "New Test Matrix" column. Items marked "N" will not be attempted during the initial three-week tunnel test, but are candidates for consideration in a possible follow-on tunnel entry at a later time. Some items are not actual test conditions, but rather are issues that should be resolved prior to the test or incorporated into test planning. These items are labeled P and are discussed below. The new proposed test matrix is shown and discussed in detail in Section 12.

10.   Summary of Attendee Comments

We asked all attendees to submit comments after the meeting summarizing their concerns and recommendations. Additional issues from the comments that were not discussed during the meeting are summarized in Table B. Many additional important issues were raised; these issues are addressed in Section 11. The relative difficulty is also included. As in Table A, the resulting test matrix priority, as determined by NREL, is included in the last column. Some of these are not actual test conditions, but rather are issues that should be considered prior to the test or incorporated into test planning. These items are labeled P and are discussed below.

Table B – Science Panel Post-Meeting Test Issues and Further Recommendations

#	Issue	Difficulty	In New Test Matrix?
dd	Leading-edge grit roughness tests	8	N
ee	Determine how tunnel turbulence spectra compare with those found in the atmospheric boundary layer at desired test velocities	5	P
ff	Determine how mean and distribution of the instantaneous Reynolds stresses vary over the desired test wind speed range	5	P
gg	Determine if there are any spectral peaks in the tunnel flow with an equivalent space scale similar to the airfoil dimensions of the turbine rotor blades	5	P
hh	Quantify tunnel horizontal shear at low velocity	5	P
ii	Profile the blades	6	P
jj	Run high priority tests first	5	P
kk	Minimize configuration changes during testing – do in off hours	2	P
ll	Have additional tests ready in case things go well	2	P
mm	Plan for failures – spares, alternative equipment, etc.	2	P
nn	Overlap in test matrix	2	P

11.   NREL Response to Concerns and Issues Raised

As expected, the Science Panel Meeting raised more issues and concerns than were solved. This section summarizes NREL's response to all recommended tests (from Table A) and follow-up Science Panel member concerns (from Table B). NREL evaluated these recommendations and concerns, taking into account the Science Panel priority and experiment configuration, and rebuilt the test matrix as shown in Section 12 below.

Two- vs. Three-Bladed Rotor (Table A, Item e)

The most significant concern is more political than scientific and is related to whether we should test a two-bladed or three-bladed rotor, or both. This stems from the fact that the NREL Wind Program's Next Generation Turbine Development Program is supporting both two- and three-bladed industry concepts. From a science perspective, the basic underlying physical aerodynamic responses are the same, regardless of the number of blades. Because this test focuses on providing data to better understand and quantify the basic science issues, we hope that critics realize that aerodynamics are aerodynamics; the politics of two- vs. three-bladed rotors does not matter here. This is not to say that these rotors behave the same. They certainly do not, and we are well aware there are many factors that affect this (e.g., rotor solidity and previous-blade shed wake interference). We have spent many years testing both types of rotors on the Unsteady Aerodynamics turbine in the field. We suspect that even if we did run both types of rotors in the wind tunnel, the scale and specific configuration differences between the test turbine and industry-scale turbines would raise additional concerns. Ideally, we hope to develop a good enough understanding of the basic 3-D aerodynamic responses so we can accurately simulate the performance of rotors, even in

stall, with any numbers of blades and any size of rotor. Therefore, we are currently planning to go into the tunnel with our existing versatile two-bladed rotor, and run in the teetered and rigid rotor configurations, both upwind and downwind. This rotor also gives us the capability to zero the pre-cone angle to better facilitate upwind and downwind operation. To switch to a three-bladed rotor is a difficult task that would probably take a week of valuable (and expensive) tunnel time. Based on the resulting data and conclusions of subsequent analyses from the two-bladed tests, we will then ascertain if three-bladed tests are needed. If so, we will schedule a follow-on wind tunnel test at a later date dedicated exclusively to using a three-bladed rotor and subjecting it to the full range of testing. This will also give us time to build up a new three-bladed rotor. The existing three-bladed rotor needs to be retrofitted with independent-blade-pitch actuators to replace the old collective-pitch system, which is problematic in maintaining accurate pitch settings. We would also like a potentially new three-bladed rotor to be versatile in setting the pre-cone angle. The current fixed 3.5° downwind pre-cone might cause some load and stability problems in an upwind test configuration.

Rotor-Wake Characterization (Table A, Items i and j)

The Science Panel felt strongly about the need to try characterizing the rotor wake. The purpose is to enable validation of wake models. Participants discussed a variety of wake-characterization measurement methods. We are working closely with NASA Ames to ascertain what types of blade-wake characterization tests are appropriate for the wind tunnel test. The most difficult methods are quantitative tests (e.g., hotwire or LDV) used to measure three components of rotor wake or induced velocity. Due to the difficult and widely varying nature of field-based test conditions, NREL has not made a significant effort to develop the capability to make this type of measurement. We are, therefore, relying on NASA Ames' expertise in this area. With only a three-week tunnel slot, NASA indicates that LDV and 3-D hotwire quantitative tests are probably not feasible because of the relative difficulty and length of time needed to obtain quality data sets.

Qualitative flow-visualization measurements (blade-tip smoke generators recorded on video, or smoke clouds and laser sheets) are simpler and more practical to conduct. NREL has used smoke generators in the past, mounted at different places on the rotating blade, to provide a basic idea of the wake nature. The generators and mounting brackets typically used were large and bulky and obviously altered the flow. We have recorded smoke-wake trace images with video cameras, but have not made an effort to measure or accurately track the wake location in the field. We have learned that this technique works well when the flow is attached, enabling visualization of tip vortex for more than three rotor cycles downwind. However, when the outboard blade section stalls, the tip-wake smoke disperses quickly—in less than a single rotor cycle. We are working with NASA Ames to explore the use of multiple tunnel-wall-mounted video cameras to track tip vortex wakes. We have field-tested smoke generators embedded into a modified tip piece that introduces smoke into the tip vortex. The smoke generator typically lasts for several minutes and visualization of the propagation of the tip vortex is excellent. We, therefore, plan to "calibrate" the video camera images so that wake location is known. NASA Ames also has experience in using smoke introduced upwind and laser sheets to locate and track tip vortices. We are continuing to evaluate this and other various potential qualitative methods for additional possible wind tunnel use.

Tower-Wake Characterization (Table A, Items s and t)

As with rotor-wake characterization, precise quantification of tower-wake characterization is also difficult. It would be useful to know the dynamic nature of the tower wake so that the tower-wake/blade interaction (e.g., shed tower vortices passing through the rotor plane) could be better characterized. However, the short duration of available tunnel time makes a detailed attempt to undertake this task unlikely. The panel proposed undertaking a detailed characterization of the tower wake as a separate task in a different wind tunnel. Currently, Mike Graham, of the Imperial College of London, is conducting an

experimental investigation of blade/wake interactions. These results may provide the basis for future investigations. During the NASA Ames test, we are planning one series of wind tunnel tests to attempt a basic tower-wake characterization. The downwind instrumented blade will be pointed into the wind (feathered) and slowly rotated through the tower wake. Planned tests are further described in the wind tunnel test series called "Tower-Wake Measurements," as described in Section 12.

Flow Quality at Low Tunnel Velocity (Table B, Item hh)

NASA Ames has indicated that uniform tunnel flow is unlikely to occur at lower operating velocities, and low-velocity tunnel flow characteristics are dependent on outdoor wind conditions. If the wind is coming from a direction that is not aligned with the tunnel inlet, the horizontal distribution of velocity across the tunnel test section can vary. This horizontal wind shear is greater at lower tunnel velocities, especially those below 35 m/s. For example, at our minimum required tunnel velocity of 5 m/s, and maximum outdoor wind of 5 m/s, the distortion in total pressure across the tunnel test section can exceed ±7% of the average dynamic pressure (q). At 15 m/s tunnel velocity and 5 m/s outdoor wind, the pressure distortion drops to ±3% of q. If the outdoor wind gusts to 10 m/s with the tunnel at 15 m/s, the distortion rises to ±7% of q. Based on NASA Ames recommendations, we are planning to run our tests late at night when lower outdoor wind-velocity conditions are more likely to occur. During testing, we plan to monitor the outside meteorological tower data. In addition, we will quantify the inflow shear by using two sonic anemometers mounted in the tunnel upwind of the turbine. It is also possible to determine how much shear is present at the rotor plane by monitoring rotating blade probe or stagnation pressure values while the turbine is operating at zero yaw conditions.

Tunnel vs. Outdoor Turbulence Scales (Table B, Items ee, ff, gg)

Debates have raged within the wind community for years over the issue of atmospheric vs. wind-tunnel turbulence-scale levels and how turbulence affects airfoil performance characterization. This is usually related to 2-D tests of airfoils in smaller wind tunnels. The general conclusion has been that it is best to conduct 2-D tests of wind turbine airfoils in low-turbulence wind tunnels to best approximate field performance. This seems contradictory in that one would think that there is much more turbulence in the outdoor field environment. The issue is instead related to the characteristic scale, rather than the amount or quantity, of the turbulence. Characteristic scales of turbulence generated in small wind tunnels can be on the order of the size of the airfoil dimensions and can certainly affect airfoil performance. Scales found in naturally occurring planetary boundary layer turbulence are typically much larger—on the order of the size of the rotor or larger—with little energy at the characteristic scale of the blade chord. There are some concerns about the scale of turbulence found in the NASA Ames tunnel and how it affects airfoil performance. NREL will be recording the data from two sonic anemometers upwind of the turbine in the tunnel. These data can be used to characterize the nature of tunnel turbulence, and will allow a comparison with previously collected outdoor field-test data. Further investigation of this is an ideal topic for a potential research partner.

Operate at Higher RPM (Table A, Item b)

To date, most field testing is conducted with the turbine operating at a fixed 72 RPM. This is because the turbine generator and gearbox provide grid-synchronous operation at 72 RPM. In conjunction with Phase IV field testing, NREL incorporated a variable-speed power electronics system into the experiment configuration to enable the turbine to be operated at speeds other than synchronous 72 RPM. The turbine can be operated with or without the power electronics system invoked. Without power electronics, the original synchronous 72 RPM is attained. Based on code simulations, we can safely operate at speeds up to 110 RPM. We have not conducted a significant amount of higher-RPM field testing for various

reasons. First, the rotor speed is usually kept at a constant 72 RPM to facilitate data comparison with results obtained from earlier phases of testing. Second, because operating the variable-speed power system generates significant electrical noise, we were concerned about the effects on measured parameters. Third, we are uneasy with running at a higher RPM than necessary due to vibration or centrifugal loads on extensive sensitive rotating instrumentation.

Seventy-two RPM corresponds to a tip velocity of 38 m/s and, at a minimal tunnel speed of approximately 5 m/s, this means the highest attainable tip speed ratio (TSR) is less than 8. This is low for a typical wind turbine, especially a two-bladed machine. At 90 RPM, a TSR in excess of 9 is attained, which is more representative of industry turbines. We certainly understand the need to run at higher RPMs during the tunnel testing to broaden the range of TSR, Re, and K data obtained. These tests will be somewhat limited because of the potential for producing greater power than the turbine generator and rotor system can handle.

Therefore, we are planning to conduct more field tests during the upcoming wind season, utilizing the variable-speed-power electronics system to run at other RPMs. This will enable us to further determine if variable-speed-electronics-induced noise is a problem, or if any of the rotating electronics systems are adversely affected. It will also help us quantify other potential mechanical problems, such as vibrations and loads on the machine and instrumentation at certain rotor speeds. We will then decide what conditions can be run in the wind tunnel.

Pitching Motions (Table A, Items c, w and x)

We revised the test matrix to include various additional series of pitching-motion tests. These tests are very simple to conduct due to the controllable turbine-pitch system. Tests were added that duplicate the pitching motion undertaken in the OSU oscillating S809 2-D airfoil tests. Smaller amplitude pitch variations were also added.

Plunging Motions (Table A, Item h)

The panel discussed various means of achieving plunging-motion data. Blade plunging motion results from teeter excursion during yawed teetered-rotor testing. Although difficult to control, the teetered-rotor tests should produce some type of sinusoidal plunging motion at 1 P (1.2 Hz) over an approximate 1 m out-of-plane tip-displacement distance. Another method would be to utilize the turbine rotor's differential blade pitch capability. The instrumented blade can be kept at a constant pitch angle while the other blade is varied in pitch to achieve teeter motion. This method might be able to produce more controlled motions at higher frequencies. Because blade teeter position is accurately monitored, the exact displacement distance is quantifiable. We plan to run some more extreme off-yaw teeter cases and single-blade pitching during field testing to better determine what types of plunging motions can be generated. The panel also discussed a technique for holding the blade in position with a cable and quick-releasing it to produce a quick plunging motion. We don't know how quickly the motion will damp out, and model simulations will be conducted to better estimate the resulting motion.

Boundary Layer Alterations (Table A, Items g and u)

Quantification of the effects of various boundary-layer alteration devices (VGs, stall strips, transition trips) were recommended, but not significantly discussed during the meeting. This is probably because extensive boundary-layer manipulator tests were undertaken previously by the NASA wind program and, more recently, by various subcontractors. This issue, due to time constraints, was not given a fair discussion at the meeting. I am including here some post-meeting comments from Herman Snel of The

Netherlands Energy Research Foundation (ECN), which better clarify the reason we are considering these types of tests:

> *"Experiments with <u>boundary layer manipulators</u> were not well received at the meeting. Perhaps I didn't explain why they are used on most of the modern stall blades. In fact, at the root, thick profiles are used (to reduce weight and costs) that have a small alfa interval between the design alfa and the maximum cl alfa. Changes of alfa with wind speed are much larger in the root region than in the tip region. As a result, the root may stall at too low wind speeds, unless stall is delayed with vortex generators. At the tip (thinner airfoils), the stall alfa may be too high in general, so that blade loading and power may overshoot. For that reason, stall strips are used in the tip region to ensure stall at a low enough alfa. The use of stall strips in the tip region also removes part of the fluctuations due to oscillation of the stall point, in time, and gives a more quiet behavior. However, there is no structured knowledge about the effect of bl manipulators in the rotating environment. The installation and removal of vortex generators (pasted on strips) and of stall strips is quite easy and quick, but of course does need a crane or something like that to reach the blades. I have made my point, you think about it and decide, it is your experiment."*

To properly address this issue, we need to conduct further research to understand the rationale behind previous boundary-layer manipulator tests, especially with regard to stall-controlled rotors, and design an appropriate test series. Again, this is an ideal topic for a potential research partner to undertake. Because of lost time from the turbine failure, it will not be possible to complete the assessment and design a comprehensive test plan for the upcoming tunnel test. Instead, a limited test series will be conducted utilizing zig-zag tape to force transition. We will consider more detailed testing for future tests, or possibly with other collaborative research partners. The main objective of the planned limited boundary-layer manipulator testing during the upcoming wind tunnel entry is to provide aerodynamic data for CFD modelers with a known air-foil transition location. The University of California–Davis Campus (UC Davis) is conducting 2-D wind tunnel experiments with an S809 airfoil model and will recommend a trip strip configuration best suited to force transition. These strips will be applied to the instrumented blade during the wind tunnel test series called "Transition Fixed," as described in Section 12.

Measure Six Net Forces on Turbine Rotor (Table A, Item k)

The Science Panel recommended measuring the six net forces on the rotor. We currently measure low-speed shaft bending on two axes (parallel and perpendicular to the instrumented blade) and low-speed shaft torque. We do not measure thrust or other forces on the shaft. We evaluated the feasibility of making direct low-speed shaft thrust measurements in the past, but the turbine mechanical-shaft-mounting configuration makes this difficult. As with measuring thrust, it is also prohibitively difficult to measure shaft X and Y forces due to the shaft-mounting configuration. We compared time-averaged measured torque measurements with torque estimated from the integrated-blade aerodynamic forces, and saw excellent agreement. From this, we can assume that thrust estimated from the aerodynamic forces is probably reasonable.

To ascertain rotor forces, we can potentially utilize the force balance system available in the NASA Ames tunnel. It will provide a measurement of the six net forces at the base of the tower. With the existing shaft-bending moment and torque measurements, and the additional tunnel force balance data, it should be possible to ascertain the remaining rotor forces and compare thrust with that estimated from the aerodynamic rotor loads. However, the tunnel force balance system will only provide time-averaged loads. The extensive system linkage (and turbine structural responses) prevents quantification of dynamic rotor loading. We are working with NASA Ames to determine if the anticipated turbine loads are within the force balance system's measurement range.

Quantify Effects of Tunnel Walls (Table A, Item l)

The impact of the turbine wake interacting with the tunnel wall is one of our ongoing concerns about obtaining useful data in the wind tunnel that is comparable to outdoor unconstrained flow. This issue was reiterated by the Science Panel and obviously needs further serious consideration. We did not attempt to quantify how significant this effect might be, especially on the yawed flow data. The worst case would be that any potential yaw data would be unusable. Our initial plan is to ask the CFD and prescribed-wake modelers to simulate turbine operation in both the enclosed tunnel and in the free-stream, at a few yaw angles. Collaborative partners in this effort are Frank Coton and Roddy Galbraith, at the University of Glasgow, and Earl Duque at NASA Ames. The differences between tunnel and free-stream model performance might provide some insight into the effect. It might then make sense to initially run the same yawed cases in the wind tunnel and compare measured performance with that estimated from the model. If the results are similar, then the guidance provided from the models at yawed flow would then dictate appropriate configurations to run in the wind tunnel. If there are significant differences, it might not be worthwhile to run extensive yawed flow conditions during the test.

Pressure Distribution with Tip Plates (Table A, Item o)

Some industry turbine designs use deployable aerodynamic tip brakes. These are essentially plates that are hinged to the tips and are held in place by electromagnets. They are deployed during over-speed conditions to slow the rotor by drag. It would be useful to obtain data to quantify how the undeployed plate affects the aerodynamic performance of the blade, especially the tip loss. This is needed to better model the performance of such turbines. It is relatively easy to change out the tip piece on the Unsteady Aerodynamics turbine's instrumented blade and to replace it with a tip plate. The existing tip piece was designed with a high-performance, low-noise shape. This was done by providing a smooth transition to the tip by fairing the suction surface into the lower surface at the tip and by smoothing a semicircular section outboard from the leading edge to the quarter chord. We plan to run a couple of cases with both the tip piece and tip block removed, where there is an abrupt truncated airfoil transition at the tip.

Improved Spanwise Resolution Inboard (Table A, Item p)

A participant made a request to try to get better spanwise resolution on the inboard section of the blade, especially at locations less than 30% span. This section is not instrumented for a couple of reasons. First, the blade is attached to the hub by a cylindrical aluminum section at the 10% span location. A carbon-fiber spar is woven around the cylindrical aluminum section. This structural spar is thickest in the root region and is greater in diameter than the airfoil thickness. The structural spar transitions from circular shape to S809 geometry in the region from 15% to 25% span. The true S809 airfoil shape starts at approximately 25% span. Pressure taps were not originally installed in this region of the blade because of both the difficulty and potential structural weakening and unspecified shape. Second, the inboard blade root flow visualization camera is located in the region from 15% to 25% span. This camera is not mounted directly to the blade, but is located approximately 30 mm above the suction surface, and probably significantly affects flow in the region when used.

Different Coning Angles (Table A, Item v)

The coning angle on the existing two-bladed hinged rotor can easily be adjusted to operate at different settings over the range of 18° downwind to 4° upwind (with the turbine in the downwind configuration). To maintain operating stability and minimized blade root loading, the turbine is typically operated at 0° coning upwind, and 3.5° downwind. At this time, we have added one highly coned rotor test where the blades are coned 18°downwind (with the turbine in the upwind configuration). We may consider adding

other intermediate coning angles, and we are conducting simulations to determine if the loads on the structure remain within tolerance at these conditions.

Higher Data Resolution Around Stall and Max Cp (Table A, Items y and z)

Existing Unsteady Aerodynamics Experiment field test data and YawDyn code simulation results were used to correlate turbine operating parameters (wind speed, nacelle yaw angle, blade pitch angle) with blade aerodynamic quantities (local velocity, angle of attack, reduced frequency). These relationships enabled turbine-operating parameters to be discretized in a manner that attacks fundamental flow physics issues, such as stall and maximum Cp, while also addressing questions conventionally related to turbine operating parameters. As a result, the test matrix described in Section 12 shows finer discretization for turbine operating parameters in regimes that are most likely to be encountered in field operation, or in regimes known to generate poorly understood responses. The test matrix exhibits similar data-resolution enhancement strategies, which will enable us to target some of the more basic fluid dynamic interactions that are known, or suspected to be, determinants of turbine performance.

Flapping Rotor Data (Table A, Item bb)

The hinged rotor could be configured to operate with each blade independently flapping. Flap motion restraints would be necessary to prevent the blades from impacting flap stops too hard. NREL designed a flap-motion-restraint system, but has not built or tested it in operation on the turbine. Flapping rotor tests were proposed to support other activities within the NREL wind program. If the turbine had not been damaged, and had operation continued during the current wind season, flapping rotor operation would have been tested in the field. Flap-motion-restraint system development and flapping rotor field-testing activities were stopped because resources were redirected to rebuilding the turbine after the boom failure to be ready for wind tunnel testing. Therefore, we do not plan to conduct flapping rotor tests in the wind tunnel.

Prescribed Disturbance Through Rotor Plane (Table A, Item cc)

Participants proposed introducing some type of prescribed disturbance into the inflow upwind of the turbine and measuring the resulting aerodynamic response through blade surface pressures. The discussion centered around generating a disturbance to simulate transients or perturbations similar to those that propagate through a turbine in the field. The difficulty lies in defining what such a disturbance would look like and then defining a scheme to generate it. We do not have sufficient time available to devise and conduct a prescribed disturbance test during this initial test period. We are, however, planning to work with the NASA Ames staff to determine what they have used in past wind tunnel tests to generate disturbances and what might be available for future tests. We also plan to discuss the issue with NREL meteorological inflow staff. This topic will be further addressed in preparation for future tests.

Test Priority and Planning (Table B, Items jj, kk, ll, mm, nn)

All the issues surrounding these suggestions were incorporated into the revised test matrix. The major difficulty is in trading off minimizing test configuration changes against obtaining high priority data first. For example, obtaining both upwind and downwind turbine operating data are high priority, but it will probably take 2-3 days to change between these two hardware configurations. Many high-priority tests are planned in both the upwind and downwind configuration. If we start out testing the turbine in the downwind configuration, it makes sense to obtain some other downwind data prior to changing to the upwind configuration. It would be impractical to switch back and forth between these two configurations (and other configurations) numerous times to follow highest priority tests because little time would be

spent in actually conducting tests. The resulting test matrix below tries to reach a practical balance in minimizing down time due to configuration changes, yet still follow highest priority requirements.

Leading-Edge Grit Roughness Testing (Table B, Item dd)

The S809 airfoil was designed to be relatively insensitive to leading-edge roughness, mainly for the purpose of maintaining turbine power production in the event of wind energy airfoil-specific field operation problems, such as insect buildup. This effect has been quantified by applying a standard pattern of grit roughness to the S809 model (in 2-D wind tunnel testing). It would also be useful to determine what the effect is on the 3-D airfoil. The standard roughness pattern for wind turbines was based on examination of insect accumulation in the field, and was jointly developed by OSU and Kenetech. The problem is that it is extremely difficult to uniformly apply the roughness to the blade. Typically, double-sided sticky tape is used with a sieve to distribute grit. It is also very difficult and time-consuming to remove the tape after the test. Therefore, because of time restraints, we are not currently planning to conduct roughness measurements during this initial test.

Profiling the Blades (Table B, Item ii)

NREL plans to have both the instrumented and non-instrumented blades profiled prior to installation on the turbine. We will use a coordinate measuring machine (CMM) to precisely determine the three-dimensional blade shape. Emphasis will be on obtaining accurate chordwise profiles close to the instrumented stations and on quantifying exact twist distribution. The CMM measurements will be to an accuracy level of ±0.005 inches (0.0278% of chord).

12.   Revised Test Matrix

Test Plan Description

The major portion of the test plan is set up to provide data to quantify blade pressure distributions under diverse operating conditions. Conditions under which blade pressure distributions will be obtained are listed. Definition of these conditions was based on the considerable input of the Science Panel; however, not all recommended tests could be accommodated. Second-priority tests were deemed to be either not as important or as more difficult than the high-priority tests, and will only be undertaken after first-priority tests are completed. If time runs short, second-priority tests will be eliminated. NREL will attempt to conduct tests from the third-priority matrix only if sufficient time remains after first- and second-priority tests are completed.

The test plan summary (shown in Figures 1 and 2) are matrices that encapsulate test activities during the projected three-week wind tunnel entry. The test plan summary is spread out over the two figures showing 30 planned test sequences (rows), with 19 columns identifying turbine configuration and time estimates for each sequence. Figure 1 shows columns 1–10. Figure 2 repeats columns 1–3, and shows the remaining columns 11–19. Each of the 30 test sequences, corresponding to one line in the summary test matrix, is further documented in the detailed test matrices appearing on the pages following the summary matrix. To facilitate cross-referencing between the summary matrix and the detailed matrices, each of the detailed matrices is marked with the appropriate Run ID# and Test Sequence, as described below.

The column entries provide key information for each test sequence, including turbine configuration, instrumentation, and data acquisition, as well as prioritization and scheduling information. Each of the

column entries is described below in more detail. The entry "As Conf," which appears in several columns of line 1, indicates that the system validation will be performed with that column parameter on the turbine "As Configured" for tests on that day.

Run ID#	Alphanumeric identification character used to tag each test sequence line in the test matrix.
Test Sequence	Text descriptor for each test sequence.
Priority	Indicates whether a test sequence has been assigned primary, secondary, or tertiary priority, as described above.
Upwind/Downwind	Indicates whether the turbine disk is upwind or downwind of tower.
Rigid/Teetered	Indicates whether the hub is rigid, or permits teeter degree of freedom. Teetered configuration will allow approximately 8.5 degrees of teeter.
Cone Angle	Angle between blade axis and plane orthogonal to rotor axis of rotation. Cone angles are positive for both upwind and downwind turbine configurations, corresponding to downstream blade tip displacement.
Yaw Angle	Angle between wind tunnel centerline and wind turbine nacelle longitudinal axis. "Locked" indicates that yaw is locked at each of several yaw angles. "Locked at 0" denotes that yaw is locked at zero yaw. "Locked/Free" indicates that the test is begun with yaw locked, and the yaw lock is then released, allowing free rotation of the nacelle.
Blade Pitch	Angle between plane orthogonal to axis rotation and blade chordline at tip. A single numeral denotes blade pitch in degrees, for the duration of that test sequence. "Fixed" indicates that blade pitch is stepped through a range of discrete pitch angles. "Slow" indicates that the blade is pitched through a range of pitch angles at a low enough rate to closely approximate steady conditions. "Sinusoidal" indicates that blade pitch is varied sinusoidally with time at angular rates high enough to elicit unsteady aerodynamic responses. Entries for Run ID#s X and Y are approximate, and will be determined at the initiation of those test sequences, when RPM (see below) has been chosen.
Parked/Rotating	In parked configuration, the instrumented blade is fixed at 12:00 position. Rotating configuration allows the turbine blades to rotate about hub axis.
RPM	Rotation rate of turbine disk in revolutions per minute. Entries for Run ID#s X and Y are approximate and will be determined at the initiation of those test sequences. Structural resonances, power electronics, and electronic noise interference probably will be the principal factors that constrain RPM.
Blade Pressure	An "X" in this column indicates that blade surface pressure data will be acquired.
Probe Pressure	An "X" in this column indicates that five-hole probes will be mounted on the blades and that inflow speed and direction data will be acquired. Otherwise, the probes and mounts will be removed, yielding a clean blade.
Slow Yaw Sweeps	An "X" in this column indicates that, in addition to collecting data sets at the fixed yaw-error positions specified in the test matrix, data sets will also be obtained during which the turbine yaw drive will be used to slowly sweep the turbine through the full range of yaw angles shown (at approximately 0.5 degree/s).
Tuft Vis.	An "X" in this column indicates that tufts will be mounted on the blade suction surface, and that a video camera will be mounted on the turbine hub to record tuft motions.
Blade Tip	"Baseline" indicates that a conventional blade tip will be mounted that makes span length 5.03 m. "Plate" signifies that a tip-vortex modification device will be added to the baseline blade tip. "Extended" denotes that the baseline blade tip will be removed, and an extended blade tip will be mounted, making blade span 5.53 m. "Visualiz" indicates that a blade tip will be mounted which is identical to the baseline tip in external conformation, but modified internally to accommodate a smoke generating device.
1 Time	Column entry exists only for priority 1 tests, and column total indicates minutes/hours required to complete only priority 1 test sequences.
1, 2 Time	Column entry exists only for priority 1 and 2 test sequences, and column total indicates minutes/hours to complete only priority 1 and 2 test sequences.
1, 2, 3 Time	Column entry exists for priority 1, 2, and 3 tests, and column total indicates minutes/hours to complete all priority 1, 2, and 3 test sequences.
Day	Indicates when during the 15 scheduled test days the test sequence will be carried out.

Overall, the test plan was formulated to address three general areas of concern. First, turbine operation and data acquisition needs to be validated at regular intervals to ensure the accuracy and reliability of the data acquired. Second, turbine operation requires characterization for diverse configurations over the broad range of conditions likely to be encountered under field operation. Finally, detailed measurements are needed to understand and predict the three-dimensional, unsteady, separated flow physics associated with the blades, inflow, and wake. Each of these three areas is prominently represented in the test matrix as described below.

Test Sequence Order, Priority, and Time Required

Test sequences will be carried out in the order shown in the summary test matrices. This order was principally determined by time, difficulty, and the risk associated with changing between upwind/downwind operation, changing between rigid/teetered hub, resetting cone angle, and reconfiguring for high RPM. Column 3 of the summary matrices contains numerals indicating the priority of each test sequence. If testing proceeds on schedule, all first- and second-priority tests will be completed. Schedule slips would require cancellation of some or all of the second-priority tests. Conversely, if testing progresses ahead of schedule, some of the third-priority test sequences could be completed. Which secondary tests can be eliminated, or which tertiary tests can be added, will be determined as testing progresses. Factors that will determine this include, but are not limited to, which test sequences have been completed successfully, the difficulty and risk associated with a configuration change, and the benefit to be gained from the data that would be acquired.

Figure 2 contains estimates of the time required to complete each test sequence. These estimates include the time required to reset test section velocity, yaw angle, and blade pitch, and to recalibrate the pressure measurement system and enter commands into the data acquisition system.

System Validation Testing

At the start of each test day, system operation will be validated using the "System Validation" sequence, designated as Run ID# A in the summary test matrix. In this sequence, the test section velocity will be set to 15.0 m/s and the blade pitch will be set at 28.4 degrees. These conditions were chosen to produce moderate angles of attack and attached flow at all five instrumented span locations. This, in turn, will yield temporally stable instrumentation output signals that should be amenable to system fault detection and diagnosis. Using software routines designed to rapidly display and assess validation data, we will make an evaluation regarding turbine and data acquisition system operation.

Aggregate Turbine Operation Testing

Most test sequences are designed to characterize turbine flow physics and structural dynamics under conditions representative of anticipated field operation. These field test sequences are designated with an "(F)" following the Test Sequence name in column 2 of the test matrix. Generally, these representative field test sequences entail acquisition of blade surface and five-hole probe pressure data, on a 5.03 m blade with conventional tip, at 72 RPM, for a range of test section speeds and yaw angles.

"Downwind Baseline," "Downwind Low Pitch," and "Downwind High Pitch" will examine downwind operation with a teetered hub and moderate rotor coning at three typical field-test blade-pitch settings. "Downwind High Cone" will enable the comparison of downwind baseline operation with moderately exaggerated cone angle. "Blade Tufts" is identical to "Downwind Baseline," except that tufts will be applied to the blade suction surface and a video camera will be mounted on the hub boom to record the tuft visualization. "Upwind Teetered" will acquire data for an upwind, teetered configuration with zero cone angle. "Upwind Baseline," "Upwind Low Pitch," and "Upwind High Pitch" will test the turbine in the upwind configuration with rigid hub and zero cone angle, for three different blade-pitch angles. "Upwind No Probes," "Upwind 2 deg Pitch," and "Upwind 4 deg pitch" will explore the upwind, rigid hub configuration with zero cone angle, for three closely spaced blade-pitch angles. These three test sequences are different from the other "(F)" sequences in that the five-hole probes will be removed to allow an aerodynamically "clean" blade, and only zero yaw conditions will be run. Similarly, "Tip Plate" and "Extended Blade" will also be carried out with five-hole probes removed and only zero-yaw conditions. "Tip Plate" will involve the addition of a tip plate (to simulate the aerodynamic effect of a tip-mounted air brake) to the conventional blade tip, while "Extended Blade" will require adding a 0.5 m

extension to the 5.03 m blade. "Medium RPM" and "High RPM" will characterize turbine operation for the upwind, rigid configuration with zero cone angle, and rotating at approximately 90 and 110 RPM, respectively, to provide high tip-speed ratio data sets.

Specific Flow Physics Testing

The remaining test sequences are designed to explore specific flow physics phenomena in a directed manner. These field test sequences are designated with a "(P)" following the Test Sequence name in column 2 of the test matrix. During these test sequences, turbine configuration or operation may deviate considerably from that mandated for routine operation. In the section below, descriptions of these test sequences are organized to best explain the rationale for performing them, and not in the order in which these sequences are scheduled to occur during wind tunnel testing.

The sequence entitled "Step AOA, Parked" requires that the turbine be configured for upwind operation, with rigid hub, and 0 degree cone angle. The hub will be parked with the instrumented blade at the 12:00 position. Then, the blade will be driven through slow-ramp and stairstep pitch-angle changes to quantify the blade 3-D static AOA response in the absence of rotational influences.

In the sequences designated "Step AOA, Probes" and "Step AOA, No Probes," the turbine will be rigged to run downwind, with a rigid hub, and the cone angle will be set at 3.4 degrees. With the hub rotating, the blade will be driven through a broad pitch-angle range, first with the yaw locked at 0.0 degrees, and then with the yaw locked at 30.0 degrees. Pitch angle will be driven through both slow-ramp and stairstep histories to thoroughly characterize blade 3-D static AOA response. These two sequences differ only in that the five-hole probes and mounting stalks will be used and then removed. These two sequences will provide quantification of 3-D blade static angle of attack response in the presence of rotational influences. In addition, these two sequences will furnish information regarding flow disruption introduced by the five-hole probes and mounting stalks.

The sequences designated "Sin AOA, Parked" require that the turbine be configured for upwind operation, with rigid hub, and zero degree cone angle. Yaw will be locked at zero, and the hub will be parked with the instrumented blade at the 12:00 position. Then, the blade will be driven through sinusoidal pitch angle changes corresponding to various reduced frequencies (K), mean angles of attack (α_m), and oscillation amplitudes (α_ω). K, α_m, and α_ω values were chosen to agree with those for existing 2-D S809 dynamic data previously acquired at OSU, and to correspond with the ranges these parameters could be expected to encounter during routine operation. Together, these data will provide blade 3-D unsteady aerodynamic response in the absence of rotational influences.

During the "Sin AOA, Rotating," the turbine will be rigged in the same way as for the "Sin AOA, Parked" sequence, except the hub will be free to rotate. As the hub rotates, the blade will be driven through sinusoidal pitch angle changes corresponding to various reduced frequencies (K), mean angles of attack (α_m), and oscillation amplitudes (α_ω). As before, K, α_m, and α_ω were chosen to agree with those for existing OSU dynamic data, and to correspond with the ranges these parameters could be expected to encounter during routine operation. The resulting data will provide blade 3-D unsteady aerodynamic response in the presence of rotational influences.

In the sequence entitled "Yaw Releases," the turbine will be configured to run downwind with a rigid hub. Cone angle will be set at 3.4 degrees, and blade pitch angle will be set at 3.0 degrees for the duration of the test sequence. With the hub rotating, the turbine will be yawed to a non-zero yaw angle, and the nacelle will be released at a predetermined hub azimuth angle. Five of these yaw and release repetitions will be completed for each combination of test section velocity and initial yaw angle.

In the "Transition Fixed" sequence, the turbine will be rigged to run upwind with a rigid hub and zero cone angle. Pitch angle will be set at 3.0 degrees for the duration of this sequence. Boundary layer trips will be applied to the surface of the blade to fix the transition location. Along with "Upwind Baseline," which corresponds to the free transition case, these results will comprise a family of data for validating CFD methodologies employing transition models.

In the "Wake Flow Vis Upwind" and "Wake Flow Vis Downwind" sequences, the conventional blade tip will be replaced with an identically shaped hollow tip designed to generate smoke and eject it into the blade tip vortex. Test section velocities, yaw angles, and blade pitch angles have been chosen, to the extent possible, to maintain attached flow and constant spanwise circulation along the blade span. As such, the visualized tip vortex should represent a major portion of the shed vorticity. The visualized flow field will be recorded via two video cameras situated to maximize angular separation between the two viewing axes, thus facilitating subsequent photogrammetric analysis.

For the "Dynamic Inflow" sequence, the turbine will be operating in the upwind, rigid hub configuration, with zero cone angle, and yaw angle locked at zero. The blades will be pitched between the initial and final blade-pitch angles at the maximum rate allowed by the pitch-drive system. Blade pitching will be preceded by a delay to allow the flow to settle prior to the pitch event. Similarly, after pitching, the pitch angle will be held to allow the flow to reach equilibrium. This delay-pitch-hold sequence will be repeated 40 times in each direction for each test section velocity. Dynamic inflow variation will be characterized using the five-hole probes mounted ahead of the blade leading edge at five span stations.

The "Tower Wake Measure" sequence will be carried out with the turbine in downwind configuration, rigid hub, 3.4 degree cone angle, and locked at zero yaw. Three test section velocities will be employed, corresponding to the subcritical, transitional, and supercritical Reynolds number regimes for the circular cross-section tower. The wake will be characterized by yawing the nacelle or rotating the instrumented blade slowly through the tower wake, with the blade pitch angle set to align the five-hole probes as closely as possible with the test section velocity vector.

The "Static Press. Calibration" sequence will provide data to enable comparison of reference pressure measured during the wind tunnel test with field tests. All differential blade pressure measurements are referenced to the pressure inside a box rotating on the hub boom. During typical field operation, a pressure transducer is also used to measure the difference between box pressure and field static pressure. Field static pressure is measured on a pitot-static probe mounted approximately 0.5D upwind of the turbine on a swiveling vane that aligns to the flow. The measured difference is applied as a correction to all blade and five-hole probe pressures. For all wind tunnel test sequences, the difference between hub box reference pressure and local barometric pressure will be measured instead. During data processing, test section static pressure calibrations (referenced to local barometric pressure) will be used to derive the pressure difference between the hub box and test section static pressure. During the "Static Press. Calibration" sequence, the reference tube will be disconnected from the tunnel reference and connected to the upwind vane static as is done in the field. This will provide a data set to compare with "Downwind Baseline" to enable the performance of the vane-mounted static probe to be

Figure 1. NREL- NASA Ames Wind Tunnel Test Plan Summary Matrix, Part 1.

NASA AMES TEST PLAN
TWISTED, TAPERED BLADES; R = 5.03m
TWO BLADE HUB

Run ID #	Test Sequence	Priority	Upwind/ Downwind	Rigid/ Teetered	Cone Angle (deg)	Yaw Angle (deg)	Blade Tip Pitch (deg)	Parked/ Rotating	RPM
A	System Validation	1	As Conf.	As Conf.	As Conf.	Locked at 0	28.4	Rotating	As Conf.
B	Downwind Baseline (F)	1	Downwind	Teetered	3.4	Locked	3.0	Rotating	72.0
C	Downwind Low Pitch (F)	1	Downwind	Teetered	3.4	Locked	0.0	Rotating	72.0
D	Downwind High Pitch (F)	1	Downwind	Teetered	3.4	Locked	6.0	Rotating	72.0
E	Yaw Releases (P)	1	Downwind	Rigid	3.4	Locked / Free	3.0	Rotating	72.0
F	Downwind High Cone (F)	1	Downwind	Rigid	18.0	Locked	3.0	Rotating	72.0
G	Upwind Teetered (F)	1	Upwind	Teetered	0.0	Locked	3.0	Rotating	72.0
H	Upwind Baseline (F)	1	Upwind	Rigid	0.0	Locked	3.0	Rotating	72.0
I	Upwind Low Pitch (F)	1	Upwind	Rigid	0.0	Locked	0.0	Rotating	72.0
J	Upwind High Pitch (F)	1	Upwind	Rigid	0.0	Locked	6.0	Rotating	72.0
K	Step AOA, Probes (P)	2	Upwind	Rigid	3.4	Locked at 0	Fixed & slow	Rotating	72.0
L	Step AOA Parked (P)	2	Upwind	Rigid	0.0	Locked at 0	Fixed & slow	Parked	0.0
M	Transition Fixed (P)	2	Upwind	Rigid	0.0	Locked	3.0	Rotating	72.0
N	Sin AOA, Rotating (P)	2	Upwind	Rigid	0.0	Locked at 0	Sinusoidal	Rotating	72.0
O	Sin AOA, Parked (P)	2	Upwind	Rigid	0.0	Locked at 0	Sinusoidal	Parked	0.0
P	Wake Flow Vis Upwind (P)	2	Upwind	Rigid	0.0	Locked	3.0/12.0	Rotating	72.0
Q	Dynamic Inflow (P)	2	Upwind	Rigid	0.0	Locked at 0	Step	Rotating	72.0
R	Step AOA, No Probes (P)	2	Upwind	Rigid	3.4	Locked at 0	Fixed & slow	Rotating	72.0
S	Upwind, No Probes (F)	2	Upwind	Rigid	0.0	Locked	3.0	Rotating	72.0
T	Upwind, 2 deg Pitch (F)	2	Upwind	Rigid	0.0	Locked at 0	2.0	Rotating	72.0
U	Upwind, 4 deg Pitch (F)	2	Upwind	Rigid	0.0	Locked at 0	4.0	Rotating	72.0
V	Tip Plate (F)	2	Upwind	Rigid	0.0	Locked at 0	3.0	Rotating	72.0
W	Extended Blade (F)	2	Upwind	Rigid	0.0	Locked at 0	3.0	Rotating	72.0
X	Medium RPM (F)	2	Upwind	Rigid	0.0	Locked at 0	3.0	Rotating	~90.0
Y	High RPM (F)	2	Upwind	Rigid	0.0	Locked at 0	3.0	Rotating	~110.0
Z	Upwind Coned (F)	3	Upwind	Rigid	3.4	Locked	3.0	Rotating	72.0
1	Wake Flow Vis Downwind (P)	3	Downwind	Teetered	3.4	Locked	3.0/12.0	Rotating	72.0
2	Blade Tufts (F)	3	Downwind	Teetered	3.4	Locked	3.0	Rotating	72.0
3	Tower Wake Measure (P)	3	Downwind	Rigid	3.4	Locked at 0	64.0	Rotating	Slow
4	Static Press. Cal (P)	3	Downwind	Either	0.0/3.4	Locked	3.0	Rotating	72.0

(F) - Test conditions representative of field operation
(P) - Test conditions designed to explore specific flow physics phenomena

Figure 2. NREL- NASA Ames Wind Tunnel Test Plan Summary Matrix, Part 2.

NASA AMES TEST PLAN
TWISTED, TAPERED BLADES; R = 5.03m
TWO BLADE HUB

Run ID #	Test Sequence	Priority	Blade Tip	Blade Press.	Probe Press.	Slow Yaw Sweeps	Tuft Vis.	1 Time (min)	1,2 Time (min)	1,2,3 Time (min)	Day
A	System Validation	1	As Conf	X	As Conf		As Conf	20	20	20	Each
B	Downwind Baseline (F)	1	Baseline	X	X			432	432	432	1-3
C	Downwind Low Pitch (F)	1	Baseline	X	X			210	210	210	1-3
D	Downwind High Pitch (F)	1	Baseline	X	X			210	210	210	1-3
E	Yaw Releases (P)	1	Baseline	X	X			332	332	332	4
F	Downwind High Cone (F)	1	Baseline	X	X			168	168	168	5
G	Upwind Teetered (F)	1	Baseline	X	X			372	372	372	6
H	Upwind Baseline (F)	1	Baseline	X	X	X		304	304	304	7-8
I	Upwind Low Pitch (F)	1	Baseline	X	X	X		166	166	166	7-8
J	Upwind High Pitch (F)	1	Baseline	X	X	X		166	166	166	7-8
K	Step AOA, Probes (P)	2	Baseline	X	X				131	131	9
L	Step AOA Parked (P)	2	Baseline	X	X				113	113	9
M	Transition Fixed (P)	2	Baseline	X	X	X			95	95	9
N	Sin AOA, Rotating (P)	2	Baseline	X	X				244	244	10
O	Sin AOA, Parked (P)	2	Baseline	X	X				267	267	11
P	Wake Flow Vis Upwind (P)	2	Visualiz	X	X				420	420	12
Q	Dynamic Inflow (P)	2	Baseline	X	X				120	120	13
R	Step AOA, No Probes (P)	2	Baseline	X					131	131	13
S	Upwind, No Probes (F)	2	Baseline	X		X			304	304	14
T	Upwind, 2 deg Pitch (F)	2	Baseline	X					42	42	15
U	Upwind, 4 deg Pitch (F)	2	Baseline	X					42	42	15
V	Tip Plate (F)	2	Plate	X					42	42	15
W	Extended Blade (F)	2	Extended	X					42	42	15
X	Medium RPM (F)	2	Baseline	X	X				118	118	15
Y	High RPM (F)	2	Baseline	X	X				78	78	15
Z	Upwind Coned (F)	3	Baseline	X	X	X				304	
1	Wake Flow Vis Downwind (P)	3	Visualiz	X	X					420	
2	Blade Tufts (F)	3	Baseline	X	X	X	X			472	
3	Tower Wake Measure (P)	3	Baseline	X	X					120	
4	Static Press. Cal (P)	3	Baseline	X	X					66	

(F) - Test conditions representative of field operation
(P) - Test conditions designed to explore specific flow physics phenomena

	Total Minutes:	2360	4549	5931
	Total Hours:	39	76	99

Figure 3. Run ID# A - System validation test sequence. This test will be repeated at various times during the wind tunnel testing to verify proper operation of turbine, instrumentation, and data-acquisition systems. Typical repetition will be at the beginning and end of each day or after changing turbine configuration.

NASA AMES TEST PLAN
TWISTED, TAPERED BLADES; R = 5.03m
TWO BLADE HUB

RUN ID#: A
SEQUENCE: System Validation

Uw (m/s)	Blade Tip Pitch (deg)	AOA at 0.30R (deg)	AOA at 0.95R (deg)	Power (kW)
15.0	28.4	8.2	-6.2	-0.05

System validation procedure:

1) Calibrate system
2) Acquire data set
3) Check data channels for activity, drift, noise, etc.
4) Compare current data with previous system validation data

Figure 4. Run ID# B – Downwind Baseline - Priority 1. Teetered rotor (3.4° cone) operation at constant blade pitch (3°), at selected yaw angles and tunnel velocities from 5-25 m/s. With five-hole leading edge pressure probes installed.

NASA AMES TEST PLAN
TWISTED, TAPERED BLADES; R = 5.03 m
TWO BLADE HUB

RUN ID#: B
SEQUENCE: Downwind Baseline (F)

Uw (m/s)	Yaw Angle																			
	0	5	10	20	30	45	60	75	90	135	180	-135	-90	-75	-60	-45	-30	-20	-10	-5
5.0	X2	X	X	X	X	X	X	X	X	X	X	X	X	X	X	X	X	X	X	X
6.0	X2		X		X												X		X	
7.0	X2	X	X	X	X	X	X	X	X	X	X	X	X	X	X	X	X	X	X	X
8.0	X2		X		X												X		X	
9.0	X2		X		X												X		X	
10.0	X2	X	X	X	X	X	X	X	X	X	X	X	X	X	X	X	X	X	X	X
11.0	X2		X		X												X		X	
12.0	X2		X		X												X		X	
13.0	X2		X		X												X		X	
14.0	X2		X		X												X		X	
15.0	X2	X	X	X	X	X	X	X	X	X	X	X	X	X	X	X	X	X	X	X
16.0	X2		X		X												X		X	
17.0	X2		X		X												X		X	
18.0	X2		X		X												X		X	
19.0	X2		X		X												X		X	
20.0	X2	X	X	X	X	X	X	X	X	X	X	X	X	X	X	X	X	X	X	X
21.0	X2		X		X												X		X	
22.0	X2		X		X												X		X	
23.0	X2		X		X												X		X	
24.0	X2		X		X												X		X	
25.0	X2	X	X	X	X	X	X	X	X	X	X	X	X	X	X	X	X	X	X	X

Each "X" entry indicates that 30 seconds of data (corresponding to 36 revolutions) will be acquired at that combination of wind speed and yaw angle.

The entry "X2" indicates that two data sets, each 30 seconds long (corresponding to 36 revolutions), will be acquired at this combination of wind speed and yaw angle. The first of these data sets will be acquired just after setting wind speed, and prior to acquiring data at any of the other yaw angles for that wind speed. The second data set will be acquired after collecting data at all of the other yaw angles, but before setting the next wind speed. This will be done to provide an indication of system viablity and data repeatability.

Shaded cells correspond to cases that may not be realizable due to excessive teeter impact loads, according to ADAMS predictions.

Figure 5. Run ID# C – Downwind Low Pitch - Priority 1. Teetered rotor (3.4° cone) operation at constant blade pitch (0°), at selected yaw angles and tunnel velocities from 5-25 m/s. With five-hole leading edge pressure probes installed.

NASA AMES TEST PLAN
TWISTED, TAPERED BLADES; R = 5.03 m
TWO BLADE HUB

RUN ID#:   C
SEQUENCE: Downwind Low Pitch (F)

Uw (m/s)	Yaw Angle																			
	0	5	10	20	30	45	60	75	90	135	180	-135	-90	-75	-60	-45	-30	-20	-10	-5
5.0	X		X		X												X		X	
6.0	X		X		X												X		X	
7.0	X		X		X												X		X	
8.0	X		X		X												X		X	
9.0	X		X		X												X		X	
10.0	X		X		X												X		X	
11.0	X		X		X												X		X	
12.0	X		X		X												X		X	
13.0	X		X		X												X		X	
14.0	X		X		X												X		X	
15.0	X		X		X												X		X	
16.0	X		X		X												X		X	
17.0	X		X		X												X		X	
18.0	X		X		X												X		X	
19.0	X		X		X												X		X	
20.0	X		X		X												X		X	
21.0	X		X		X												X		X	
22.0	X		X		X												X		X	
23.0	X		X		X												X		X	
24.0	X		X		X												X		X	
25.0	X		X		X												X		X	

Each "X" entry indicates that 30 seconds of data (corresponding to 36 revolutions) will be acquired at that combination of wind speed and yaw angle.

Shaded cells correspond to cases that may not be realizable due to excessive teeter impact loads, according to ADAMS predictions.

Figure 6. Run ID# D – Downwind High Pitch - Priority 1. Teetered rotor (3.4° cone) operation at constant blade pitch (6°), at selected yaw angles and tunnel velocities from 5-25 m/s. With five-hole leading edge pressure probes installed.

NASA AMES TEST PLAN
TWISTED, TAPERED BLADES; R = 5.03 m
TWO BLADE HUB

RUN ID#: D
SEQUENCE: Downwind High Pitch (F)

Uw (m/s)	Yaw Angle																			
	0	5	10	20	30	45	60	75	90	135	180	-135	-90	-75	-60	-45	-30	-20	-10	-5
5.0	X		X		X												X		X	
6.0	X		X		X												X		X	
7.0	X		X		X												X		X	
8.0	X		X		X												X		X	
9.0	X		X		X												X		X	
10.0	X		X		X												X		X	
11.0	X		X		X												X		X	
12.0	X		X		X												X		X	
13.0	X		X		X												X		X	
14.0	X		X		X												X		X	
15.0	X		X		X												X		X	
16.0	X		X		X												X		X	
17.0	X		X		X												X		X	
18.0	X		X		X												X		X	
19.0	X		X		X												X		X	
20.0	X		X		X												X		X	
21.0	X		X		X												X		X	
22.0	X		X		X												X		X	
23.0	X		X		X												X		X	
24.0	X		X		X												X		X	
25.0	X		X		X												X		X	

Each "X" entry indicates that 30 seconds of data (corresponding to 36 revolutions) will be acquired at that combination of wind speed and yaw angle.

Shaded cells correspond to cases that may not be realizable due to excessive teeter impact loads, according to ADAMS predictions.

Figure 7. Run ID# E - Yaw Releases - Priority 1. Downwind rigid rotor (3.4° cone) operation at constant blade pitch (3°). Yaw releases at selected initial yaw angles and tunnel velocities from 5-20 m/s. With five-hole leading edge pressure probes installed.

NASA AMES TEST PLAN
TWISTED, TAPERED BLADES; R = 5.03 m
TWO BLADE HUB

RUN ID#: E
SEQUENCE: Yaw Releases (P)

Uw (m/s)	Initial Yaw Angle																
	0	5	10	20	30	45	60	90	135	180	-135	-90	-45	-30	-20	-10	-5
5.0			X5	X5		X5		X5				X5	X5		X5	X5	
6.0																	
7.0																	
8.0																	
9.0																	
10.0			X5	X5		X5		X5				X5	X5		X5	X5	
11.0																	
12.0																	
13.0																	
14.0																	
15.0			X5	X5		X5		X5				X5	X5		X5	X5	
16.0																	
17.0																	
18.0																	
19.0																	
20.0																	

Each "X5" entry indicates that five yaw releases will be completed for that combination of wind speed and initial yaw angle. All yaw releases will be initiated at the same blade azimuth, and data acquisition will persist for 30 seconds to permit steady state to be reached.

Figure 8. Run ID# F – Downwind High Cone - Priority 1. Downwind rigid rotor (18° cone) operation at constant blade pitch (3°), at selected yaw angles and tunnel velocities from 5-25 m/s. With five-hole leading edge pressure probes installed.

NASA AMES TEST PLAN
TWISTED, TAPERED BLADES; R = 5.03 m
TWO BLADE HUB

RUN ID#: F
SEQUENCE: Downwind High Cone (F)

Uw (m/s)	Yaw Angle																			
	0	5	10	20	30	45	60	75	90	135	180	-135	-90	-75	-60	-45	-30	-20	-10	-5
5.0	X2	X	X	X														X	X	X
6.0	X2		X																X	
7.0	X2	X	X	X														X	X	X
8.0	X2		X																X	
9.0	X2		X																X	
10.0	X2	X	X	X														X	X	X
11.0	X2		X																X	
12.0	X2		X																X	
13.0	X2		X																X	
14.0	X2		X																X	
15.0	X2	X	X	X														X	X	X
16.0	X2		X																X	
17.0	X2		X																X	
18.0	X2		X																X	
19.0	X2		X																X	
20.0	X2	X	X	X														X	X	X
21.0																				
22.0																				
23.0																				
24.0																				
25.0																				

Each "X" entry indicates that 30 seconds of data (corresponding to 36 revolutions) will be acquired at that combination of wind speed and yaw angle.

The entry "X2" indicates that two data sets, each 30 seconds long (corresponding to 36 revolutions), will be acquired at this combination of wind speed and yaw angle. The first of these data sets will be acquired just after setting wind speed, and prior to acquiring data at any of the other yaw angles for that wind speed. The second data set will be acquired after collecting data at all of the other yaw angles, but before setting the next wind speed. This will be done to provide an indication of system viability and data repeatability.

Shaded cells correspond to cases that may not be realizable due to excessive yaw shaft loads, according to ADAMS predictions.

Figure 9. Run ID# G - Upwind Teetered – Priority 1 upwind teetered (0° cone) operation at constant blade pitch (3°), at selected yaw angles and tunnel velocities from 5-25 m/s. With five-hole leading edge pressure probes installed.

NASA AMES TEST PLAN
TWISTED, TAPERED BLADES; R = 5.03 m
TWO BLADE HUB

RUN ID#: G
SEQUENCE: Upwind Teetered (F)

Uw (m/s)	Yaw Angle																			
	0	5	10	20	30	45	60	75	90	135	180	-135	-90	-75	-60	-45	-30	-20	-10	-5
5.0	X2	X	X	X	X	X	X	X	X	X	X	X	X	X	X	X	X	X	X	X
6.0	X2		X		X												X		X	
7.0	X2	X	X	X	X	X	X	X	X	X	X	X	X	X	X	X	X	X	X	X
8.0	X2		X		X												X		X	
9.0	X2		X		X												X		X	
10.0	X2	X	X	X	X	X	X	X	X	X	X	X	X	X	X	X	X	X	X	X
11.0	X2		X		X												X		X	
12.0	X2		X		X												X		X	
13.0	X2		X		X												X		X	
14.0	X2		X		X												X		X	
15.0	X2	X	X	X	X	X	X	X	X	X	X	X	X	X	X	X	X	X	X	X
16.0	X2		X		X												X		X	
17.0	X2		X		X												X		X	
18.0	X2		X		X												X		X	
19.0	X2		X		X												X		X	
20.0	X2	X	X	X	X	X	X	X	X	X	X	X	X	X	X	X	X	X	X	X
21.0	X2		X		X												X		X	
22.0	X2		X		X												X		X	
23.0	X2		X		X												X		X	
24.0	X2		X		X												X		X	
25.0	X2	X	X	X	X	X	X	X	X	X	X	X	X	X	X	X	X	X	X	X

Each "X" entry indicates that 30 seconds of data (corresponding to 36 revolutions) will be acquired at that combination of wind speed and yaw angle.

The entry "X2" indicates that two data sets, each 30 seconds long (corresponding to 36 revolutions), will be acquired at this combination of wind speed and yaw angle. The first of these data sets will be acquired just after setting wind speed, and prior to acquiring data at any of the other yaw angles for that wind speed. The second data set will be acquired after collecting data at all of the other yaw angles, but before setting the next wind speed. This will be done to provide an indication of system viablity and data repeatability.

Shaded cells correspond to cases that may not be realizable due to excessive teeter impact loads, according to ADAMS predictions.

Figure 10. Run ID# H- Upwind Baseline - Priority 1. Upwind rigid rotor (0° cone) operation at constant blade pitch (3°), at selected yaw angles and tunnel velocities from 5-25 m/s. With five-hole leading edge pressure probes installed.

NASA AMES TEST PLAN
TWISTED, TAPERED BLADES; R = 5.03 m
TWO BLADE HUB

RUN ID#: H
SEQUENCE: Upwind Baseline (F)

Uw (m/s)	Yaw Angle																			
	0	5	10	20	30	45	60	75	90	135	180	-135	-90	-75	-60	-45	-30	-20	-10	-5
5.0	X2	X	X	X	X	X	X	X	X	X	X									
6.0	X2		X		X															
7.0	X2	X	X	X	X	X	X	X	X	X	X									
8.0	X2		X		X															
9.0	X2		X		X															
10.0	X2	X	X	X	X	X	X	X	X	X	X									
11.0	X2		X		X															
12.0	X2		X		X															
13.0	X2		X		X															
14.0	X2		X		X															
15.0	X2	X	X	X	X	X	X	X	X	X	X									
16.0	X2		X		X															
17.0	X2		X		X															
18.0	X2		X		X															
19.0	X2		X		X															
20.0	X2	X	X	X	X	X	X	X	X	X	X									
21.0	X2		X		X															
22.0	X2		X		X															
23.0	X2		X		X															
24.0	X2		X		X															
25.0	X2	X	X	X	X	X	X	X	X	X	X									

Each "X" entry indicates that 30 seconds of data (corresponding to 36 revolutions) will be acquired at that combination of wind speed and yaw angle.

The entry "X2" indicates that two data sets, each 30 seconds long (corresponding to 36 revolutions), will be acquired at this combination of wind speed and yaw angle. The first of these data sets will be acquired just after setting wind speed, and prior to acquiring data at any of the other yaw angles for that wind speed. The second data set will be acquired after collecting data at all of the other yaw angles, but before setting the next wind speed. This will be done to provide an indication of system viablity and data repeatability.

Figure 11. Run ID# I – Upwind Low Pitch - Priority 1. Upwind rigid rotor (0° cone) operation at constant blade pitch (0°), at selected yaw angles and tunnel velocities from 5-25 m/s. With five-hole leading edge pressure probes installed.

NASA AMES TEST PLAN
TWISTED, TAPERED BLADES; R = 5.03 m
TWO BLADE HUB

RUN ID#: I
SEQUENCE: Upwind Low Pitch (F)

Uw (m/s)	Yaw Angle																			
	0	5	10	20	30	45	60	75	90	135	180	-135	-90	-75	-60	-45	-30	-20	-10	-5
5.0	X		X		X															
6.0	X		X		X															
7.0	X		X		X															
8.0	X		X		X															
9.0	X		X		X															
10.0	X		X		X															
11.0	X		X		X															
12.0	X		X		X															
13.0	X		X		X															
14.0	X		X		X															
15.0	X		X		X															
16.0	X		X		X															
17.0	X		X		X															
18.0	X		X		X															
19.0	X		X		X															
20.0	X		X		X															
21.0	X		X		X															
22.0	X		X		X															
23.0	X		X		X															
24.0	X		X		X															
25.0	X		X		X															

Each "X" entry indicates that 30 seconds of data (corresponding to 36 revolutions) will be acquired at that combination of wind speed and yaw angle.

Figure 12. Run ID# J – Upwind High Pitch - Priority 1. Upwind rigid rotor (0° cone) operation at constant blade pitch (6°), at selected yaw angles and tunnel velocities from 5-25 m/s. With five-hole leading edge pressure probes installed.

NASA AMES TEST PLAN
TWISTED, TAPERED BLADES; R = 5.03 m
TWO BLADE HUB

RUN ID#: J
SEQUENCE: Upwind High Pitch (F)

Uw (m/s)	Yaw Angle																			
	0	5	10	20	30	45	60	75	90	135	180	-135	-90	-75	-60	-45	-30	-20	-10	-5
5.0	X		X		X															
6.0	X		X		X															
7.0	X		X		X															
8.0	X		X		X															
9.0	X		X		X															
10.0	X		X		X															
11.0	X		X		X															
12.0	X		X		X															
13.0	X		X		X															
14.0	X		X		X															
15.0	X		X		X															
16.0	X		X		X															
17.0	X		X		X															
18.0	X		X		X															
19.0	X		X		X															
20.0	X		X		X															
21.0	X		X		X															
22.0	X		X		X															
23.0	X		X		X															
24.0	X		X		X															
25.0	X		X		X															

Each "X" entry indicates that 30 seconds of data (corresponding to 36 revolutions) will be acquired at that combination of wind speed and yaw angle.

Figure 13. Run ID# K – Varying AOA With Probes - Priority 2. Upwind rigid rotor (3.4° cone) operation at zero yaw, with ramped and stepped blade pitch variations, at selected tunnel velocities from 6-20 m/s. With five-hole leading edge pressure probes removed.

NASA AMES TEST PLAN
TWISTED, TAPERED BLADES; R = 5.03m
TWO BLADE HUB

RUN ID#: K
SEQUENCE: Step AOA, Probes (P)

Uw (m/s)	Yaw (deg)	Initial Tip Pitch (deg)	0.30R AOA at Initial Pitch (deg)	0.95R AOA at Initial Pitch (deg)	Final Tip Pitch (deg)	0.30R AOA at Final Pitch (deg)	0.95R AOA at Final Pitch (deg)	Pitch Rate (deg/s)	Pitching
6.0	0.0	32.0	-16.0	-20.1	-15.0	20.0	20.1	0.180	continuous ramp
6.0	0.0	-15.0	20.0	20.1	32.0	-16.0	-20.1	-0.180	continuous ramp
6.0	0.0	32.0	-16.1	-20.1	-15.0	20.0	20.1	step up then step down	5.0 deg step, 3.0 s delay, 5.0 s data
6.0	30.0	32.0	-16.1	-20.1	-15.0	20.0	20.1	step up then step down	5.0 deg step, 3.0 s delay, 5.0 s data
10.0	0.0	37.0	-9.0	-2.0	-15.0	36.0	26.8	0.180	continuous ramp
10.0	0.0	-15.0	36.0	26.8	37.0	-9.0	-2.0	-0.180	continuous ramp
10.0	0.0	37.0	-9.0	-2.0	-15.0	36.0	26.8	step up then step down	5.0 deg step, 3.0 s delay, 5.0 s data
10.0	30.0	37.0	-9.0	-2.0	-15.0	36.0	26.8	step up then step down	5.0 deg step, 3.0 s delay, 5.0 s data
15.0	0.0	40.0	-1.6	-16.3	-15.0	48.2	34.0	0.180	continuous ramp
15.0	0.0	-15.0	48.2	34.0	40.0	-1.6	-16.3	-0.180	continuous ramp
15.0	0.0	40.0	-1.6	-16.3	-15.0	48.2	34.0	step up then step down	5.0 deg step, 3.0 s delay, 5.0 s data
15.0	30.0	40.0	-1.6	-16.3	-15.0	48.2	34.0	step up then step down	5.0 deg step, 3.0 s delay, 5.0 s data
20.0	0.0	44.0	1.3	-14.4	28.0	14.7	-0.8	0.180	continuous ramp
20.0	0.0	28.0	14.7	-0.8	44.0	1.3	-14.4	-0.180	continuous ramp
20.0	0.0	44.0	1.3	-14.4	28.0	14.7	-0.8	step up then step down	5.0 deg step, 3.0 s delay, 5.0 s data
20.0	30.0	44.0	1.3	-14.4	28.0	14.7	-0.8	step up then step down	5.0 deg step, 3.0 s delay, 5.0 s data

The column titled "Pitching" describes how the blade will be pitched to acquire static data. The entry "continuous ramp" indicates that pitching will be carried out at 0.180 degrees per second through the range indicated in the columns to the left. The entry "5.0 deg step, 3.0 s delay, 5.0 s data" indicates that, through the range indicated in the columns to the left, the blade will be stepped in pitch to the each angle, 3.0 seconds will be allowed to elapse to stabilize the flow, and then 5.0 seconds of data will be acquired.

Figure 14. Run ID #L - Varying AOA Parked - Priority 2. Parked rotor with ramped and stepped blade pitch variations, at selected tunnel velocities from 20-40 m/s. With five-hole leading edge pressure probes installed.

NASA AMES TEST PLAN
TWISTED, TAPERED BLADES; R = 5.03m
TWO BLADE HUB

RUN ID#: L
SEQUENCE: Step AOA Parked (P)

Uw	Initial Tip Pitch (deg)	0.30R AOA at Initial Pitch (deg)	0.95R AOA at Initial Pitch (deg)	Final Tip Pitch (deg)	0.30R AOA at Final Pitch (deg)	0.95R AOA at Final Pitch (deg)	Pitch Rate (deg/s)	Pitching
20.0	90.0	-16.1	-0.3	-15.0	88.9	104.7	0.180	continuous ramp
20.0	-15.0	88.9	104.7	90.0	-16.1	-0.3	-0.180	continuous ramp
20.0	90.0	-16.1	-0.3	-15.0	88.9	104.7	step up then step down	5.0 deg step, 3.0 s delay, 5.0 s data
30.0	90.0	-16.1	-0.3	-15.0	88.9	104.7	0.180	continuous ramp
30.0	-15.0	88.9	104.7	90.0	-16.1	-0.3	-0.180	continuous ramp
30.0	90.0	-16.1	-0.3	-15.0	88.9	104.7	step up then step down	5.0 deg step, 3.0 s delay, 5.0 s data
40.0	90.0	-16.1	-0.3	-15.0	88.9	104.7	0.180	continuous ramp
40.0	-15.0	88.9	104.7	90.0	-16.1	-0.3	-0.180	continuous ramp
40.0	90.0	-16.1	-0.3	-15.0	88.9	104.7	step up then step down	5.0 deg step, 3.0 s delay, 5.0 s data

The column titled "Pitching" describes how the blade will be pitched to acquire static data. The entry "continuous ramp" indicates that pitching will be carried out at 0.180 degrees per second through the range indicated in the columns to the left. The entry "5.0 deg step, 3.0 s delay, 5.0 s data" indicates that, through the range indicated in the columns to the left, the blade will be stepped in pitch to the each angle, 3.0 seconds will be allowed to elapse to stabilize the flow, and then 5.0 seconds of data will be acquired.

Figure 15. Run ID# M – Transition Fixed - Priority 2. Upwind rigid rotor (0° cone) operation at constant blade pitch (3°), at selected yaw angles, and velocities from 5-15 m/s. With five-hole leading edge pressure probes installed. With NASA-recommended trip-strip installed.

NASA AMES TEST PLAN
TWISTED, TAPERED BLADES; R = 5.03 m
TWO BLADE HUB

RUN ID#: M
SEQUENCE: Transition Fixed (P)

Uw	Yaw Angle																			
(m/s)	0	5	10	20	30	45	60	75	90	135	180	-135	-90	-75	-60	-45	-30	-20	-10	-5
5.0	X		X		X				X											
6.0	X		X		X															
7.0	X		X		X				X											
8.0	X		X		X															
9.0	X		X		X															
10.0	X		X		X				X											
11.0	X		X		X															
12.0	X		X		X															
13.0	X		X		X															
14.0	X		X		X															
15.0	X		X		X				X											
16.0																				
17.0																				
18.0																				
19.0																				
20.0																				
21.0																				
22.0																				
23.0																				
24.0																				
25.0																				

Each "X" entry indicates that 30 seconds of data (corresponding to 36 revolutions) will be acquired at that combination of wind speed and yaw angle.

The entry "X2" indicates that two data sets, each 30 seconds long (corresponding to 36 revolutions), will be acquired at this combination of wind speed and yaw angle. The first of these data sets will be acquired just after setting wind speed, and prior to acquiring data at any of the other yaw angles for that wind speed. The second data set will be acquired after collecting data at all of the other yaw angles, but before setting the next wind speed. This will be done to provide an indication of system viability and data repeatability.

Figure 16. Run ID# N - Sinusoidal AOA - Priority 2. Upwind rigid rotor (0° cone) operation with sinusoidally varying blade pitch, at constant yaw (0°) and constant tunnel velocity (15 m/s). With five-hole leading edge pressure probes installed.

NASA AMES TEST PLAN
TWISTED, TAPERED BLADES; R = 5.03m
TWO BLADE HUB

RUN ID#: N
SEQUENCE: Sin AOA, Rotating (P)

WIND SPEED = 15.0 m/s AND YAW = 0.0 deg THROUGHOUT THIS SERIES DATA WILL BE ACQUIRED FOR 40 SUCCESSIVE BLADE PITCH CYCLES

NOTE: Rows for each span station are divided into two sets, and are separated by a heavy horizontal line. The first set of rows consists of combinations of K, mean AOA, and omega AOA that the blades would likely experience during routine operation. The second set of rows contains combinations of K, mean AOA, and omega AOA corresponding to those tested at Ohio State University using an S809 airfoil section under two-dimensional conditions.

Span Station	Chord (m)	Total Local U (m/s)	Local Re	Local K	Mean AOA (deg)	Omega AOA (deg)	Freq (Hz)	Tip Min Pitch (deg)	Tip Max Pitch (deg)	Power Caution
1	0.711	18.78	862,352	0.1000	-4.00	4.00	0.84161	38.20	46.82	X
1	0.711	19.01	872,914	0.1000	10.00	4.00	0.85434	21.02	31.02	
1	0.711	18.91	868,322	0.1000	24.00	5.00	0.84957	4.25	14.93	X
1	0.711	19.00	872,455	0.1000	38.00	7.00	0.84957	-12.27	2.69	
1	0.711	18.73	860,056	0.1250	-5.00	1.00	1.04246	42.73	44.69	X
1	0.711	18.86	866,026	0.1250	11.00	2.00	1.06363	22.42	27.24	
1	0.711	18.88	866,944	0.1250	27.00	5.00	1.06363	1.08	11.88	
1	0.711	18.71	859,138	0.1500	-7.00	4.00	1.25159	41.55	49.81	X
1	0.711	18.77	861,893	0.1500	7.00	4.00	1.26369	25.10	34.42	
1	0.711	18.81	863,730	0.1500	21.00	5.00	1.2621	6.99	18.49	X
1	0.711	18.90	867,863	0.1500	35.00	5.00	1.2621	-7.04	3.80	
1	0.711	18.73	860,056	0.1750	-5.00	3.00	1.47362	40.54	46.88	X
1	0.711	18.89	867,403	0.1750	11.00	3.00	1.48078	21.34	28.32	
1	0.711	18.91	868,322	0.1750	28.00	3.00	1.47441	2.14	8.72	
1	0.711	18.74	860,516	0.2000	-4.00	2.00	1.67558	40.52	44.88	X
1	0.711	19.00	872,455	0.2000	15.00	2.00	1.69436	17.34	21.96	
1	0.711	18.83	864,648	0.2000	10.00	4.00	1.68497	21.43	30.61	
1	0.711	18.74	860,516	0.2000	-4.00	4.00	1.67558	38.36	47.04	X
1	0.711	18.66	856,842	0.2000	5.00	3.00	1.67829	29.05	35.87	
1	0.711	19.00	872,455	0.2000	15.00	3.00	1.69436	16.16	23.14	
1	0.711	18.75	860,975	0.2125	-3.00	1.00	1.78683	40.54	42.76	X
1	0.711	18.76	861,434	0.2125	3.00	1.00	1.78683	33.73	35.71	
1	0.711	18.75	860,975	0.2125	-3.00	2.00	1.78683	39.47	43.83	X
1	0.711	18.75	860,975	0.2125	3.00	2.00	1.78683	32.54	36.90	

Figure 16 (continued). Run ID# N - Sinusoidal AOA - Priority 2. Upwind rigid rotor (0° cone) operation with sinusoidally varying blade pitch, at constant yaw (0°) and constant tunnel velocity (15 m/s). With five-hole leading edge pressure probes installed.

Span Station	Chord (m)	Total Local U (m/s)	Local Re	Local K	Mean AOA (deg)	Omega AOA (deg)	Freq (Hz)	Tip Min Pitch (deg)	Tip Max Pitch (deg)	Power Caution
1	0.711	18.86	866,026	0.025	8.00	5.50	0.213	21.68	35.30	
1	0.711	18.86	866,026	0.025	14.00	5.50	0.213	14.52	27.98	
1	0.711	18.96	870,618	0.025	20.00	5.50	0.213	7.92	20.22	
1	0.711	18.90	867,863	0.025	8.00	10.00	0.213	15.99	40.41	
1	0.711	18.80	863,271	0.025	14.00	10.00	0.213	9.46	33.50	
1	0.711	18.86	866,026	0.025	20.00	10.00	0.213	3.48	25.78	X
1	0.711	18.85	865,567	0.050	8.00	5.50	0.415	21.71	35.27	
1	0.711	18.86	866,026	0.050	14.00	5.50	0.415	14.16	27.82	
1	0.711	18.97	871,077	0.050	20.00	5.50	0.420	7.83	20.19	X
1	0.711	18.87	866,485	0.050	8.00	10.00	0.415	15.97	40.39	
1	0.711	18.75	860,975	0.050	14.00	10.00	0.412	9.39	33.53	X
1	0.711	18.84	865,108	0.050	20.00	10.00	0.415	3.43	25.93	X
1	0.711	18.88	866,944	0.075	8.00	5.50	0.640	21.62	35.36	
1	0.711	18.89	867,403	0.075	14.00	5.50	0.640	14.26	27.88	X
1	0.711	18.99	871,995	0.075	20.00	5.50	0.640	7.75	20.11	X
1	0.711	18.93	869,240	0.075	8.00	10.00	0.640	15.97	40.39	X
1	0.711	18.85	865,567	0.075	14.00	10.00	0.640	9.19	33.29	X
1	0.711	18.93	869,240	0.075	20.00	10.00	0.640	3.07	25.55	X
1	0.711	18.83	864,648	0.100	8.00	5.50	0.850	21.58	35.24	
1	0.711	18.82	864,189	0.100	14.00	5.50	0.850	14.15	27.49	X
1	0.711	18.80	863,271	0.100	20.00	5.50	0.850	7.71	20.23	X
1	0.711	18.80	863,271	0.100	14.00	10.00	0.850	8.90	33.18	X
1	0.711	18.80	863,271	0.100	20.00	10.00	0.850	2.71	25.53	X
2	0.627	23.19	939,048	0.0625	-7.00	2.00	0.74644	39.89	44.15	X
2	0.627	23.19	939,048	0.0625	3.00	2.00	0.74309	28.72	33.22	
2	0.627	23.42	948,362	0.0625	12.00	4.00	0.73195	15.64	24.82	
2	0.627	23.21	939,858	0.0750	-5.00	2.00	0.87631	37.83	42.09	
2	0.627	23.47	950,386	0.0750	9.00	2.00	0.90145	21.52	26.02	
2	0.627	23.50	951,601	0.0750	23.00	5.00	0.89318	3.20	13.78	
2	0.627	23.30	943,502	0.0750	37.00	6.00	0.87742	-12.01	0.43	
2	0.627	23.21	939,858	0.1000	-4.00	2.00	1.17313	36.63	40.89	
2	0.627	23.47	950,386	0.1000	9.00	2.00	1.1935	21.46	26.08	
2	0.627	23.49	951,196	0.1000	23.00	2.00	1.19494	6.31	10.67	
2	0.627	23.35	945,527	0.1000	37.00	4.00	1.1865	-9.98	-1.60	
2	0.627	23.31	943,907	0.1000	7.00	6.00	1.1865	19.48	33.00	
2	0.627	23.08	934,594	0.1250	-2.00	1.00	1.47537	35.69	37.73	
2	0.627	23.30	943,502	0.1250	5.00	1.00	1.47775	27.65	29.77	
2	0.627	23.34	945,122	0.1250	13.00	1.00	1.4838	18.19	20.31	

Figure 16 (continued). Run ID# N - Sinusoidal AOA - Priority 2. Upwind rigid rotor (0° cone) operation with sinusoidally varying blade pitch, at constant yaw (0°) and constant tunnel velocity (15 m/s). With five-hole leading edge pressure probes installed.

Span Station	Chord (m)	Total Local U (m/s)	Local Re	Local K	Mean AOA (deg)	Omega AOA (deg)	Freq (Hz)	Tip Min Pitch (deg)	Tip Max Pitch (deg)	Power Caution
2	0.627	23.31	943,907	0.025	8.00	5.50	0.294	18.60	31.36	
2	0.627	23.36	945,932	0.025	14.00	5.50	0.307	12.12	24.36	
2	0.627	23.39	947,147	0.025	20.00	5.50	0.307	5.95	17.53	
2	0.627	23.25	941,478	0.025	8.00	10.00	0.294	13.50	36.46	
2	0.627	23.34	945,122	0.025	14.00	10.00	0.296	7.38	29.92	X
2	0.627	23.17	938,238	0.025	20.00	10.00	0.294	1.47	22.71	X
2	0.627	23.35	945,527	0.050	8.00	5.50	0.584	18.60	31.36	
2	0.627	23.34	945,122	0.050	14.00	5.50	0.584	11.95	24.53	X
2	0.627	23.39	947,147	0.050	20.00	5.50	0.584	5.77	17.59	X
2	0.627	23.33	944,717	0.050	8.00	10.00	0.584	13.45	36.69	X
2	0.627	23.24	941,073	0.050	14.00	10.00	0.584	7.01	29.63	X
2	0.627	23.30	943,502	0.050	20.00	10.00	0.584	1.19	22.45	X
2	0.627	23.32	944,312	0.075	8.00	5.50	0.899	18.60	31.36	
2	0.627	23.34	945,122	0.075	14.00	5.50	0.899	11.65	24.33	X
2	0.627	23.37	946,337	0.075	20.00	5.50	0.899	5.55	17.43	X
2	0.627	23.33	944,717	0.075	8.00	10.00	0.893	13.34	36.30	X
2	0.627	23.34	945,122	0.075	14.00	10.00	0.883	6.86	29.62	X
2	0.627	23.40	947,552	0.075	20.00	10.00	0.883	0.81	22.53	X
2	0.627	23.30	943,502	0.100	8.00	5.50	1.194	18.67	31.29	
2	0.627	23.27	942,288	0.100	14.00	5.50	1.187	11.85	24.19	X
2	0.627	23.29	943,098	0.100	20.00	5.50	1.194	5.61	17.43	X
3	0.542	28.17	986,065	0.0375	-7.00	1.00	0.60909	36.00	38.04	
3	0.542	28.10	983,615	0.0375	-1.00	1.00	0.60909	29.19	31.31	
3	0.542	28.22	987,816	0.0375	5.00	2.00	0.62325	21.07	25.79	
3	0.542	28.12	984,315	0.0375	7.00	10.00	0.60909	9.94	32.54	X
3	0.542	28.11	983,965	0.0375	15.00	10.00	0.60909	1.87	23.33	X
3	0.542	28.08	982,915	0.0375	23.00	10.00	0.60909	-6.05	14.47	
3	0.542	27.98	979,415	0.0500	-5.00	1.00	0.82856	33.77	35.75	
3	0.542	28.28	989,916	0.0500	8.00	2.00	0.84113	17.49	22.15	
3	0.542	28.49	997,267	0.0500	21.00	4.00	0.84113	1.92	10.28	
3	0.542	28.63	1,002,167	0.0500	34.00	5.00	0.84113	-12.04	-1.84	
3	0.542	28.78	1,007,418	0.0500	11.00	11.00	0.84113	4.58	29.04	X
3	0.542	28.06	982,215	0.0625	-4.00	1.00	1.03148	32.74	34.72	
3	0.542	28.30	990,616	0.0625	8.00	2.00	1.02671	17.49	22.15	
3	0.542	28.33	991,666	0.0625	20.00	2.00	1.05504	4.95	9.31	
3	0.542	28.41	994,466	0.0625	32.00	2.00	1.05504	-7.02	-2.80	
3	0.542	28.54	999,017	0.0625	10.00	8.00	1.04437	8.75	26.61	X
3	0.542	28.34	992,016	0.0625	26.00	7.00	1.05504	-6.26	8.32	
3	0.542	28.18	986,415	0.0750	-3.00	1.00	1.24921	31.51	33.47	
3	0.542	28.43	995,166	0.0750	12.00	1.00	1.26178	14.29	16.47	
3	0.542	28.32	991,316	0.0750	28.00	2.00	1.26178	-2.74	1.24	
3	0.542	28.23	988,166	0.0750	10.00	3.00	1.24284	14.44	21.06	X
3	0.542	28.30	990,616	0.0750	23.00	3.00	1.26178	1.03	7.39	

Figure 16 (continued). Run ID# N - Sinusoidal AOA - Priority 2. Upwind rigid rotor (0° cone) operation with sinusoidally varying blade pitch, at constant yaw (0°) and constant tunnel velocity (15 m/s). With five-hole leading edge pressure probes installed.

Span Station	Chord (m)	Total Local U (m/s)	Local Re	Local K	Mean AOA (deg)	Omega AOA (deg)	Freq (Hz)	Tip Min Pitch (deg)	Tip Max Pitch (deg)	Power Caution
3	0.542	28.24	988,516	0.025	8.00	5.50	0.419	13.75	26.21	
3	0.542	28.46	996,217	0.025	14.00	5.50	0.428	7.52	19.28	
3	0.542	28.33	991,666	0.025	20.00	5.50	0.428	1.53	12.89	
3	0.542	28.40	994,116	0.025	8.00	10.00	0.419	8.99	31.27	X
3	0.542	28.25	988,866	0.025	14.00	10.00	0.419	2.96	24.44	X
3	0.542	28.21	987,466	0.025	20.00	10.00	0.419	-2.80	17.72	X
3	0.542	28.35	992,366	0.050	8.00	5.50	0.842	13.65	25.99	X
3	0.542	28.23	988,166	0.050	14.00	5.50	0.842	7.39	19.37	X
3	0.542	28.38	993,416	0.050	20.00	5.50	0.842	1.45	12.81	
3	0.542	28.29	990,266	0.050	8.00	10.00	0.842	8.86	31.10	X
3	0.542	28.44	995,517	0.050	14.00	10.00	0.842	2.81	24.37	X
3	0.542	28.41	994,466	0.050	20.00	10.00	0.842	-3.32	17.74	X
3	0.542	28.27	989,566	0.075	8.00	5.50	1.243	13.73	25.91	X
3	0.542	28.14	985,015	0.075	14.00	5.50	1.249	7.33	19.15	X
3	0.542	28.33	991,666	0.075	20.00	5.50	1.262	1.40	12.86	
3	0.542	28.47	996,567	0.100	8.00	5.50	1.685	13.83	25.81	X
3	0.542	28.49	997,267	0.100	14.00	5.50	1.684	7.25	19.07	X
3	0.542	28.58	1,000,417	0.100	20.00	5.50	1.679	1.27	13.09	X
4	0.457	33.68	994,049	0.0250	-5.00	1.00	0.57853	28.94	31.06	
4	0.457	33.86	999,362	0.0250	5.00	1.00	0.61211	17.32	19.44	
4	0.457	33.70	994,639	0.0250	15.00	3.00	0.5841	4.81	11.17	
4	0.457	33.95	1,002,018	0.0250	16.00	11.00	0.57853	-4.23	18.53	X
4	0.457	33.68	994,049	0.0375	-5.00	1.00	0.86771	28.94	31.06	
4	0.457	34.05	1,004,970	0.0375	10.00	2.00	0.86771	10.86	15.08	
4	0.457	33.87	999,657	0.0375	26.00	2.00	0.86771	-5.11	-1.13	
4	0.457	33.63	992,573	0.0375	15.00	10.00	0.86771	-2.50	18.48	X
4	0.457	33.79	997,296	0.0500	-4.00	1.00	1.1744	27.89	30.01	
4	0.457	34.09	1,006,150	0.0500	13.00	1.00	1.1744	8.91	10.87	
4	0.457	34.08	1,005,855	0.0500	30.00	2.00	1.1744	-9.18	-5.20	
4	0.457	33.98	1,002,904	0.0500	4.00	2.00	1.1744	17.31	21.67	
4	0.457	34.04	1,004,674	0.0500	12.00	2.00	1.1744	8.92	13.12	
4	0.457	33.96	1,002,313	0.0500	25.00	2.00	1.1744	-4.25	0.11	
4	0.457	34.12	1,007,036	0.0500	10.00	3.00	1.1744	9.79	16.15	X
4	0.457	34.07	1,005,560	0.0500	27.00	3.00	1.1744	-7.35	-0.99	

Figure 16 (continued). Run ID# N - Sinusoidal AOA - Priority 2. Upwind rigid rotor (0° cone) operation with sinusoidally varying blade pitch, at constant yaw (0°) and constant tunnel velocity (15 m/s). With five-hole leading edge pressure probes installed.

Span Station	Chord (m)	Total Local U (m/s)	Local Re	Local K	Mean AOA (deg)	Omega AOA (deg)	Freq (Hz)	Tip Min Pitch (deg)	Tip Max Pitch (deg)	Power Caution
4	0.457	34.05	1,004,970	0.025	8.00	5.50	0.584	9.25	21.17	X
4	0.457	34.08	1,005,855	0.025	14.00	5.50	0.584	3.46	14.70	
4	0.457	33.62	992,278	0.025	20.00	5.50	0.600	-2.73	8.63	
4	0.457	33.78	997,001	0.025	8.00	10.00	0.584	4.83	26.41	X
4	0.457	33.92	1,001,133	0.025	14.00	10.00	0.584	-1.21	19.61	X
4	0.457	33.83	998,476	0.025	20.00	10.00	0.567	-7.31	13.21	
4	0.457	33.98	1,002,904	0.050	8.00	5.50	1.175	9.05	21.21	X
4	0.457	33.96	1,002,313	0.050	14.00	5.50	1.175	3.13	14.79	X
4	0.457	34.05	1,004,970	0.050	20.00	5.50	1.175	-2.84	8.74	
4	0.457	33.82	998,181	0.075	14.00	5.50	1.752	3.07	14.73	X
4	0.457	33.86	999,362	0.075	20.00	5.50	1.752	-2.97	8.49	
5	0.381	38.98	959,150	0.0125	-4.00	1.00	0.4329	24.31	26.99	
5	0.381	39.22	965,055	0.0125	5.00	1.00	0.4329	13.59	15.71	
5	0.381	39.10	962,102	0.0125	15.00	4.00	0.4329	0.12	8.36	
5	0.381	39.15	963,333	0.0125	6.00	7.00	0.4329	5.97	21.55	X
5	0.381	39.07	961,364	0.0125	13.00	8.00	0.4329	-1.93	14.69	
5	0.381	39.15	963,333	0.0125	22.00	11.00	0.4329	-14.41	8.41	
5	0.381	39.23	965,301	0.0125	16.00	15.00	0.4329	-12.34	19.26	X
5	0.381	38.94	958,165	0.0250	-4.00	1.00	0.82601	24.41	26.89	
5	0.381	39.18	964,071	0.0250	16.00	2.00	0.82601	1.04	5.22	
5	0.381	39.90	981,787	0.0250	10.00	8.00	0.82601	0.71	17.99	X
5	0.381	39.57	973,667	0.0250	22.00	8.00	0.82601	-11.49	5.49	
5	0.381	39.19	964,317	0.0375	-3.00	1.00	1.22517	22.89	25.37	
5	0.381	39.39	969,238	0.0375	9.00	1.00	1.25876	9.19	11.31	
5	0.381	39.47	971,207	0.0375	9.00	2.00	1.25876	8.12	12.38	
5	0.381	39.17	963,825	0.0375	21.00	2.00	1.22517	-4.03	0.33	
5	0.381	39.49	971,699	0.025	8.00	5.50	0.826	5.38	17.48	X
5	0.381	39.40	969,484	0.025	14.00	5.50	0.826	-0.55	10.97	
5	0.381	39.55	973,175	0.025	20.00	5.50	0.826	-6.75	4.77	
5	0.381	39.83	980,065	0.025	8.00	10.00	0.826	0.70	22.72	X
5	0.381	39.72	977,358	0.025	14.00	10.00	0.826	-5.41	15.83	X
5	0.381	39.57	973,667	0.025	20.00	10.00	0.826	-11.56	9.42	
5	0.381	39.44	970,469	0.050	14.00	5.50	1.670	-1.08	11.00	
5	0.381	39.46	970,961	0.050	20.00	5.50	1.627	-6.91	4.77	

Figure 17. Run ID#O- Sinusoidal AOA Parked - Priority 2. Parked rotor with sinusoidally varying blade pitch, at selected tunnel velocities from 20-40 m/s. With five-hole leading edge pressure probes installed.

NASA AMES TEST PLAN
TWISTED, TAPERED BLADES; R = 5.03m
TWO BLADE HUB

RUN ID#: O
SEQUENCE: Sin AOA, Parked (P)

YAW = 0.0 deg THROUGHOUT THIS SERIES
DATA WILL BE ACQUIRED FOR 40 SUCCESSIVE BLADE PITCH CYCLES

NOTE: Rows for each span station are divided into two sets, and are separated by a heavy horizontal line.
The first set of rows consists of combinations of K, mean AOA, and omega AOA that the blades would likely experience during routine operation. The second set of rows contains combinations of K, mean AOA, and omega AOA corresponding to those tested at Ohio State University using an S809 airfoil section under two-dimensional conditions.

Span Station	Chord (m)	Uw (m/s)	Local Re	Local K	Mean AOA (deg)	Omega AOA (deg)	Blade Pitch Freq (Hz)	Tip Min Pitch (deg)	Tip Max Pitch (deg)
1	0.711	18.90	867,863	0.1000	-4.00	4.00	0.846	73.88	81.88
1	0.711	18.90	867,863	0.1000	10.00	4.00	0.846	59.88	67.88
1	0.711	18.90	867,863	0.1000	24.00	5.00	0.846	44.88	54.88
1	0.711	18.90	867,863	0.1000	38.00	7.00	0.846	28.88	42.88
1	0.711	18.90	867,863	0.1000	52.00	7.00	0.846	14.88	28.88
1	0.711	18.90	867,863	0.1250	11.00	2.00	1.058	60.88	64.88
1	0.711	18.90	867,863	0.1250	27.00	5.00	1.058	41.88	51.88
1	0.711	18.90	867,863	0.1250	44.00	7.00	1.058	22.88	36.88
1	0.711	18.90	867,863	0.1500	7.00	4.00	1.269	62.88	70.88
1	0.711	18.90	867,863	0.1500	21.00	5.00	1.269	47.88	57.88
1	0.711	18.90	867,863	0.1500	35.00	5.00	1.269	33.88	43.88
1	0.711	18.90	867,863	0.1750	11.00	3.00	1.481	59.88	65.88
1	0.711	18.90	867,863	0.1750	28.00	3.00	1.481	42.88	48.88
1	0.711	18.90	867,863	0.2000	-4.00	2.00	1.692	75.88	79.88
1	0.711	18.90	867,863	0.2000	15.00	2.00	1.692	56.88	60.88
1	0.711	18.90	867,863	0.2000	10.00	4.00	1.692	59.88	67.88
1	0.711	18.90	867,863	0.2000	-4.00	4.00	1.692	73.88	81.88
1	0.711	18.90	867,863	0.2000	5.00	3.00	1.692	65.88	71.88
1	0.711	18.90	867,863	0.2000	15.00	3.00	1.692	55.88	61.88
1	0.711	18.90	867,863	0.2125	-3.00	1.00	1.798	75.88	77.88
1	0.711	18.90	867,863	0.2125	3.00	1.00	1.798	69.88	71.88
1	0.711	18.90	867,863	0.2125	-3.00	2.00	1.798	74.88	78.88
1	0.711	18.90	867,863	0.2125	3.00	2.00	1.798	68.88	72.88

Figure 17 (continued). Run ID# O - Sinusoidal AOA Parked - Priority 2. Parked rotor with sinusoidally varying blade pitch, at selected tunnel velocities from 20-40 m/s. With five-hole leading edge pressure probes installed.

Span Station	Chord (m)	Uw (m/s)	Local Re	Local K	Mean AOA (deg)	Omega AOA (deg)	Blade Pitch Freq (Hz)	Tip Min Pitch (deg)	Tip Max Pitch (deg)
1	0.711	18.90	867,863	0.0250	8.0	5.5	0.212	60.38	71.38
1	0.711	18.90	867,863	0.0250	14.0	5.5	0.212	54.38	65.38
1	0.711	18.90	867,863	0.0250	20.0	5.5	0.212	48.38	59.38
1	0.711	18.90	867,863	0.0250	8.0	10.0	0.212	55.88	75.88
1	0.711	18.90	867,863	0.0250	14.0	10.0	0.212	49.88	69.88
1	0.711	18.90	867,863	0.0250	20.0	10.0	0.212	43.88	63.88
1	0.711	18.90	867,863	0.0500	8.0	5.5	0.423	60.38	71.38
1	0.711	18.90	867,863	0.0500	14.0	5.5	0.423	54.38	65.38
1	0.711	18.90	867,863	0.0500	20.0	5.5	0.423	48.38	59.38
1	0.711	18.90	867,863	0.0500	8.0	10.0	0.423	55.88	75.88
1	0.711	18.90	867,863	0.0500	14.0	10.0	0.423	49.88	69.88
1	0.711	18.90	867,863	0.0500	20.0	10.0	0.423	43.88	63.88
1	0.711	18.90	867,863	0.0750	8.0	5.5	0.635	60.38	71.38
1	0.711	18.90	867,863	0.0750	14.0	5.5	0.635	54.38	65.38
1	0.711	18.90	867,863	0.0750	20.0	5.5	0.635	48.38	59.38
1	0.711	18.90	867,863	0.0750	8.0	10.0	0.635	55.88	75.88
1	0.711	18.90	867,863	0.0750	14.0	10.0	0.635	49.88	69.88
1	0.711	18.90	867,863	0.0750	20.0	10.0	0.635	43.88	63.88
1	0.711	18.90	867,863	0.1000	8.0	5.5	0.846	60.38	71.38
1	0.711	18.90	867,863	0.1000	14.0	5.5	0.846	54.38	65.38
1	0.711	18.90	867,863	0.1000	20.0	5.5	0.846	48.38	59.38
1	0.711	18.90	867,863	0.1000	8.0	10.0	0.846	55.88	75.88
1	0.711	18.90	867,863	0.1000	14.0	10.0	0.846	49.88	69.88
1	0.711	18.90	867,863	0.1000	20.0	10.0	0.846	43.88	63.88
2	0.627	23.30	943,502	0.0625	3.00	2.00	0.739	78.62	82.62
2	0.627	23.30	943,502	0.0625	12.00	4.00	0.739	67.62	75.62
2	0.627	23.30	943,502	0.0750	9.00	2.00	0.887	72.62	76.62
2	0.627	23.30	943,502	0.0750	23.00	5.00	0.887	55.62	65.62
2	0.627	23.30	943,502	0.0750	37.00	6.00	0.887	40.62	52.62
2	0.627	23.30	943,502	0.0750	52.00	6.00	0.887	25.62	37.62
2	0.627	23.30	943,502	0.1000	9.00	2.00	1.183	72.62	76.62
2	0.627	23.30	943,502	0.1000	23.00	2.00	1.183	58.62	62.62
2	0.627	23.30	943,502	0.1000	37.00	4.00	1.183	42.62	50.62
2	0.627	23.30	943,502	0.1000	7.00	6.00	1.183	70.62	82.62
2	0.627	23.30	943,502	0.1250	5.00	1.00	1.479	77.62	79.62
2	0.627	23.30	943,502	0.1250	13.00	1.00	1.479	69.62	71.62

Figure 17 (continued). Run ID# O - Sinusoidal AOA Parked - Priority 2. Parked rotor with sinusoidally varying blade pitch, at selected tunnel velocities from 20-40 m/s. With five-hole leading edge pressure probes installed.

Span Station	Chord (m)	Uw (m/s)	Local Re	Local K	Mean AOA (deg)	Omega AOA (deg)	Blade Pitch Freq (Hz)	Tip Min Pitch (deg)	Tip Max Pitch (deg)
2	0.627	23.30	943,502	0.0250	8.0	5.5	0.296	70.12	81.12
2	0.627	23.30	943,502	0.0250	14.0	5.5	0.296	64.12	75.12
2	0.627	23.30	943,502	0.0250	20.0	5.5	0.296	58.12	69.12
2	0.627	23.30	943,502	0.0250	8.0	10.0	0.296	65.62	85.62
2	0.627	23.30	943,502	0.0250	14.0	10.0	0.296	59.62	79.62
2	0.627	23.30	943,502	0.0250	20.0	10.0	0.296	53.62	73.62
2	0.627	23.30	943,502	0.0500	8.0	5.5	0.591	70.12	81.12
2	0.627	23.30	943,502	0.0500	14.0	5.5	0.591	64.12	75.12
2	0.627	23.30	943,502	0.0500	20.0	5.5	0.591	58.12	69.12
2	0.627	23.30	943,502	0.0500	8.0	10.0	0.591	65.62	85.62
2	0.627	23.30	943,502	0.0500	14.0	10.0	0.591	59.62	79.62
2	0.627	23.30	943,502	0.0500	20.0	10.0	0.591	53.62	73.62
2	0.627	23.30	943,502	0.0750	8.0	5.5	0.887	70.12	81.12
2	0.627	23.30	943,502	0.0750	14.0	5.5	0.887	64.12	75.12
2	0.627	23.30	943,502	0.0750	20.0	5.5	0.887	58.12	69.12
2	0.627	23.30	943,502	0.0750	8.0	10.0	0.887	65.62	85.62
2	0.627	23.30	943,502	0.0750	14.0	10.0	0.887	59.62	79.62
2	0.627	23.30	943,502	0.0750	20.0	10.0	0.887	53.62	73.62
2	0.627	23.30	943,502	0.1000	8.0	5.5	1.183	70.12	81.12
2	0.627	23.30	943,502	0.1000	14.0	5.5	1.183	64.12	75.12
2	0.627	23.30	943,502	0.1000	20.0	5.5	1.183	58.12	69.12
3	0.542	28.30	990,616	0.0375	-1.00	1.00	0.623	87.02	89.02
3	0.542	28.30	990,616	0.0375	5.00	2.00	0.623	80.02	84.02
3	0.542	28.30	990,616	0.0375	15.00	10.00	0.623	62.02	82.02
3	0.542	28.30	990,616	0.0375	23.00	10.00	0.623	54.02	74.02
3	0.542	28.30	990,616	0.0500	8.00	2.00	0.831	77.02	81.02
3	0.542	28.30	990,616	0.0500	21.00	4.00	0.831	62.02	70.02
3	0.542	28.30	990,616	0.0500	34.00	5.00	0.831	48.02	58.02
3	0.542	28.30	990,616	0.0500	47.00	5.00	0.831	35.02	45.02
3	0.542	28.30	990,616	0.0500	11.00	11.00	0.831	65.02	87.02
3	0.542	28.30	990,616	0.0500	23.00	12.00	0.831	52.02	76.02
3	0.542	28.30	990,616	0.0625	8.00	2.00	1.039	77.02	81.02
3	0.542	28.30	990,616	0.0625	20.00	2.00	1.039	65.02	69.02
3	0.542	28.30	990,616	0.0625	32.00	2.00	1.039	53.02	57.02
3	0.542	28.30	990,616	0.0625	44.00	4.00	1.039	39.02	47.02
3	0.542	28.30	990,616	0.0625	10.00	8.00	1.039	69.02	85.02
3	0.542	28.30	990,616	0.0625	26.00	7.00	1.039	54.02	68.02
3	0.542	28.30	990,616	0.0625	42.00	7.00	1.039	38.02	52.02
3	0.542	28.30	990,616	0.0750	12.00	1.00	1.247	74.02	76.02
3	0.542	28.30	990,616	0.0750	28.00	2.00	1.247	57.02	61.02
3	0.542	28.30	990,616	0.0750	10.00	3.00	1.247	74.02	80.02
3	0.542	28.30	990,616	0.0750	23.00	3.00	1.247	61.02	67.02

Figure 17 (continued). Run ID# O - Sinusoidal AOA Parked - Priority 2. Parked rotor with sinusoidally varying blade pitch, at selected tunnel velocities from 20-40 m/s. With five-hole leading edge pressure probes installed.

Span Station	Chord (m)	Uw (m/s)	Local Re	Local K	Mean AOA (deg)	Omega AOA (deg)	Blade Pitch Freq (Hz)	Tip Min Pitch (deg)	Tip Max Pitch (deg)
3	0.542	28.30	990,616	0.0250	8.0	5.5	0.416	73.52	84.52
3	0.542	28.30	990,616	0.0250	14.0	5.5	0.416	67.52	78.52
3	0.542	28.30	990,616	0.0250	20.0	5.5	0.416	61.52	72.52
3	0.542	28.30	990,616	0.0250	8.0	10.0	0.416	69.02	89.02
3	0.542	28.30	990,616	0.0250	14.0	10.0	0.416	63.02	83.02
3	0.542	28.30	990,616	0.0250	20.0	10.0	0.416	57.02	77.02
3	0.542	28.30	990,616	0.0500	8.0	5.5	0.831	73.52	84.52
3	0.542	28.30	990,616	0.0500	14.0	5.5	0.831	67.52	78.52
3	0.542	28.30	990,616	0.0500	20.0	5.5	0.831	61.52	72.52
3	0.542	28.30	990,616	0.0500	8.0	10.0	0.831	69.02	89.02
3	0.542	28.30	990,616	0.0500	14.0	10.0	0.831	63.02	83.02
3	0.542	28.30	990,616	0.0500	20.0	10.0	0.831	57.02	77.02
3	0.542	28.30	990,616	0.0750	8.0	5.5	1.247	73.52	84.52
3	0.542	28.30	990,616	0.0750	14.0	5.5	1.247	67.52	78.52
3	0.542	28.30	990,616	0.0750	20.0	5.5	1.247	61.52	72.52
3	0.542	28.30	990,616	0.1000	8.0	5.5	1.662	73.52	84.52
3	0.542	28.30	990,616	0.1000	14.0	5.5	1.662	67.52	78.52
3	0.542	28.30	990,616	0.1000	20.0	5.5	1.662	61.52	72.52
4	0.457	33.90	1,000,542	0.0250	5.00	1.00	0.590	82.56	84.56
4	0.457	33.90	1,000,542	0.0250	15.00	3.00	0.590	70.56	76.56
4	0.457	33.90	1,000,542	0.0250	16.00	11.00	0.590	61.56	83.56
4	0.457	33.90	1,000,542	0.0250	28.00	13.00	0.590	47.56	73.56
4	0.457	33.90	1,000,542	0.0375	10.00	2.00	0.885	76.56	80.56
4	0.457	33.90	1,000,542	0.0375	26.00	2.00	0.885	60.56	64.56
4	0.457	33.90	1,000,542	0.0375	42.00	3.00	0.885	43.56	49.56
4	0.457	33.90	1,000,542	0.0375	15.00	10.00	0.885	63.56	83.56
4	0.457	33.90	1,000,542	0.0375	28.00	10.00	0.885	50.56	70.56
4	0.457	33.90	1,000,542	0.0375	42.00	10.00	0.885	36.56	56.56
4	0.457	33.90	1,000,542	0.0500	13.00	1.00	1.181	74.56	76.56
4	0.457	33.90	1,000,542	0.0500	30.00	2.00	1.181	56.56	60.56
4	0.457	33.90	1,000,542	0.0500	4.00	2.00	1.181	82.56	86.56
4	0.457	33.90	1,000,542	0.0500	12.00	2.00	1.181	74.56	78.56
4	0.457	33.90	1,000,542	0.0500	25.00	2.00	1.181	61.56	65.56
4	0.457	33.90	1,000,542	0.0500	10.00	3.00	1.181	75.56	81.56
4	0.457	33.90	1,000,542	0.0500	27.00	3.00	1.181	58.56	64.56

Figure 17 (continued). Run ID# O - Sinusoidal AOA Parked - Priority 2. Parked rotor with sinusoidally varying blade pitch, at selected tunnel velocities from 20-40 m/s. With five-hole leading edge pressure probes installed.

Span Station	Chord (m)	Uw (m/s)	Local Re	Local K	Mean AOA (deg)	Omega AOA (deg)	Blade Pitch Freq (Hz)	Tip Min Pitch (deg)	Tip Max Pitch (deg)
4	0.457	33.90	1,000,542	0.0250	8.0	5.5	0.590	75.06	86.06
4	0.457	33.90	1,000,542	0.0250	14.0	5.5	0.590	69.06	80.06
4	0.457	33.90	1,000,542	0.0250	20.0	5.5	0.590	63.06	74.06
4	0.457	33.90	1,000,542	0.0250	8.0	10.0	0.590	70.56	90.56
4	0.457	33.90	1,000,542	0.0250	14.0	10.0	0.590	64.56	84.56
4	0.457	33.90	1,000,542	0.0250	20.0	10.0	0.590	58.56	78.56
4	0.457	33.90	1,000,542	0.0500	14.0	5.5	1.181	69.06	80.06
4	0.457	33.90	1,000,542	0.0500	20.0	5.5	1.181	63.06	74.06
4	0.457	33.90	1,000,542	0.0750	14.0	5.5	1.771	69.06	80.06
4	0.457	33.90	1,000,542	0.0750	20.0	5.5	1.771	63.06	74.06
5	0.381	39.30	967,024	0.0125	5.00	1.00	0.410	83.65	85.65
5	0.381	39.30	967,024	0.0125	15.00	4.00	0.410	70.65	78.65
5	0.381	39.30	967,024	0.0125	13.00	8.00	0.410	68.65	84.65
5	0.381	39.30	967,024	0.0125	22.00	11.00	0.410	56.65	78.65
5	0.381	39.30	967,024	0.0125	16.00	15.00	0.410	58.65	88.65
5	0.381	39.30	967,024	0.0125	24.00	17.00	0.410	48.65	82.65
5	0.381	39.30	967,024	0.0125	33.00	18.00	0.410	38.65	74.65
5	0.381	39.30	967,024	0.0250	16.00	2.00	0.821	71.65	75.65
5	0.381	39.30	967,024	0.0250	37.00	3.00	0.821	49.65	55.65
5	0.381	39.30	967,024	0.0250	10.00	8.00	0.821	71.65	87.65
5	0.381	39.30	967,024	0.0250	22.00	8.00	0.821	59.65	75.65
5	0.381	39.30	967,024	0.0250	37.00	8.00	0.821	44.65	60.65
5	0.381	39.30	967,024	0.0375	9.00	1.00	1.231	79.65	81.65
5	0.381	39.30	967,024	0.0375	9.00	2.00	1.231	78.65	82.65
5	0.381	39.30	967,024	0.0375	21.00	2.00	1.231	66.65	70.65
5	0.381	39.30	967,024	0.0250	8.0	5.5	0.821	76.15	87.15
5	0.381	39.30	967,024	0.0250	14.0	5.5	0.821	70.15	81.15
5	0.381	39.30	967,024	0.0250	20.0	5.5	0.821	64.15	75.15
5	0.381	39.30	967,024	0.0250	8.0	10.0	0.821	71.65	91.65
5	0.381	39.30	967,024	0.0250	14.0	10.0	0.821	65.65	85.65
5	0.381	39.30	967,024	0.0250	20.0	10.0	0.821	59.65	79.65
5	0.381	39.30	967,024	0.0500	14.0	5.5	1.642	70.15	81.15
5	0.381	39.30	967,024	0.0500	20.0	5.5	1.642	64.15	75.15

Figure 18. Run ID# P - Wake Flow Visualization - Priority 2. Upwind rigid rotor (0° cone) operation at fixed blade pitch settings of 3° and 12°, at selected yaw angles and tunnel velocities from 5-12 m/s. With five-hole leading edge pressure probes installed. With blade tip smoke flow visualization.

NASA AMES TEST PLAN
TWISTED, TAPERED BLADES; R = 5.03 m
TWO BLADE HUB

RUN ID#: P
SEQUENCE: Wake Flow Vis Upwind (P)

Uw (m/s)	Yaw Angle																
	0	5	10	20	30	45	60	90	135	180	-135	-90	-45	-30	-20	-10	-5
5.0	X		X	X	X	X	X										
6.0																	
7.0	X		X	X	X	X	X										
8.0																	
9.0																	
10.0	X		X	X	X												
11.0																	
12.0	X		X														
13.0																	
14.0																	
15.0																	
16.0																	
17.0																	
18.0																	
19.0																	
20.0																	

Each "X" entry indicates that the wake will be visualized for approximately 1 minute at that combination of wind speed and yaw angle.

BLADE PITCH ANGLE = 3.0 deg FOR 5.0 m/s AND 7.0 m/s
BLADE PITCH ANGLE = 12.0 deg FOR 10.0 m/s AND 12.0 m/s

Figure 19. Run ID# Q - Dynamic Inflow - Priority 2. Upwind rigid rotor (0° cone) operation at zero yaw, with stepped blade pitch variations, at selected tunnel velocities from 5-15 m/s. With five-hole leading edge pressure probes installed.

NASA AMES TEST PLAN
TWISTED, TAPERED BLADES; R = 5.03m
TWO BLADE HUB

RUN ID#: Q
SEQUENCE: Dynamic Inflow (P)

Uw (m/s)	Initial Tip Pitch (deg)	Final Tip Pitch (deg)	Pitch Rate (deg/s)	Delay Time (s)	Hold Time (s)	Number of Pitches
5.0	-6.0	10.0	66.0	15.0	15.0	20
5.0	-6.0	10.0	66.0	15.0	15.0	20
8.0	0.0	18.0	66.0	10.0	10.0	20
8.0	0.0	18.0	66.0	10.0	10.0	20
10.0	6.0	24.0	66.0	8.0	8.0	20
10.0	6.0	24.0	66.0	8.0	8.0	20
15.0	18.0	36.0	66.0	5.0	5.0	40

"Initial Tip Pitch" column entries indicate tip pitch angle prior to pitching, and "Final Tip Pitch" column entries denote tip pitch after pitching. "Delay Time" is the time period allowed to elapse prior to initiating the next pitch. "Hold Time" is the time allowed to elapse before pitching back to the intial pitch angle. Data will be acquired during the entire series of pitches specified in the column titled "Number of Pitches."

Figure 20. Run ID# R – Varying AOA Without Probes - Priority 2. Upwind rigid rotor (3.4° cone) operation at zero yaw, with ramped and stepped blade pitch variations, at selected tunnel velocities from 6-20 m/s. With five-hole leading edge pressure probes installed.

NASA AMES TEST PLAN
TWISTED, TAPERED BLADES; R = 5.03m
TWO BLADE HUB

RUN ID#:   R
SEQUENCE: Step AOA, No Probes (P)

Uw (m/s)	Yaw (deg)	Initial Tip Pitch (deg)	0.30R AOA at Initial Pitch (deg)	0.95R AOA at Initial Pitch (deg)	Final Tip Pitch (deg)	0.30R AOA at Final Pitch (deg)	0.95R AOA at Final Pitch (deg)	Pitch Rate (deg/s)	Pitching
6.0	0.0	32.0	-16.0	-20.1	-15.0	20.0	20.1	0.180	continuous ramp
6.0	0.0	-15.0	20.0	20.1	32.0	-16.0	-20.1	-0.180	continuous ramp
6.0	0.0	32.0	-16.1	-20.1	-15.0	20.0	20.1	step up then step down	5.0 deg step, 3.0 s delay, 5.0 s data
6.0	30.0	32.0	-16.1	-20.1	-15.0	20.0	20.1	step up then step down	5.0 deg step, 3.0 s delay, 5.0 s data
10.0	0.0	37.0	-9.0	-2.0	-15.0	36.0	26.8	0.180	continuous ramp
10.0	0.0	-15.0	36.0	26.8	37.0	-9.0	-2.0	-0.180	continuous ramp
10.0	0.0	37.0	-9.0	-2.0	-15.0	36.0	26.8	step up then step down	5.0 deg step, 3.0 s delay, 5.0 s data
10.0	30.0	37.0	-9.0	-2.0	-15.0	36.0	26.8	step up then step down	5.0 deg step, 3.0 s delay, 5.0 s data
15.0	0.0	40.0	-1.6	-16.3	-15.0	48.2	34.0	0.180	continuous ramp
15.0	0.0	-15.0	48.2	34.0	40.0	-1.6	-16.3	-0.180	continuous ramp
15.0	0.0	40.0	-1.6	-16.3	-15.0	48.2	34.0	step up then step down	5.0 deg step, 3.0 s delay, 5.0 s data
15.0	30.0	40.0	-1.6	-16.3	-15.0	48.2	34.0	step up then step down	5.0 deg step, 3.0 s delay, 5.0 s data
20.0	0.0	44.0	1.3	-14.4	28.0	14.7	-0.8	0.180	continuous ramp
20.0	0.0	28.0	14.7	-0.8	44.0	1.3	-14.4	-0.180	continuous ramp
20.0	0.0	44.0	1.3	-14.4	28.0	14.7	-0.8	step up then step down	5.0 deg step, 3.0 s delay, 5.0 s data
20.0	30.0	44.0	1.3	-14.4	28.0	14.7	-0.8	step up then step down	5.0 deg step, 3.0 s delay, 5.0 s data

The column titled "Pitching" describes how the blade will be pitched to acquire static data. The entry "continuous ramp" indicates that pitching will be carried out at 0.180 degrees per second through the range indicated in the columns to the left. The entry "5.0 deg step, 3.0 s delay, 5.0 s data" indicates that, through the range indicated in the columns to the left, the blade will be stepped in pitch to the each angle, 3.0 seconds will be allowed to elapse to stabilize the flow, and then 5.0 seconds of data will be acquired.

Figure 21. Run ID# S – Upwind Clean Blade (no probes) - Priority 2. Upwind rigid rotor (0° cone) operation at constant blade pitch (3°), at selected yaw angles and tunnel velocities from 5-25 m/s. With five-hole leading edge pressure probes removed.

NASA AMES TEST PLAN
TWISTED, TAPERED BLADES; R = 5.03 m
TWO BLADE HUB

RUN ID#: S
SEQUENCE: Upwind, No Probes (F)

Uw (m/s)	Yaw Angle																			
	0	5	10	20	30	45	60	75	90	135	180	-135	-90	-75	-60	-45	-30	-20	-10	-5
5.0	X2	X	X	X	X	X	X	X	X	X	X									
6.0	X2		X		X															
7.0	X2	X	X	X	X	X	X	X	X	X	X									
8.0	X2		X		X															
9.0	X2		X		X															
10.0	X2	X	X	X	X	X	X	X	X	X	X									
11.0	X2		X		X															
12.0	X2		X		X															
13.0	X2		X		X															
14.0	X2		X		X															
15.0	X2	X	X	X	X	X	X	X	X	X	X									
16.0	X2		X		X															
17.0	X2		X		X															
18.0	X2		X		X															
19.0	X2		X		X															
20.0	X2	X	X	X	X	X	X	X	X	X	X									
21.0	X2		X		X															
22.0	X2		X		X															
23.0	X2		X		X															
24.0	X2		X		X															
25.0	X2	X	X	X	X	X	X	X	X	X	X									

Each "X" entry indicates that 30 seconds of data (corresponding to 36 revolutions) will be acquired at that combination of wind speed and yaw angle.

The entry "X2" indicates that two data sets, each 30 seconds long (corresponding to 36 revolutions), will be acquired at this combination of wind speed and yaw angle. The first of these data sets will be acquired just after setting wind speed, and prior to acquiring data at any of the other yaw angles for that wind speed. The second data set will be acquired after collecting data at all of the other yaw angles, but before setting the next wind speed. This will be done to provide an indication of system viablity and data repeatability.

Figure 22. Run ID# T – Upwind 2° Pitch Power Curve - Priority 2. Upwind rigid rotor (cone) operation at zero yaw and constant blade pitch (2°), and tunnel velocities from 5-25 m/s. With five-hole leading edge pressure probes removed.

NASA AMES TEST PLAN
TWISTED, TAPERED BLADES; R = 5.03 m
TWO BLADE HUB

RUN ID#: T
SEQUENCE: Upwind, 2 deg Pitch (F)

Uw (m/s)	Yaw Angle																			
	0	5	10	20	30	45	60	75	90	135	180	-135	-90	-75	-60	-45	-30	-20	-10	-5
5.0	X																			
6.0	X																			
7.0	X																			
8.0	X																			
9.0	X																			
10.0	X																			
11.0	X																			
12.0	X																			
13.0	X																			
14.0	X																			
15.0	X																			
16.0	X																			
17.0	X																			
18.0	X																			
19.0	X																			
20.0	X																			
21.0	X																			
22.0	X																			
23.0	X																			
24.0	X																			
25.0	X																			

Each "X" entry indicates that 30 seconds of data (corresponding to 36 revolutions) will be acquired at that combination of wind speed and yaw angle.

Figure 23. Run ID# U - 4° Pitch Power Curve - Priority 2. Upwind rigid rotor (0° cone) operation at zero yaw and constant blade pitch (4°), at selected tunnel velocities from 5-25 m/s. With five-hole leading edge pressure probes removed.

NASA AMES TEST PLAN
TWISTED, TAPERED BLADES; R = 5.03 m
TWO BLADE HUB

RUN ID#: U
SEQUENCE: Upwind, 4 deg Pitch (F)

Uw (m/s)	Yaw Angle																			
	0	5	10	20	30	45	60	75	90	135	180	-135	-90	-75	-60	-45	-30	-20	-10	-5
5.0	X																			
6.0	X																			
7.0	X																			
8.0	X																			
9.0	X																			
10.0	X																			
11.0	X																			
12.0	X																			
13.0	X																			
14.0	X																			
15.0	X																			
16.0	X																			
17.0	X																			
18.0	X																			
19.0	X																			
20.0	X																			
21.0	X																			
22.0	X																			
23.0	X																			
24.0	X																			
25.0	X																			

Each "X" entry indicates that 30 seconds of data (corresponding to 36 revolutions) will be acquired at that combination of wind speed and yaw angle.

Figure 24. Run ID# V - Tip Plate Power Curve - Priority 2. Upwind rigid rotor (0° cone) operation at zero yaw and constant blade pitch (3°), at selected tunnel velocities from 5-25 m/s. With five-hole leading edge pressure probes removed. With tip plate installed.

NASA AMES TEST PLAN
TWISTED, TAPERED BLADES; R = 5.03 m
TWO BLADE HUB

RUN ID#: V
SEQUENCE: Tip Plate (F)

Uw (m/s)	Yaw Angle																			
	0	5	10	20	30	45	60	75	90	135	180	-135	-90	-75	-60	-45	-30	-20	-10	-5
5.0	X																			
6.0	X																			
7.0	X																			
8.0	X																			
9.0	X																			
10.0	X																			
11.0	X																			
12.0	X																			
13.0	X																			
14.0	X																			
15.0	X																			
16.0	X																			
17.0	X																			
18.0	X																			
19.0	X																			
20.0	X																			
21.0	X																			
22.0	X																			
23.0	X																			
24.0	X																			
25.0	X																			

Each "X" entry indicates that 30 seconds of data (corresponding to 36 revolutions) will be acquired at that combination of wind speed and yaw angle.

Figure 25. Run ID# W - Extended Rotor Power Curve - Priority 2. Upwind rigid rotor (0° cone) operation at zero yaw and constant blade pitch (3°), at selected tunnel velocities from 5-25 m/s. With five-hole leading edge pressure probes removed. With extended blade tips installed to achieve rotor diameter of 5.53m (optimum for two-bladed rotor).

NASA AMES TEST PLAN
TWISTED, TAPERED BLADES; R = 5.03 m
TWO BLADE HUB

RUN ID#: W
SEQUENCE: Extended Blade (F)

Uw	Yaw Angle																			
(m/s)	0	5	10	20	30	45	60	75	90	135	180	-135	-90	-75	-60	-45	-30	-20	-10	-5
5.0	X																			
6.0	X																			
7.0	X																			
8.0	X																			
9.0	X																			
10.0	X																			
11.0	X																			
12.0	X																			
13.0	X																			
14.0	X																			
15.0	X																			
16.0	X																			
17.0	X																			
18.0	X																			
19.0	X																			
20.0	X																			
21.0	X																			
22.0	X																			
23.0	X																			
24.0	X																			
25.0	X																			

Each "X" entry indicates that 30 seconds of data (corresponding to 36 revolutions) will be acquired at that combination of wind speed and yaw angle.

Figure 26. Run ID# X – Medium RPM - Priority 2. Upwind rigid rotor (0° cone) operation at constant blade pitch (~0°), at yaw angles and tunnel velocities from 5-15 m/s. With five-hole leading edge pressure probes installed. Operation at medium RPM (~90 RPM).

NASA AMES TEST PLAN
TWISTED, TAPERED BLADES; R = 5.03 m
TWO BLADE HUB

RUN ID#: X
SEQUENCE: Medium RPM (F)

Uw (m/s)	Yaw Angle																			
	0	5	10	20	30	45	60	75	90	135	180	-135	-90	-75	-60	-45	-30	-20	-10	-5
5.0	X	X	X	X	X												X	X	X	X
6.0	X		X		X															
7.0	X	X	X	X	X												X	X	X	X
8.0	X		X		X															
9.0	X		X		X															
10.0	X	X	X	X	X												X	X	X	X
11.0	X		X		X															
12.0	X		X		X															
13.0	X		X		X															
14.0	X		X		X															
15.0	X	X	X	X	X												X	X	X	X
16.0																				
17.0																				
18.0																				
19.0																				
20.0																				
21.0																				
22.0																				
23.0																				
24.0																				
25.0																				

Each "X" entry indicates that 30 seconds of data (corresponding to 36 revolutions) will be acquired at that combination of wind speed and yaw angle.

The entry "X2" indicates that two data sets, each 30 seconds long (corresponding to 36 revolutions), will be acquired at this combination of wind speed and yaw angle. The first of these data sets will be acquired just after setting wind speed, and prior to acquiring data at any of the other yaw angles for that wind speed. The second data set will be acquired after collecting data at all of the other yaw angles, but before setting the next wind speed. This will be done to provide an indication of system viablity and data repeatability.

Figure 27. Run ID# Y – High RPM - Priority 2. Upwind rigid rotor (0° cone) operation at constant blade pitch (~-4°), at selected yaw angles and tunnel velocities from 5-15 m/s. With five-hole leading edge pressure probes installed. Operation at highest RPM (~110 RPM).

NASA AMES TEST PLAN
TWISTED, TAPERED BLADES; R = 5.03 m
TWO BLADE HUB

RUN ID#: Y
SEQUENCE: High RPM (F)

Uw	Yaw Angle																			
(m/s)	0	5	10	20	30	45	60	75	90	135	180	-135	-90	-75	-60	-45	-30	-20	-10	-5
5.0	X	X	X	X	X												X	X	X	X
6.0	X		X		X															
7.0	X	X	X	X	X												X	X	X	X
8.0	X		X		X															
9.0	X		X		X															
10.0	X	X	X	X	X												X	X	X	X
11.0	X		X		X															
12.0																				
13.0																				
14.0																				
15.0																				
16.0																				
17.0																				
18.0																				
19.0																				
20.0																				
21.0																				
22.0																				
23.0																				
24.0																				
25.0																				

Each "X" entry indicates that 30 seconds of data (corresponding to 36 revolutions) will be acquired at that combination of wind speed and yaw angle.

The entry "X2" indicates that two data sets, each 30 seconds long (corresponding to 36 revolutions), will be acquired at this combination of wind speed and yaw angle. The fist of these date sets will be acquired just after setting wind speed, and prior to acquiring data at any of the other yaw angles for that wind speed. The second data set will be acquired after collecting data at all of the other yaw angles, but before setting the next wind speed. This will be done to provide an indication of system viability and data repeatability.

Figure 28. Run ID# Z -Upwind Rigid Rotor Coned Downwind - Priority 3. Rigid rotor (3.4° cone) operation at constant blade pitch (3°), at selected yaw angles and tunnel velocities from 5-25 m/s. With five-hole leading edge pressure probes installed.

NASA AMES TEST PLAN
TWISTED, TAPERED BLADES; R = 5.03 m
TWO BLADE HUB

RUN ID#: Z
SEQUENCE: Upwind Coned (F)

Uw	Yaw Angle																			
(m/s)	0	5	10	20	30	45	60	75	90	135	180	-135	-90	-75	-60	-45	-30	-20	-10	-5
5.0	X2	X	X	X	X	X	X	X	X	X	X									
6.0	X2		X		X															
7.0	X2	X	X	X	X	X	X	X	X	X	X									
8.0	X2		X		X															
9.0	X2		X		X															
10.0	X2	X	X	X	X	X	X	X	X	X	X									
11.0	X2		X		X															
12.0	X2		X		X															
13.0	X2		X		X															
14.0	X2		X		X															
15.0	X2	X	X	X	X	X	X	X	X	X	X									
16.0	X2		X		X															
17.0	X2		X		X															
18.0	X2		X		X															
19.0	X2		X		X															
20.0	X2	X	X	X	X	X	X	X	X	X	X									
21.0	X2		X		X															
22.0	X2		X		X															
23.0	X2		X		X															
24.0	X2		X		X															
25.0	X2	X	X	X	X	X	X	X	X	X	X									

Each "X" entry indicates that 30 seconds of data (corresponding to 36 revolutions) will be acquired at that combination of wind speed and yaw angle.

The entry "X2" indicates that two data sets, each 30 seconds long (corresponding to 36 revolutions), will be acquired at this combination of wind speed and yaw angle. The first of these data sets will be acquired just after setting wind speed, and prior to acquiring data at any of the other yaw angles for that wind speed. The second data set will be acquired after collecting data at all of the other yaw angles, but before setting the next wind speed. This will be done to provide an indication of system viability and data repeatability.

Figure 29. Run ID# 1 - Wake Flow Visualization Downwind - Priority 3. Downwind teetered rotor (3.4° cone) operation at blade pitch settings of 3° and 12°, at selected yaw angles and tunnel velocities from 5-12 m/s. With five-hole leading edge pressure probes installed. With blade-tip smoke-flow visualization.

NASA AMES TEST PLAN
TWISTED, TAPERED BLADES; R = 5.03 m
TWO BLADE HUB

RUN ID#: 1
SEQUENCE: Wake Flow Vis Downwind (P)

Uw (m/s)	Yaw Angle																
	0	5	10	20	30	45	60	90	135	180	-135	-90	-45	-30	-20	-10	-5
5.0	X		X	X	X	X	X										
6.0																	
7.0	X		X	X	X	X	X										
8.0																	
9.0																	
10.0	X		X	X	X												
11.0																	
12.0	X		X														
13.0																	
14.0																	
15.0																	
16.0																	
17.0																	
18.0																	
19.0																	
20.0																	

Each "X" entry indicates that the wake will be visualized for approximately 1 minute at that combination of wind speed and yaw angle.

BLADE PITCH ANGLE = 3.0 deg FOR 5.0 m/s AND 7.0 m/s
BLADE PITCH ANGLE = 12.0 deg FOR 10.0 m/s AND 12.0 m/s

Figure 30. Run ID# 2– Blade Flow Visualization Tufts Installed - Priority 3. Downwind teetered rotor (3.4° cone) operation at constant blade pitch (3°), at selected yaw angles and tunnel velocities from 5-25 m/s. With five-hole leading edge pressure probes installed.

NASA AMES TEST PLAN
TWISTED, TAPERED BLADES; R = 5.03 m
TWO BLADE HUB

RUN ID#: 2
SEQUENCE: Blade Tufts (F)

Uw (m/s)	Yaw Angle																			
	0	5	10	20	30	45	60	75	90	135	180	-135	-90	-75	-60	-45	-30	-20	-10	-5
5.0	X2	X	X	X	X	X	X	X	X	X	X	X	X	X	X	X	X	X	X	X
6.0	X2		X		X												X		X	
7.0	X2	X	X	X	X	X	X	X	X	X	X	X	X	X	X	X	X	X	X	X
8.0	X2		X		X												X		X	
9.0	X2		X		X												X		X	
10.0	X2	X	X	X	X	X	X	X	X	X	X	X	X	X	X	X	X	X	X	X
11.0	X2		X		X												X		X	
12.0	X2		X		X												X		X	
13.0	X2		X		X												X		X	
14.0	X2		X		X												X		X	
15.0	X2	X	X	X	X	X	X	X	X	X	X	X	X	X	X	X	X	X	X	X
16.0	X2		X		X												X		X	
17.0	X2		X		X												X		X	
18.0	X2		X		X												X		X	
19.0	X2		X		X												X		X	
20.0	X2	X	X	X	X	X	X	X	X	X	X	X	X	X	X	X	X	X	X	X
21.0	X2		X		X												X		X	
22.0	X2		X		X												X		X	
23.0	X2		X		X												X		X	
24.0	X2		X		X												X		X	
25.0	X2	X	X	X	X	X	X	X	X	X	X	X	X	X	X	X	X	X	X	X

Each "X" entry indicates that 30 seconds of data (corresponding to 36 revolutions) will be acquired at that combination of wind speed and yaw angle.

The entry "X2" indicates that two data sets, each 30 seconds long (corresponding to 36 revolutions), will be acquired at this combination of wind speed and yaw angle. The first of these data sets will be acquired just after setting wind speed, and prior to acquiring data at any of the other yaw angles for that wind speed. The second data set will be acquired after collecting data at all of the other yaw angles, but before setting the next wind speed. This will be done to provide an indication of system viablity and data repeatability.

Shaded cells correspond to cases that may not be realizable due to excessive teeter impact loads, according to ADAMS predictions.

Figure 31. Run ID# 3 - Tower Wake Measurement - Priority 3. Downwind rigid rotor (3.4° cone) slow rotation at zero yaw and constant blade pitch (64°), at tunnel velocities of 7, 15, and 25 m/s. With five-hole leading edge pressure probes installed.

NASA AMES TEST PLAN
TWISTED, TAPERED BLADES; R = 5.03 m
TWO BLADE HUB

 RUN ID#: 3
SEQUENCE: Tower Wake Measure (P)

Uw (m/s)	Tower Diam. (m)	Re	Re Range
7.0	0.4	180,833	Subcritical
15.0	0.4	387,499	Transitional
25.0	0.4	645,832	Supercritical

At each wind speed, the instrumented blade will be rotated slowly or stepped in azimuth through the tower wake. This will enable tower wake profiling with the five hole probes mounted upstream of the instrumented blade leading edge.

Figure 32. Run ID# 4 - Static Pressure Calibration - Priority 3. Downwind rotor, either rigid (0° cone) or teetered (3.4° cone) operation at 0°, 10°, and 30° yaw and constant blade pitch (3°). With five-hole leading edge pressure probes installed. Configured to measure differential pressure between blade reference and upwind static probe.

NASA AMES TEST PLAN
TWISTED, TAPERED BLADES; R = 5.03 m
TWO BLADE HUB

RUN ID#: 4
SEQUENCE: Static Press. Cal (P)

Uw	Yaw Angle																			
(m/s)	0	5	10	20	30	45	60	75	90	135	180	-135	-90	-75	-60	-45	-30	-20	-10	-5
5.0	X		X		X															
6.0	X																			
7.0	X		X		X															
8.0	X																			
9.0	X																			
10.0	X		X		X															
11.0	X																			
12.0	X																			
13.0	X																			
14.0	X																			
15.0	X		X		X															
16.0	X																			
17.0	X																			
18.0	X																			
19.0	X																			
20.0	X		X		X															
21.0	X																			
22.0	X																			
23.0	X																			
24.0	X																			
25.0	X		X		X															

Each "X" entry indicates that 30 seconds of data (corresponding to 36 revolutions) will be acquired at that combination of wind speed and yaw angle.

The entry "X2" indicates that two data sets, each 30 seconds long (corresponding to 36 revolutions), will be acquired at this combination of wind speed and yaw angle. The first of these data sets will be acquired just after setting wind speed, and prior to acquiring data at any of the other yaw angles for that wind speed. The second data set will be acquired after collecting data at all of the other yaw angles, but before setting the next wind speed. This will be done to provide an indication of system viablity and data repeatability.

Appendix A. NREL – NASA Ames 10 m HAWT Unsteady Rotor Aerodynamics Wind Tunnel Test

Science Panel Meeting #1, October 5-6, 1998
National Wind Technology Center (NWTC), Boulder Colorado

Final Agenda

Monday, October 5

Session 1. Overview

7:45	**Continental breakfast (to be brought in)**	
8:00	Welcome and introductions	Simms
8:30	Wind turbine aerodynamics overview	Robinson
9:00	IEC wind turbine design process overview	Butterfield
9:30	Turbulence inflow characteristics overview	Kelley
10:00	Break	

Session 2. Wind Turbine Aerodynamics "Engineering Methods"

In this session, the various methods used to estimate wind turbine aerodynamic responses for engineering purposes (e.g. for inclusion in full turbine structural dynamics models) are identified and briefly described. In addition to including models that account for the effects of dynamic stall, these methods also typically incorporate models of 3-D responses (e.g. delayed stall and tip loss effects). Presenters will summarize method objectives, including, for example, who developed the method, what models are included in it, how it was tuned and validated, and modifications made to fix problems and improve performance.

10:15	AeroDyn	Hansen/ Pierce
10:30	European Models and EU Joule project summaries	Bjorck/ Madsen/ Rasmussen /Smith /Snel
11:15	Group comments and discussion	

Session 3. Beddoes- Leishman Dynamic Stall Model

This session provides a forum for users of the Beddoes- Leishman (and other similar models) to focus on issues specific to semi-empirical dynamic stall models. Users will also address issues related to associated 3-D effects models. Each presenter will provide the following: 1) a brief description of modeling needs and efforts including typical applications; 2) identification of model shortcomings, perceived limitations, and problems encountered; 3) a summary chart depicting model strengths and weaknesses; 4) a summary of needed improvements; and 5) specific information that the NREL wind tunnel test could provide to enable better model utilization and/ or validation.

11:30	Original model development and intent	Leishman
12:00	**Lunch (to be brought in)**	
12:30	As implemented in AeroDyn	Pierce/ Hansen
13:15	As implemented by FFA Sweden	Bjorck
14:00	Break	
14:15	As implemented by Garrad-Hassan UK	Smith
15:00	As implemented by Riso Denmark	Madsen/ Rasmussen
15:45	Break	
16:00	As implemented by ECN Netherlands	Snel
16:45	Group comments and discussion	
18:30	**Dinner (to be provided – Hotel Boulderado, 13th and Spruce, Boulder)**	

Tuesday, October 6

Session 4. 3-D Effects Models

In this session, users of various other 3-D effects models will address the same five specific topics: 1) brief description of modeling needs and efforts, including typical applications; 2) identification of model shortcomings, perceived limitations, and problems encountered; 3) a summary chart depicting model strengths and weaknesses; 4) summary of needed improvements; and 5) specific information that the NREL wind tunnel test could provide to enable better model utilization and/ or validation.

7:45	**Continental breakfast (to be brought in)**	
8:00	Skewed wake modeling	Holley
8:30	Corrigan/Du delayed stall model/ Prandtl tip loss model	Whale/ Tangler
9:30	Potential of CFD to improve engineering methods	Duque/ Van Dam

Session 5. Test Description

10:15	Break/ Tour of experimental facility	
11:15	Review of turbine systems, planned field testing, and data processing	Simms/ Hand
12:00	**Lunch (to be brought in)**	
12:30	Planned wind tunnel test logistics	Fingersh
13:00	Strawman of test matrix and research issues addressed	Robinson
14:00	Break	

Session 6. Conclusion and Wrap-up

14:15	Group discussion - test priorities to address research needs	
16:00	Comments and summary by technical oversight committee.	Carr/ Galbraith/ Leishman/ McCroskey

Minutes and Follow-up

All presenters are requested to bring a copy of their presentation to be included in the meeting minutes, or, if possible, email the presentation in electronic format (Power Point 2-slide per page handout format is preferable) to dave_simms@nrel.gov.

Meeting minutes, including presentations, will be compiled and provided to all participants at a later time. All participants are requested to submit 1-2 pages of summary comments within a few days following the meeting. The comments should identify key meeting issues and other significant concerns. NREL will review participant comments and summarize results into the meeting minutes.

Appendix B: Science Panel Addresses and Phone Number

Technical Oversight:

Larry Carr, (650) 604-4143
  lcarr@mail.arc.nasa.gov
  NASA Ames Research Center
  Mail Stop 260-1
  Moffett Field, CA 94035-1000
  Fax: (650) 604-4511
  http://www.arc.nasa.gov

Roddy Galbraith, +44 141 330 5295
  r.a.m.galbraith@aero.gla.ac.uk
  Department of Aerospace Engineering
  University of Glasgow
  Glasgow G12 8QQ, Scotland UK
  Fax: +44 141 330-5560
  http://www.aero.gla.ac.uk

Gordon Leishman,(301)405-1126
  leishman@eng.umd.edu
  Alfred Gessow Rotorcraft Center
  Department of Aerospace Engineering
  University of Maryland
  College Park, MD
  Fax: (301) 314-9001
  http://www.enae.umd.edu/AGRC/aero.html

Jim McCroskey, (650) 604-6428
  wmccroskey@mail.arc.nasa.gov
  NASA Ames Research Center
  Mail Stop 258-1
  Moffett Field, CA 94035-1000
  Fax: (650) 604-2238
  http://www.arc.nasa.gov

International Partners:

Anders Björck, +46 8 634 13 65
  bka@ffa.se
  FFA – The Aeronautical Research Institute of Sweden
  PO Box 11021
  Ranhammersvagen 14
  S-161 11 Bromma, Sweden
  Fax: +46 8 25 34 81
  http://www.ffa.se/windenergy/windenergy.html

Helge Madsen, +45 4237 2965
  helge.aagaard.madsen@risoe.dk
Flemming Rasmussen, +45 4677 5048
  flemming.rasmussen@risoe.dk
Niels Sorensen, +45 4677 5043
  nns@risoe.dk
  RISØ National Laboratory
  Test Station for Wind Turbines
  PO Box 49
  DK-4000 Roskilde, Denmark
  Fax: +45 4677 4677
  http://www.risoe.dk

Takis Chaviaropoulos, +30 1 603 99 00
  tchaviar@cres.gr
Nikos Stefanatos, +30 1 603 99 00
  nstefan@cresdb.cress.ariadne-t.gr
  CRES Centre for Renewable Energy Sources
  19th Km Marathonos Ave.
  19009 Pikermi,
  Greece
  Fax: +30 1 603 99 05

Stig Oye, +45 4525 4311
  s.oye@et.dtu.dk
  Technical University of Denmark
  Department of Energy Engineering
  Building 404
  2800 Lyngby, Denmark
  Fax: +45 4588 2421

Robert Rawlinson-Smith, +44 1275 394360
  smith@bristol.garradhassan.co.uk
  Garrad-Hassan and Partners Limited
  The Coach House
  Folleigh Lane, Long Ashton
  Bristol BS189JB, United Kingdom
  Fax: +44 1275 394361

Herman Snel, +31 224 564170
  snel@ecn.nl
Arno Brand, +31 224 564912
  brand@ecn.nl
Gerard Schepers, +31 224 564894
  schepers@ecn.nl
  ECN – Netherlands Energy Research Foundation
  Westerduinweg 3, PO Box 1
  1755 ZG Petten, The Netherlands
  Fax: +31 224 563214
  http://www.ecn.nl

International Partners Continued:

Mike Graham, +44 171 589 5074
  mgraham@ic.ac.uk
  Imperial College
  Department of Aeronautics
  London SW7 2BY
  United Kingdom
  Fax: +44 171 584 8120

Nando Timmer, +31 15 2781093
  nando@dutlls1.lr.tudelft.nl
Albert Bruining, +31 15 2785167 or 2781999
  a.bruining@ct.tudelft.nl
  Delft University of Technology
  Institute for Wind Energy
  Stevinweg 1, 2628 CN
  Delft, The Netherlands
  Fax: +31 15 2783533 or 2611465, respectively
  http://www.tudelft.nl

Frank Coton, +44 141 330 4305
  f.coton@aero.gla.ac.uk
  Department of Aerospace Engineering
  University of Glasgow
  Glasgow G12 8QQ, Scotland UK
  Fax: +44 141 330-5560
  http://www.aero.gla.ac.uk

Y. Shimizu, +81 59 231 9382
  shimizu@mach.mie-u.ac.jp
Takao Maeda, +81 59 231 9382
  maeda@mach.mie-u.ac.jp
  Department of Mechanical Engineering
  Mie University
  1515 Kamihama-cho Tsu
  Mie 514-8507, Japan
  Fax: +81 59 231 1572

NREL Subcontractors:

Earl Duque, (650) 604-4489
  eduque@mail.arc.nasa.gov
  Aeromechanics Branch
  NASA Ames Research Center
  Mail Stop 258-1
  Moffett Field, CA 94035-1000
  Fax: (650) 604-5173
  http://www.arc.nasa.gov

Al Eggers, (650) 493-3439
  ranninc@pacbell.net
  RANN Inc.
  744 San Antonio Rd Ste 26
  Palo Alto, CA. 94303
  Fax: (650) 493-2975

Philippe Giguere, (661) 823-6479
  Philippe.Giguere@enron.com
  Zond Energy Systems, Inc.
  13681 Chantico Road
  Tehachapi, CA 93561
  Fax: (805) 823-6804
  http://www.zond.com

Craig Hansen, (801) 278-7852
  chansen@windwardengineering.com
  Windward Engineering
  4661 Holly Lane
  Salt Lake City, UT 84117
  Fax: (801) 272-4132

Bill Holley, (925) 484-2985
  bill_holley@compuserve.com
  3731 Oak Brook Court
  Pleasanton CA 94588
  Fax: (925) 461-4377

Bob Kufeld, (650) 604-5664
  rkufeld@mail.arc.nasa.gov
Wayne Johnson, (650) 604-2242
  wrjohnson@mail.arc.nasa.gov
  Rotorcraft Aeromechanics Branch
  NASA Ames Research Center
  Code AAR, Mail Stop T12-B
  Moffett Field, CA 94035-1000
  Fax: (650) 604-5173
  http://www.arc.nasa.gov

Lakshmi Sankar, (404) 894-3014
  lsankar@aerospace.gatech.edu
  School of Aerospace Engineering
  Georgia Institute of Technology
  400 10th St. N. W.
  Atlanta, GA 30332-0150
  Fax: (404) 894-2760
  http://www.gatech.edu/

Michael Selig, (217) 244-5757
  m-selig@uiuc.edu
  Dept. of Aeronautical and Astronautical Engineering
  University of Illinois
  104 S. Wright Street (306 Talbot Lab)
  Urbana, IL 61801-2935
  Fax: (217) 244-0720
  http://www.aae.uiuc.edu

NREL Subcontractors Cont:

Case Van Dam, (530) 752-7741
  cpvandam@ucdavis.edu
  University of California, Davis
  Department of Mechanical & Aerospace Engineering
  2132A Bainer Hall
  Davis, CA 95616-5294
  Fax: (530) 752-4158
  http://www.ucdavis.edu

Bob Wilson, (541) 737-2218
  wilsonr@engr.orst.edu
  Oregon State University
  Department of Mechanical Engineering
  204 Rogers Hall
  Corvallis, Oregon 97331-6001
  Fax: (541) 737-2600
  http://www.engr.orst.edu

Sandia:

Dale Berg, (505) 844-1030
  deberg@sandia.gov
Walt Wolfe, (505) 844-4387
  wpwolfe@sandia.gov
  Sandia National Laboratories
  PO Box 5800
  MS 0708
  Albuquerque, NM 87185-0708
  Fax: (505) 845-9500

NREL:

Gunjit Bir, (303) 384-6953
  gunjit_bir@nrel.gov
Marshall Buhl, (303) 384-6914
  marshall_buhl@nrel.gov
Sandy Butterfield, (303)384-6902
  sandy_butterfield@nrel.gov
Palmer Carlin, (303) 384-6945
  palmer_carlin@nrel.gov
Jason Cotrell, (303) 384-7056
  jason_cotrell@nrel.gov
Lee Fingersh, (303) 384-6929
  lee_fingersh@nrel.gov
Maureen Hand, (303) 384-6933
  maureen_hand@nrel.gov
Sue Hock, (303) 384-6950
  sue_hock@nrel.gov
Neil Kelley, (303) 384-6923
  neil_kelley@nrel.gov
Scott Larwood, (303) 384-6948
  scott_larwood@nrel.gov
Kirk Pierce, (303) 384-7081
  kirk_pierce@nrel.gov

Mike Robinson, (303) 384-6947
  mike_robinson@nrel.gov
Scott Schreck, (303) 384-7102
  scott_schreck@nrel.gov
Dave Simms, (303) 384-6942
  dave_simms@nrel.gov
Jim Tangler, (303) 384-6934
  jim_tangler@nrel.gov
Bob Thresher ,(303) 384-6922
  bob_thresher@nrel.gov
Alan Wright, (303) 384-6928
  alan_wright@nrel.gov
  NREL NWTC
  1617 Cole Blvd.
  Golden, CO. 80401
  Fax: (303) 384-6901
  http://www.nrel.gov/wind
  http://wind2.nrel.gov/amestest

DOE:

Lew Pratsch, (202) 586-1512
  lew.pratsch@hq.doe.gov
  US Department of Energy
  Office of Geothermal and Wind Technology
  EE-12/5H072
  1000 Independence Ave. SW
  Washington, DC. 20585-0121
  Fax: (202) 586-8185

Appendix C:

Presentation by M. Robinson, NREL

Science Panel Considerations

⬥NREL

- Aerodynamics Models Used For Design Are One The Most Critical Links In The Advancement Of Wind Technology
  - Affects all aspects of design
  - Serious reservations about the assumptions and applicability of current models
  - Do not want to miss a unique opportunity to improve existing models and to explore new methods!

Meeting Agenda & Technical Overviews

⬥NREL

- Science Review:
  - IEC Design Standards & Turbine Design Process
  - Inflow Conditions & Modeling
  - Overview of the Current Aerodynamics Models (Momentum Theory) Being Used In The Design Process
  - Use of the Beddoes-Leishman Dynamic Stall Model
  - Corrections for 3-D Effects
    - Skewed wake
    - Delayed stall
    - Tip loses
    - Potential for CFD to Provide Some Insight Into 3-D Effects and Improve Engineering Methods

NREL Meeting Agenda & Technical Overviews

- Test Overview:
  - Experimental Capabilities
  - Turbine Mechanical and Instrumentation Systems
  - Data Reduction, Processing & Availability
  - Test Logistics
  - Discussion of Test Matrix & Research Issues

NREL Questioning The Fundamentals

- **Current Modeling Approach:**
  - Sectional 2-D Airfoil Properties Used as Initial Guess
  - Axial Induction Determined From Momentum Conservation
  - Wake Model Used to Adjust Axial Induction (Skewed Wakes)
  - Beddoes-Leishman Used to Obtain Unsteady Effects
  - Total Load Determined From Integration Of Sectional Properties

BEM Power Prediction

Blade tip pitch angle = 3 degrees
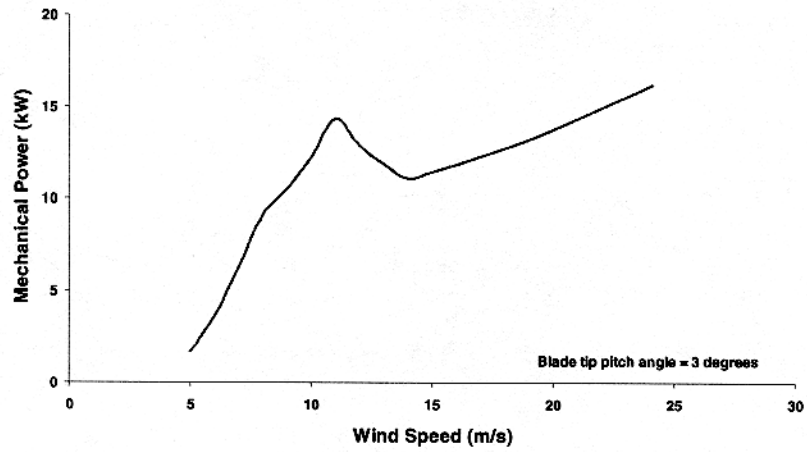
Cycle-Averaged Power Performance

PROP Prediction
Phase IV Baseline Cycles

Blade tip pitch angle = 3 degrees
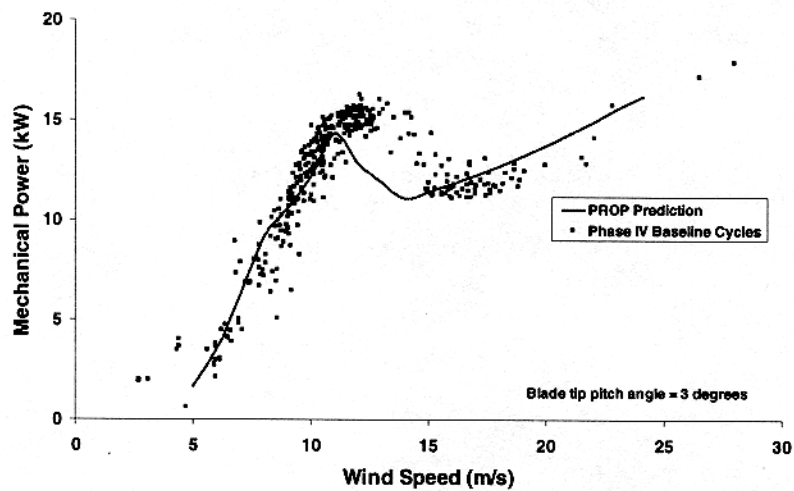
Instantaneous Power Performance
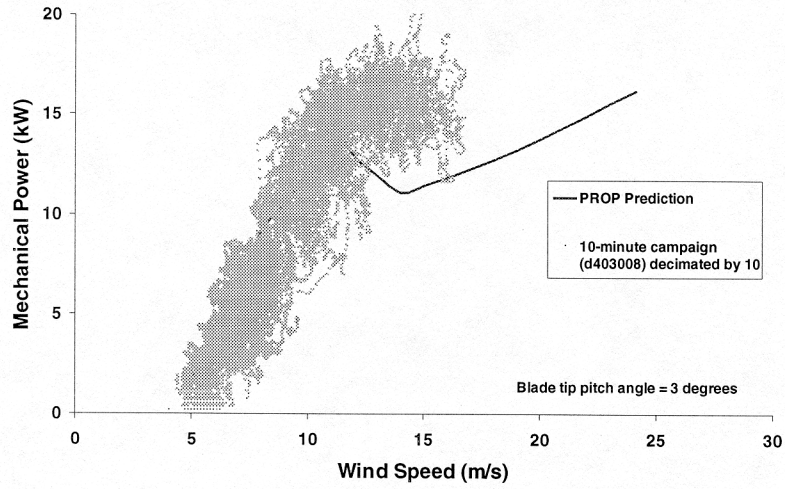
2-D Wind Tunnel Aerodynamic Performance
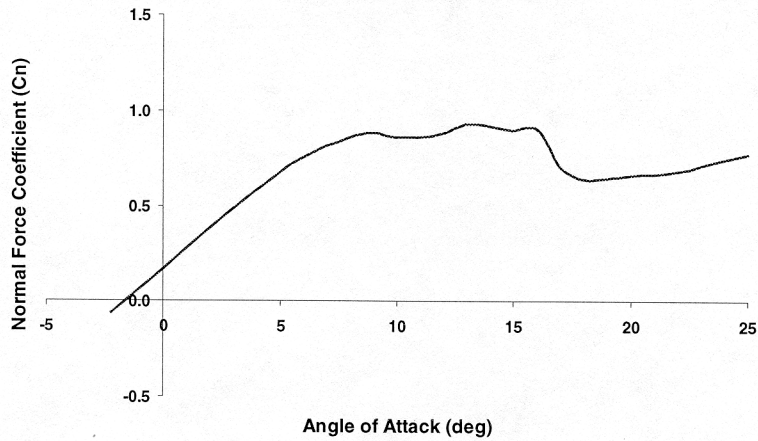
Cycle-Average Aerodynamic Performance
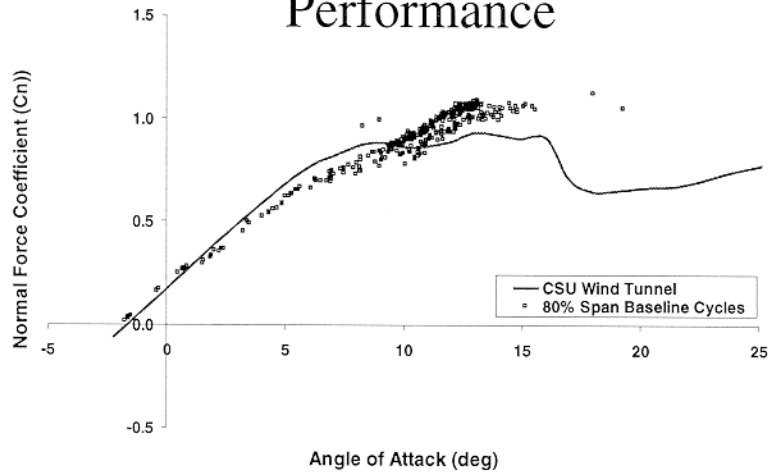
Instantaneous Aerodynamic Performance
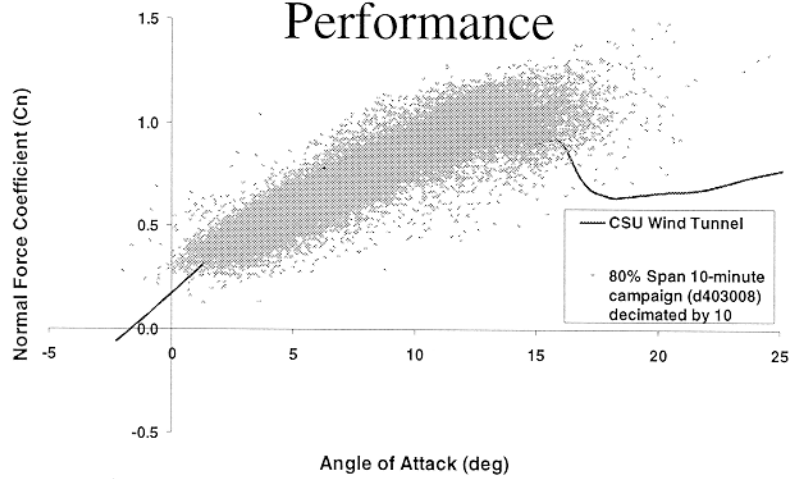
Phase IV Aerodynamic Performance
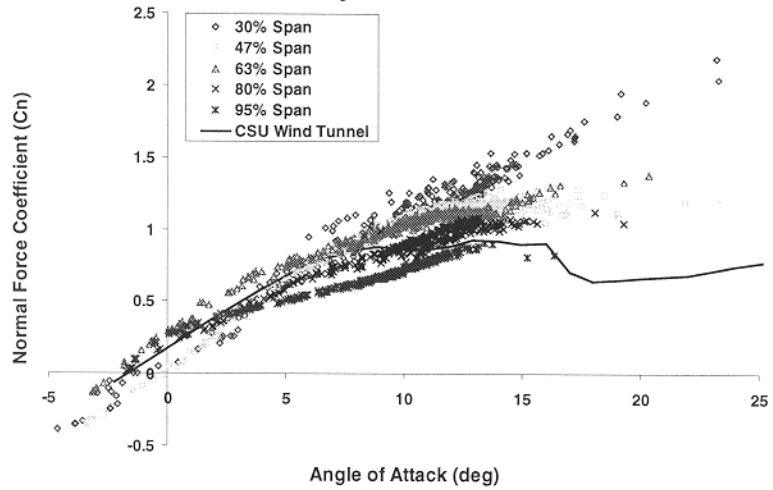
NREL Unsteady Aerodynamics Experiment
Blade Angle of Attack Histories (YawDyn)
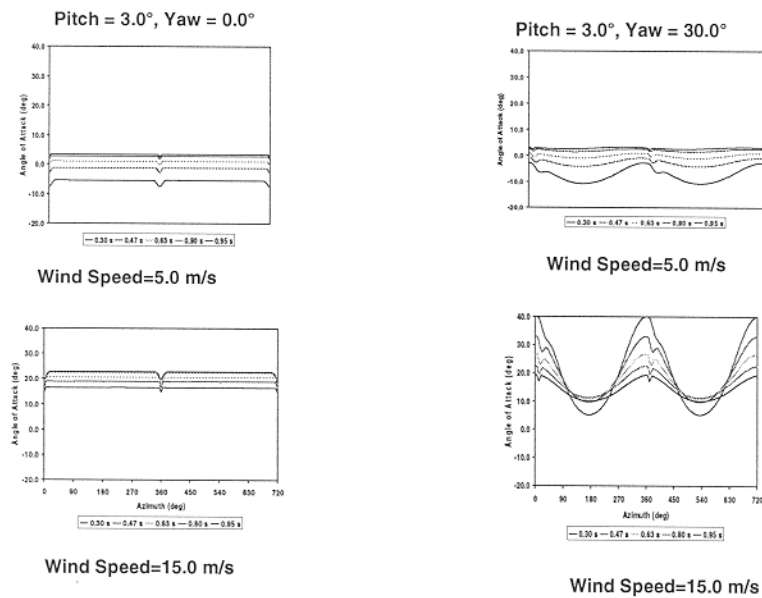
Program Goals

- **Make The Best Use Of This Opportunity:**
  - Improve Existing Modeling Capabilities
  - Validate Current Methods and Procedures
  - Develop New and Improved Methods Through a Better Appreciation Of The 3-D Fluid Physics
  - Are There Other Opportunities That We may Be Missing?

Appendix D:

Presentation by S. Butterfield, NREL

"The Big Picture"

•High Reliability

•Low Cost (Creative Design & low margins)

•Standards and Certification Bodies are attempting to Quantify "Safe Designs"!?

•Must quantify margins on design loads (20 - 30 year fatigue)

•Must quantify confidence in margins

6/17/97   1   **National Wind Technology Center**

How Accurate Do The Models Need To Be?

IEC 61400-1 Ed2 Safety of Wind Turbines

•Minimum material factor of 1.35

•Loads factor minimum is 1.0

•No Guidance on determining 50 year design fatigue load spectrum

•No uncertainty estimate of loads predictions required

6/17/97   2   **National Wind Technology Center**

Design Analysis Process

More Accurate Design Tools are the Key to High Reliability and Lower Cost

Inflow Models → Velocity Distributions → Aero Models → Aero Forces → Dynamic Simulator → Loads → Stress Analysis → Fatigue Analysis

Confidence (uncertainty) in each step?
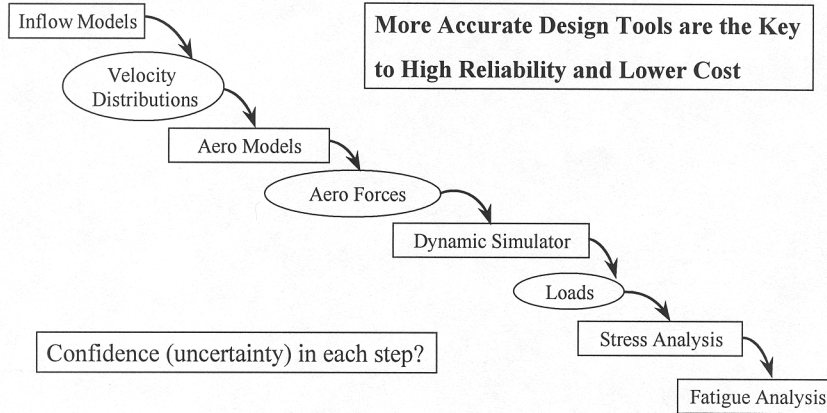
6/17/97   3   National Wind Technology Center

Simulation Results Vary Widely

Blade out-of-plane bending moment (kNm)

Max load response vs. Simulation no. (B1_Moop)
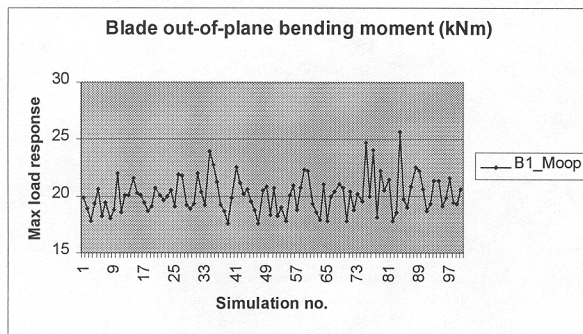
6/17/97   4   National Wind Technology Center

D-3

Needs:

•Physics must be as close to reality as practical with reasonable simulation run times to get statistical significance (30 yr. fatigue spectrum).

•Must have estimate of uncertainty for predicted applied loads

•Must be able to predict applied loads during abnormal operating conditions well

>transient inflow

>high yaw errors

>transients due to control operations

•Must have means of estimating long term extreme statistics of inflow

Critical Models

•Turbulence

•Steady Stall

•Dyn. Stall

•Dyn Wake

•Skewed Wake

6/17/97   5   **National Wind Technology Center**

Appendix E:

Presentation by N. Kelley, NREL

Turbulent Inflow Characteristics Overview

Neil Kelley
NREL/NWTC

October 5, 1998   Unsteady Rotor Aerodynamics Science Panel Meeting

Overall Goals

- **To explain the observed wind turbine loading spectral distributions in terms of the fluid dynamic processes taking place within the atmospheric boundary layer.**

- **To apply this knowledge in the testing and estimating the life of structural components.**

2

Questions to be Answered...

- **What is the mechanism or mechanisms responsible for producing structural responses from turbulent inflow events?**

- **What is the turbulent structure(s) responsible for such responses?**

- **Does our current turbulence simulation capability produce such structures?**

3

A Summary of Previous Activities...

- **Extensive wind season boundary layer measurements taken from two 50-m towers upwind and downwind of a large wind farm in San Gorgonio Pass (1989)**

- **Extensive, though limited, inflow turbulence measurements taken in conjunction with dual turbine testing within San Gorgonio wind farm (1990)**

- **Expanded and enhanced original Veers' SNLWIND turbulence simulation using information gathered from above into SNLWIND-3D which provides a much more realistic turbulent wind field (1992)**

4

San Gorgonio Measurements...
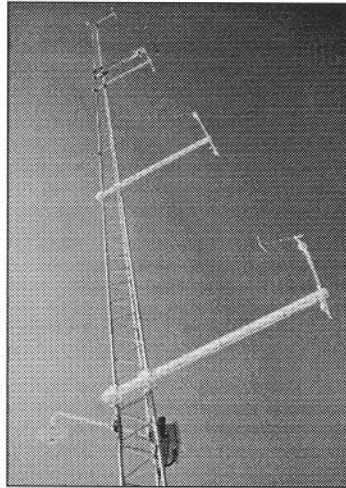
- Fast-response cups and vanes at 5, 10, 20, 50 m levels
- High-resolution sonic anemometer at 23 m (hub-height)
- Temperature/Dewpoint at 5 m
- Temperature difference between 50 and 5 m
- Barometric pressure at 5 m
- Global solar radiation

5

San Gorgonio Upwind Met Tower
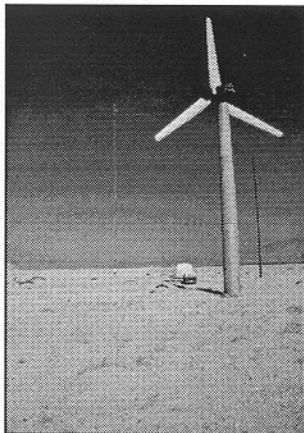
View upwind of tower
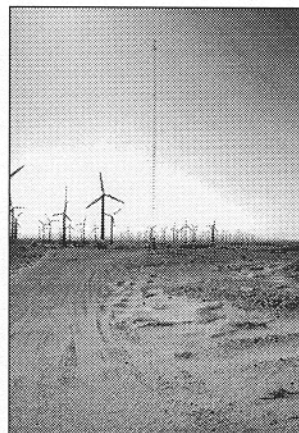
View downwind of tower

6

San Gorgonio Downwind Tower

Downwind (outflow) tower
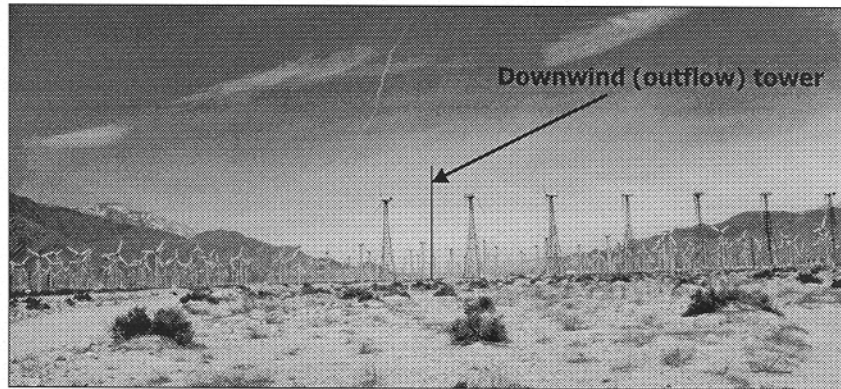
View looking towards prevailing wind direction

7

Role of Complex Terrain to South ...
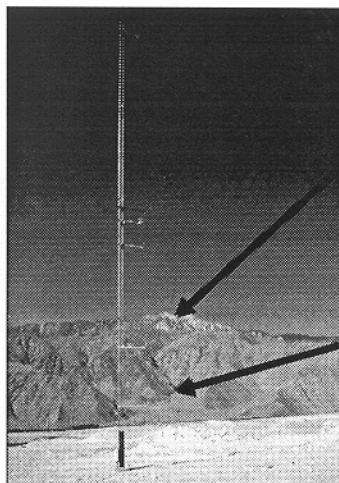
Mt. San Jacinto
12,000 ft peak

Blaisdell Canyon
*source of
nocturnal drainage
winds which increase
turbine fatigue damage*

8

Previous Activities - cont'd

- Used the San Gorgonio Micon 65/13 turbine data set to identify the potential of various inflow turbulence statistical parameters for scaling fatigue load spectra (1993)

- Compared San Gorgonio turbine load spectra with those found in northern Europe using the WISPER protocol (1994)

- Investigated using a Bergey EXCEL-S 10 kW turbine as a turbulence/loads sensor combined with online turbulence parameter measurements (1995)

- Performed a complete diurnal wind cycle numerical simulation of inflow and loading for two turbines (Micon 65 and AWT-26) at the upwind and downwind locations in the San Gorgonio wind farm (1996)

9

Initial conclusions . . .

- The turbulent loading of a wind turbine is an <u>event-driven process</u>

- Large loading events result from rotors encountering <u>spatially and temporally coherent turbulent structures</u>

- The number and severity of these structures depends on the local diurnal variation of the wind profile and stability of the atmospheric boundary layer as well as terrain characteristics

- The frequency and severity of such structures is much greater within multi-row wind farms though local topographies can conceivably produce similar conditions

- Most damaging loads tend to occur during day/night transition

10

Factors influencing inflow turbulence characteristics ...

upwind fetch characteristics

wind driving mechanism/ local area circulations

boundary layer vertical stability

free stream turbulence structure

upwind turbine wakes

turbine turbulence inflow structure

(Wind farms)

11

Planetary Boundary Layer (PBL) Diurnal Structure

Sunrise

Capping Inversion

Sunset

Height (km)

Inversion Layers

"Mixed Layer" Depth

z_i

0.5

Surface Layers

h

Wind turbines

0.0 0600 0900 1200 1500 1800 2100 0000 0500

Local Standard Time (LST)

12

Daytime (unstable) Boundary Layer Characteristics

Velocity Profile

1.5 km

Potential Temperature Profile

Dust Devil Circulation

surface
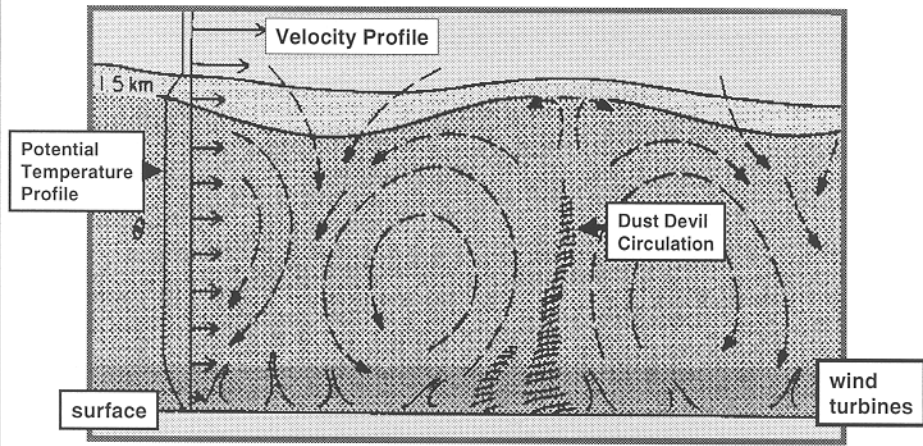
wind turbines

13

Stable (Nocturnal) Boundary Layer Characteristics

θ

Velocity Profile

Wave motions: *a source of coherent structures*

wave motions

200 m

coherent structures

wind turbines

surface
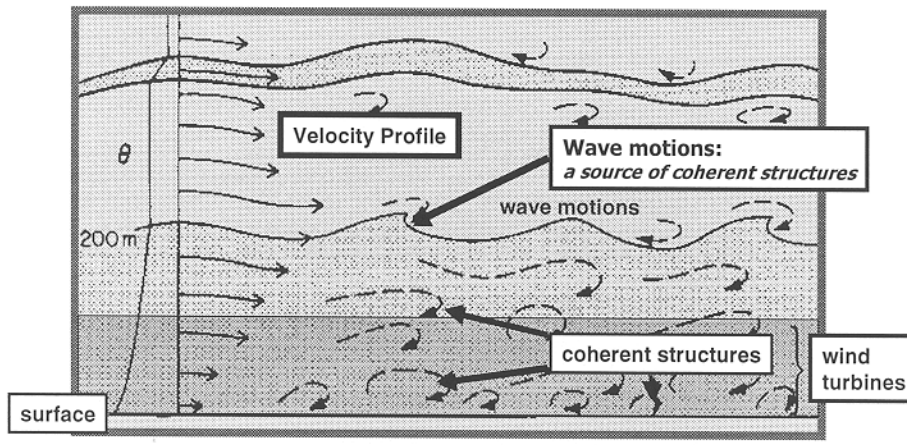
14

Impact of Boundary Layer Coherent Turbulence on Wind Turbine Rotor Loads

15

Sensitivity of Blade Loads with Stability
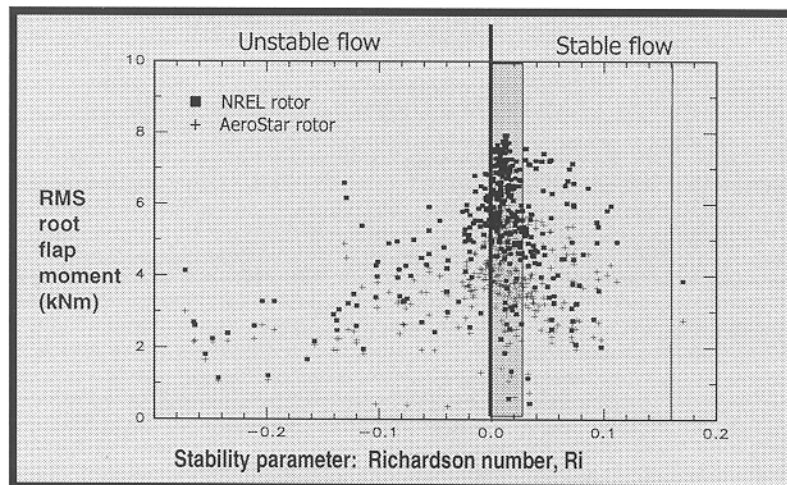
16
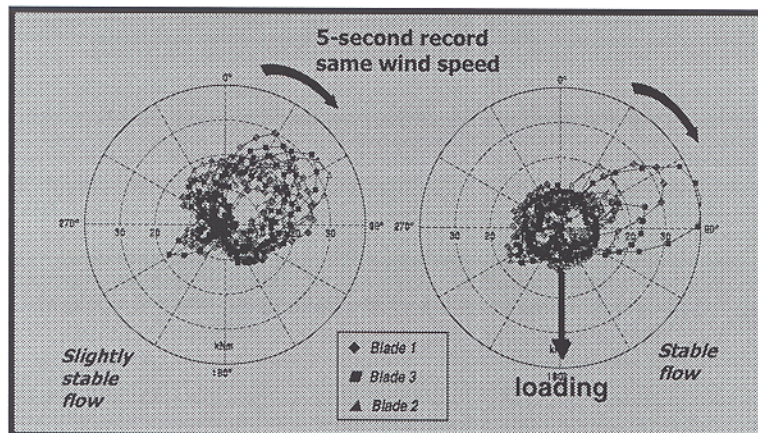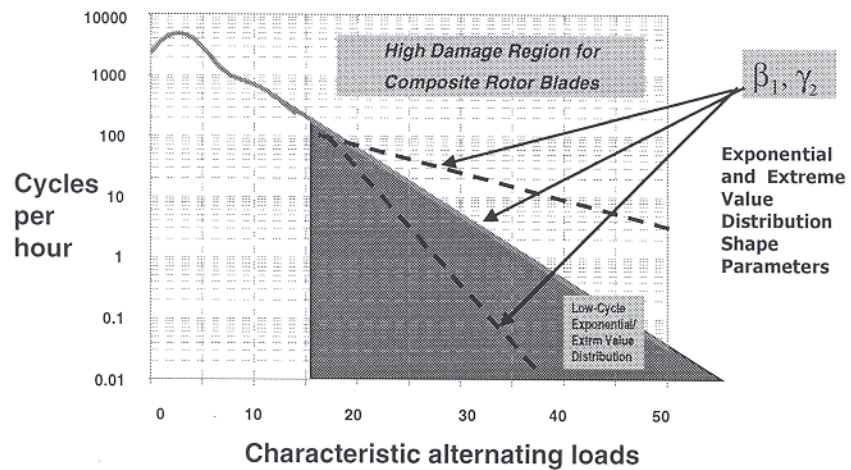
Characteristic Turbulence Time Scales for Wind Farm Environment
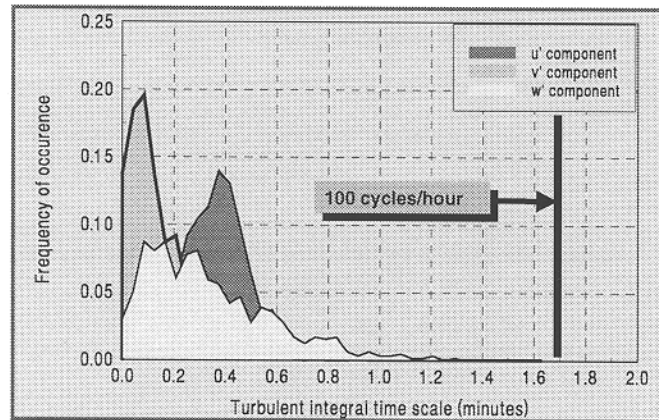
19

Variation of (-u'w')$^{1/2}$ and Flapwise Moment versus Stability
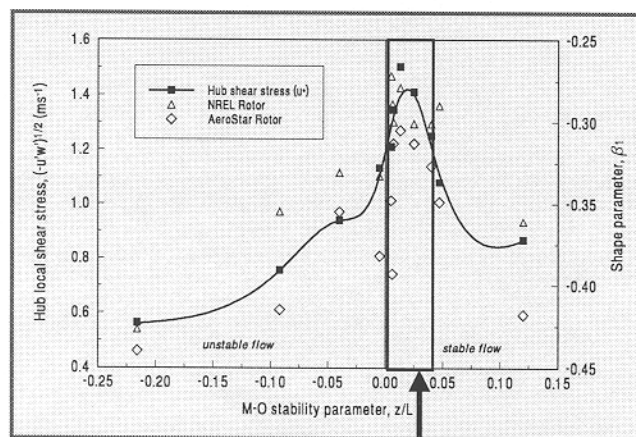
20

Variation of $(-u'w')^{1/2}$ and Edgewise Moment versus Stability
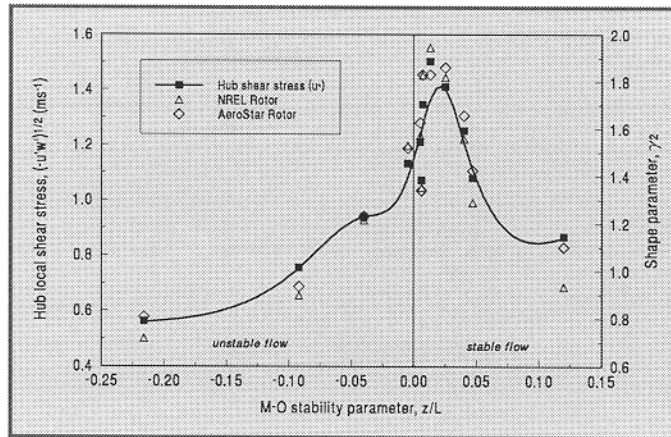
Observed Largest Peak Flapwise Loads vs Stability and Wind Component Correlations $(u_i'u_j')/\sigma_i\sigma_j$
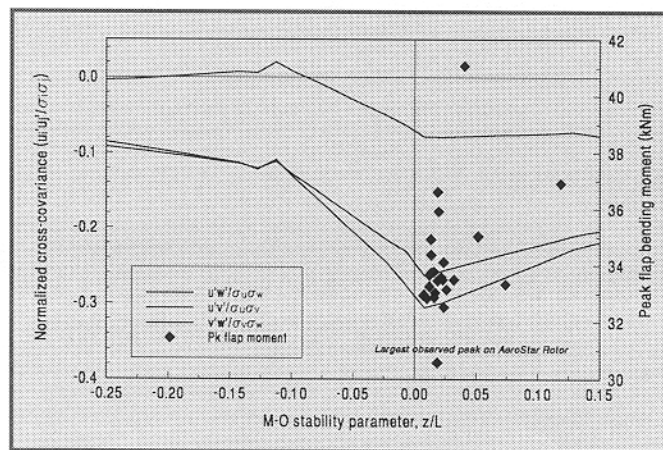
SNLWIND-3D/ADAMS Simulation

17 m/s San Gorgonio Simulated Turbulence

AWT-26 turbine ADAMS-Predicted Response
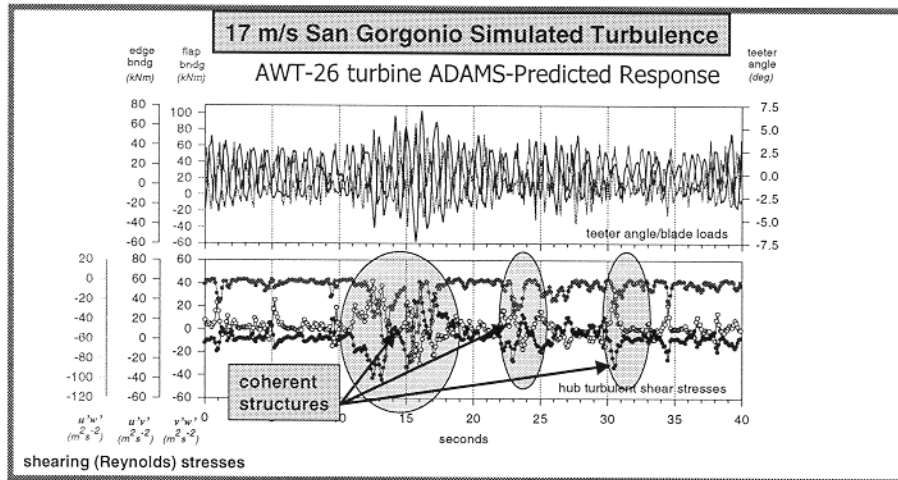
Our Current Working Hypotheses

- Structural loading peaks and minimums seen result from turbine rotors encountering organized inhomogenities in the inflow

- These inhomogenities or coherent elements are associated with local maxima in the Reynolds (shearing) stress field

- These encounters can be represented as a series of stochastic events

- These events can be described by a parametric statistical process which is scaled by boundary layer turbulence characteristics

Appendix F:

Presentation by C. Hansen, University of Utah

The AeroDyn Wind Turbine Aerodynamics Analysis

Craig Hansen

Mechanical Engineering Department

University of Utah

(801) 581-4145

hansen@me.mech.utah.edu

Wind Tunnel Test Planning Meeting   University of Utah, October, 1998

YawDyn and AeroDyn for ADAMS

- Two codes for combined aerodynamic and structural dynamic analysis of horizontal-axis wind turbines
- They share the same (AeroDyn) aerodynamics subroutines
- They differ greatly in their level of structural detail and ease of use
  - YawDyn has four degrees of freedom (written at U. of Utah)
  - ADAMS has unlimited degrees of freedom but long learning curve (commercial software)

Wind Tunnel Test Planning Meeting   University of Utah, October, 1998

Overview of the Aerodynamics Model

- Blade-element/momentum method used for quasi-steady inflow
  - Skewed wake correction to induction factor
  - Prandtl tip loss model
- Dynamic inflow option
  - Replaces BEM theory
  - Based upon method of Pitt and Peters, terms up to 3p
  - Induced velocity distribution depends upon aerodynamic thrust and pitch and yaw moments
- Dynamic stall based upon Beddoes-Leishman method
  - Lift, drag and pitching moment coefficients
- Momentum balance uses static airfoil characteristics
- Final force determination uses dynamic characteristics
- 3-D delayed stall implemented only via airfoil tables

Suggested Tests (Teetering and Rigid Hub)

- Steady-state operation at yaw angles of 0, ±20°, ±40°, ±60°, 80°, 90°, 120°, 150°, 180°
  - Rotors operate in this range, particularly with some IEC gust conditions
  - Throughout maximum range of wind speeds and pitch angles (not just positive power range)
  - Operation at multiple rotor speeds to broaden the reduced frequency and Reynolds number range
- Dynamic inflow tests
  - Abrupt pitch changes over full range of pitch angles and TSR
  - Yaw releases from 30° and 60° over wide range of wind speeds

Suggested Tests (Continued)

- Parked rotor over full range of pitch/yaw angles
  - Need to achieve $-180° < \alpha < 180°$ and a range of sweep angles
- Wake profiles and flow visualization in addition to existing field test instrumentation
- Fast-response tower shadow measurements during rotor tests
- Particular interest in blade tip region
  - Known problems in models, may be quite important to aerodynamic damping under extreme (i.e. design) conditions
- Simple models, together with wind tunnel limits, can be used to map out a quantitative test matrix

Appendix G:

Presentations by:
H. Snel, ECN
H. Madsen, RISO
A. Bjorck FFA

Overview of EC/EU Projects on Wind Turbine Rotor Aerodynamics for Aeroelastic Response Calculations

or:

From Benchmark to Benchmark

Overview EC Projects Aero

- WTBE-ML: Wind Turbine Benchmark Exercise on Mechanical Loads (EN3W/C1/151/NL) '85-'88
  - ECN, CRAA, FFA+TG, GH, RISØ, SPE, TUDk, VUB, WEG
- Aerodynamics of a Horizontal Axis Wind Turbine in Natural Conditions (EN3W.0032-DK) '86-'90
  - RISØ
- Response of Stall Regulated - Stall Induced Vibrations (JOUR-0076) '90-'93
  - RISØ, ECN, GH
- Dynamic Inflow I + extension (JOUR 0083) '90-'94
  - ECN, DUT, GH, NTUA+ULH, SPE, TUDk, TG, UniSt
- Dynamic Inflow II (JOU2-CT92-0186) '92-'95
  - ECN, DUT, GH, NTUA+ULH, SPE, TUDk, TG, UniSt

Overview Joule Projects cnt'd

- NEWDESI: New Generation of Design Tools for HAWTS (JOU2-CT92-0113 '92-'95)
  - **NTUA**, CRES, IAMRA, GH, LAMDA, STU
- Dynamic Stall and 3D Effects (JOU2-CT93-0345) '94-'95
  - **FFA**, Cranfield, CRES, DUT, ECN+NLR, GH, IC, NTUA+ULH, RISØ, TUDk, UB
- Stallvib: Prediction of Dynamic Loads and Induced Vibrations in Stall (JOR3-CT95-0047) '96-'98
  - **RISØ**, Bonus, DUT, ECN, FFA, TG, TUDk
- VISCWIND: CFD Codes for Wind Turbines (JOR3-CT95-0007) '96-'98
  - **TUDk**, CRES, NTUA, VUB?, RISØ?

Overview Joule Projects cnt'd

New Benchmark ......

- VEWTDC: Verification of European Wind Turbine Design Codes (JOR3-CT98-0267), just started
  - **ECN**, CRES, GH, NTUA, RISØ, SPE, TG, TUDk, WindMaster

WTBE-ML

- Comparison of the (then) state of the art aero-elastic design (and certification) computer codes.
- Some conclusions:
  - Loads in main components can be predicted within 20-35% error **if not in stall or in yaw**
  - Fundamental limitations mainly in aerodynamics:
    - transient and dynamic effects (inflow and stall);
    - aero characteristics, especially in stall

Dynamic Inflow I and II

- Subject: 'Rotor scale' (not dynamic stall which is chord scale) unsteady effects due to:
  - Blade pitch or tip pitch variations
  - Wind Speed variations
  - Yaw misalignment
- Results:
  - Dynamic inflow 'engineering' model: equilibrium momentum balance (algebraic equations) changed into dynamic balance (o.d.e's)
  - Yaw model that describes first harmonic inflow distribution in rotorplane

Prediction of Dynamic Loads and Induced Vibrations in Stall
STALLVIB

Helge Aagaard Madsen

Flemming Rasmussen

Wind Energy and Atmospheric Physics Dept.

Risø National Laboratory

Denmark

e-mail: helge.aagaard.madsen@risoe.dk

e-mail: flemming.rasmussen@risoe.dk

The STALLVIB Project

- EU funded project (JOULE III Programme)
- carried out in the two years period from 1996-1998
- participants

Teknikgruppen	**(SE)**
FFA	**(SE)**
ECN	**(NL)**
Delft Univ.	**(NL)**
Imperial Col.	**(UK)**
DTU	**(DK)**
Bonus Energy A/S (DK)	
Risø	**(DK)**

Project objectives

- Improvement of the prediction capabilities with respect to dynamic loads in stall and stall induced vibrations

- Establishment of guidelines aiming at achieving safety margins against stall induced vibrations.

Observed Problem
500 kW turbine
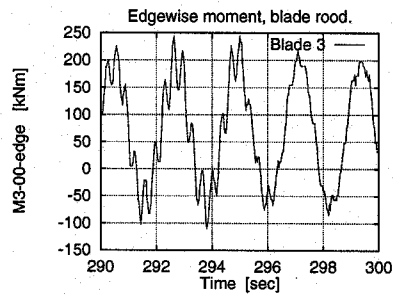
Edgewise blade root bending moment for a 500 kW turbine during operation in stall. Damped edgewise vibrations.
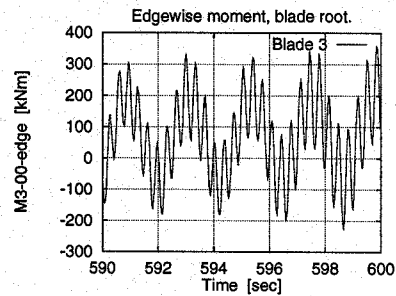
Edgewise blade root bending moment for a 500 kW turbine during operation in stall. Undamped edgewise vibrations at the edgewise natural frequency have started.

Observed Problem
500 kW turbines

Edgewise blade root bending moment. 23.2 m/s.
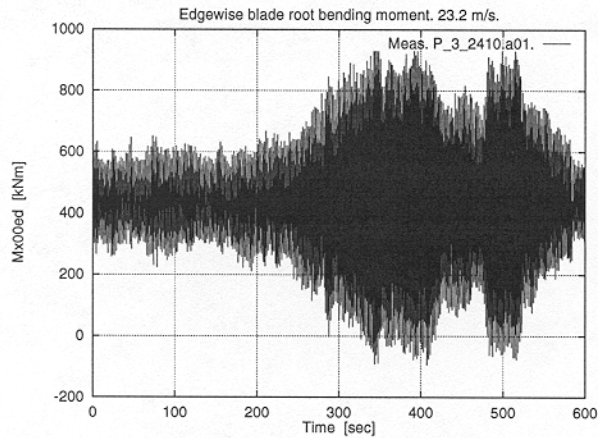
GENERAL APPROACH

USING MODELS WITH INCREASING COMPLEXITY

- a simple quasi-steady aerodynamic model for a blade section

- a simple quasi-steady aerodynamic model combined with a mode shape representation of a single blade

- including stall hysteresis model in the above models

- full aeroelastic simulations

LOCAL AERODYNAMIC DAMPING ON A BLADE SECTION
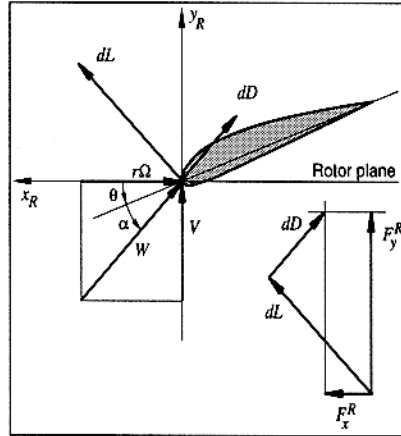
$$\left\{ \begin{matrix} F_x^R \\ F_y^R \end{matrix} \right\} \cong \left\{ \begin{matrix} F_{x0}^R \\ F_{y0}^R \end{matrix} \right\} + \left[\begin{matrix} c_{xx}^R & c_{xy}^R \\ c_{yx}^R & c_{yy}^R \end{matrix} \right] \left\{ \begin{matrix} \dot{x}_R \\ \dot{y}_R \end{matrix} \right\}$$

The Coefficients in the Damping Matrix

$$c_{xx}^R(r,V) = \frac{1}{2} c\rho \frac{r\Omega}{W} \left[\left(\frac{2r^2\Omega^2 + V^2}{r\Omega} \right) C_D - V \frac{\partial C_D}{\partial \alpha} - V C_L + \frac{V^2}{r\Omega} \frac{\partial C_L}{\partial \alpha} \right] \quad \boxed{\text{(in-plane)}}$$

$$c_{xy}^R(r,V) = \frac{1}{2} c\rho \frac{r\Omega}{W} \left[-V C_D - r\Omega \frac{\partial C_D}{\partial \alpha} + \left(\frac{2V^2 + r^2\Omega^2}{r\Omega} \right) C_L + V \frac{\partial C_L}{\partial \alpha} \right]$$

$$c_{yx}^R(r,V) = \frac{1}{2} c\rho \frac{r\Omega}{W} \left[-V C_D + \frac{V^2}{r\Omega} \frac{\partial C_D}{\partial \alpha} - \left(\frac{2r^2\Omega^2 + V^2}{r\Omega} \right) C_L + V \frac{\partial C_L}{\partial \alpha} \right]$$

$$c_{yy}^R(r,V) = \frac{1}{2} c\rho \frac{r\Omega}{W} \left[\left(\frac{2V^2 + r^2\Omega^2}{r\Omega} \right) C_D + V \frac{\partial C_D}{\partial \alpha} + V C_L + r\Omega \frac{\partial C_L}{\partial \alpha} \right] \quad \boxed{\text{(out-of-plane)}}$$

Airfoil Data for a 18% Section

Airfoil data.
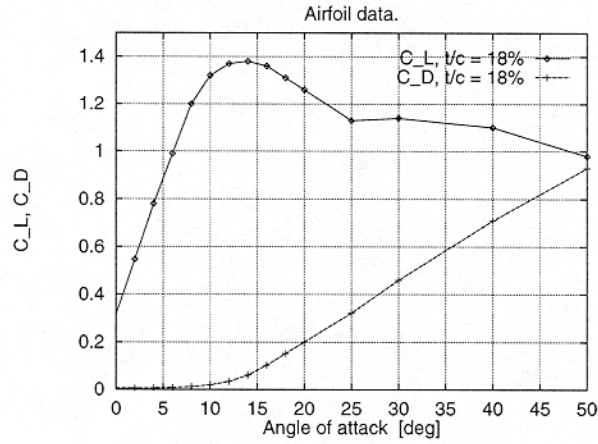
Damping as function of wind speed
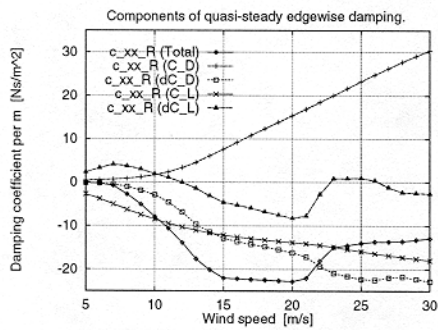
in-plane damping components   out-of-plane damping components
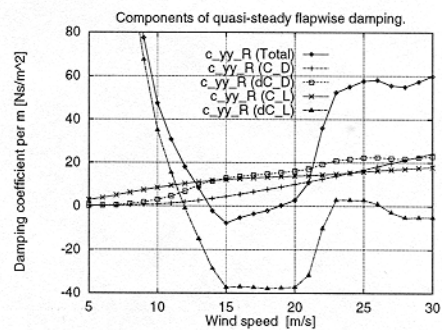
G-9

Damping Coefficient as Function of Vibration Direction

Local damping coefficient at radius 14 m.
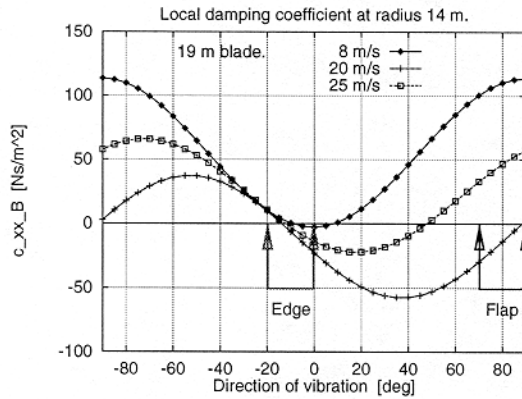
$$c_{xx}^{B}(\theta_{RB}) = \cos^2(\theta_{RB})c_{xx}^{R} + \cos(\theta_{RB})\sin(\theta_{RB})(c_{xy}^{R} + c_{yx}^{R}) + \sin^2(\theta_{RB})c_{yy}^{R}$$

11/16/98   NREL-NASA Ames Science Panel Meeting #1   11

Damping Coefficient as Function of Power

$$c_{xx}^{R}(r,V) = -\frac{2}{r^2\Omega^2}P_u(r,V) + \frac{V}{r^2\Omega^2}\frac{\partial P_u(r,V)}{\partial V}$$

11/16/98   NREL-NASA Ames Science Panel Meeting #1   12

Modal Aerodynamic Damping for a Blade

$$c_n(r) = c_{xx}^{Bn}(r)\varphi_{n0}^2(r)$$

Where $\varphi_{n0}(r)$ is the local amplitude of the nth mode shape of the blade and $c_{xx}^{Bn}(r)$ is the damping coefficient in the local direction of vibration for mode shape n

Mode Shapes and Vibration Directions

1st flapwise and edgewise mode shapes. Ex1.
Flapwise: 1.805 Hz.
Edgewise: 2.963 Hz.

Mode shape vibration direction. Ex1.
Flapwise: -90 deg.
Edgewise: 0 deg.

Logarithmic Decrement

1st edgewise mode. Ex1.

Airfoil t/c = 18%

Tip pitch = 0 deg.

1st flapwise mode. Ex1.

Airfoil t/c = 18%

Tip pitch = 0 deg.
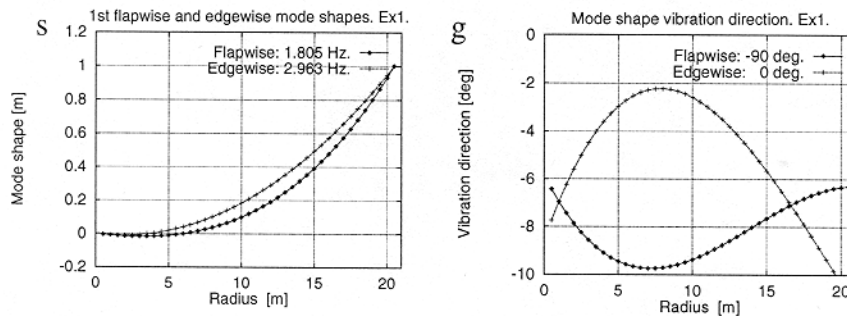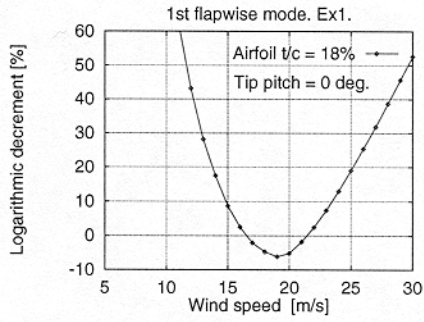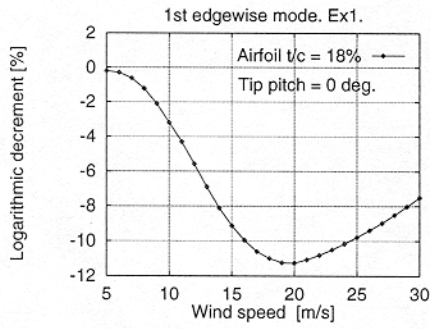
Logarithmic Decrement per Unit Length

1st edgewise mode. Ex1.

18 m/s

1st flapwise mode. Ex1.

18 m/s

G-12
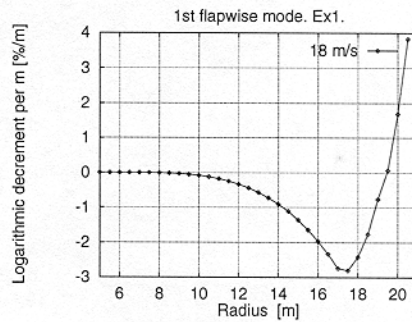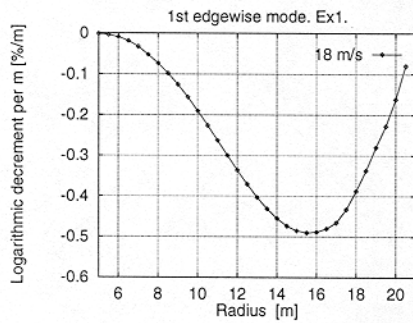
Including Stall Hysteresis

- update of dynamic stall models with respect to in-plane vibrations, the varying relative velocity and the model parameters

- try to extract information from the different field rotor experiments as basis for update of models

---

Risø Implementation of the Beddoes-Leishman Dynamic Stall model in the aeroelastic code HawC
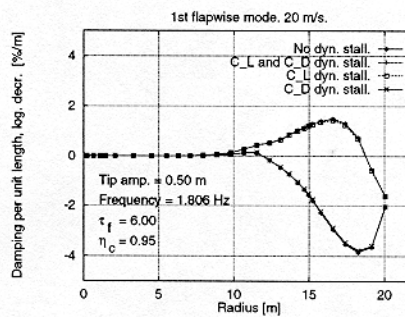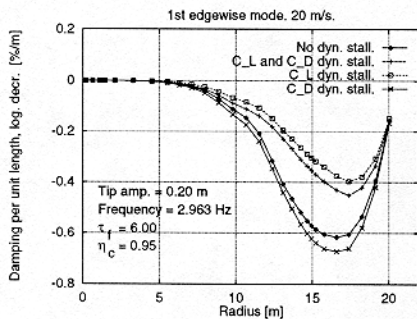
Risø Implementation of the Beddoes-Leishman Dynamic Stall model in the aeroelastic code HawC
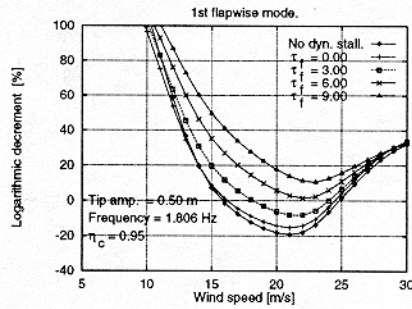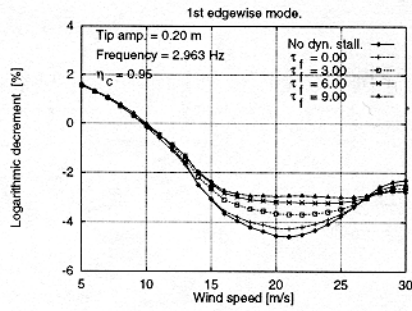
FFA Implementation and Modification of the Beddoes-Leishman Dynamic Stall model
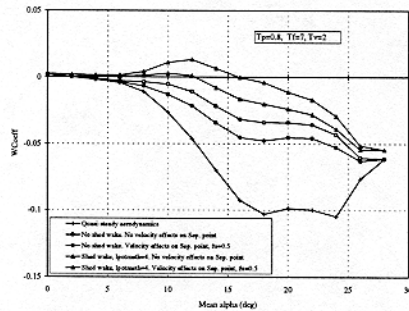
Coupled Rotor Modes and Edgewise Vibrations

LM-19.0. Mode shape 7 : 2.921 Hz.
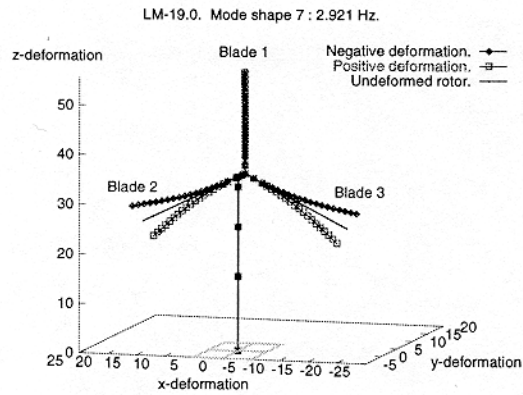
In-plane inertia force in stationary coordinates due to deformation in edgewise mode shapes (local whirl)
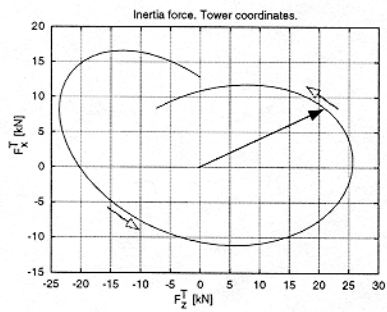
One period of the edgewise vibration   One complete rotor revolution
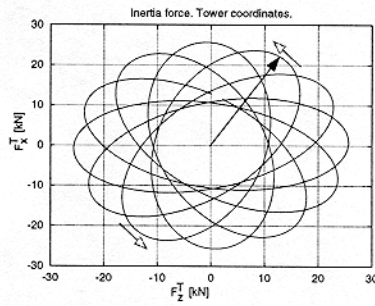
Rotor global whirl frequencies. Case 2.

$IT = 2.5\ e5\ kgm^2$
$kN = 4.0\ e7\ Nm/rad$
$kxT = 6.0\ e7\ Nm/rad$
$kzT = 0.75\ kxT$

1st whirl backwards.
1st whirl forwards.
2nd whirl backwards.
2nd whirl forwards.

LM-19.0. Mode shape 9: 3.550 Hz.

Negative deformation.
Positive deformation.
Undeformed rotor.

z-deformation

x-deformation

y-deformation
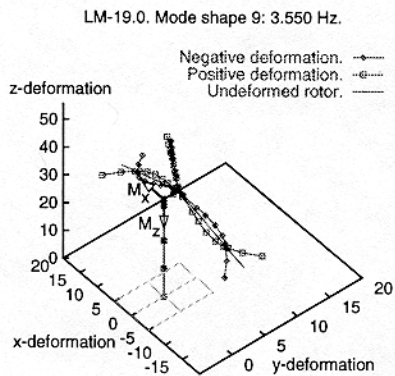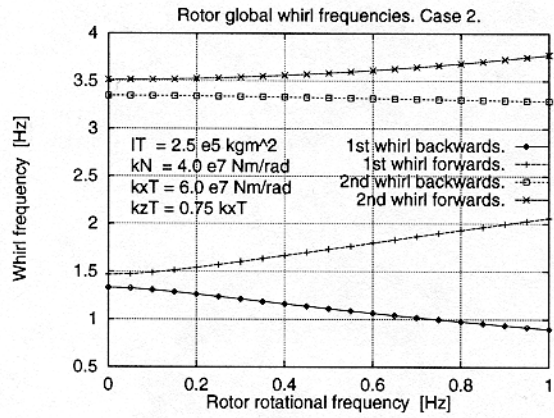
Effect of changing main shaft stiffness
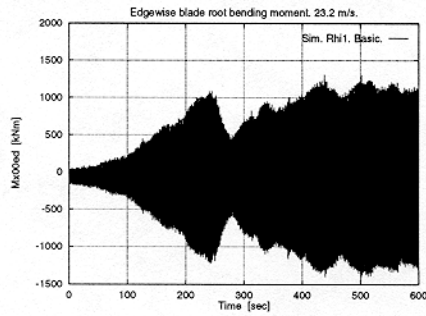
Normal shaft stiffness
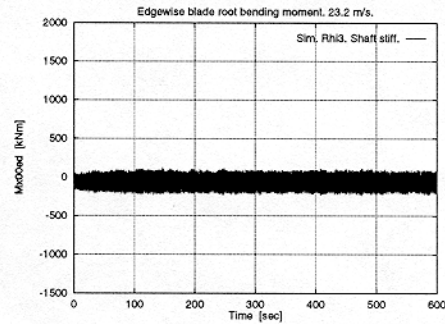
Increased shaft stiffness

Conclusions from STALLVIB

using a simple quasi- steady aerodynamic model for a two-dimensional blade section showed the importance of:

- the quasi steady C_L and C_D characteristics
- the direction of vibration of the blade section

- using a simple quasi- steady aerodynamic model ing a simple mode shape representation of the blade. This part of the work showed the importance of:

  - the mode shape of the blade
  - the mode shape vibrational direction

Appendix H:

Presentation by G. Leishmann, University of Maryland

"Leishman-Beddoes" Dynamic Stall Model: Original Development & Intent

Presented at:

National Wind Technology Center,
National Renewable Energy Laboratory,
Boulder, Colorado
Oct. 5, 1998

by

J. Gordon Leishman,
Dept. of Aerospace Engineering,
University of Maryland, College Park,
Maryland 20742

Ph: (301) 405-1126
FAX: (301) 314-9001
e-mail: leishman@eng.umd.edu
http://www.enae.umd.edu/AGRC/aero.html

Helicopter Rotor Flow Structure

Main rotor/tail rotor interactions

Dynamic stall on retreating blade

Blade/tip vortex interactions

Main rotor/empennage interactions

Rotor wake/airframe interactions

Hub wake

Tip vortices

Transonic flow / shock induced separation on advancing blade
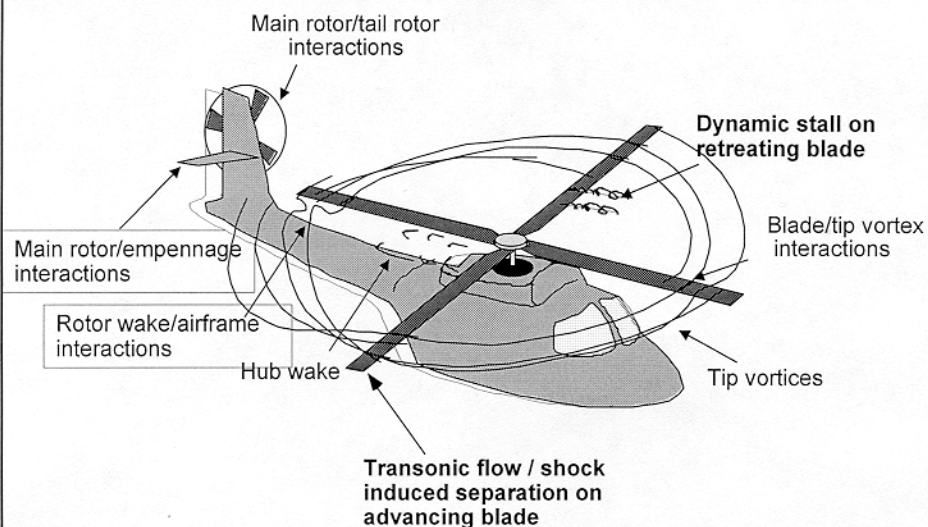
JGL 10/98

Environment for Typical Section

High Lift Boundary
(Dynamic stall)

Stall Boundary
(Affected by airfoil shape)

High Speed Boundary
(Shock induced separation)

170 knots

155 knots

Angle of attack (deg.)

Mach number, M
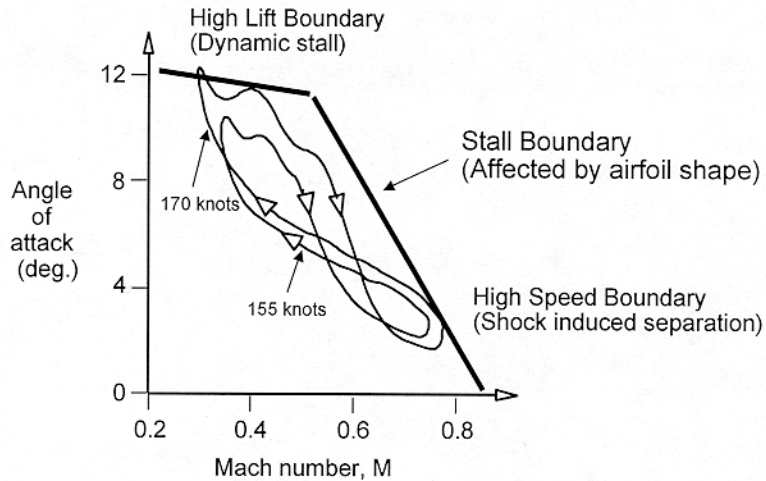
JGL 10/98

Semi-Empirical Models

❏ Designed for use in rotor airloads and aeroelastic applications (comprehensive models). Computationally inexpensive.

❏ Used to predict integrated unsteady airloads (i.e., lift, moment & drag) to a 'best attainable' level of approximation.

❏ Root for most models is in linearized unsteady thin airfoil theory.

❏ For 'non-linear' part various levels of sophistication possible, but some models have limited physical basis (e.g., sythesization methods).

❏ Limited in application by range of experimental data used for formulation and/or validation purposes.

❏ Mainly validated against data from pitch oscillation experiments, yet substantialn AoA from blade flapping (plunge) wake inflow (convecting non-uniform vertical upwash).

❏ Generally give better rotor airloads predictions than without these models. Yet, validation is difficult because of other uncertainties.

JGL 10/98

Time-Delay Method (Beddoes, 1976)

❏ *Formulated in time-domain.*

❏ *Indicial method using Duhamel superposition. Versatile.*

❏ *Incompressible Wagner indicial function and non-circulatory (apparentcy.*

❏ *Dynamic stall forces and moments modeled as a series of discrete events linked by statistically measured 'delay' terms.*

❏ *Stall onset based on delayed AoA criterion.*

❏ *Did not reduce to static airfoil characteristics in limit as k --> 0.*

❏ *Tendency to suffer from numerical problems from 'switch states,' particularly for predicting stall onset, which can cause problems when coupled to an elastic blade model.*

❏ *Did not distinguishertical velocity across the chord, e.g., gusts, BVI etc.*

Motivation for New Model (1983)

❏ *Existing model not fully adequate to model the behavior of some rotor airfoils, especially those that exhibit trailing-edge separation.*

❏ *Existing unsteady attached flow model based on 'incompressible' assumptions. Inadequate for many problems. But retain versatility of indicial approach.*

❏ *Properly delinate mode of forcing on indicial responses, i.e., AoA, plunge, pitch rate, non-uniform vertical velocity.*

❏ *Unsteady drag model in existing model not fully adequate.*

❏ *Existing stall onset model (delayed AoA) not accurate enough for newer airfoils.*

❏ *Existing 'switch' states are often problematic (e.g., stall onset).*

❏ *Better numerical solutions required for convolution process. Preferred scheme depends on time constants of dynamic system.*

❏ *Must have a lesser dependence on measured unsteady airfoil data.*

❏ *Better validation required (data for 14 airfoils available from ARA).*

Original Objectives of L-B Model

❏ *Emphasis on modeling unsteady attached flow (lift, moment & drag).*

❏ *Retain indicial formulation. New root of model is in subsonic unsteady airfoil theory.*

❏ *Must represent compressibility effects (Mach number dependent amplitude & phasing effects on airloads).*

❏ *Model the nonlinear trailing-edge stall characteristic of modern cambered helicopter airfoil sections.*

❏ *Model must reduce to static airloads as k--> 0.*

❏ *Accurately define dynamic stall onset conditions (I.e. separation).*

❏ *Must use a minimum number of empirical coefficients. Most should be derivable from quasi-steady airfoil data.*

❏ *Must be well validated with measured airfoil data, minimizing empiricism as improved understanding is obtained.*

❏ *Should retain numerical efficiency as far as possible compared to existing models.*

L-B Aerodynamic Model (1986/88)

❏ *Three main subsystems:*
  - *Attached flow subsystem (subsonic linear theory)*
  - *Trailing-edge separation subsystem (Kirchhoff/Helmholtz theory)*
  - *Leading-edge separation onset system*
  - *Vortex induced airloads subsystem*

❏ *Each subsystem is a simplified representation of the physics associated with key elements of the unsteady airfoil behavior and dynamic stall process.*

❏ *Subsystems arranged in "open-loop" or Kelvin chain, where the output from one subsystem forms the input to the next.*

❏ *As few empirical coefficients as possible. All have some physical significance, most can be derived from static airfoil results.*

❏ *Extensive validation with experimental results at subsystem level and for full model.*

❏ *Published at AHS Forum 1986 & in revised form in JAHS 1988.*

Extensions to Basic Model (1987-97)

- Refined subsonic indicial response functions for attached flow. (AIAA JofA 1987, AIAA JofA 1994).
- Extension to handle sweep (yawed) flow conditions (AHSJ 1988, Sikorsky 1984).
- State-space (ODE) version of basic model (AIAAJ 1989, SDM 1989).
- Distinguishitch vs. plunge effects on stall onset (AHSJ 1991).
- Representation of unsteady free-stream effects (AHSJ 1991).
- Unsteady flap motion (AIAA JofA 1993, JofA 1995).
- Three-dimensional (finite-wing) effects (Ames Workshop 1994, Sikorsky 1995).
- Non-stationary convecting gust type problems (AIAAJ 1997).
- Improved numerical methods for Duhamel superposition (1997).

Attached Flow Subsystem

- Indicial responses for lift and moments (generalized in terms of mode of forcing and Mach number alone).
- Indicial lift and moments resulting from AoA, pitch rate, stationary sharp edge gusts.
- Basis in subsonic linear theory (Lomax) and experimental data in the frequency domain, which are used to relate back to the indicial response. CFD used to supplement results.
- Exponential form of indicial response approximation lends easily to Duhamel superposition for arbitrary forcing:
  - finite difference approx. leads to one-step recursive formulation
  - transfer function leads to state-space form (ODE's)
- Numerically efficient - all prior time history accommodateddy drag model based on leading-edge suction concept.

Trailing-Edge Separation

- *Trailing-edge separation model based on Kirchhoff/Helmholtz theory. Analytic results for lift, moment & drag for flat plate with defined separation point.*
- *Airfoil static lift measurements used to derive 'effective' separation point from C_N vs. AoA data.*
- *Effective separation point (as function of AoA) can be generalizd empiricallyas a function of AoA.*
- *By cross-plotting 'f' versus the centerfunction of AoA.*
- *The pressure drag can also be computed as a function of 'f'.*

$$C_N = C_N^c \left[\frac{1 + \sqrt{f}}{2} \right]^2$$
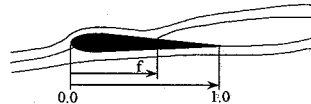
Unsteady Effects on Separation Point

- *Time-dependent effects introduced into the separation point movement by two additional first-order systems that represent:*
  - *effect of unsteady pressure distribution on b.l. response (outer solution)*
  - *effects of unsteadiness within boundary layer itself (inner solution)*
- *The latter model is equivalent to the Prandtl 'spring-mass-damper' model used to explain b.l. behavior.*
- *The time constants of these two systems (T_p and T_f) are obtained from measurements of unsteady pressure response at airfoil l.e. and calculations performed using unsteady boundary layer theory and verified by correlation studies.*
- *The contribution of the motion to l.e. pressure lag (and T_p) can be further decomposed into "AoA" contributions and "pitch rate" contributions.*
- *The resulting system produces a hysteresis effect on airloads.*

JGL 10/98

Stall-Onset Model

□ The onset of leading-edge separation is dependent upon the attainment of high suction pressure & adverse pressure gradient.

□ Indicial method does not readily lend to the calculation of unsteady chordwise pressure without significant cost.

□ Therefore, an integrated parameter is required that can be related to the pressure distribution to determine stall onset.

□ It is possible to correlate a critical value of the normal (lift) force that is coincident with the collapse in l.e. pressure at stall (C_{N_1})

□ Under unsteady conditions there is essentially a first-order type lag between the instantaneous normal force, $C_N(t)$, and the unsteady l.e. pressure response.

□ The computed normal force can be used via a first-order system to create a pseudo value of normal force (C_N') such that when $C_N' = C_{N1}$ then l.e. separation is said to occur.

JGL 10/98

Dynamic Stall Vortex Loading

□ Modeled as another first-order dynamic system.

□ Effects of accretionted for via 'excess lift.'

□ When rate of change of lift is high, vortex induced loads are high.

□ In the limit as the forcing becomes zero (q-s case), the accumulatednt time constant.

□ Center of pressure movement linked to stall onset model, with statistically determined vortex convection time-constant.

JGL 10/98

Sub-System Coupling Coefficients

❑ *Various 'coupling' strategies between sub-systems are imposed based on correlation studies with unsteady airfoil measurements.*

❑ *All are feed-forward adjustments to sub-system time constants, and have a hierarchicalic and computational overhead.*

❑ *However, coupling strategies lead to significant improvement in predictive capabilities for combined forcing conditions.*
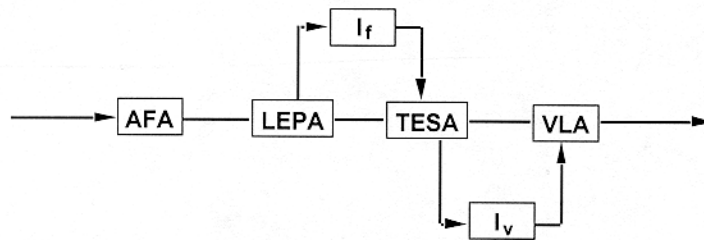
JGL 10/98

Pitch Oscillation: Attached Flow

NACA 23010, M=0.6, k=0.13

JGL 10/98

H-9

Plunge Oscillation: Attached Flow

NACA 23010, Plunge, M=0.4, k=0.12

Pitch Oscillation: Light Stall

NACA 23010, M=0.6, k=0.09

Pitch Oscillation: Dynamic Stall

NACA 23010, M=0.4, k=0.062

Pitch Oscillation: Dynamic Stall

NACA 23010, M=0.4, k=0.12

Plunge Oscillation: Dynamic Stall

NACA 23010, M=0.4, k=0.13

Pitch Oscillation: Post Stall

NACA 23010, M=0.6, k=0.085
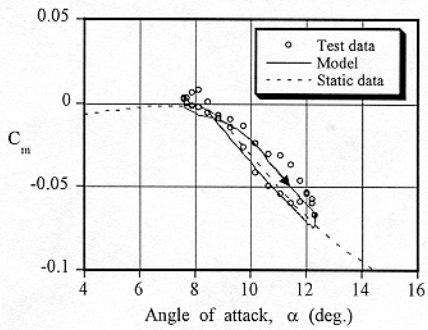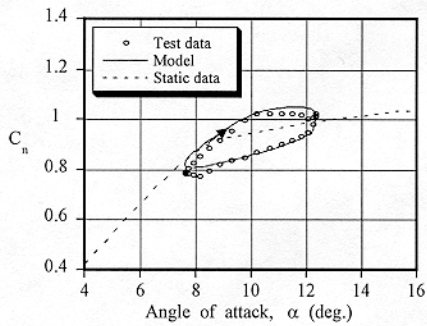
Appendix I:

Presentation by K. Pierce, NREL

The Beddoes-Leishman Model as Implemented in AeroDyn

Kirk Pierce

NREL / NWTC

October 5, 1998

Outline

- The Beddoes-Leishman Dynamic Stall Model
- Modification to the Model
- 2-D Wind Tunnel Comparisons
- Comparisons with CER Data
- Difficulties with the Model
- Conclusions
- Other Issues

The Beddoes-Leishman Model for Unsteady Aerodynamics and Dynamic Stall

- Only steady 2-D airfoil data are required for implementation of model.
- Model is semi-empirical, based on airfoil indicial response.
- The airfoil response to a general angle of attack history is computed by superposition of airfoil indicial responses.
- The non-linear trailing edge separation is modeled based upon Kirchoff flow:

$$C_N = C_{N\alpha}(\alpha - \alpha_0)\left(\frac{1 + \sqrt{f}}{2}\right)^2$$

$$C_C = \eta C_{N\alpha}(\alpha - \alpha_0)\alpha\sqrt{f}$$

where C_N is the normal force coefficient, C_C is the chordwise force coefficient, $C_{N\alpha}$ is the lift curve slope, α is the angle of attack, α_0 is the zero lift angle of attack, and f is the separation point.

The Beddoes-Leishman Model for Unsteady Aerodynamics and Dynamic Stall

- The vortex shedding is modeled as an increase in circulation near the airfoil.
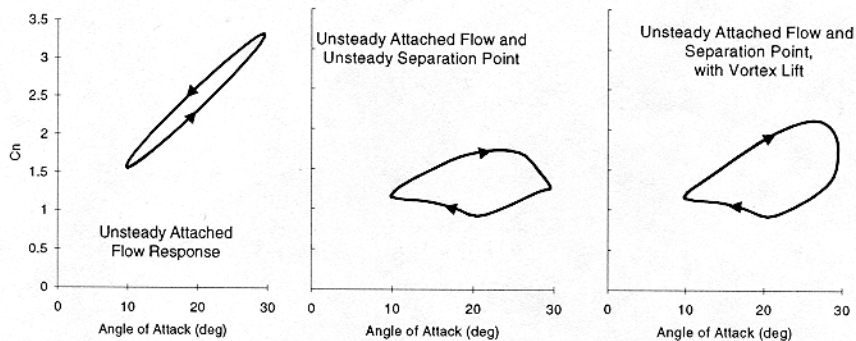
Modifications to the Model

- Published results consider angles of attack from -10° to +30°, however wind turbines often operate outside this range.
- The method was used without modification for the range +90 to -90.
- To extend the model for angles of attack beyond -90° and +90° the angle of attack is mirrored about +90° or -90°.

Effective Angle of Attack / Angle of Attack
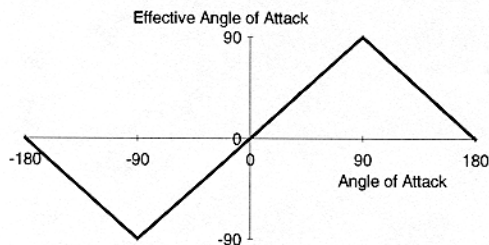
Modifications to the Model
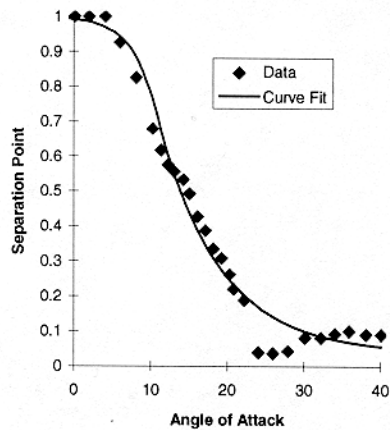
- Exponential curve fit representation of separation point did not accurately follow data.

Modifications to the Model

- Coefficients regenerated from the exponential curve representation did not accurately reproduce static values.
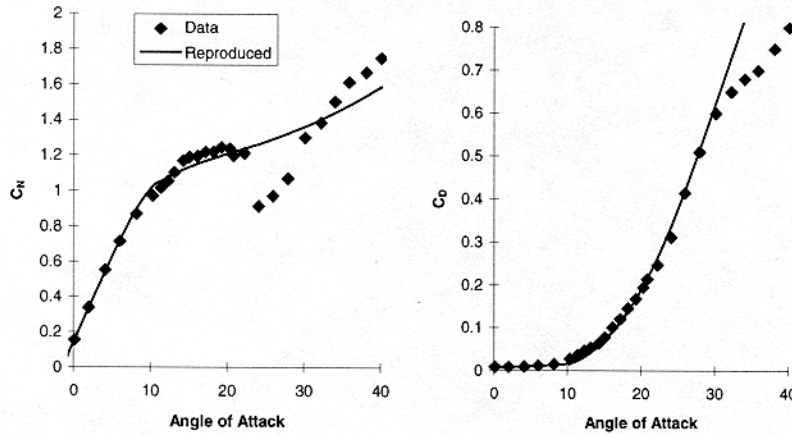
Modifications to the Model

- Use of two separation parameter tables, one for C_N and one for C_C.
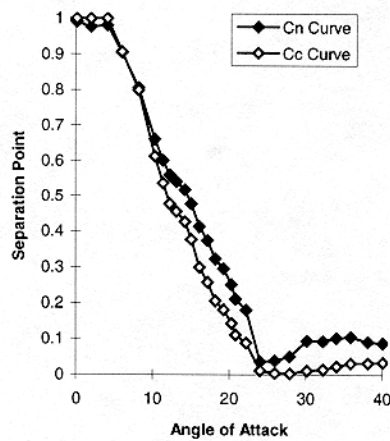
$$C_N = C_{N\alpha}(\alpha - \alpha_0)\left(\frac{1 + \sqrt{f_N}}{2}\right)^2$$

$$f_N = \left(2\sqrt{\frac{C_N}{C_{N\alpha}(\alpha - \alpha_0)}} - 1\right)^2$$

$$C_C = \eta C_{N\alpha}(\alpha - \alpha_0)\alpha\sqrt{f_C}$$

$$f_C = \left(\frac{C_C}{\eta C_{N\alpha}(\alpha - \alpha_0)\alpha}\right)^2$$

I-5

Modifications to the Model

- Use of two separation parameter curves allows the model to accurately regenerate force coefficients for very general inputs.
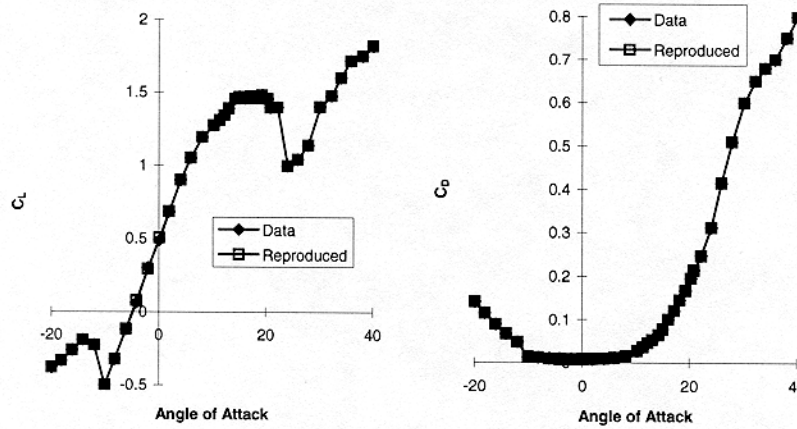
Modifications to the Model

- Hysterisis for unusual angle of attack ranges.
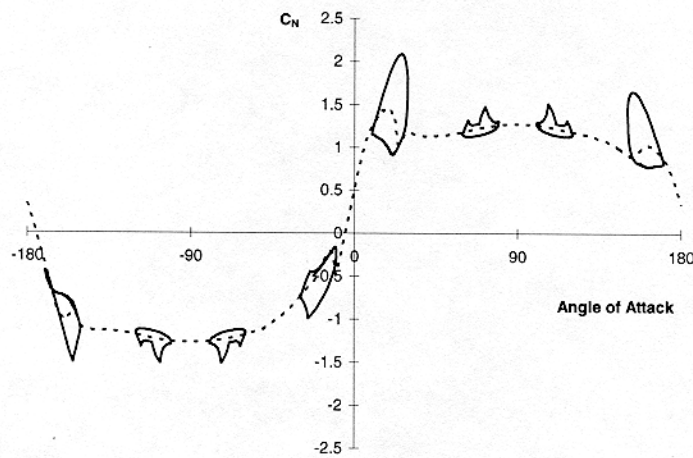
Modifications to the Model

- Vortex effect on C_C

$$C_{C_v} = C_{N_v} \alpha (1 - \tau_v)$$

- Polynomial curve fit to C_M not used to model unsteady separation point effect on C_M.
- C_M unsteady separation effects determined by lookup of C_M at lagged effective angle of attack.

$$\alpha_f' = \alpha_f - D_{\alpha_n}$$

$$D_{\alpha_n} = D_{\alpha_{n-1}} \exp\left(\frac{-\Delta S}{T_\alpha}\right) + \left(\alpha_{f_n} - \alpha_{f_{n-1}}\right) \exp\left(\frac{-\Delta S}{2T_\alpha}\right)$$

Comparisons with 2-D Wind Tunnel Data

- OSU unsteady aerodynamic data for three airfoils.
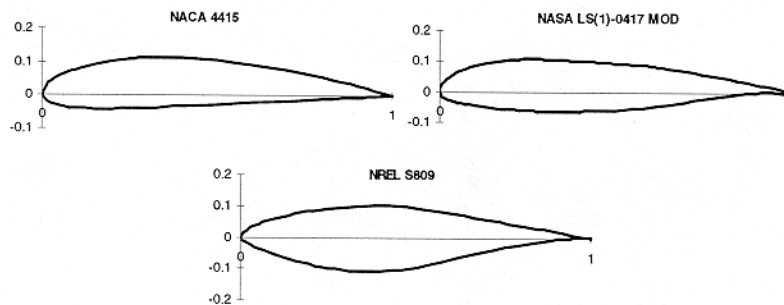
Comparisons with 2-D Wind Tunnel Data

- **NACA 4415 CL and CD comparisons, including separation point shifting. High amplitude oscillation.**
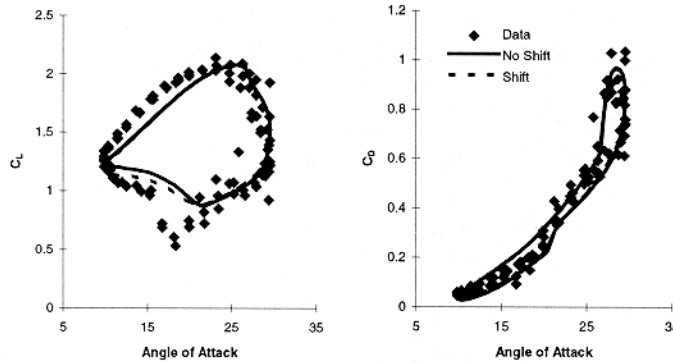
Comparisons with 2-D Wind Tunnel Data

- **NACA 4415 CL and CD comparisons, including separation point shifting. Low amplitude oscillation.**
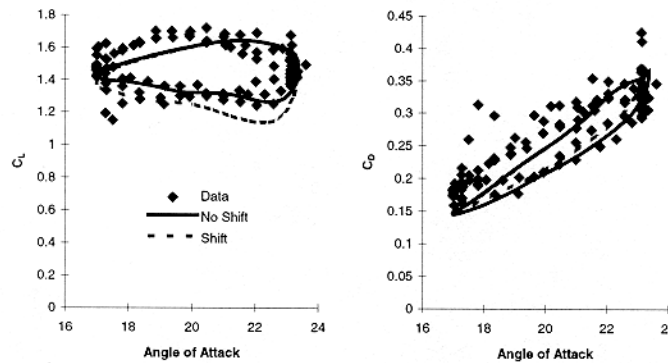
Comparisons with 2-D Wind Tunnel Data

- S809 $\alpha=14+10\sin\omega t$, k=.026, M=0.1
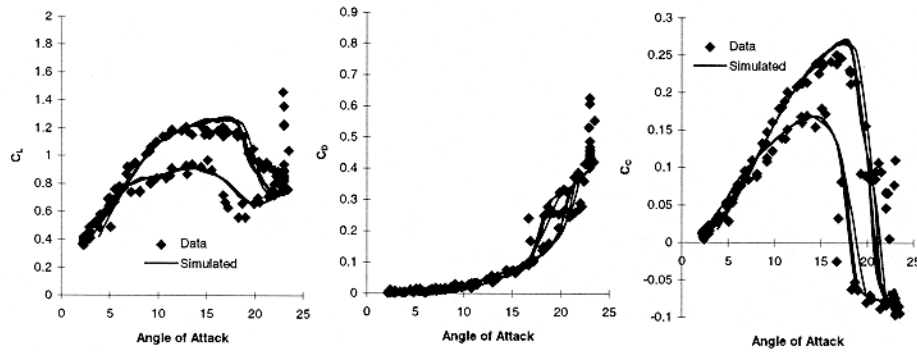
Comparisons with 2-D Wind Tunnel Data

- LS(1)-0417 $\alpha=14+10\sin\omega t$, k=.052, M=0.1
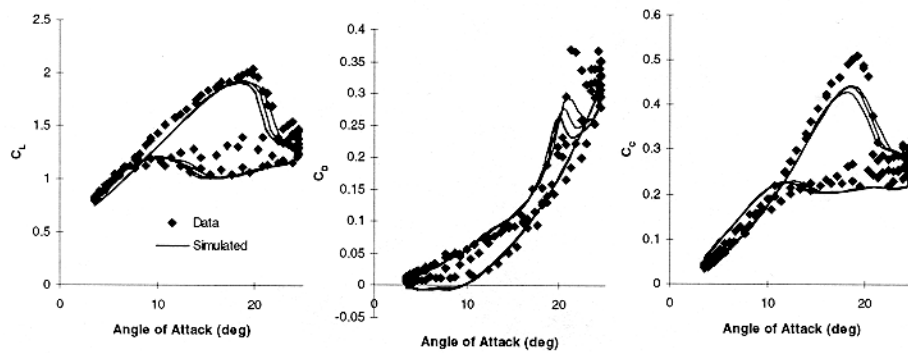
Comparisons with 2-D Wind Tunnel Data

- **NACA 4415 $\alpha=20+10\sin\omega t$, k=.096, M=0.1**
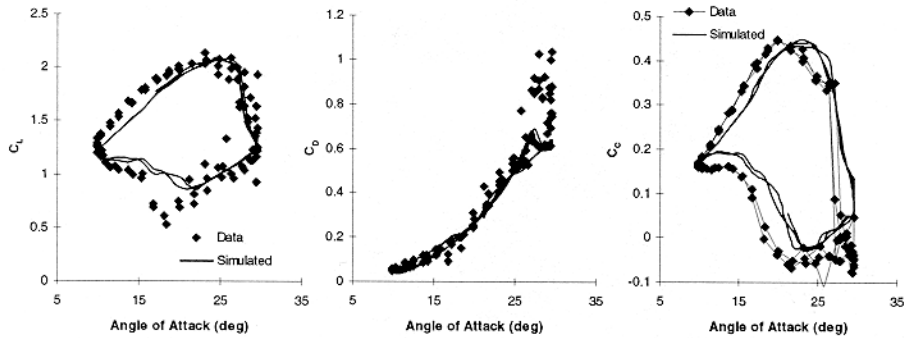
Comparisons with 2-D Wind Tunnel Data

- Moment coefficients
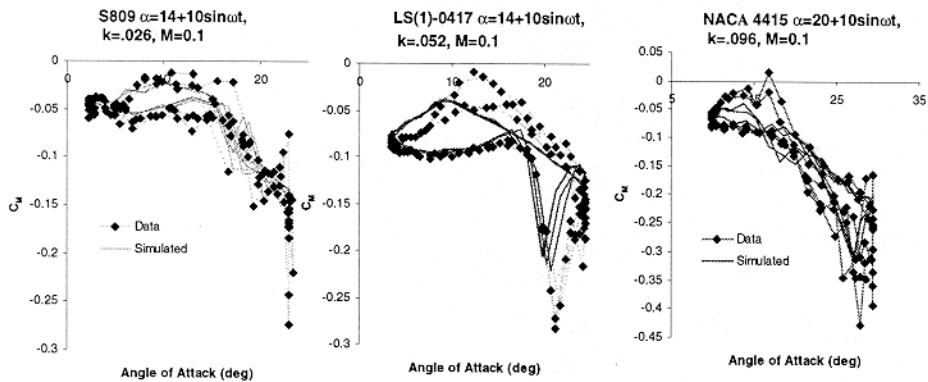
Comparisons to CER Data

- **80% radius C$_N$ comparison**
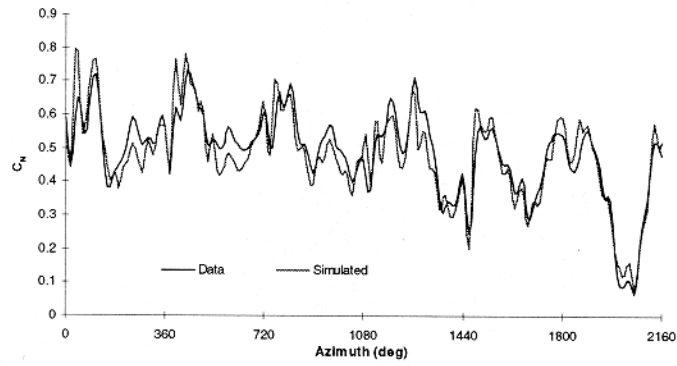
Comparisons to CER Data

- **Initial 30% span C$_N$ comparison.**
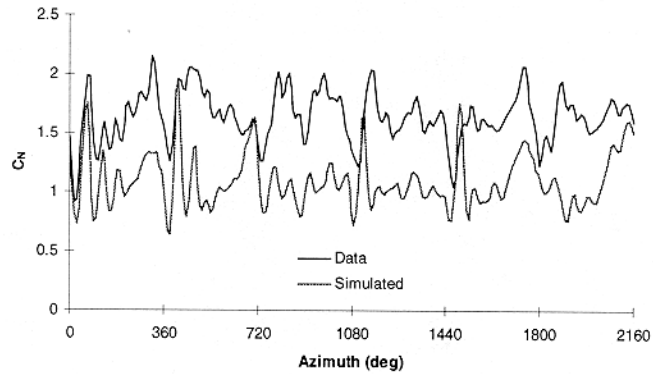
Comparisons to CER Data

- **Delayed static stall and ringing of angle of attack flag at 30% span location.**
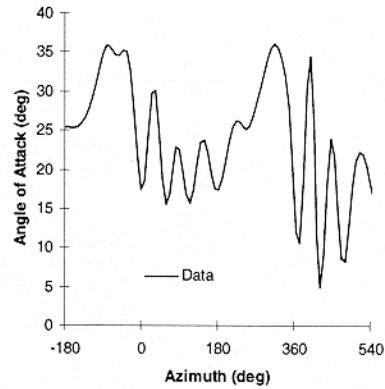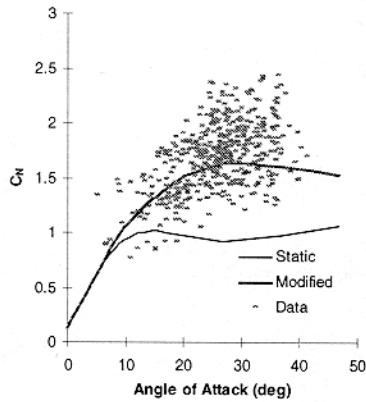
Comparisons to CER Data

- **30% span C_N comparison using modified static data.**
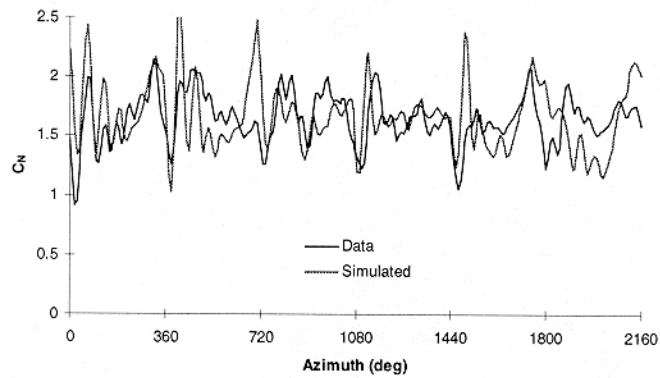
Difficulties with the model

- Attached flow hysterisis seem too wide for higher reduced frequency low Mach number cases.
- For low mean angle of attack cases flow reattaches too soon.

LS(1)-0417 $\alpha=8+10\sin\omega t$, k=.082, M=.1
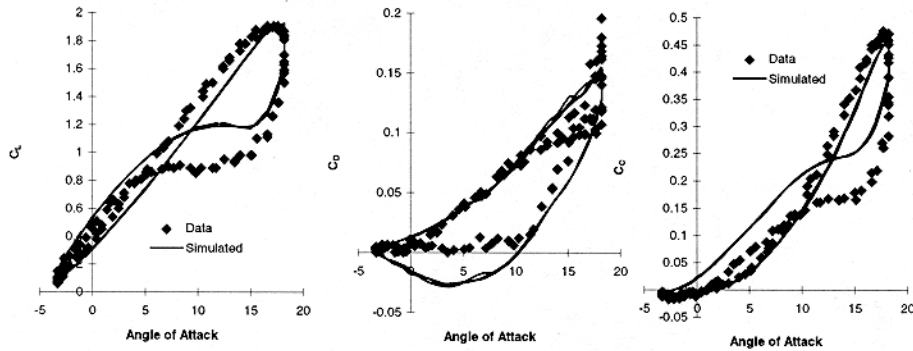
Difficulties with the model

- **Difficulties with impulsive terms at low velocities.**

$$\Delta C_{N\alpha}^{I} = \frac{4}{M}\phi_{\alpha}^{I}\Delta\alpha \qquad\qquad \Delta C_{M\alpha}^{I} = -\frac{1}{M}\phi_{\alpha M}^{I}\Delta\alpha$$

$$\Delta C_{Nq}^{I} = -\frac{1}{M}\phi_{q}^{I}\Delta q \qquad\qquad \Delta C_{Mq}^{I} = -\frac{7}{12M}\phi_{qM}^{I}\Delta q$$
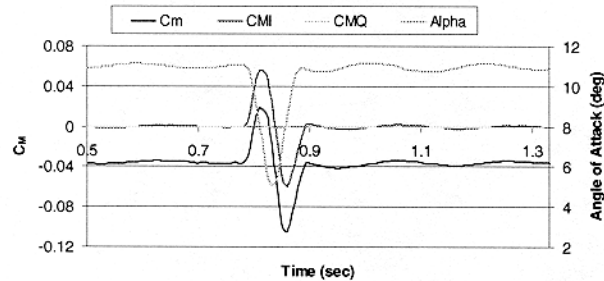
Conclusions

- Modifications allow the model to accurately reproduce static data and generate coefficients for the entire angle of attack range.
- Comparisons between predicted and measured aerodynamic force coefficients are generally in good agreement.
- The model seems capable of accurate simulation of measured coefficients for the 80% span of the CER.
- It is also capable of modeling the 30% span coefficients if static data are modified to account for the delayed static stall.
- Improvements could be made in stability of non-circulatory component, prediction of maximum drag, and flow reattachment for low mean angle of attack.

Other Issues

- Pitch versus plunge versus ΔV airfoil response.
- 3-D effects
- Develop attached flow response for incompressible flow?

Appendix J:

Presentation by A. Bjorck, FFA

Presentation of the FFA use of the Beddoes-Leishman model including FFA-modifications of the model

NREL-NASA Ames test
Panel meeting#1 October 5-6 1998

Presentation by Anders Björck, FFA

Background:

A dynamic stall model was needed for the aeroelastic simulation code, VIDYN, used in Sweden (Code developed by a consultancy company Teknikgruppen)

FFA have experience from co-ordinating the EU JOULE II project "Dynamic stall and 3D effects".

Recent experience comes from work within the "Stallvib" project concerning mainly edge wise vibrations

When the Beddoes model was going to be implemented, a few things were thought of:

- For oscillations in the lead-lag direction, both the angle of attack and the relative velocity will change.

- The drag will contribute to the aerodynamic damping to a much higher extent than for flap-wise oscillations.

The treatment of drag and a varying velocity was given therefore given new attention.

This presentation

- Basic features of the FFA-Beddoes dynamic stall model

- Some comments from the use to calculate aerodynamic damping of edgewise vibrations.

- Comments on limitations, problems and needed improvements

Dynamic stall model used by FFA:

Origin: Beddoes-Leishman model, Øye-model.

Steps of calculation, more or less like original Beddoes model:

1) Compute impulsive loads

2) Compute shed wake effects. $\alpha_E = \alpha_{75} - \alpha_i$

   α_{75} is the angle of attack at x/c=75%, including pitch rate effects

3) Compute a shift in angle of attack due to leading edge pressure response. Time constant T_p.
   $=> \alpha_p => f_p$

4) Compute a lag in the separation point position.

   $$\frac{df}{ds} = \frac{f_p - f}{T_f} \qquad \text{non-dimensional time } s = \frac{2tV_{rel}}{c}$$

   Compute dynamic $C_l = C_{l,f}$ from an equation linking C_l to f. (f having the interpretation as the point of separation.)

5) Compute vortex lift. Assumed to act only in the direction normal to the chord.

6) Add components of lift: Impulsive lift, vortex lift and $C_{l,f}$

7) Add components of drag: Static drag, induced drag, vortex drag and separation drag.

The model is used with the f-function linked to the lift and works in C_l and C_d.

The model uses a $C_l(f)$-function borrowed from Øye.

$$C_l = f \cdot C_{l,inv}(\alpha_E) + (1-f) \cdot C_{l,sep}(\alpha_E) \qquad (1)$$
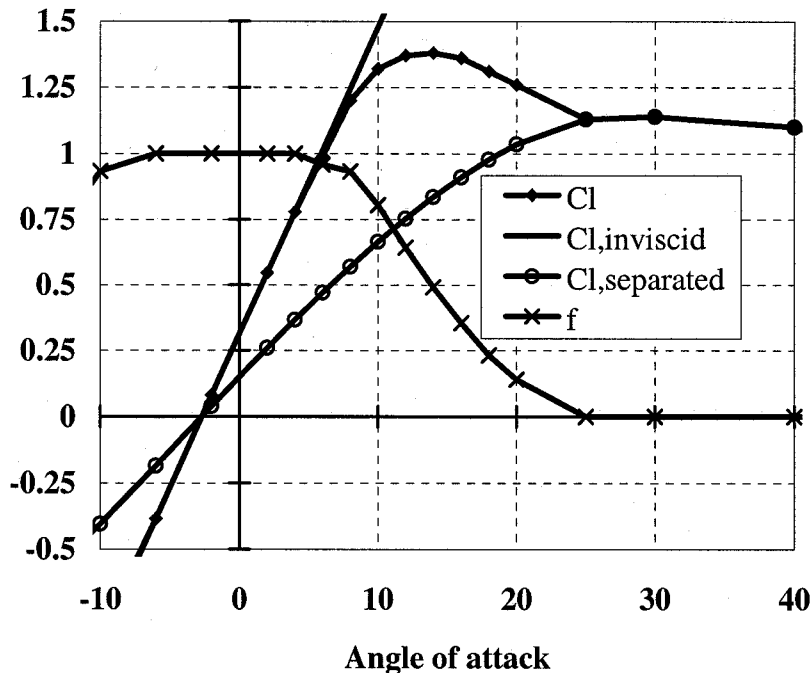
Figure 1. Static C_l and f-function.

The definition of $C_{l,sep}$ is rather arbitrary, which is undesired.

It is therefore planned to use the "Kirchoff" formulation

$$C_l = 0.25 \cdot C_{l_\alpha}\left(1+\sqrt{f}\right)^2(\alpha - \alpha_0) \qquad (2)$$

with the static $f(\alpha)$ function computed from eq (2) with the static $C_l(\alpha)$ curve. This reduces the arbitrariness in the use of the model.

Changes to the Beddoes dynamic stall model.

Varying velocity: $V_{rel} = V_{rel}(t)$

Two effects adressed:

I) The shed wake

II) Boundary layer effects

Further, the drag is modelled with three componenents added to the static value. The drag includes changes due to three components: induced drag, vortex drag and "separation drag"

```
cdind=sin(alfa75(ib,ir)-alfaeq)*(clf-cl_imp)
cdsep=acd(ipr)*(clstat-clf+cl_imp)
cdvor=cnv(ib,ir)*sin(alfa(ib,ir))
cd=cdstat+cdind+cdsep+cdvor
```

acd is an empirical constant.

Shed Wake effects

Original Beddoes:

A step in angle of attack gives the circulatory lift

$$\Delta C_{l_c} = C_{l_\alpha} \phi_c \Delta \alpha \tag{3}$$

$$\phi_c = 1 - A_1 \, exp(-b_1 \beta s) - A_2 \, exp(-b_2 \beta s) \tag{4}$$

Change 1. Gamma formulation (From Harris)

Equation (3) is replaced by equation (5)

$$\Delta \Gamma = C_{l_\alpha} \cdot c \cdot 0.5 \cdot \phi_c \cdot \Delta w \tag{5}$$

(w is the velocity component normal to the airfoil. Small angle approximations is are used and $w = V_{rel}(\alpha_{75} - \alpha_0)$)

Further changes:

$\Delta \alpha$ is exchanged with $\dfrac{\Delta C_{l,est}}{C_{l_\alpha}}$ \hfill (6)

or Δw with $\dfrac{C_{l,est}}{C_{l_\alpha}} \cdot \Delta V_{rel} + \dfrac{\Delta C_{l,est}}{C_{l_\alpha}} \cdot V_{rel}$ \hfill (7)

$C_{l,est}$ is obtained by (at each time step) first running steps 3-4 in the model with $\alpha_E = \alpha_{75}$

Boundary layer effects due to changes in the relative velocity

Reference to L. E. Ericsson, 1988

The unsteady Bernoulli equation at the edge of the boundary layer can be written as, (Incompressible flow)

$$\frac{\partial C_{pe}}{\partial \xi} = -2q_e \frac{\partial q_e}{\partial \xi} - 2\frac{c}{V_{rel}^2}\left(q_e \frac{\partial V_{rel}}{\partial t} + V_{rel}\frac{\partial q_e}{\partial t} \right) \qquad (8)$$

where $\xi = s/c$ (or x/c), $\qquad q_e = \dfrac{U_e}{V_{rel}} \qquad V_{rel} = U_\infty$

The first term is the gradient for the static case. For an accelerating free-stream with $\partial V / \partial t > 0$ the effective pressure gradient at the edge of the boundary layer becomes more favourable, resulting in less separation.

Assuming that α is constant gives $V_{rel}\dfrac{\partial q_e}{\partial t} = 0$. Eq. (8) then becomes:

$$\frac{\partial C_{pe}}{\partial \xi} = -2q_e \frac{\partial q_e}{\partial \xi} - 2\frac{c}{V_{rel}^2}\frac{\partial V_{rel}}{\partial t}q_e \qquad (9)$$

The second term in the equation can be viewed as the modification of $\dfrac{\partial C_{pe}}{\partial \xi}$ due to a varying velocity and

$$\Delta \frac{\partial C_{pe}}{\partial \xi} = -2\frac{c}{V_{rel}^2}\frac{\partial V_{rel}}{\partial t}q_e = -4\gamma q_e \qquad (10)$$

where γ is the non-dimensional velocity change rate

The velocity effect on the pressure gradient is translated into a change in angle of attack.

The point of separation, f, is determined using this corrected angle of attack as step 2b in the dynamic stall model.

The assumption is: At $\alpha = \alpha + \Delta\alpha_v$, the pressure gradient for the case with varying V_{rel}, is the same as for the case with constant V_{rel} at α.

$\Delta\alpha$ could then be computed as

$$\Delta\alpha_v = -\Delta\frac{\partial C_{pe}}{\partial\xi} \Bigg/ \frac{\partial^2 C_{pe}}{\partial\xi\partial\alpha} \qquad (11)$$

inserting $\Delta\dfrac{\partial C_{pe}}{\partial\xi}$ from eq. (10) we get

$$\Delta\alpha_v = -\gamma\cdot 4\cdot q_e \Bigg/ \frac{\partial^2 C_{pe}}{\partial\xi\partial\alpha} \qquad (12)$$

The change in angle of attack is used to define a corrected angle of attack as a step 3b.

$$\alpha_v = \alpha - \gamma\cdot f_u$$

The angle of attack, α, is here the effective angle of attack or the angle of attack α_E corrected for the inviscid pressure response, α_p.

f_u is presently a constant. Based on investigations of pressure distributions the value used for f_u is presently set to 0.5.

f_u as a function of angle of attack should however be examined. One problem is the lack of experiments or CFD calculations for tuning.

Some conclusions from application of the model

- Different ways of taking the effects of a varying relative velocity into account have a rather large effect on the value of aerodynamic damping for edgewise vibrations.

- The drag is important for the calculation of edgewise damping. (Static value and dynamic changes)

Questions and model limitations

- How should shed wakes be taken into account considering the 3D wake? (The shed wake behind an element does not stretch out to ±infinity in the spanwise direction)

- 3D viscous effects not considered by FFA other than using 3D corrected static data as model input.

- A good modelling of vortex lift, especially with respect to 3D effects. (For the real situation, radial segments not are uncoupled)

Problems encountered

- How should parameters be tuned? Definition of a sensible objective function.

- Data from experiments or possibly CFD calculations at for relevant situations.

Strengths and weaknesses

Strength

The model is based on some physics. This means that there is hope that one could find a set of constants that works with some satisfaction for a range of airfoils.

Considering computational effectiveness, it is definitively suited for use in aeroelastic codes.

It can be exetended.

Weakness

It's a 2D model used for 3D calculations.

References to the FFA-model:

Björck, A. et al " Computations of Aerodynamic Damping for Blade Vibrations in Stall" Paper Presented at the European Wind Energy Conference, EWEC'97 Dublin, Ireland, October 1997

Jörgen Thirstrup Petersen, Helge Aagard Madsen, Anders Björck, Peter Envoldsen, Stig Öye, Hans Ganander och Danny Winkelaar. "Preiction of Dynamic Loads and Induced Vibrations in stall", Risoe-R-1045(EN), 1998

Björck, A "The FFA Dynamic Stall Model. The Beddoes-Leishman Dynamic Stall Model Modified for Lead-Lag Oscillations". Presentard vid IEA 10th Symposium on Aerodynamics of Wind Turbines i Edingburgh, 16-17 December 1996. Proceedings utgivna av Maribo Pederesen, DTU Danmark

References referred to:

Harris, A. "The role of unsteady aerodynamics in vertical axis wind turbines", Presented at BWEA workshop "recent development of wind turbines", held in Nottingham, England, February 1990.

Ericsson, L.E., and Reding, J.P., "Fluid Mechanics of Dynamic Stall Part II. Prediction of Full Scale Characteristics", Journal of Fluids and Structures (1988) 2, page 113-143.

FFA dynamic stall calculations, STALLVIB project

Dynamic stall model with different models for the shed wake

Oscillations in lead-lag, (delta=90), amplitude:s,amp=0.2, k=0.189

Tp=0.8, Tf=7, Tv=2, fufac=0.5

Static data from file: lm18oc_1.cls
file:oc_212211_s , lpotmeth=1, alfa-shift due to du/dt, fufac=0.5
file:oc_222211_s , lpotmeth=2, alfa-shift due to du/dt, fufac=0.5
file:oc_232211_s , lpotmeth=3, alfa-shift due to du/dt, fufac=0.5
file:oc_242211_s , lpotmeth=4, alfa-shift due to du/dt, fufac=0.5
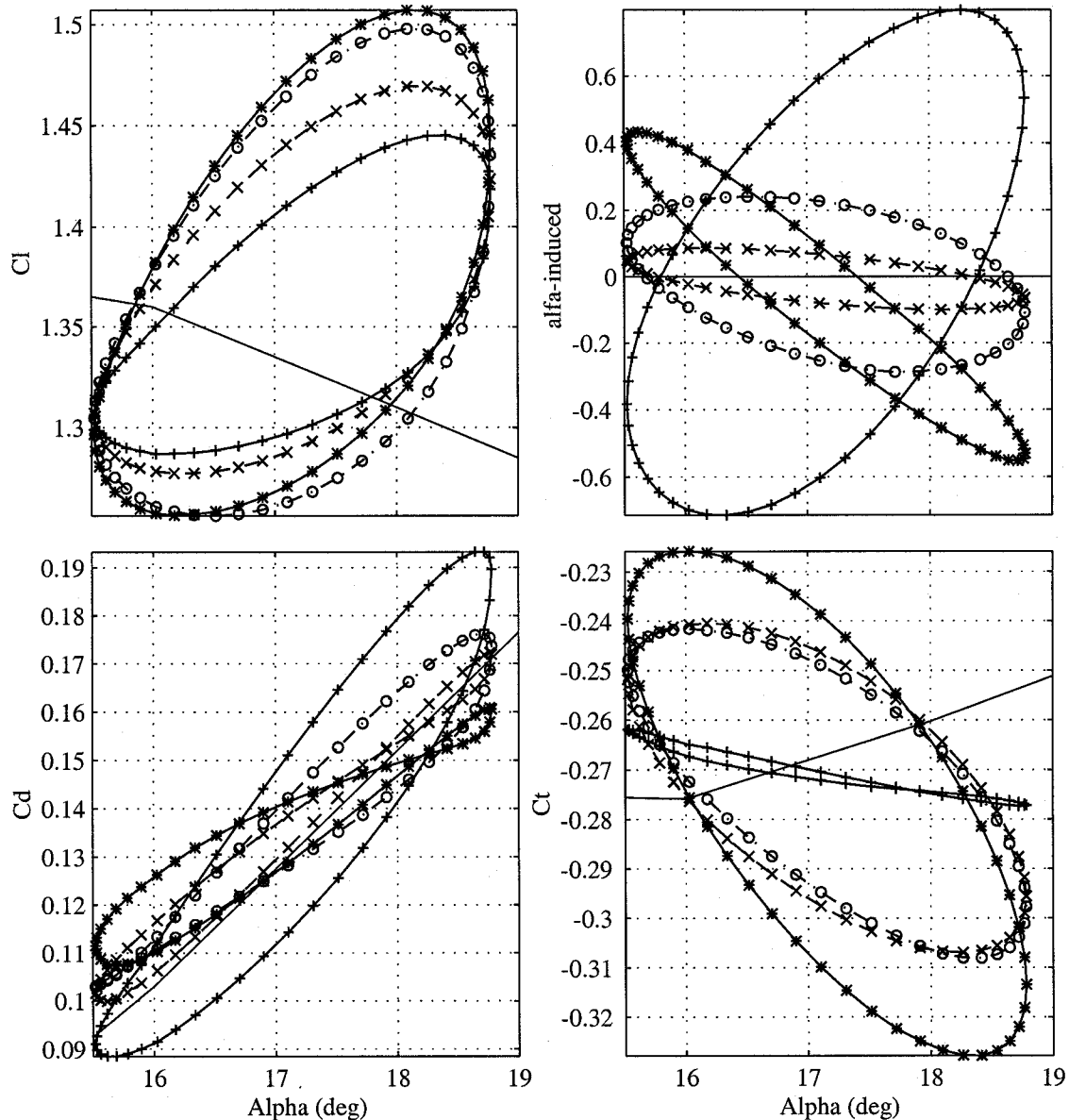
Figure 2 Calculations with the FFA Beddoes model

Lpotmeth=1: Beddoes original shed wake effect calc.

Lpotmeth=2: eq (6) used instead of $\Delta\alpha$

Lpotmeth=3: eq (5)

Lpotmeth=4: eq (7) used instead of Δw

A measure of aerodynamic damping

F_p is the aerodyanmic force parallel to the direction of translation (in the opposite direction)
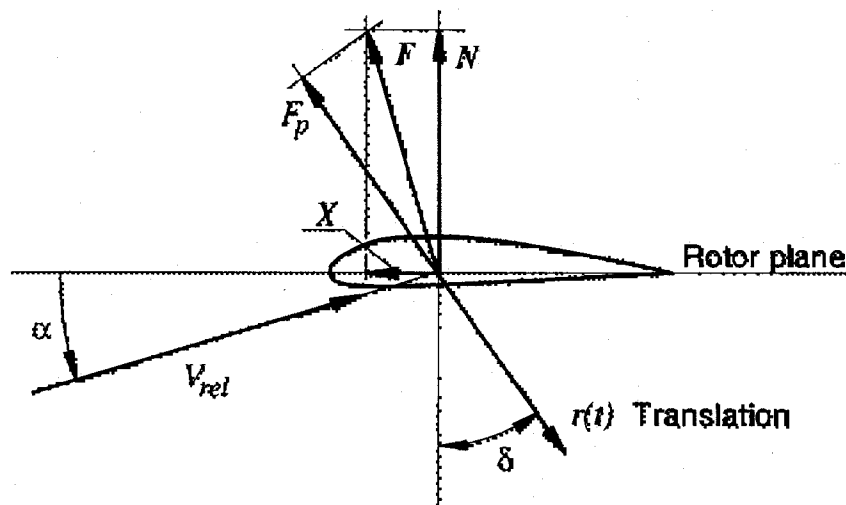
Figure 3 Forced oscillations of a blade section

$$F_p = N \cdot cos(\delta) + X \cdot sin(\delta)$$

For constant amplitude oscillations compute the work per cycle:

$$W = \oint F_p \cdot dr = c \cdot \oint F_p \cdot ds$$

Free stream velocity: $\qquad V_{rel}$

Reduced frequency: $\qquad k = \dfrac{\omega \cdot c}{2 \cdot V_{rel}}$

Translation in meter $\qquad r$

Relative translation $\qquad r/c$

Oscillations $\qquad s = s_{amp} \cdot cos(\omega t)$

Define the aerodynamic work per cycle for oscillations in the aerofoil normal direction using quasi-steady aerodynamics and small angles: W_{qs}

$$L = N = 2 \cdot \pi \cdot \alpha \cdot \tfrac{1}{2} \cdot \rho \cdot c \cdot V^2$$

$$W_{qs} = 4 \cdot \pi^2 \cdot \tfrac{1}{2} \cdot \rho \cdot V^2 \cdot k \cdot \left(c \cdot s_{amp}\right)^2$$

(Two dimensions; work per unit length)

For oscillations in a general δ-direction, with non-linear aerodynamics including dynamic stall, define a coefficient proportional to the aerodynamic damping:

$Wcoeff = W/W_{qs}$
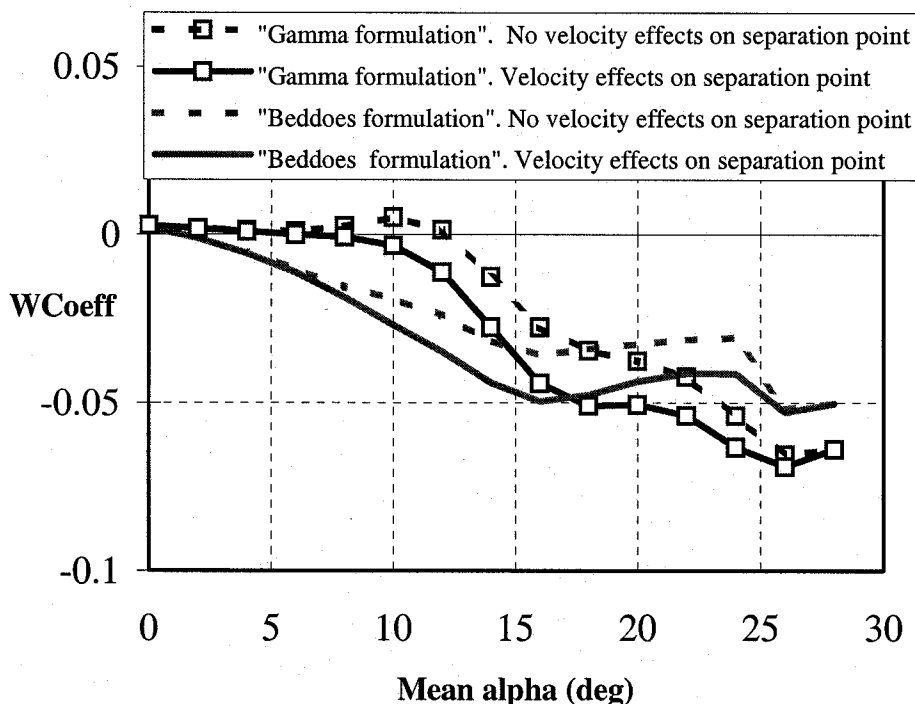
Figure 4 Results from calculations of damping. Oscillation amplitude s/c=±0.2 at a reduced frequency k=0.2.
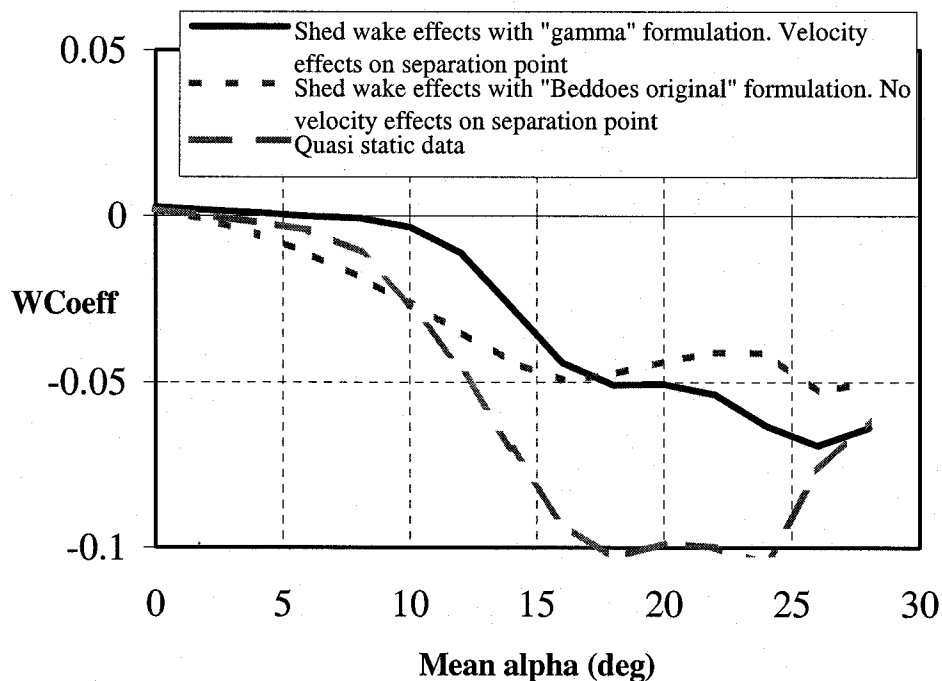
Figure 5 Results from calculations of damping. Oscillation amplitude s/c=±0.2 at a reduced frequency k=0.2
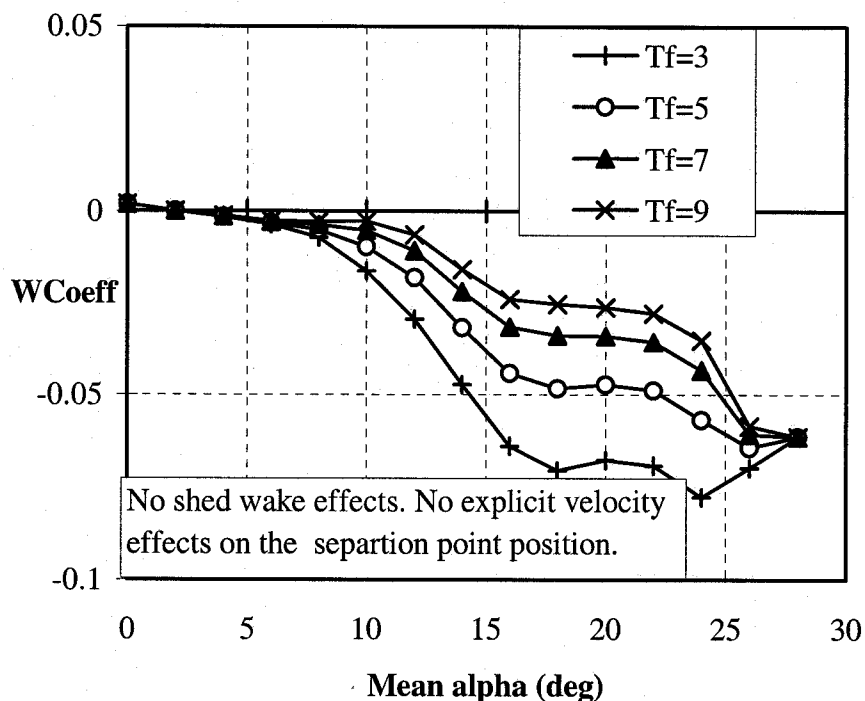
Figure 6 Results from calculations of damping. Oscillation amplitude s/c=±0.2 at a reduced frequency k=0.2. various values of Tf
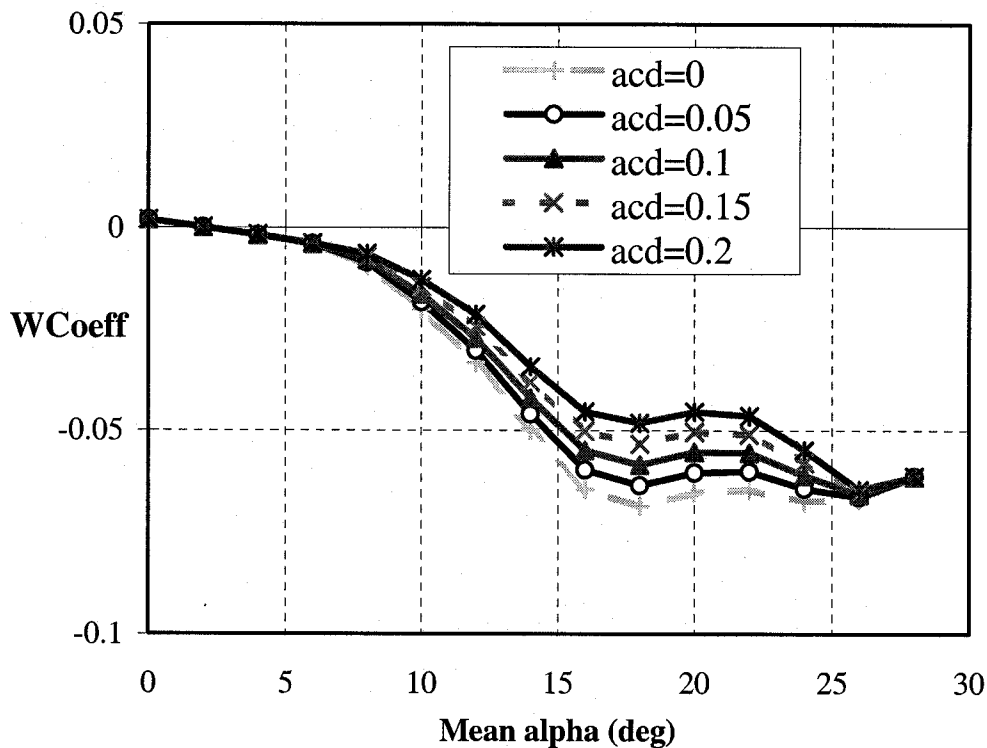
Figure 7 Results from calculations of damping. Oscillation amplitude s/c=±0.2 at a reduced frequency k=0.2. Various values for the constant acd in the calculation of separation drag

Appendix K:

Presentation by H. Snel, ECN

Engineering models used at ECN
(PHATAS code)

- Prandtl tip correction
- Empiric relation between inflow and axial force for turbulent wake state
- Dynamic inflow: dynamic momentum-force balance on annulus level
- 3D effects (especially in stall) on sectional aero-characteristics with help of 'RFOIL'
- Dynamic stall model including self excited vortex shedding
- Improved (2nd harmonic) inflow distribution for yawed flow (skewed wake)

Framework for Discussion

What are the present problems, uncertainties, etc

$\updownarrow$

How can these be (partially) solved by NREL
NASA-Ames wind tunnel measurements

Prandtl tip correction

Applied in usual way: F is Prandtl correction factor
  Fu_i is average induction over annulus, u_i is local
  induction at blade position

$$F = \frac{2}{\pi}\arccos\left\{\exp\left(\frac{-B(1-r/R)}{2\sin\phi_{\text{inf}}\, r/R}\right)\right\}$$

This is the only place where B (number of Blades)
  enters explicitly in the BEM formulae

Prandtl tip correction cnt'd

- **Known problem of BEM:**
  generally predictions (power, loads) are in better
  agreement with measurements for 3 bladed rotors
  than for 2 bladed rotors
- Since number of blades only enters through tip
  correction, this correction needs correction
- Possible ways:
  - compare measured tip loads for 2 and 3 bladed rotors
  - measure inflow distribution in rotor plane
  - compare with FreeVortex Wake solutions

Dynamic Inflow equation.

$$CRf\left(\frac{r}{R}\right)\frac{du_i}{dt} + 4u_i(U_w - u_i) = \frac{\Delta D_{ax}}{2\pi r \rho \Delta r}$$

transient   Equilibrium

C is a semi-empirical constant (non-dimensional time)
$f(r/R)$ is an analytical form that scales the time constant
with respect to radial position:
       at tip $f(1) = 0$, at centre, $f(0) = 1$

Dynamic inflow

Time constant only globally validated, through load
responses to pitching transients on Esbjerg turbine

Measuring blade pressure distribution responses to
pichting transients, at different radial positions,
this can be more fundamentally validated (tuned)

Problem: seperate 'profile' dynamics from 'inflow'
dynamics (different time scales $\longrightarrow$ possible)

3D effects in stall

3D boundary layer equations in polar coordinates, fixed to a rotating blade

r, V

z, W

blade rotational speed = Ω rad/s

$s = r\theta$, u
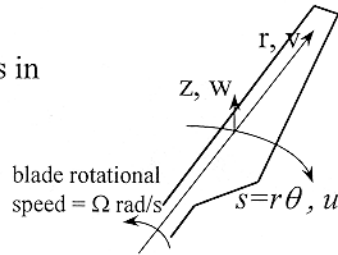
$$\frac{\partial u}{\partial s} + \frac{v}{r} + \frac{\partial v}{\partial r} + \frac{\partial w}{\partial z} = 0$$

$$u\frac{\partial u}{\partial s} + v\frac{\partial u}{\partial r} + w\frac{\partial u}{\partial z} = -\frac{1}{\rho}\frac{\partial p}{\partial s} + \frac{1}{\rho}\frac{\partial \tau_s}{\partial z} + 2\Omega v - \frac{uv}{r}$$

$$u\frac{\partial v}{\partial s} + v\frac{\partial v}{\partial r} + w\frac{\partial v}{\partial z} = -\frac{1}{\rho}\frac{\partial p}{\partial r} + \frac{1}{\rho}\frac{\partial \tau_r}{\partial z} - \frac{(u-\Omega r)^2}{r}$$

3D effects in stall, cnt'd

Attached flow order or magnitude consideration (Fogarty, 1950), based on $u = O(\Omega r)$

$$\frac{\partial u}{\partial s} + \boxed{\frac{v}{r} + \frac{\partial v}{\partial r}} + \frac{\partial w}{\partial z} = 0$$

$$u\frac{\partial u}{\partial s} + \boxed{v\frac{\partial u}{\partial r}} + w\frac{\partial u}{\partial z} = -\frac{1}{\rho}\frac{\partial p}{\partial s} + \frac{1}{\rho}\frac{\partial \tau_s}{\partial z} \boxed{+ 2\Omega v - \frac{uv}{r}}$$

$$\boxed{u\frac{\partial v}{\partial s} + v\frac{\partial v}{\partial r} + w\frac{\partial v}{\partial z} = -\frac{1}{\rho}\frac{\partial p}{\partial r} + \frac{1}{\rho}\frac{\partial \tau_r}{\partial z} - \frac{(u-\Omega r)^2}{r}}$$

▨ :Terms of $O(c/r)^2$ or smaller with respect to rest, can be discardes, hence 2D

Order of magnitude analysis for separared flow
(Snel, 1991)

Assumption:
  $u<<\Omega r,$
  chordwise pressure gradient relatively small
  Coriolis force $2\Omega v$ driving force in chordwise mom.
  and hence scales with chordwise accelaration:

$$O\left(u\frac{\partial u}{\partial s}\right) = O(\Omega v) \rightarrow O(u) = O(\Omega c v)$$

Second relation from radial momentum:
radial accelaration scales with radial pressure gradient and centr.
force term:

$$O\left(u\frac{\partial v}{\partial s}\right) = O(\Omega^2 r) \rightarrow O(uv) = O(\Omega^2 rc)$$

Order of magnitude analysis for separared flow cnt'd

Combine two expressions:

$$u = O\left(\Omega r^{1/3} c^{2/3}\right)$$
$$v = O\left(\Omega r^{2/3} c^{1/3}\right)$$

$$\longrightarrow \quad \frac{v}{u} = O\left(\frac{r}{c}\right)^{1/3}$$

Hence, important radial flows

Substitution of scaling into bl eq's

$$\frac{\partial u}{\partial s} + \boxed{\frac{v}{r} + \frac{\partial v}{\partial r}} + \frac{\partial w}{\partial z} = 0$$

$$u\frac{\partial u}{\partial s} + \boxed{v\frac{\partial u}{\partial r}} + w\frac{\partial u}{\partial z} = -\frac{1}{\rho}\frac{\partial p}{\partial s} + \frac{1}{\rho}\frac{\partial \tau_s}{\partial z} + 2\Omega v \boxed{-\frac{uv}{r}}$$

$$u\frac{\partial v}{\partial s} + \boxed{v\frac{\partial v}{\partial r}} + w\frac{\partial v}{\partial z} = -\frac{1}{\rho}\frac{\partial p}{\partial r} + \frac{1}{\rho}\frac{\partial \tau_r}{\partial z} - \frac{(u - \Omega r)^2}{r}$$

$\boxed{}$: Terms of $O(c/r)^{2/3}$ with respect to rest, neglected

Application

The '2.5D' boundary layer equations implemented within XFOIL (Drela, '85): $\longrightarrow$ RFOIL

- additional terms in chordwise mom. eq.
- additional radial mom. eq. including v profile family
- can still be solved in chordwise stepping fashion because of 2D convective accelaration terms

RFOIL can be used to construct 'corrected' sectional characteristics

Example of rotating airfoil characteristics, as calculated by RFOIL

C_l
C_d

rotating, c/r=0.2

2D

α
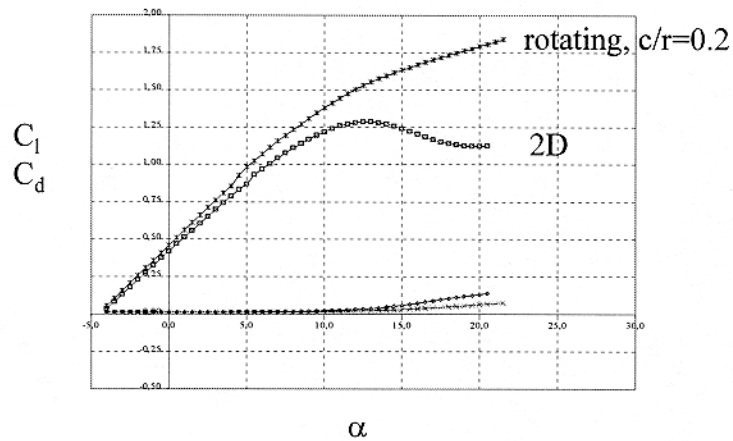
Remaining problems

Validation done with FFA measurements in Chinese Tunnel:

- few measurements in 'deeper' stall,
- difficulties with definition
- basic tendency: RFOIL overestimates 3D rotating effects.
- Practical solution used is to use $(c/r)_{calc} = (c/r)_{real}/1.5$

Need for **better validation** (measured pressure distributions in deep stall), and subsequent RFOIL improvement

RFOIL gives solution till about $\alpha = 25$. Deep stall: NavStok

Dynamic Stall

Basic Model:

$$c_l = c_{l,\text{steady}} + \Delta c_{l,1} + \Delta c_{l,2}$$

$\Delta c_{l,1}$ of forcing frequency

$\Delta c_{l,2}$ for higher frequency dynamics
(self excited vortex shedding?)

$\Delta c_{l,1}$ model

First order ordinary differential equation for
evolution, following forcing frequency in ft_1:

$$\tau \; \frac{d\Delta c_{l,1}}{dt} + cf_{10}\Delta c_{l,1} = ft_1$$

$$\tau = c \, / \, 2U$$

'Damper spring model'

Forcing term and coefficient for $\Delta c_{l,1}$

$$cf_{10} = \frac{1+0.5\dfrac{d\Delta C_{l,pot}}{dt}}{8*(1+60\tau\dfrac{d\alpha}{dt})} \qquad\qquad ft_1 = \tau\frac{d\Delta C_{l,pot}}{dt}$$

with

$$\Delta C_{l,pot} = C_{l,pot} - C_{l,steady} = 2\pi\sin(\alpha - \alpha_0) - C_{l,steady}$$

$\Delta C_{1,2}$ model

$$\tau^2\frac{d^2\Delta c_{l2}}{dt^2} + cf_{21}\frac{d\Delta c_{l2}}{dt} + cf_{20}\Delta c_{l,pot} = ft_2$$

$$cf_{21} = C\tau\, k_s\{-0.01(\Delta c_{l,pot} - 0.5) + \Delta c_{l2}^{\,2}\}$$

$$ft_2 = \text{combination of } \Delta c_{l,pot} \text{ and } d\Delta c_{l,pot}/dt$$

cf_{21} is a vanderPol type damping term, that gives
self excited oscillations, frequency determined by cf_{20}

Problems

Validation from field experiments is practically
impossible because of stochastic wind.

As a result, validation is practically zero !!!

Aero-elastic stability is to a large degree dependent
on dynamic stall, for C_l and for C_d, hence
validation is urgent

Validation

Possibilities for validation:

- 1P variations can be made with yaw misalignment,
  however this increases the uncertainties in angles
  of attack (inflow!)

- fast pitch oscillation in axially symmetric flow is
  'purer'

Yaw misalignment modelling

Inflow distrubution in annulus is deterministically non-axi symmetric;

First harmonic modelling as resulting from Joule:

$$u_i = u_{i,0}\left[1 - f\left(r/R\right)\tan\frac{\chi}{2}\sin\Phi_{az}\right]$$

with χ = wake skew angle

Newer modelling including 2nd harmonic and phases directly induced from flow field measurements in Delft open jet wind tunnel

Remaining problems

Model works fine in some occasions, but lousy in others:

      Validation, validation and validation

Best validation through blade load and flow field measurements, next best only blade load measurements, but as function of azimuth

Miscellaneous but important problems and some questions

- Influence of boundary layer manipulators (vortex generators, stall strips, tripping devices, etc) on sectional properties
- Radial region influenced by bl manipulators
- Flow viz possible? Stall flags? smoke for detection of wake vorticity?
- Flow field measurement possible? (hot wires, laser-doppler, piv)?

Aerodynamic measurements in large wind tunnel

NREL plans for experiments with 10 m diameter rotor of NREL field tests in NASA-Ames wind tunnel	European plans for rotor and flow field measurements on sophisticated wind tunnel model in large wind tunnel

SYNERGY
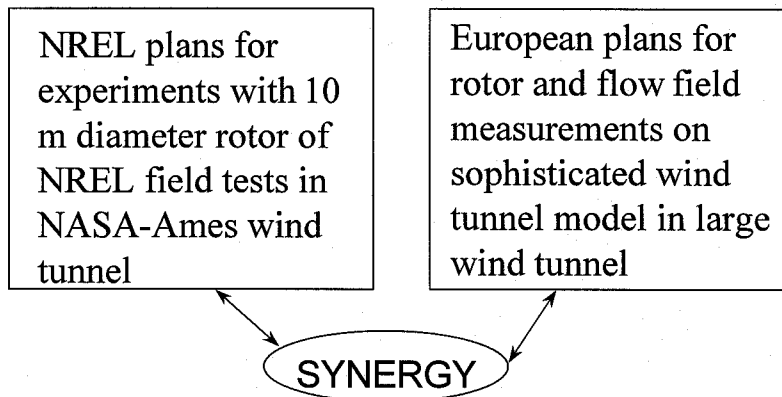
Aerodynamic measurements in large wind tunnel

AIM: Improvement of aerodynamic modules of wind turbine design and analysis methods

- Performance prediction, especially in stall conditions
- Load and load fluctuation prediction especially in stall and yaw misalignment conditions
- Quantify influence of vortex generators and stall strips on blade
- Data base for validation Navier Stokes solvers

WHY?

- Improve power predictions capabilities from 10-15% error to 5-10% error : reduce measurement time and REDUCE TIME TO MARKET
- Improve fatigue load prediction for yaw error conditions: one of the main fatigue drivers: REDUCE SAFETY FACTORS, AND COST
- Organise knowlegde of vortex generators and stall strip behaviour for better use of thick profiles to: REDUCE BLADE WEIGHT AND COST

Why in wind tunnel and Why together

- Field measurements are very valuable but wind speed cannot be quantified with sufficient accuracy
- Field measurements together with tunnel measurements more then duplicates value of both
- Synergy of collaboration
  - reduces costs (one data acquisistion system)
  - unites more brains
  - enables broader scope (2 and 3 bladed rotors)

Appendix L:

Presentation by F. Rasmussen, RISO

Presentation not Available

Appendix M:

Presentation by R. Rawlinson-Smith, GH

Three Dimemsional Model of Dynamic Stall

NREL Science Panel
Meeting #1
5-6 October 1998

Robert Rawlinson-Smith
Garrad Hassan and Partners Ltd.

The problem(s)

Poor prediction of the peak power of stall regulated wind turbines

Poor prediction of the dynamic behaviour of stall regulated wind turbines

The model

Extension of the Beddoes dynamic stall model

Use of Kirchoff parameter to model the delay of trailing edge separation

Use of (c/r) parameter to determine extent of the delay

Quasi-static movement of separation point
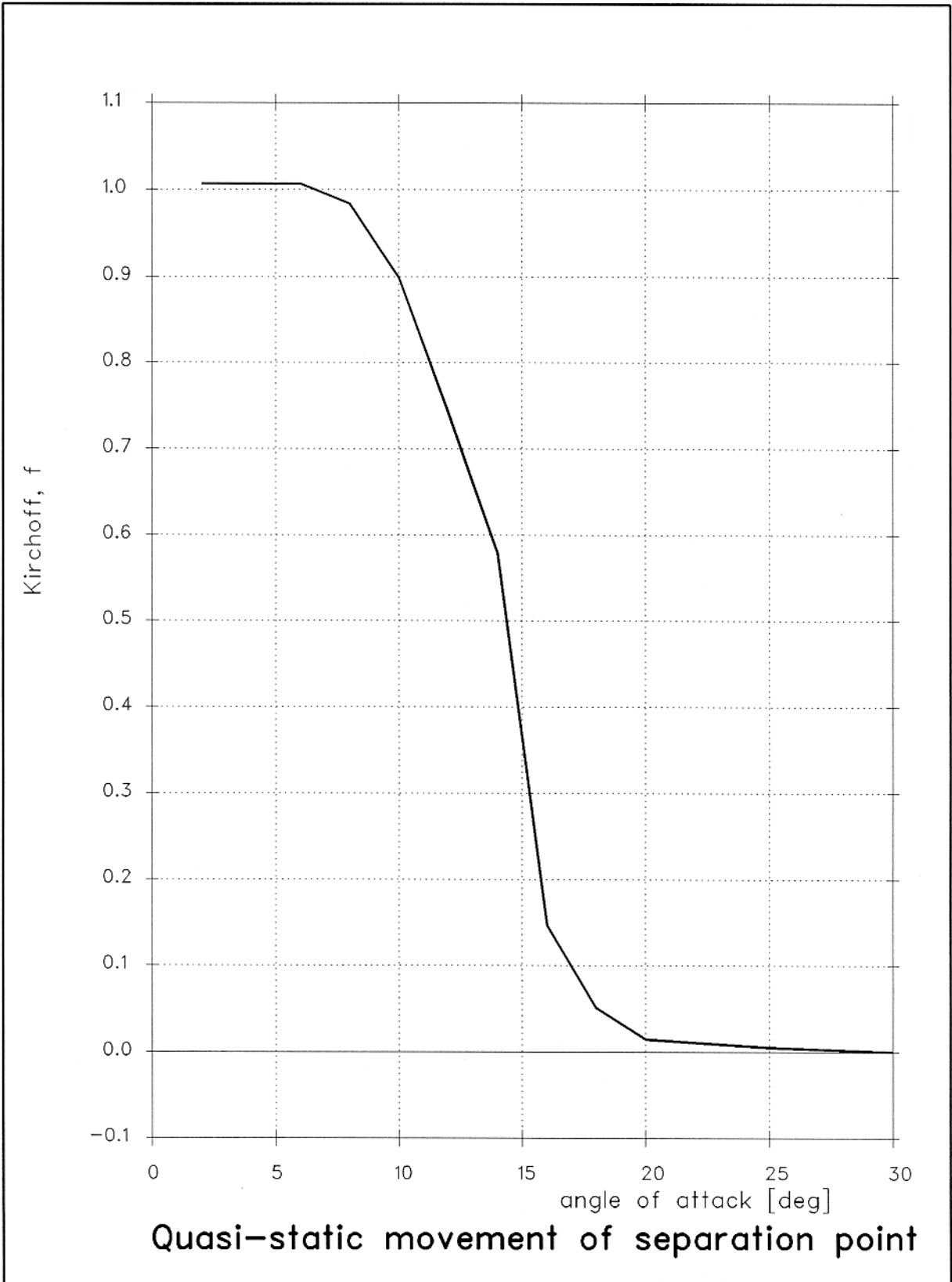
Prediction methods

- *Quasi-steady using 2D aerofoil data*

- *Using 2D aerofoil data and standard dynamic stall model*

- *Quasi-steady using 3D aerofoil data*

- *Using 2D data and 3D dynamic stall model*

Danwin Turbine

Three bladed stall regulated

180kW, 22m diameter

NACA 63-2xx aerofoils

Danwin turbine power curve

Legend:
- —— measured
- ········ 2d quasi-static
- – – – 2d dynamic stall
- –·–·– 3d quasi-static
- ○ 3d dynamic stall

Axes: wind speed [m/s] (horizontal), electrical power [kW] (vertical)
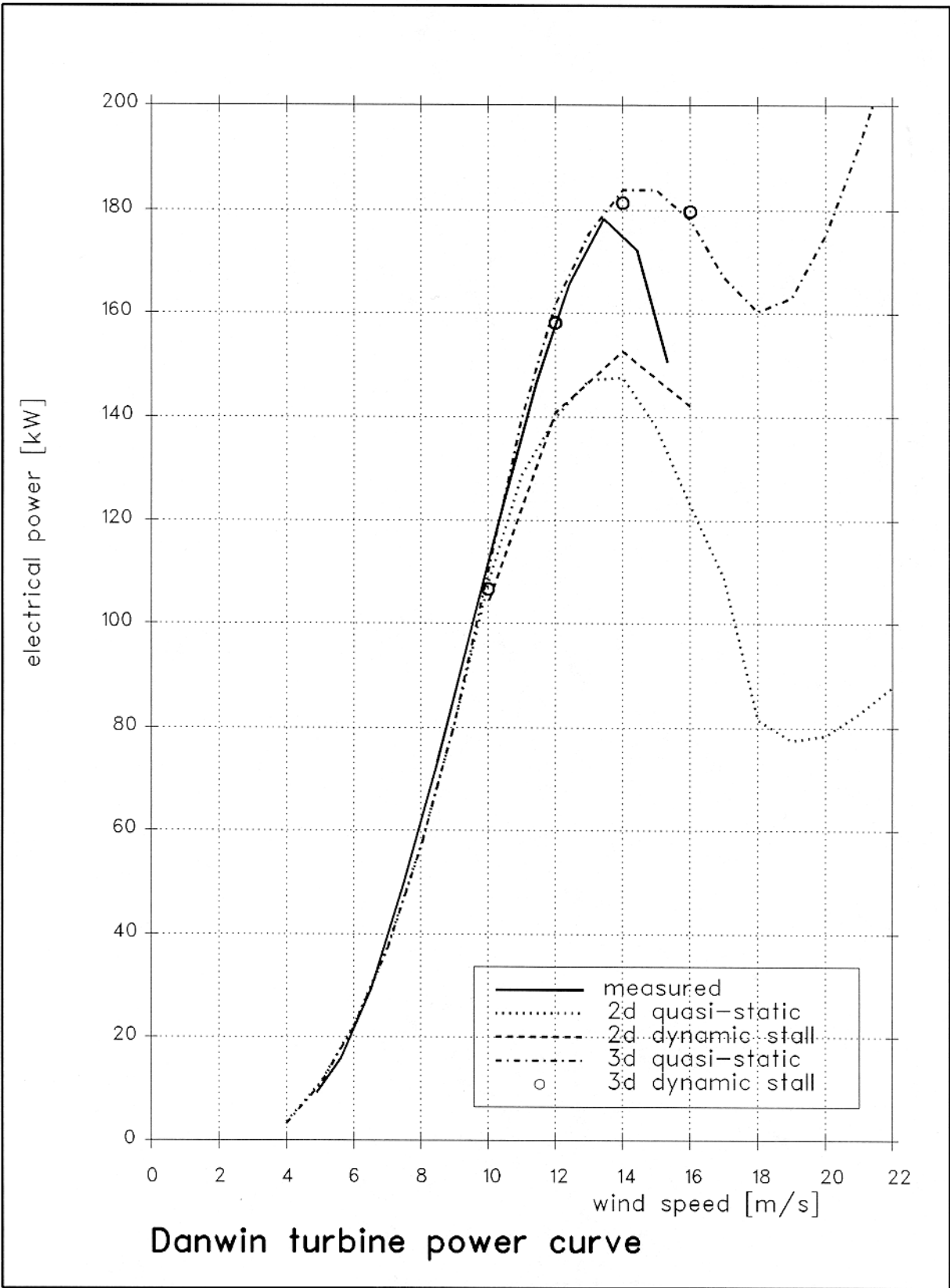
Dynamic loads - load case

Wind speed - 14.8 m/s

Turbulence intensity - 11.8%

Flapwise bending load predicted
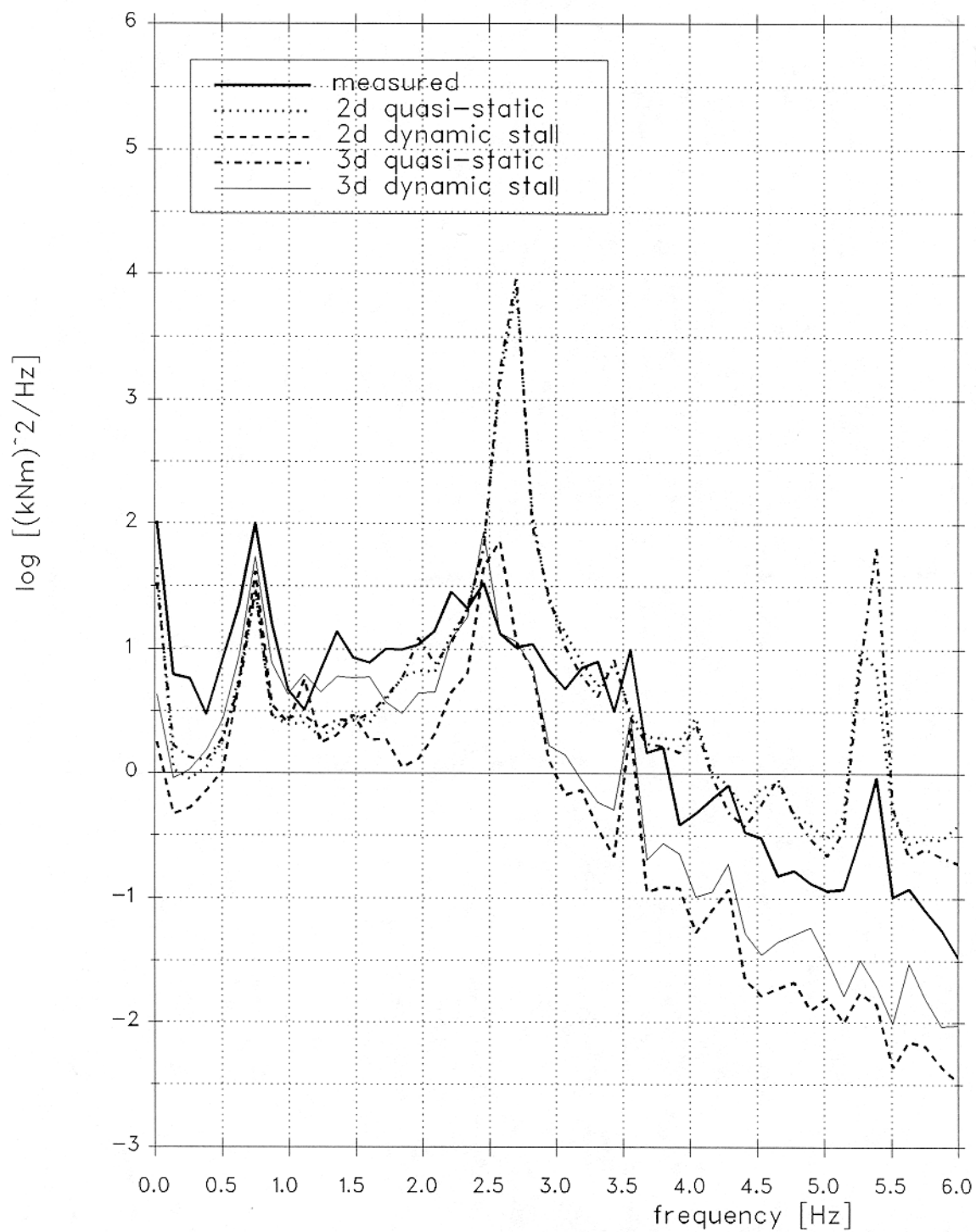
Danwin turbine flapwise bending moment

Concluding remarks

Improved prediction of steady state performance

Improved prediction of dynamic loading

Detailed verification requires access to suitable aerodynamic measurement data sets

Limitations

High reduced frequencies
at inboard stations

Trailing edge
vs
Leading edge
separation

Stochastic input
to periodic model?

Important parameters (1)

*Reduced frequencies
corresponding to*

*- fundamental blade
  frequencies*
- 1P

Separation position
*- versus angle of attack
   as a function of radial
   station*

Important parameters (2)

Vortex formation

Conditions
for onset of
vortex motion

Speed of vortex
motion

DEVELOPMENT OF A THREE DIMENSIONAL
MODEL OF DYNAMIC STALL

R I Rawlinson-Smith
Garrad Hassan and Partners Ltd
The Coach House, Folleigh Lane, Long Ashton, Bristol BS18 9JB, UK

ABSTRACT: An existing engineering model of dynamic stall has been developed to include the effects of three dimensional flow on a Horizontal Axis Wind Turbine. Application of the new model within the Garrad Hassan aeroelastic code BLADED is shown to improve not only the prediction of peak power but also that of the dynamic behaviour of stall regulated machines at high wind speeds.

KEYWORDS: Dynamic stall, Three dimensional flow effects, Stall induced vibrations, Stall rotation effects

1. INTRODUCTION

The peak power of stall regulated horizontal axis wind turbines is poorly predicted when using standard combined blade element and momentum theory in combination with two dimensional aerofoil characteristics.

Previous work [1, 2] has sought to address this problem by concentrating on the production of 'three dimensionalised' aerofoil data for use in the calculation of the steady state performance of wind turbines. These data however are not generally useful for the prediction of wind turbine loading as they represent the average force coefficients variation with angle of attack for different blade radial stations; implicitly included in this averaged data are the mean effects of the three dimensionality and unsteadiness associated with the wind turbine flowfield.

The work reported here has sought to address the effects of both three dimensionality and the unsteadiness by including an empirical model of three dimensional effects within an existing semi-empirical model of dynamic stall.

This paper summarises the work performed by Garrad Hassan (GH) in the development of their engineering models within the Joule project 'Dynamic Stall and Three Dimensional Effects' (JOU2-CT93-0345).

2. THE MODEL

The Beddoes model [3] of dynamic stall uses a combination of indicial aerodynamics and the Kirchoff representation of trailing edge separation to generate unsteady aerofoil characteristics. The Kirchoff model uses the following equation to relate the quasi-static chordwise location of the separation point, f, to the lift coefficient, C_L, through the angle of attack, α.

$$C_L = 2\pi(1 + f^{0.5})^2 \, \alpha \, /4$$

A typical example of the quasi-static variation of the parameter f with angle of attack is shown in Figure 2.1. At low angles of attack the flow is fully attached to the aerofoil (f = 1), as the angle of attack increases towards stall the separation point moves forward (f ~ 0.5 at steady stall) until it reaches the leading edge (f = 0) for fully separated flow. This quasi-static relationship is determined for any particular aerofoil by using steady wind tunnel test data. In the unsteady aerodynamic model time delays are applied to this quasi-static relationship to account for the lag in the movement of the separation position due to unsteady pressure and boundary layer responses.

One effect of the three dimensional nature of the flowfield on the performance of the aerofoil sections used to make up a wind turbine blade is that the forward movement of the separation position is delayed due to modification of the flow in the boundary layer near the root of the blade caused by radial pressure gradients [2]. To incorporate this effect within the Beddoes dynamic stall model is quite simple; by applying an empirical correction to the relationship between the separation point position and angle of attack determined from the quasi-static C_L - α curve it is possible to extend the linear range of the C_L curve therefore giving rise to higher mean lift coefficients. The parameter $(c/r)^2$ is identified in [2] as being significant in determining the extent of the delay in the forward movement of the separation point and has therefore been used here. The delay is defined as a deficit in angle of attack, α_{def}, using the following relationship

$$\alpha_{def} = k(c/r)^2$$

where k is an empirical factor. The delay is imposed in the context of an unsteady variation in angle of attack.

3. DANWIN TURBINE

The JOULE Project 'Dynamic Loads in Wind Farms' JOU2-CT92-0094 has used measurements from the Alsvik wind farm which is situated in level terrain, on the west coast of the Swedish island of Gotland. It consists of 4 Danwin 180 kW, fixed speed, stall regulated wind turbines.

One of the machines was extensively instrumented and a large database of high quality measurements exist for the turbine operating both in and out of the wake(s) of the adjacent turbines.

REFERENCES

[1] Rasmussen F R et al, Investigation of the aerodynamics and structural dynamics of the Danwin 180 kW, Riso-M-2727, June 1983

[2] Snel H et al, Sectional prediction of 3-D effects for stalled flow on rotating blades and comparison with measurements, ECWEC '93, Travemunde, March 1993

[3] Beddoes T S and Leishman J G, A semi-empirical model for dynamic stall, Journal of the American Helicopter Society, July 1989

[4] Montgomerie B, The Influence of 3D effects in lift and drag on the performance of a stalled horizontal axis wind turbine rotor, IEA meeting on Aerodynamics, 21-23 Nov 1994, Lyngby, Denmark

[5] Rasmussen F R, Petersen J T, Winkelaar D and Rawlinson-Smith R I, Response of stall regulated wind turbines- Stall induced vibrations, Riso-R-691(EN), June 1993
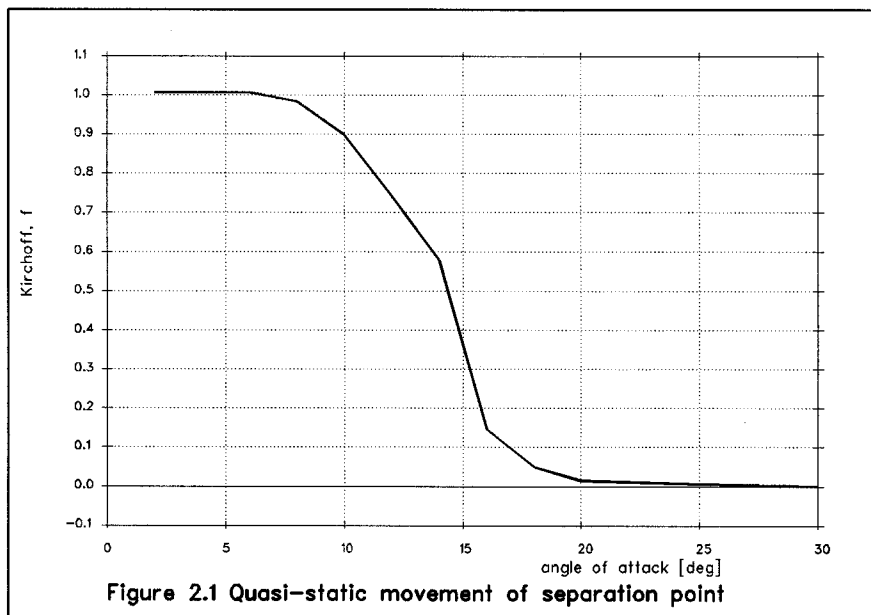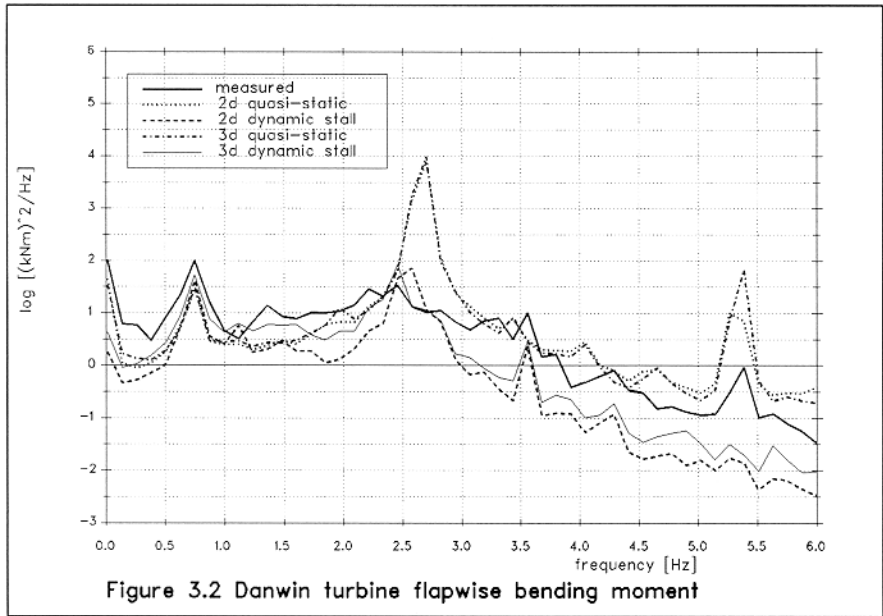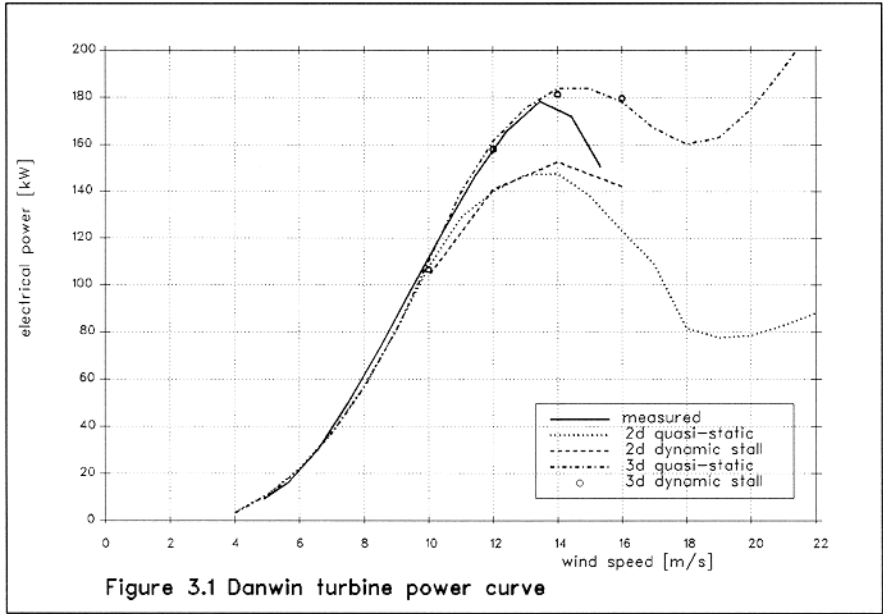
Figure 2.1 Quasi-static movement of separation point

Figure 3.1 Danwin turbine power curve

Figure 3.2 Danwin turbine flapwise bending moment

NREL Science Panel

Meeting #1
5-6 October 1998

Robert Rawlinson-Smith
Garrad Hassan and Partners Ltd

BLADED for Windows
A Design Tool

- Interaction of:
  - wind
  - aerodynamics
  - structural dynamics
  - power train
  - control
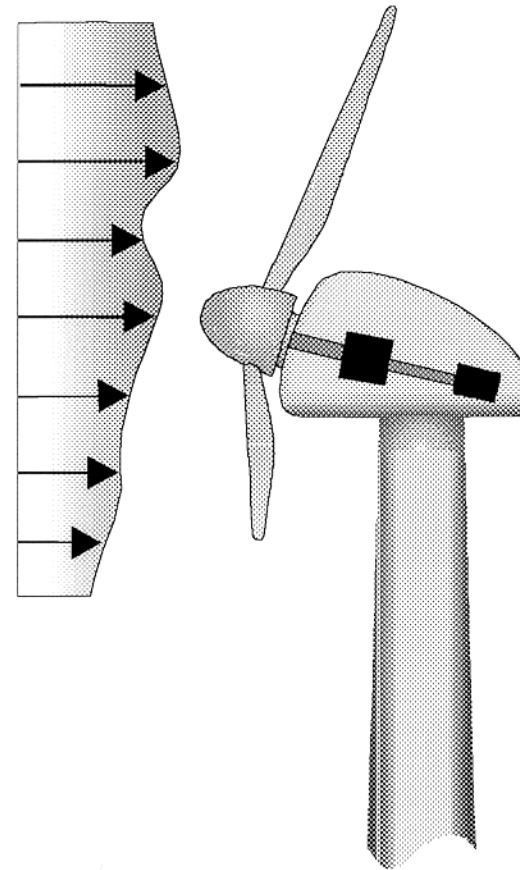
Wind Modelling

- *Wind shear*
  - *exponential, logarithmic or user-specified*
- *Tower shadow*
  - *potential flow dipole or user specifed cosine model*
- *Upflow and upwind wake profile*
- *Turbulence*
  - *single or three components*
  - *von Karman or Kaimal spectral models*
- *Deterministic transients*
  - *wind speed, wind direction, wind shear*

Aerodynamics

- *Blade element theory*
- *Prandtl tip and hub loss*
- *Options for inflow calculation*
  - *equilibrium wake*
  - *frozen wake*
  - *dynamic wake based on Pitt and Peters*
- *Dynamic stall model based on Leishman-Beddoes*

Structural Dynamics

- *Modal analysis of rotor blades and tower*
- *Structural degrees of freedom*
  - *blade flapwise bending*
  - *blade edgewise bending*
  - *rotor teeter*
  - *nacelle yaw*
  - *tower fore-aft*
  - *tower lateral*
- *Coupling of component modes and aeroelastic feedback*

Power Train and Control

- ## Power train

  - mounting flexibilty
  - brake models
  - shaft flexibility
  - generator models

- ## Control

  - fixed / variable speed
  - active pitch / active stall
  - supervisory control
  - interface to external controller
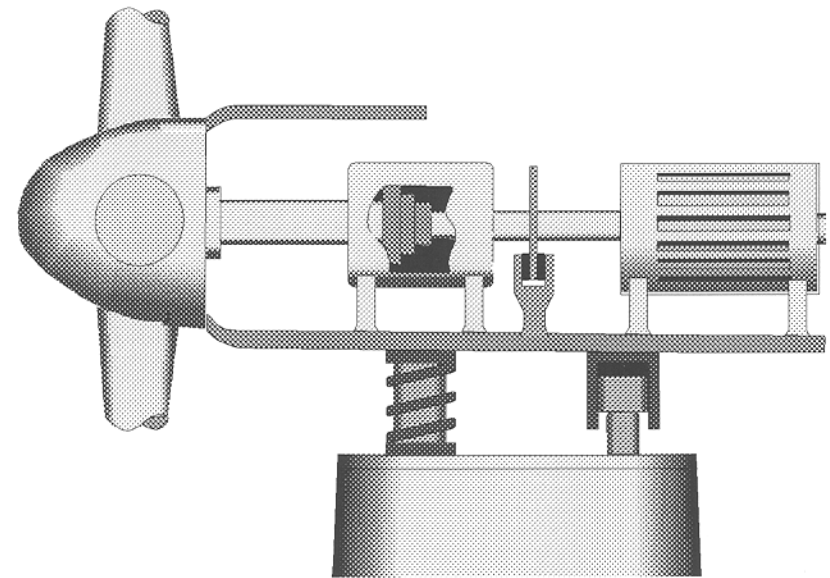
Appendix N:

Presentation by B. Holley, RANN

Small Wind Turbine Aerodynamic Issues

W.E. Holley, et. al.

RANN, Inc.

Palo Alto, CA

October, 1998

Typical Small Wind Turbine Configuration

- Free yaw with tail vane
- Yawing/furling for load and overspeed control

Typical Example:
Sencenbaugh S-1000 Turbine

SENCENBAUGH
WIND
ELECTRIC

NORMAL OPERATIONAL MODE

WIND

WIND

OVERSPEED CONTROL MODE
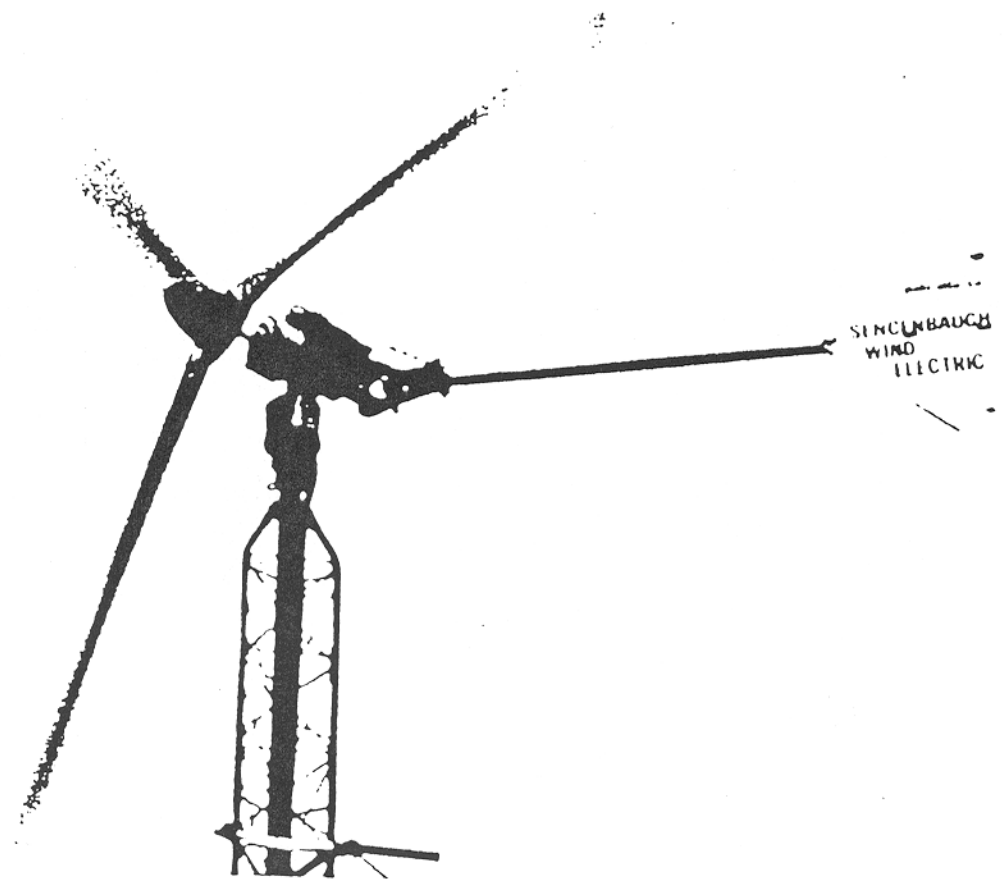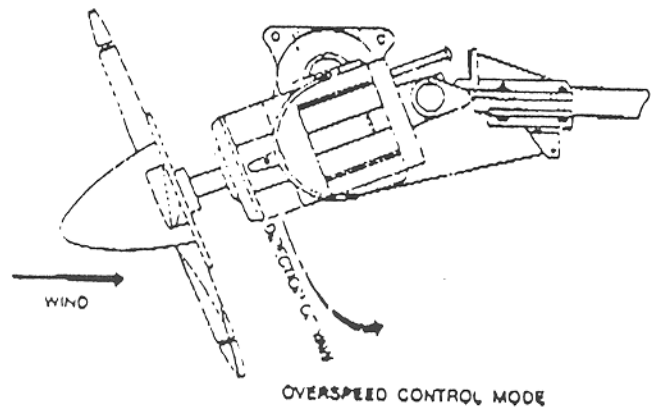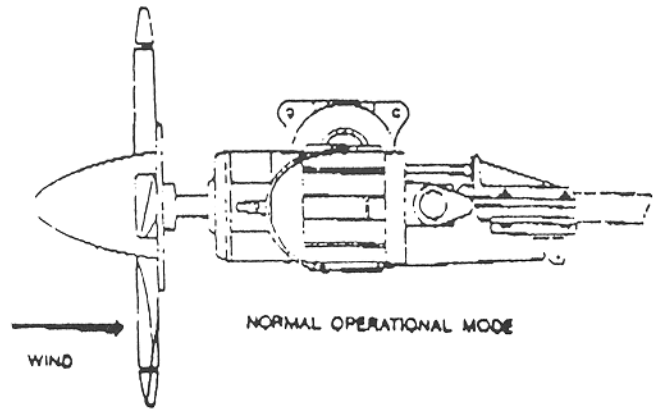
Critical Design Issues

- Reliable initiation of furling
- Loads for peak power and loss of load design situations
- Stable progressive furling with increasing wind speed with no "limit cycling"

Aerodynamic Issues Re. Yaw/Furl Equilibrium

- Skewed Wake
  - Induced effects at rotor
  - Induced effects at tail
- Dynamic Stall

Skewed Wake

Preliminary comparison of YawDyn model
with Coleman, 1945

$$a = a_0 \left(1 + \left(\tfrac{15\pi}{32} \right)\left(\tfrac{r}{R} \right) \sin \psi \tan \tfrac{\chi}{2} \right)$$

N-8

Assumptions for Model Equivalence

- Spanwise linearization of exact solution
- Wake skew angle used in tangent expression
- Constant spanwise circulation

Skewed Helical Vortex Wake

(a)　　　　　　　　　　(b)　　　　　　　　　　(c)
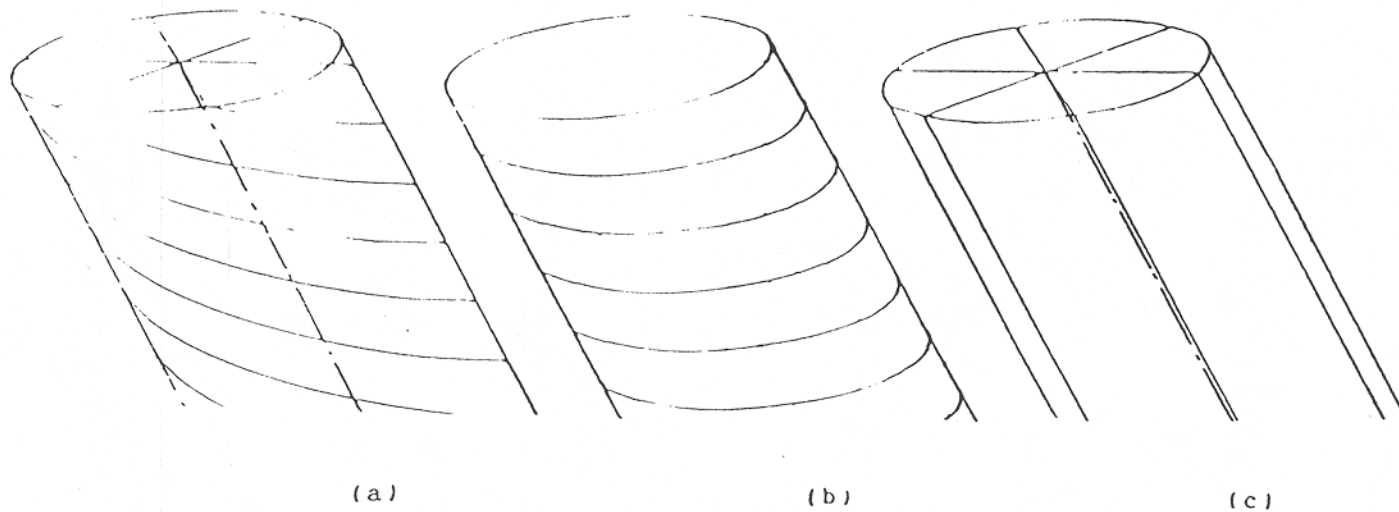
Figure 1. Representation of Skewed Helical Vortex Wake by
Circular and Linear Vortex Wakes

Coordinate System

Figure 2. Coordinate System for Obtaining Induced Velocities
at Rotor Disk

Radial Variation of Induced Velocity for Large Skew Angles

(Helicopter Case)

Eqn.(12)

Eqn.(11)

$\frac{V_i}{V_i'}$

1.0

.8

.6

.4

.2

0

-.2

-1.0   -.8   -.6   -.4   -.2   0   +.2   +.4   +.6   +.8   +1.0

$\psi = \pi$

$\bar{r} \cos \psi$

$\psi = 0$

NATIONAL ADVISORY
COMMITTEE FOR AERONAUTICS
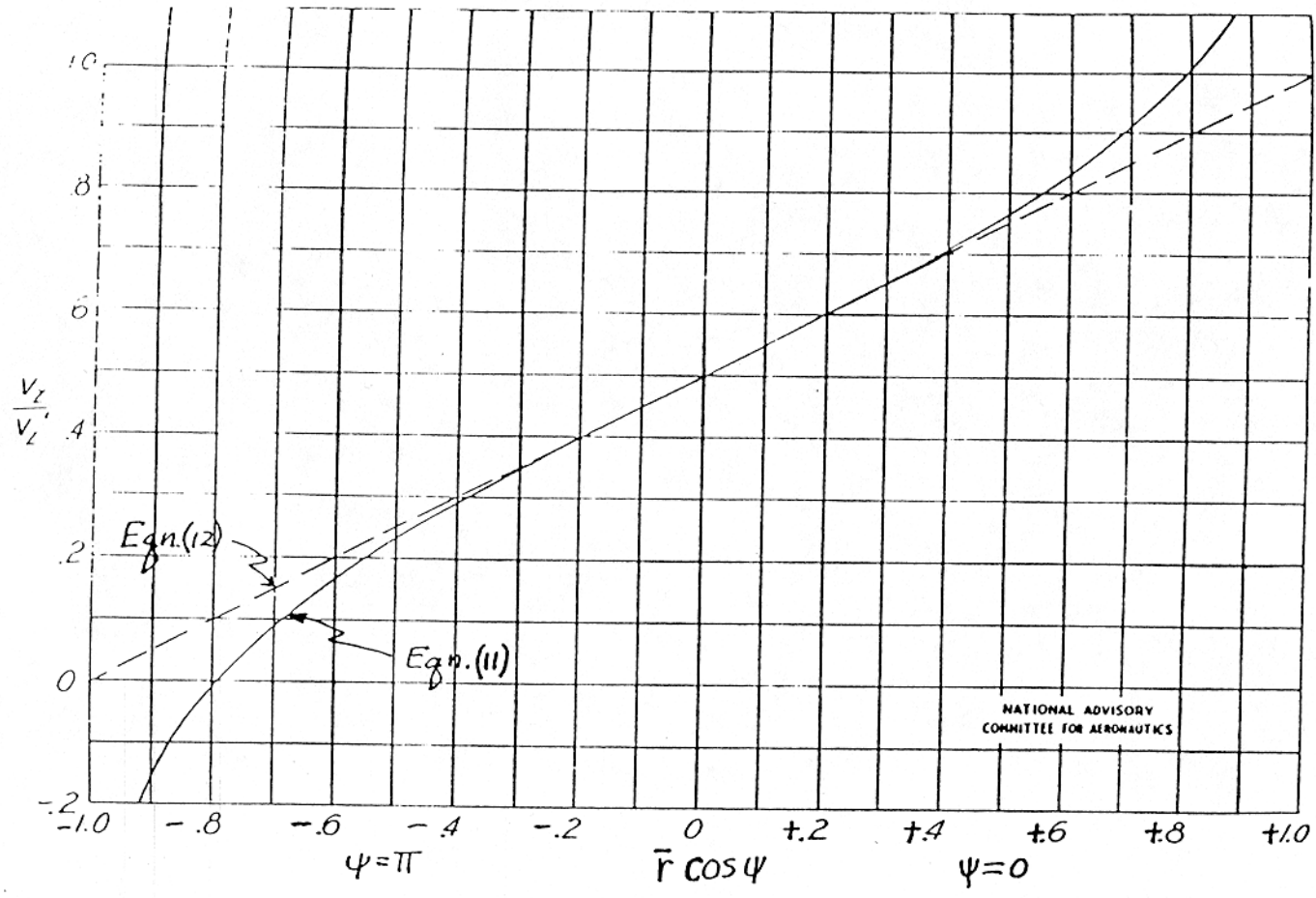
Relation Between Yaw and Wake Skew Angles

Figure 4. Variation of Wake Skew Angle with Rotor Yaw Angle for Various Values of a_o
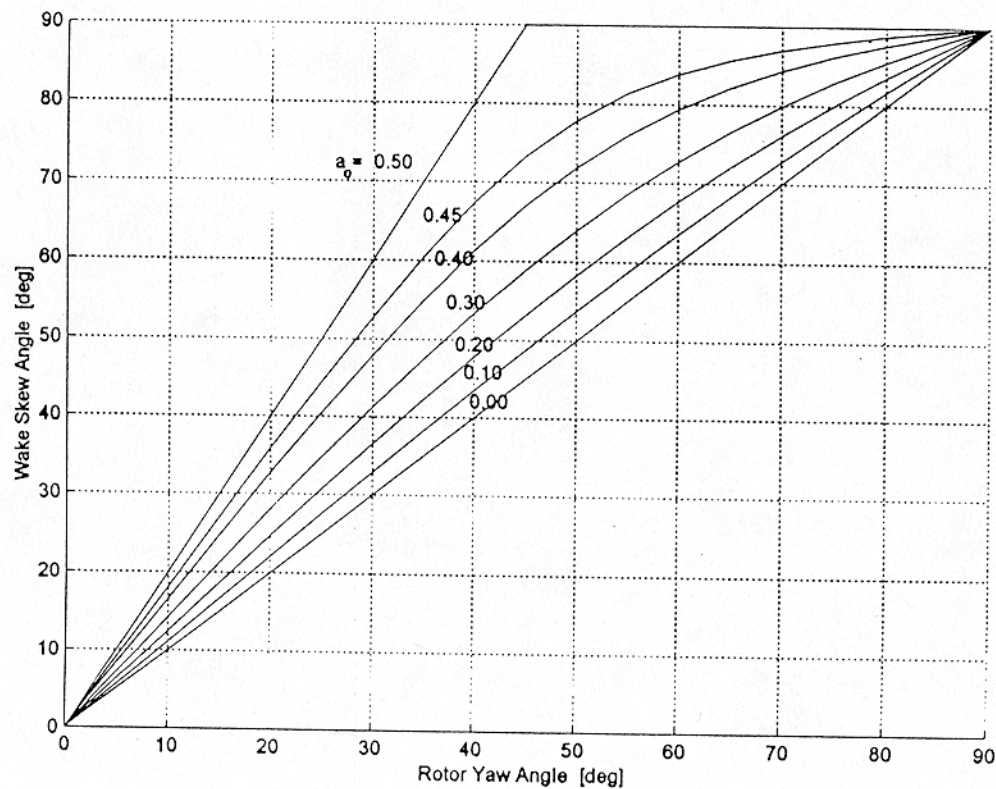
Variation of "Coefficient"

Figure 5. Variation of K' with Wake Skew Angle
for Various Tip Loss Corrections
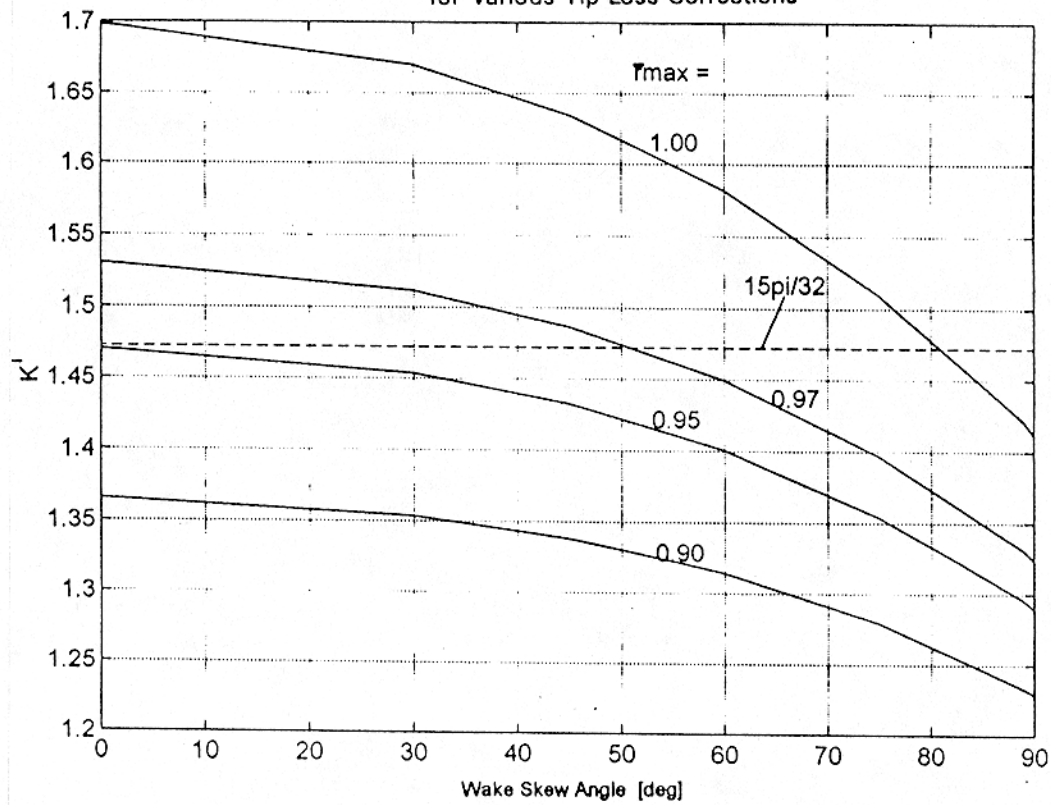
Preliminary Evaluation of Dynamic Stall Effect

- S-1000 Rotor Parameters
- Calculations used YawDyn
- Forces and moments computed with and without dynamic stall

Figure 13. Estimated Yawing Coefficient Due to Thrust Without Dynamic Stall Effects
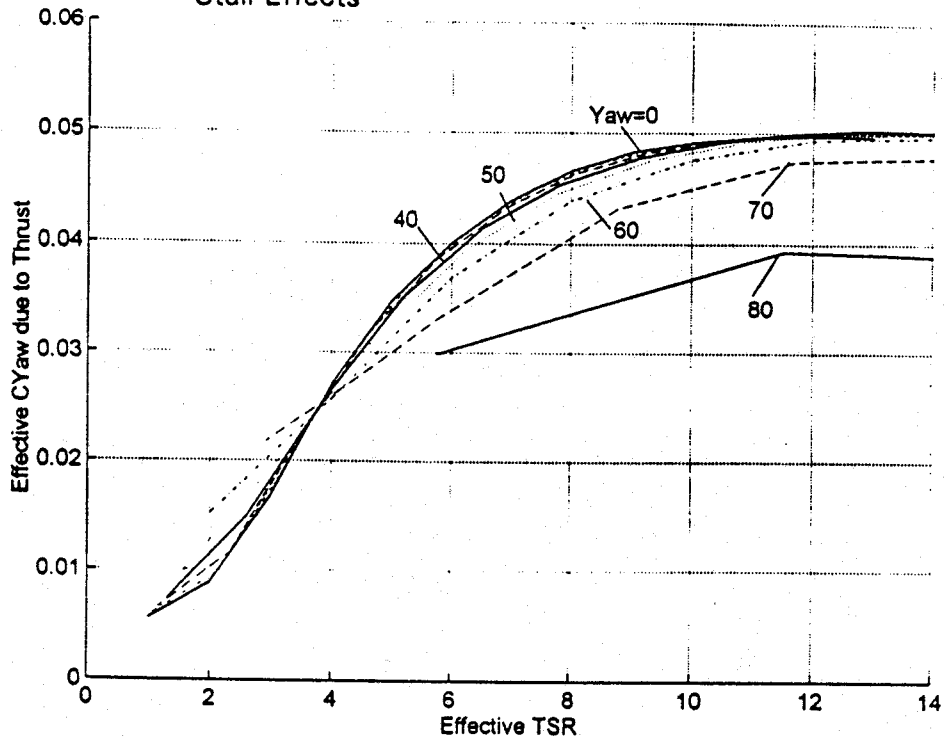
Figure 14. Estimated Yawing Coefficient Due to Thrust With Dynamic Stall Effects

N-16
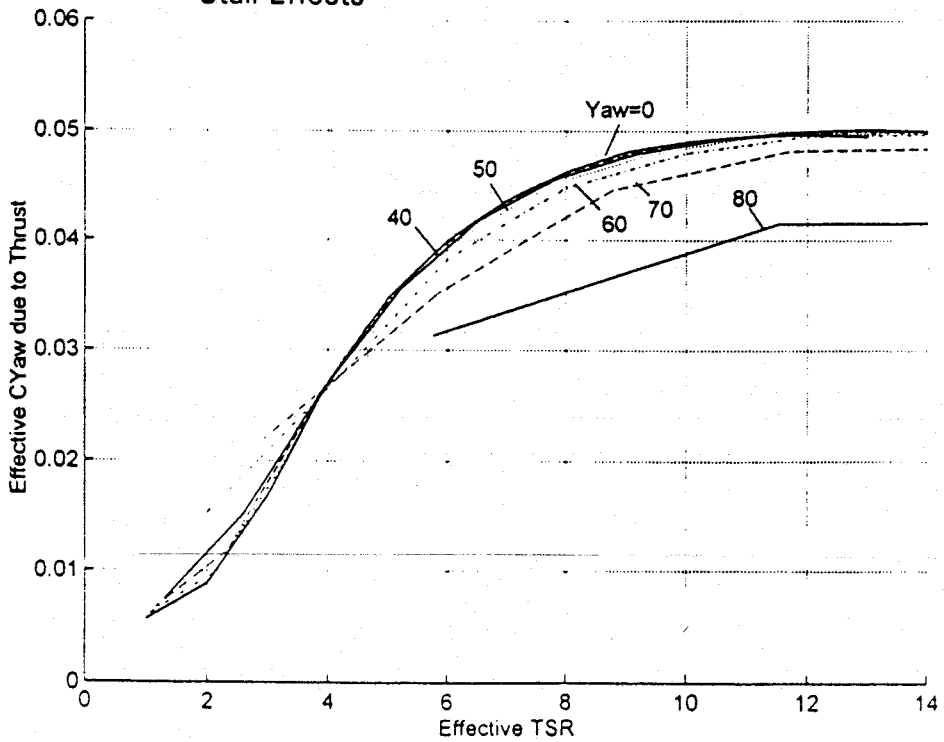
Figure 15. Estimated Yawing Couple Coefficient Without Dynamic Stall Effects
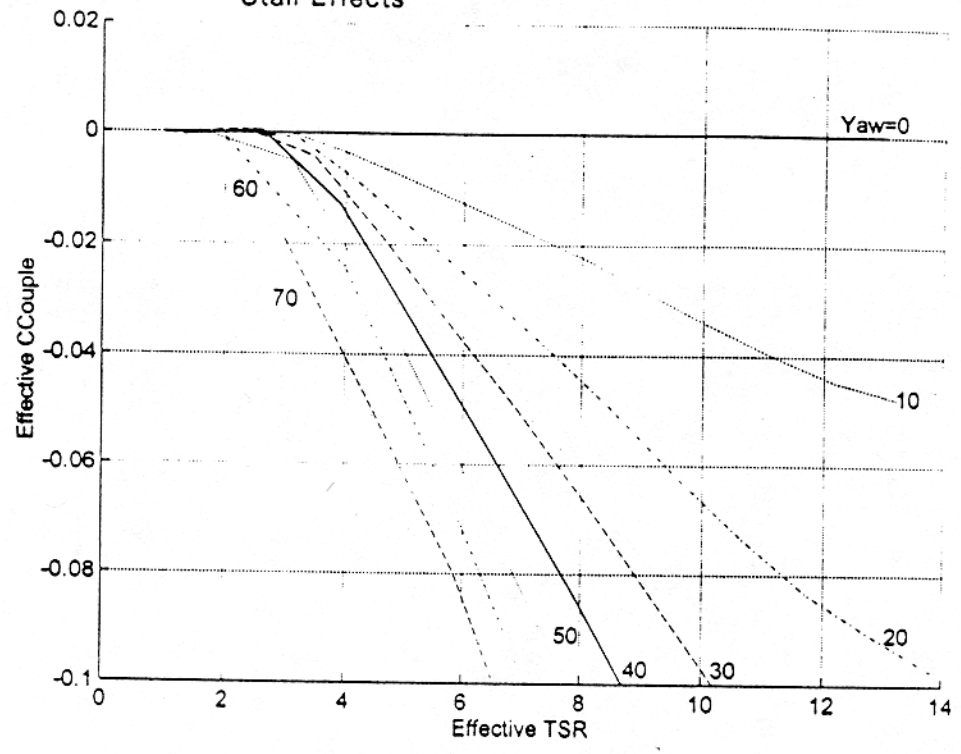
Figure 16. Estimated Yawing Couple Coefficient With Dynamic Stall Effects
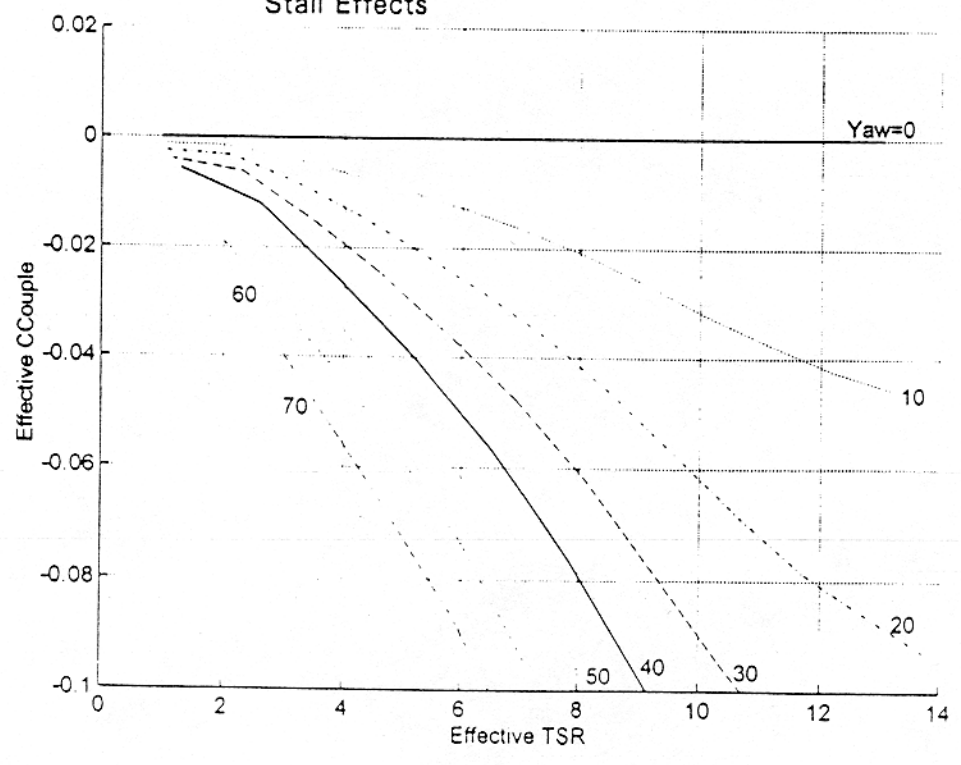
Figure 21. Estimated Yawing Coefficient Due to Side Force Without Dynamic Stall Effects
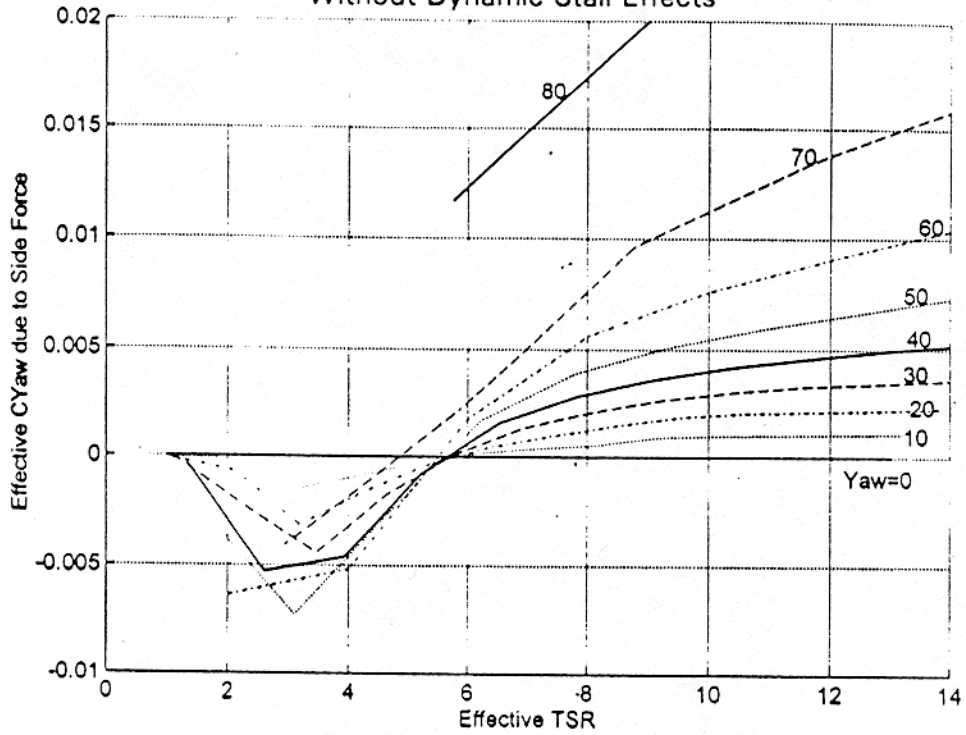
Figure 22. Estimated Yawing Coefficient Due to Side Force With Dynamic Stall Effects

N-18
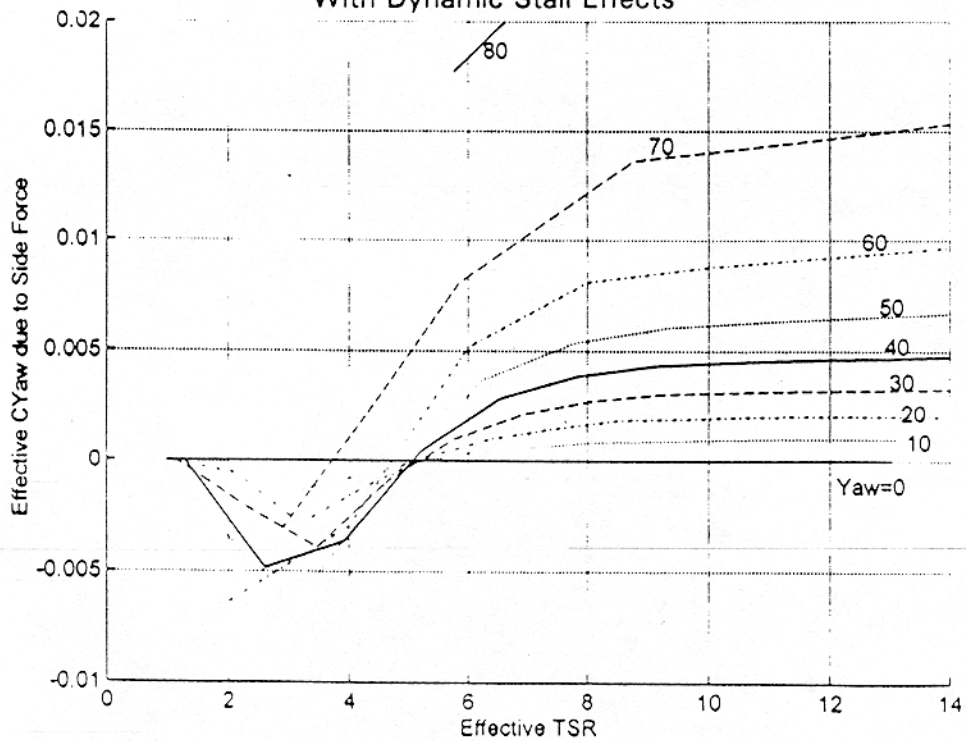
Figure 23. Estimated Net Yawing Coefficient Without Dynamic Stall Effects
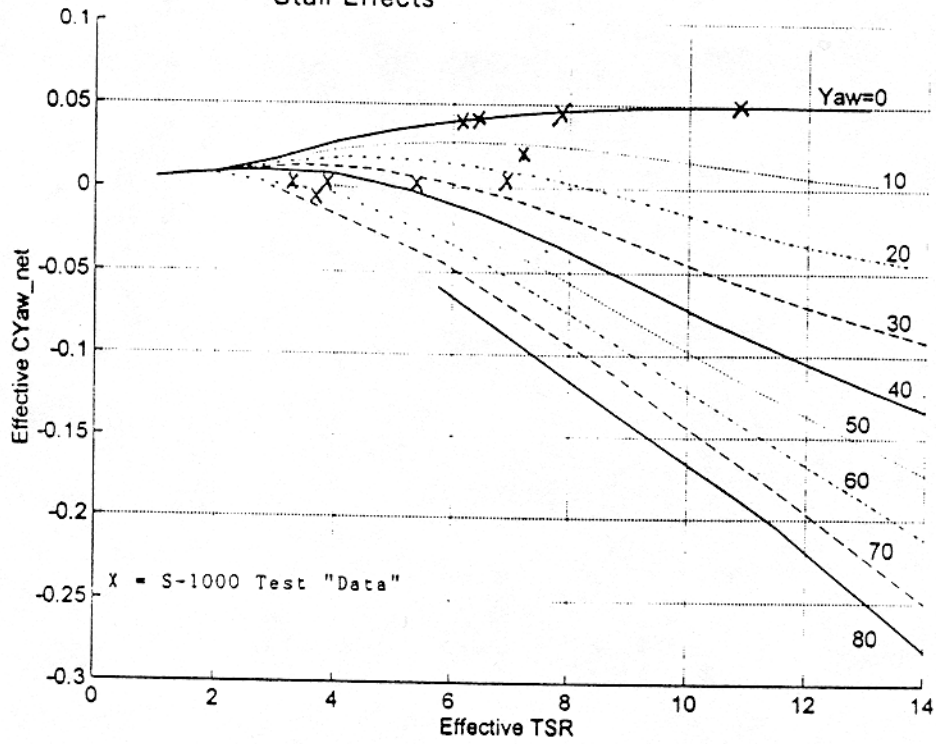
Figure 24. Estimated Net Yawing Coefficient With Dynamic Stall Effects
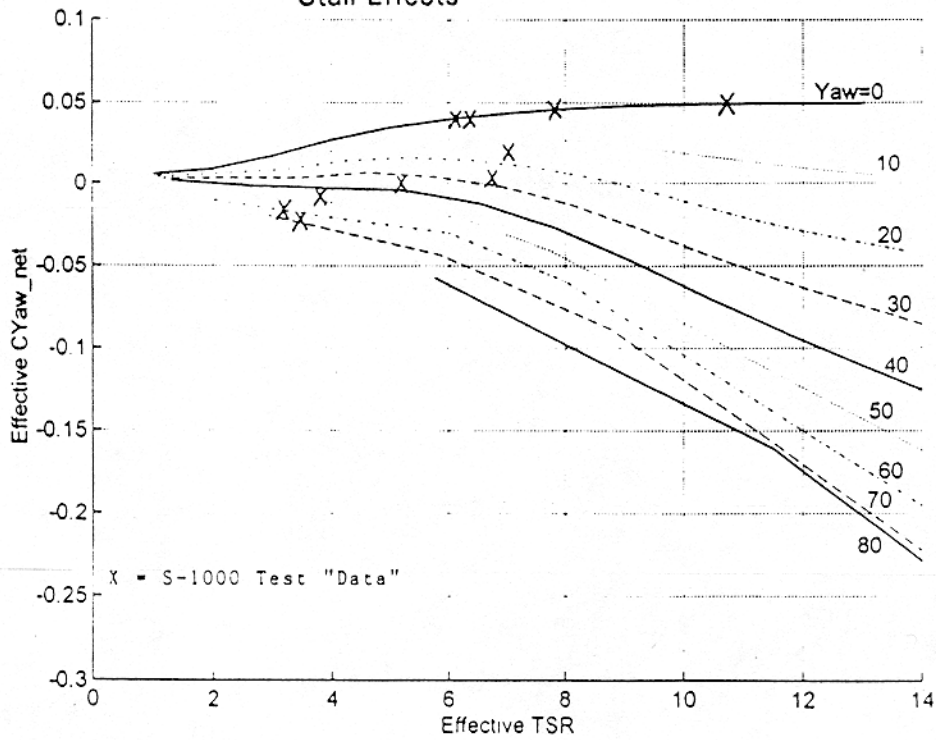
Induced Velocity Effect
at the Tail

- S-1000 Rotor Parameters

- Calculations used YawDyn

- Tail assumed fully immersed in far wake or free stream

Figure 32. Variation of Yaw Angle with Wind Speed

Vertical Tail in Far Wake
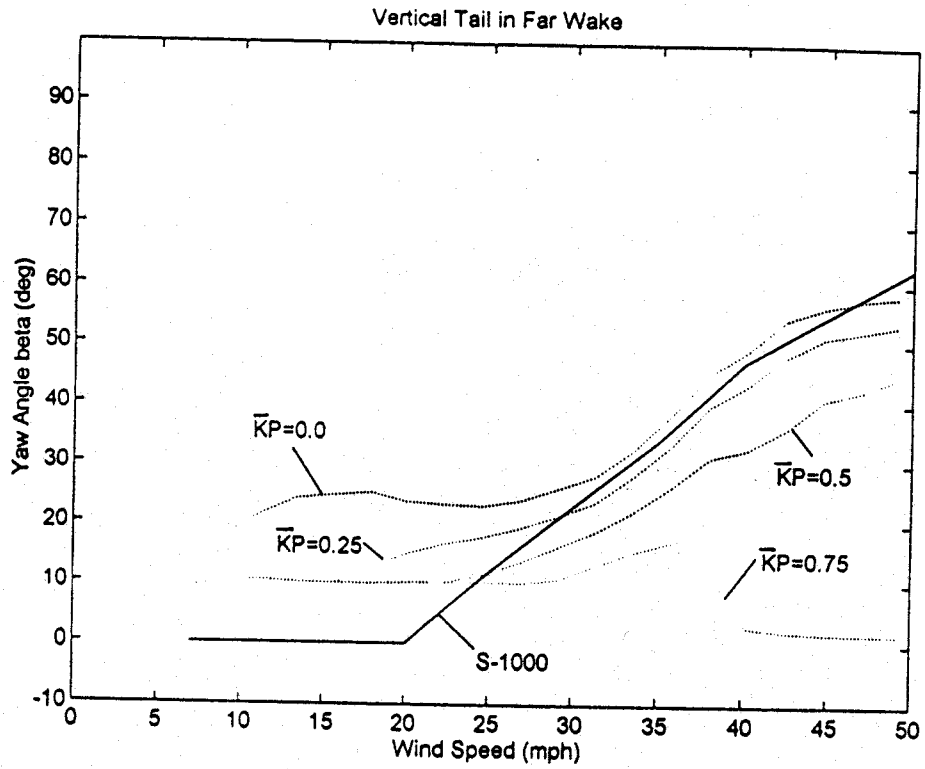
Figure 33. Variation of Furl Angle with Wind Speed

Vertical Tail in Far Wake
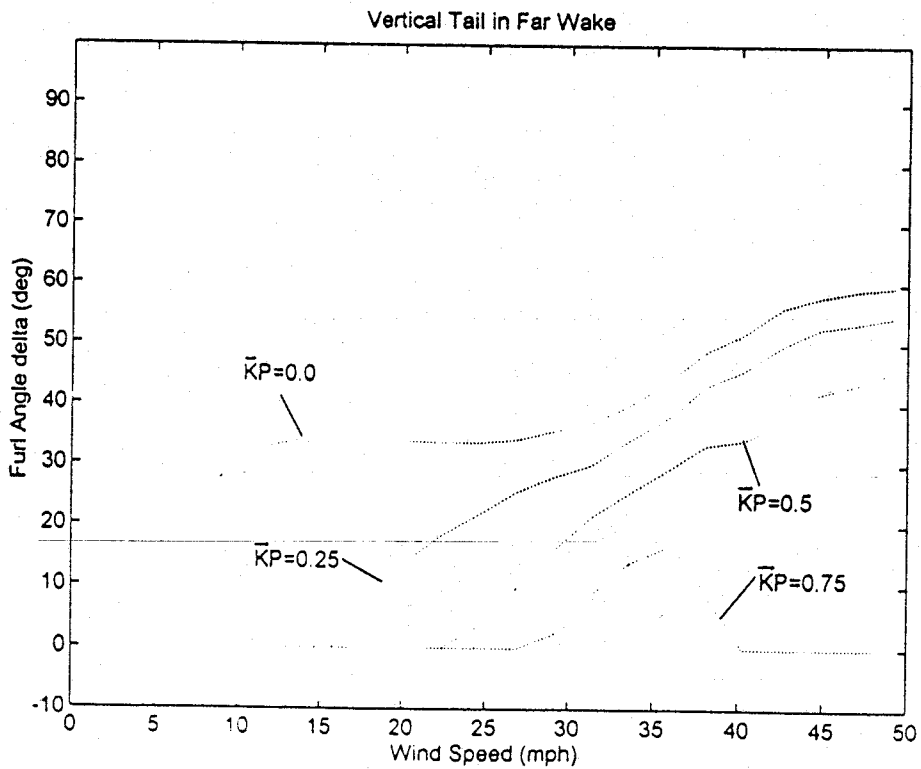
Figure 34. Variation of Yaw Angle with Wind Speed

Vertical Tail in Undisturbed Flow
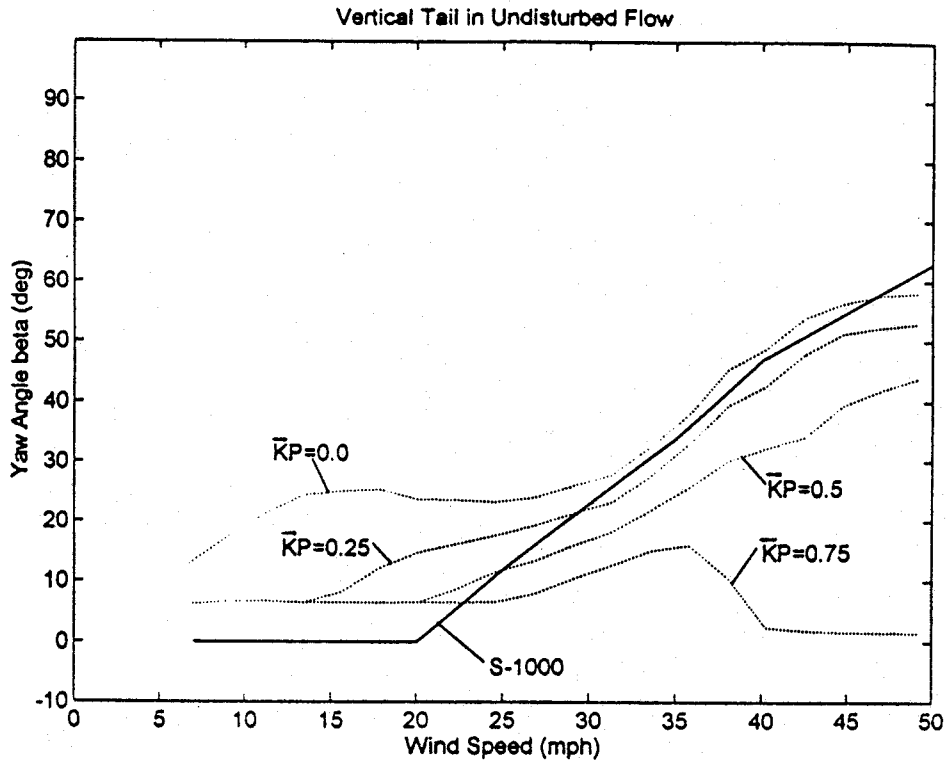
Figure 35. Variation of Furl Angle with Wind Speed

Vertical Tail in Undisturbed Flow
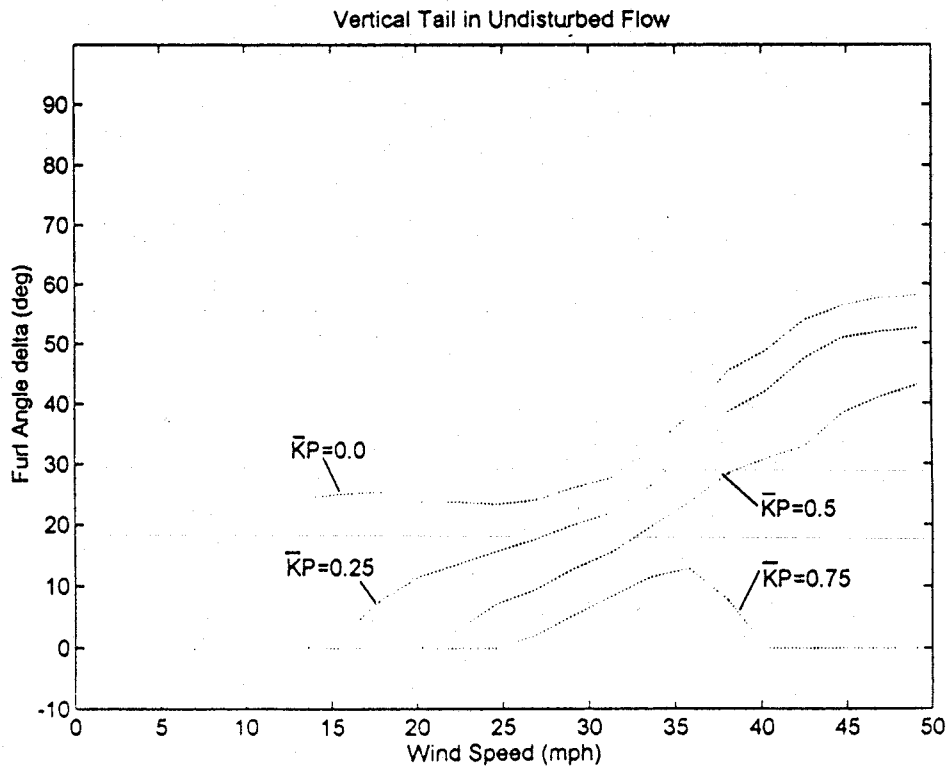
Recommendations for Wind Tunnel Experiment

- Measure wake skew angle as well as yaw angle
- Measure induced velocity in wake near nominal tail position
- Measure all six net forces and moments on rotor
- Measure high tip-speed as well as low tip speed conditions
- Determine effect of wind tunnel walls on wake expansion and straightening

Appendix O:

Presentation by J. Whale, University of Illinois

The Lifting-Surface Inflow Correction Method (LSIM)

J. Whale and M.S.Selig

Dept. of Aeronautical and Astronautical Engineering

University of Illinois at Urbana-Champaign

J.L.Tangler

NREL Technical Monitor

NREL-NASA Ames Tests Science Panel, Oct. 1998

1

Overview

- **Statement of the problem**
  - ➤ Objective
  - ➤ Approach
- **Strategy**
- **Testing the method**
- **Results**
- **Comparison with wind-tunnel method**
- **Conclusions and Recommendations**
- **Future Work**

O-3

Objective

- Objective : accurate 3D measurements from full-scale wind turbines to use in BEM design codes

- Aim: find relationship between measured flow angle (β) and (sectional) angle of attack (α)
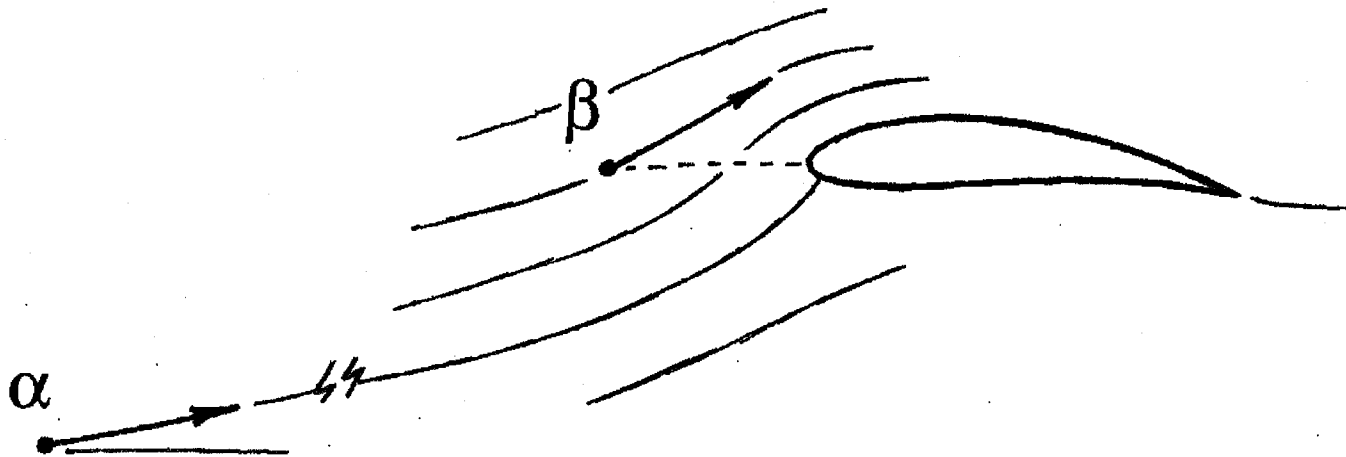
Approach

- Previous approach: essentially 2D methods e.g. blade section in a wind tunnel)

- Current approach: use a 3D code with input data that reflects 3D flow physics (post-stall effects)

2-D ⇨ Cl = 1   **3-D ⇨ Cl = 2**

β_{2-D}

Γ_{2-D}

α

$\beta_{3-D} > \beta_{2-D}$

$\Gamma_{3-D} > \Gamma_{2-D}$

α
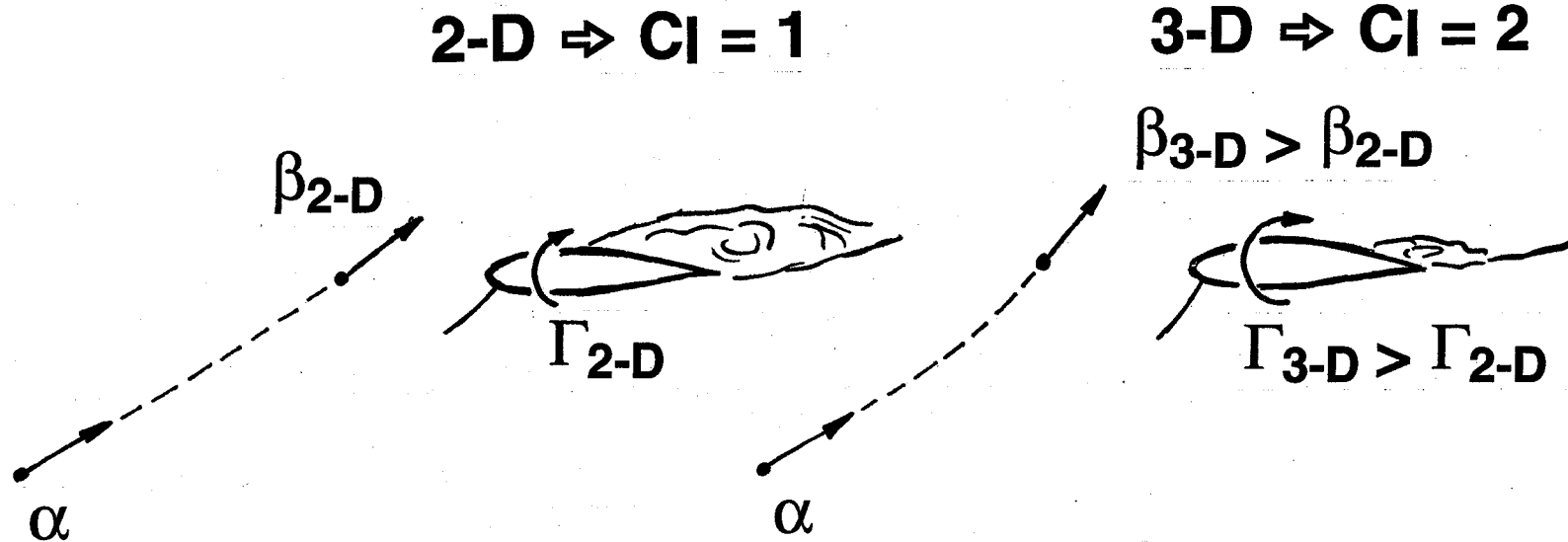
Strategy

- ## 3D vortex panel code -

  Lifting Surface Aerodynamics and Performance Analysis of Rotors in Axial Flight (LSAF)

  - ➤ Adapted from helicopter theory
  - ➤ Simulates rotor and wake as lattice of lifting surfaces
  - ➤ Prescribed wake model
  - ➤ Combines lifting surface method with blade-element analysis
  - ➤ INPUT: airfoil performance tables - c_l, c_d vs. α
  - ➤ OUTPUT: inflow angle at field point - β vs. α

O-9

START

The Lifting-Surface Inflow Correction Method (LSIM)

Make initial estimate of the β–α relationship

Convert raw c_n–β, c_t–β data to c_l–α data and use together with suitable c_d–α data as airfoil tables for input to LSAF

Run LSAF to produce new 3D β–α relationship

Converged solution for β–α curve?

NO

YES

Apply β–α correction to raw c_n–β, c_t–β data to produce final solutions for c_l–α, c_{dp}–α

END

NREL-NASA Ames Tests Science Panel, Oct. 1998

Testing the Method

- ## Available Field Measurement Data
  - ➢ International Energy Agency (IEA) -
    Field Rotor Aerodynamics (Annex XIV)

- ## Combined Experiment Rotor (CER) at NREL
  - ➢ Comprehensive instrumentation system
  - ➢ S809 profile (2D data wind tunnel from Delft)
  - ➢ Most recent campaigns - Phase III, Phase IV
  - ➢ Pressure taps, flags, probes at 4(5) spanwise stations

O-8

CER Performance Data - Phase III
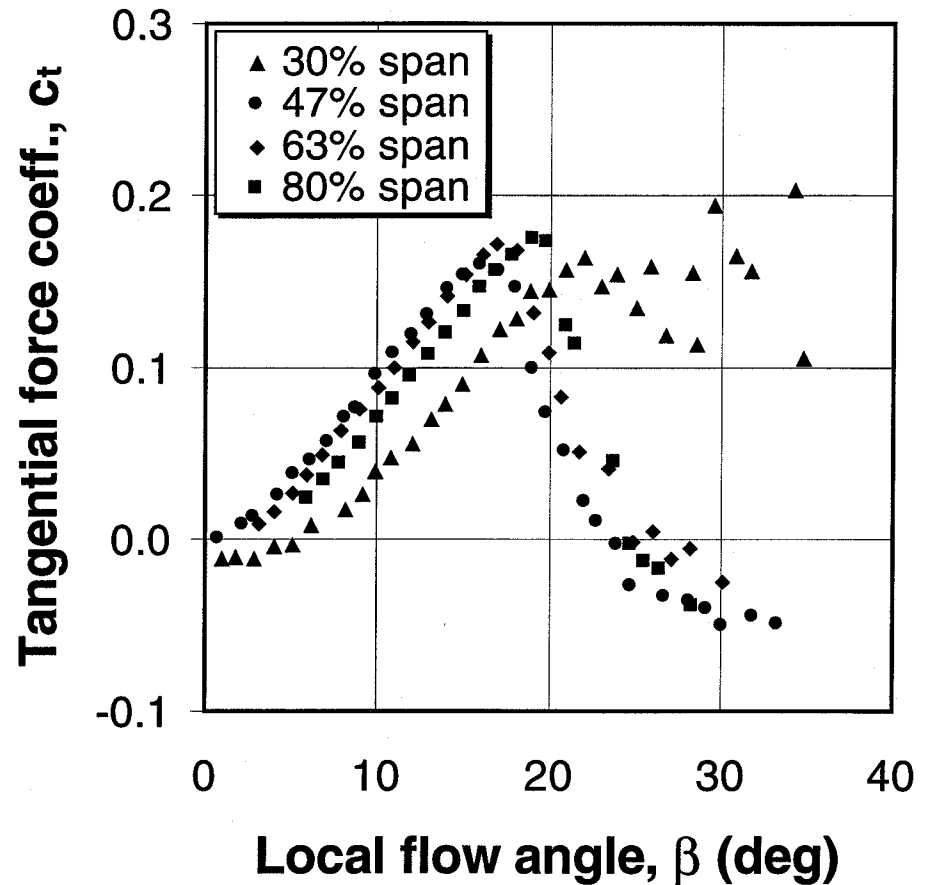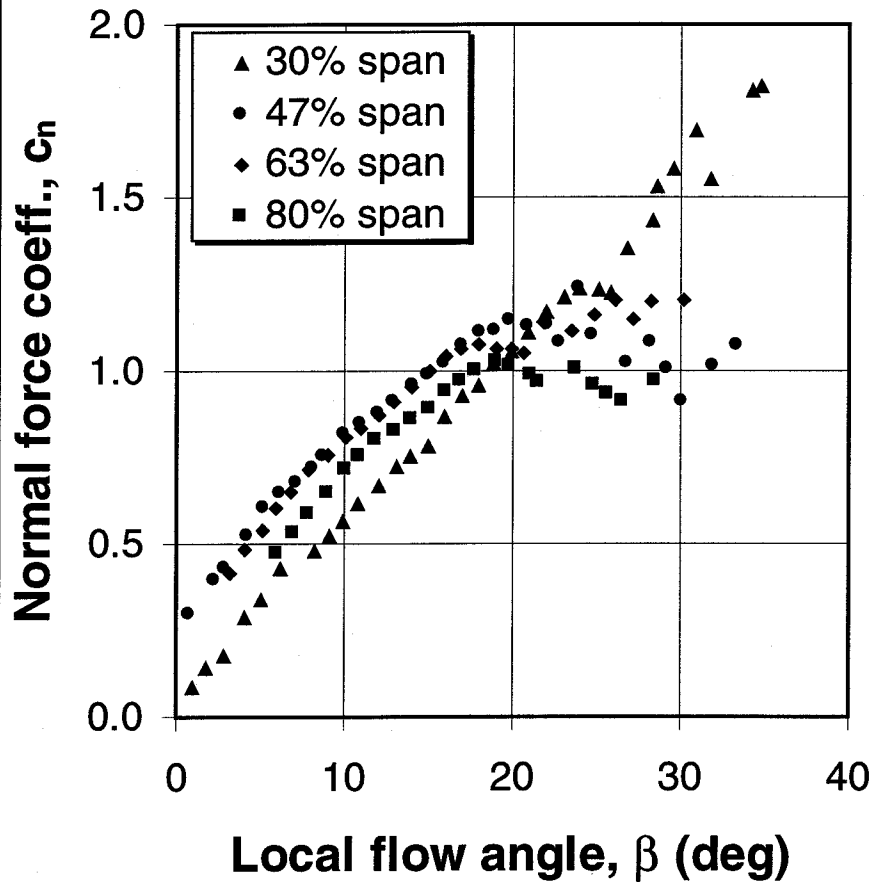
Features of the CER Data

- Spread of data below stall

  ➤ Low c_n and c_t values at 30% span

  ➤ Contradicts trends in spanwise upwash effects ?

- Post-stall data

  ➤ High c_t values

  ➤ Higher c_n at 63% than 47%

  ➤ Contradicts idea of enhanced inboard lift ?

- Use hypothetical data in order to test LSIM

O-10
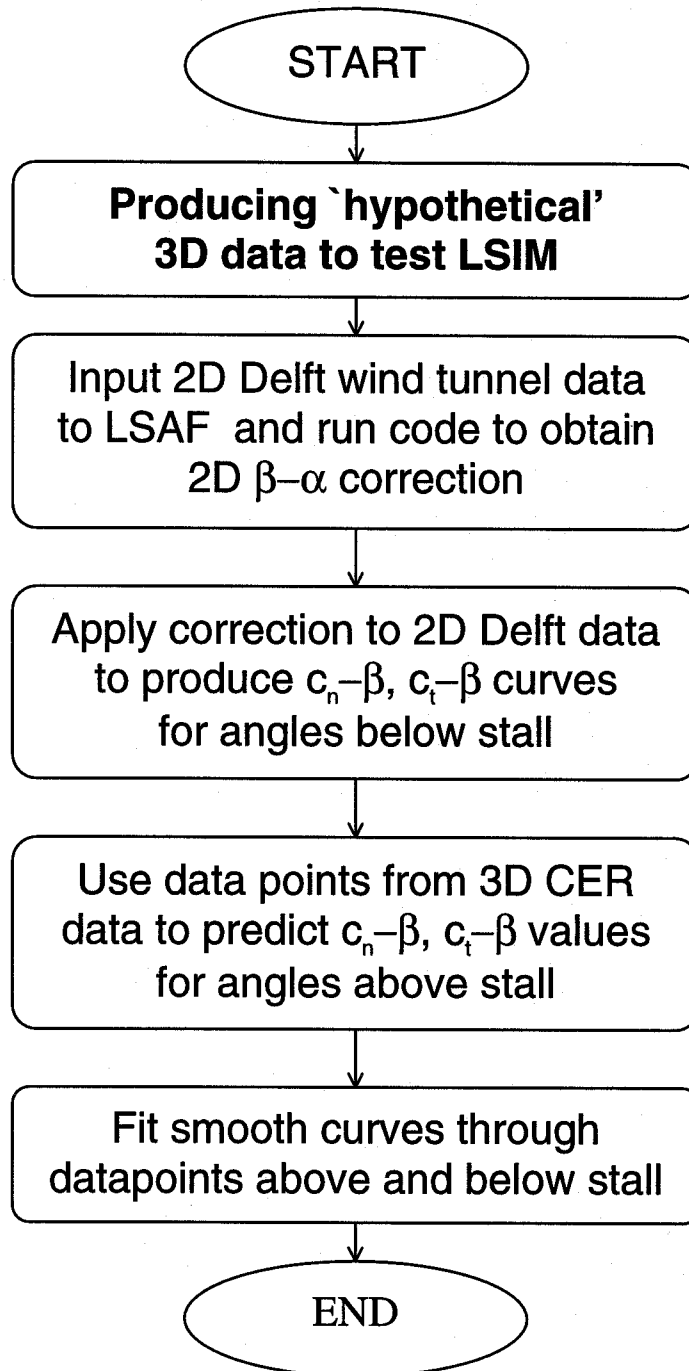
Hypothetical Performance Data

11
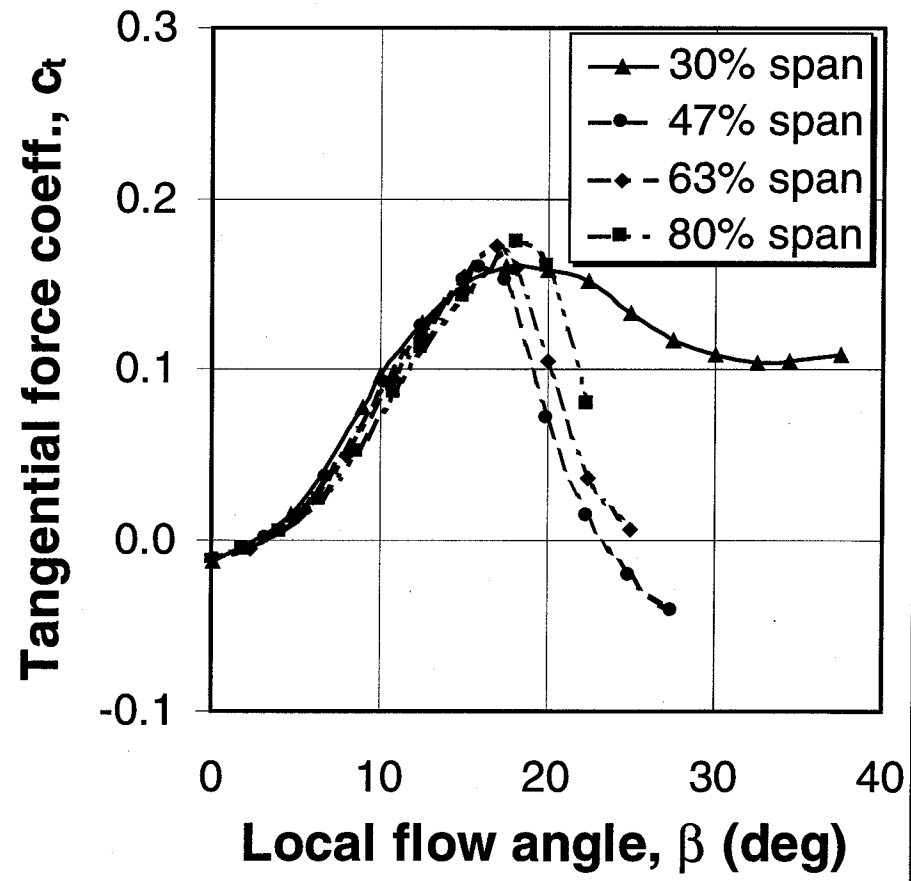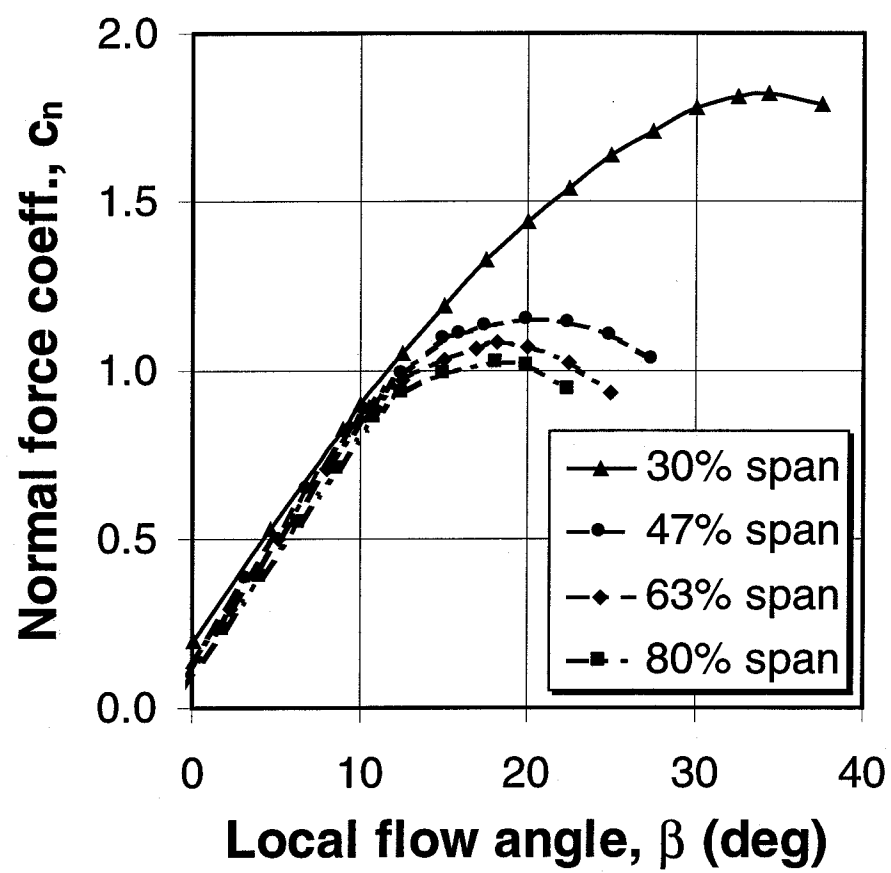
Vortex Panel Simulations

NREL S809 Profile
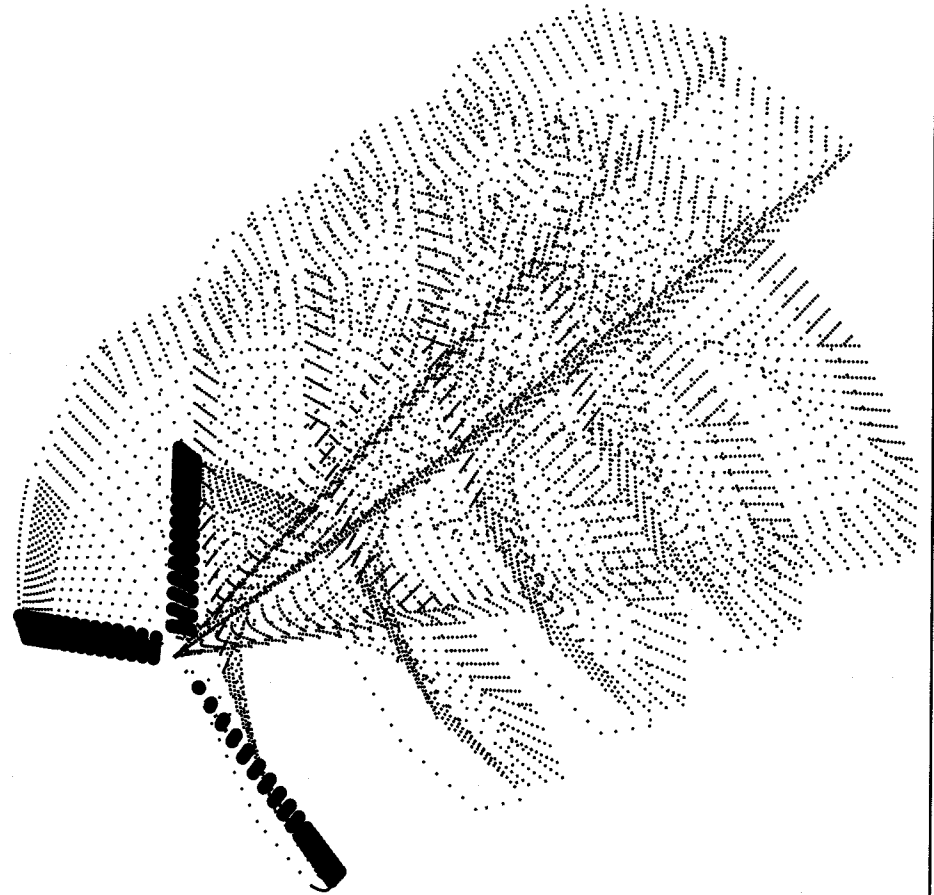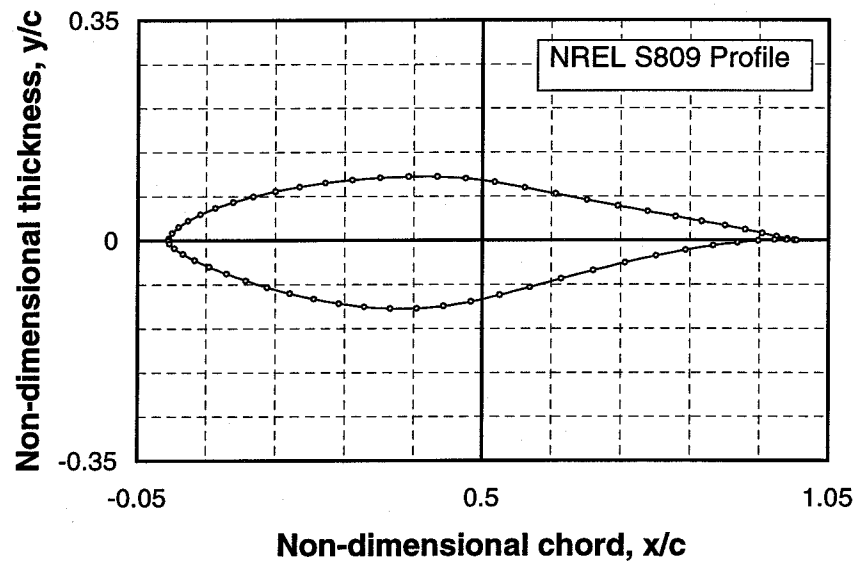
Corrected Inflow Angle

13
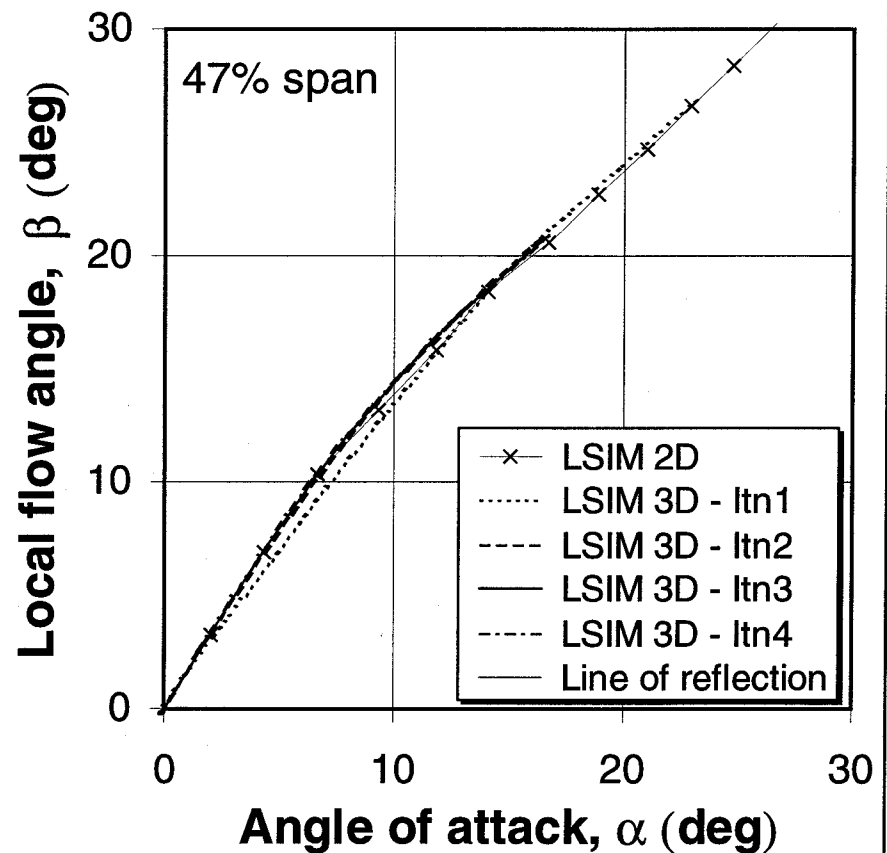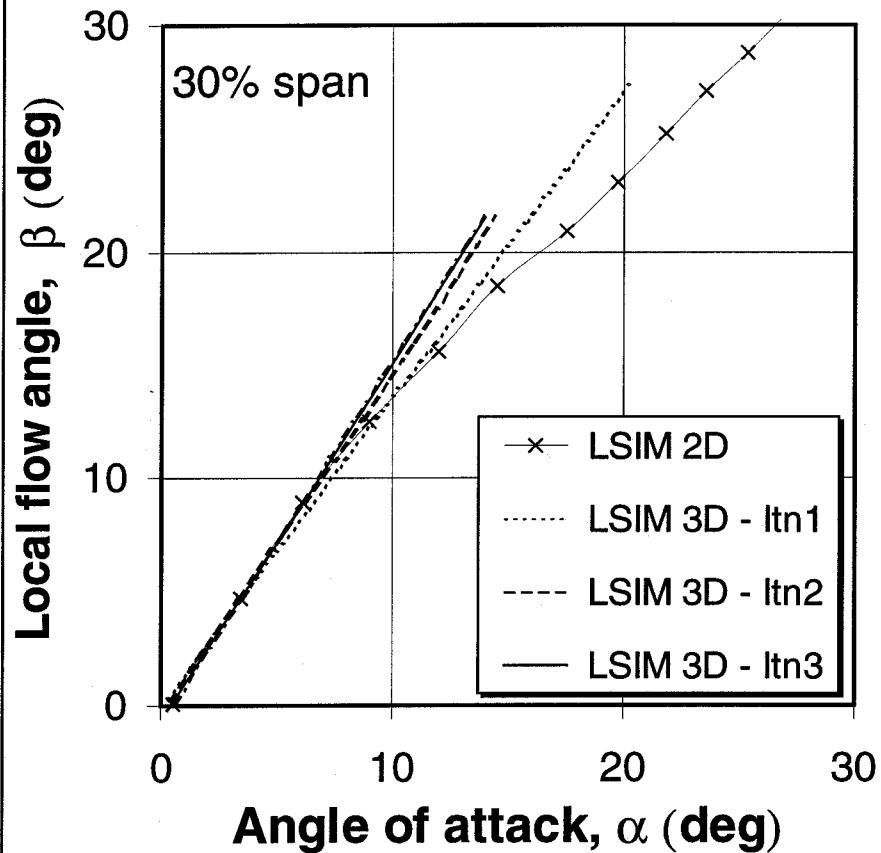
Corrected Lift

$$c_l = c_n \cos\alpha - c_t \sin\alpha$$
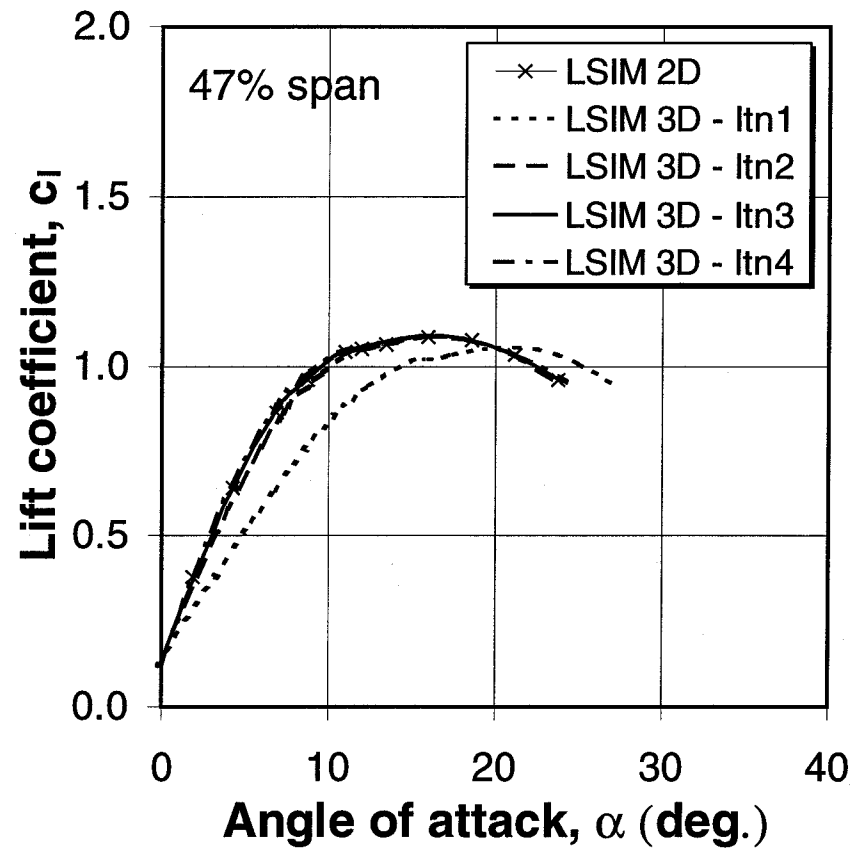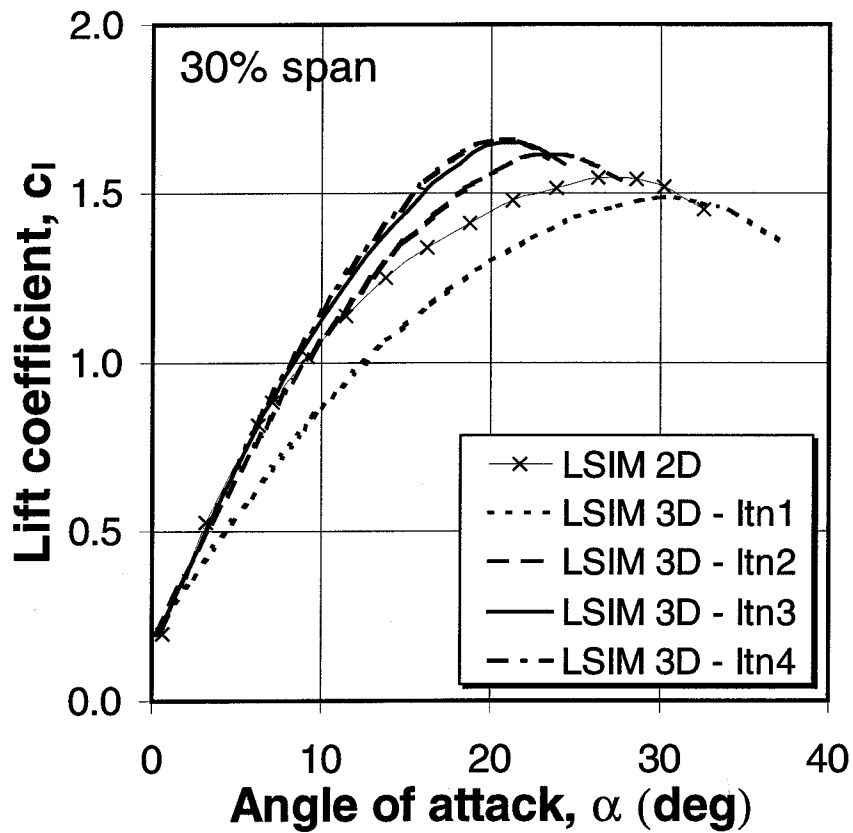
Corrected Pressure Drag

$$c_{dp} = c_t \cos\alpha + c_n \sin\alpha$$
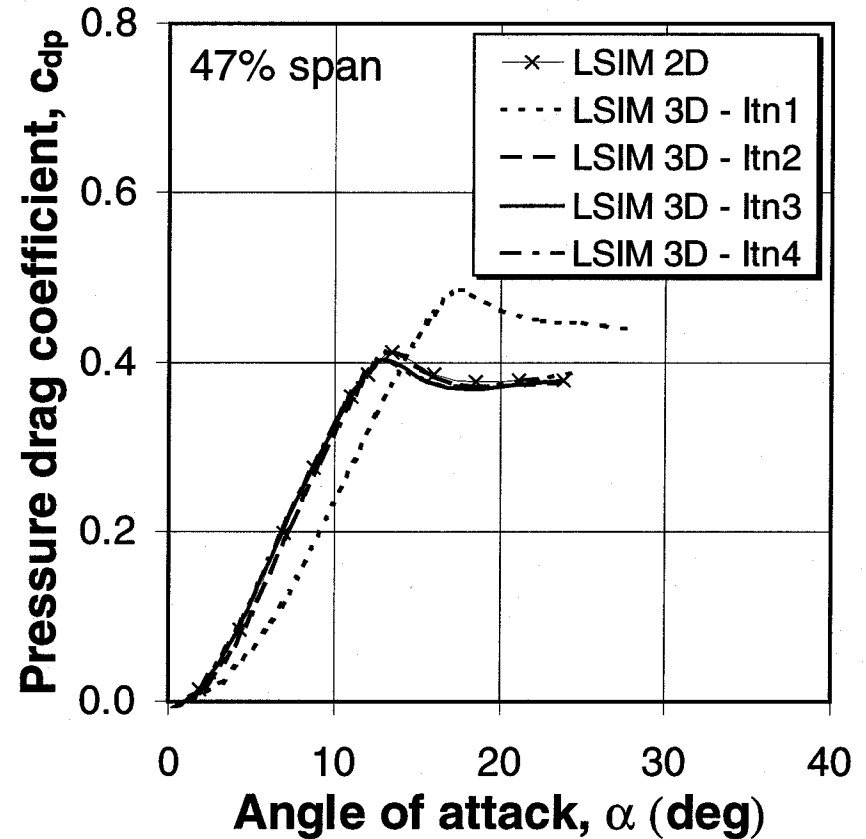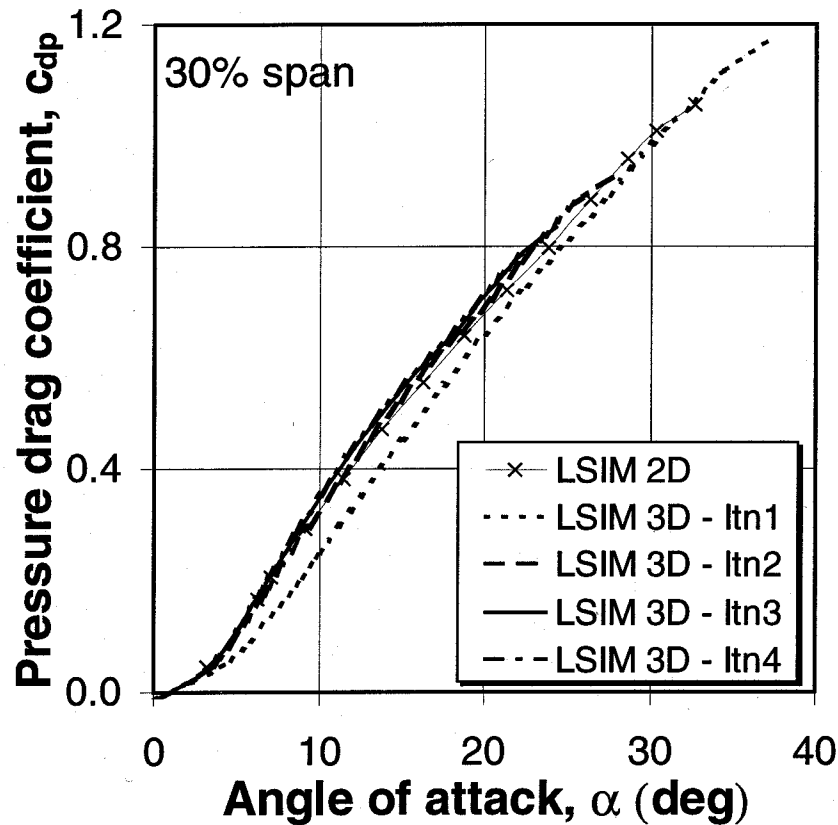
Corrected Forces
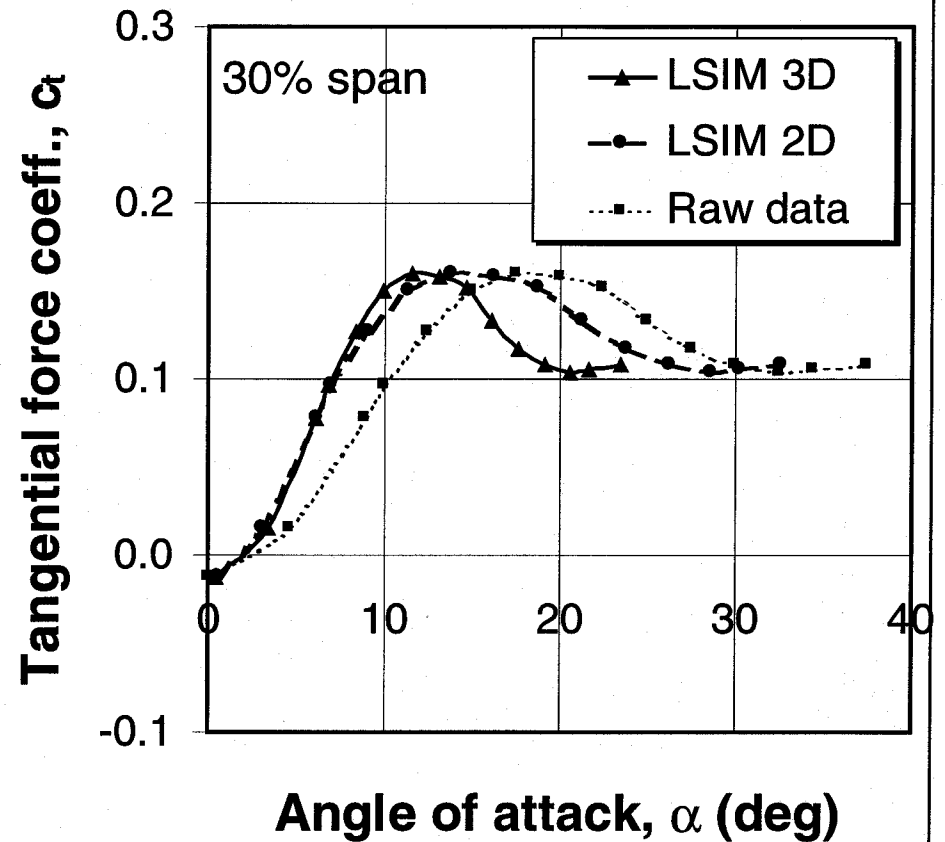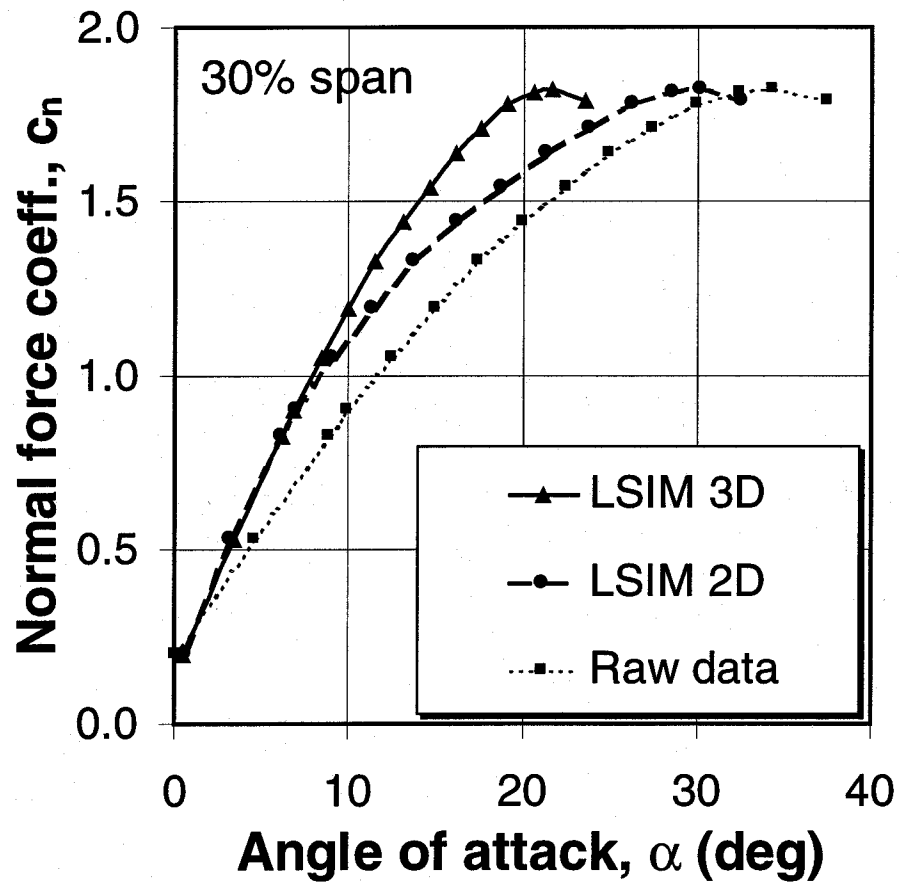
Summary

- Results for 30% span suggest that inboard of the rotor there is a significant difference between applying the 3D LSIM method and using 2D approach

- Results for 47%, 63%, 80% suggest that outboard of the rotor, a 2D LSIM method provides adequate results

- $C_{dp\ 3\text{-}D} > C_{dp\ 2\text{-}D}$ at inboard stations
  - LSIM ✓
  - PROPID/WTPREP ✓
  - Flow Physics ??
  - Measurements from other turbines?

O-18

Comparison with Wind Tunnel Method

O-19
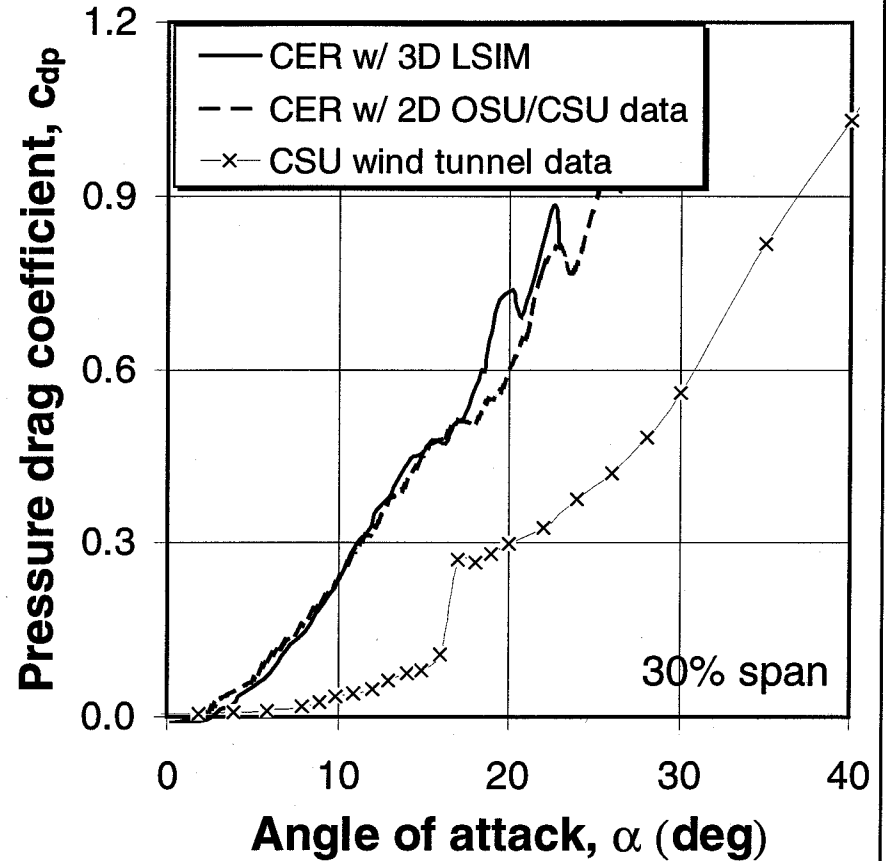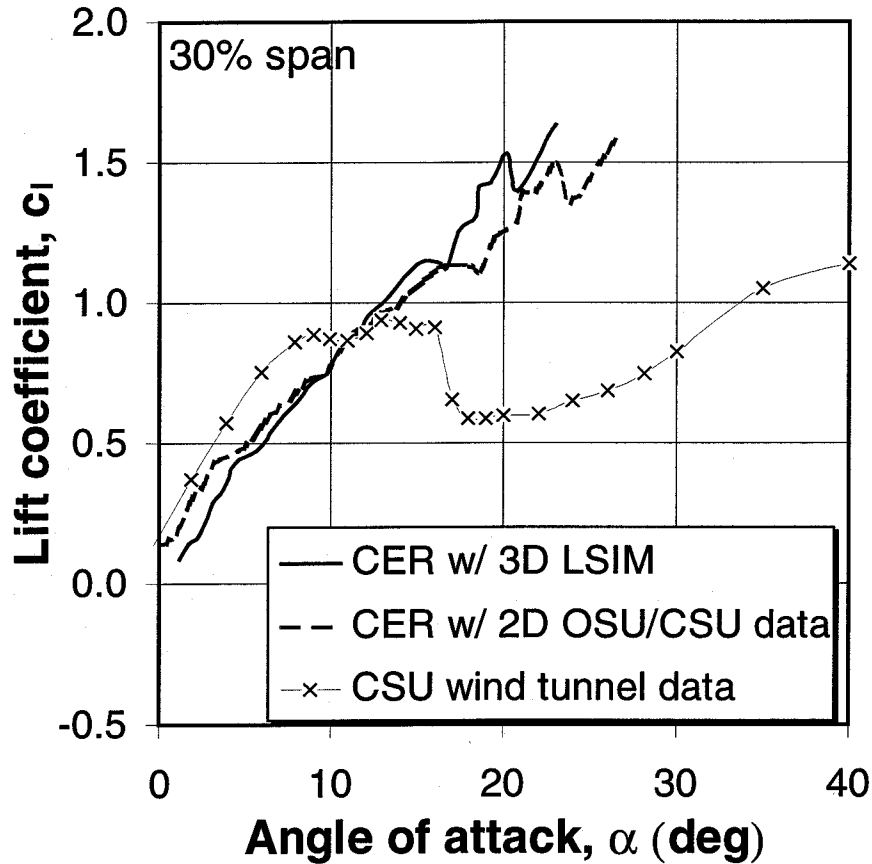
Error Analysis
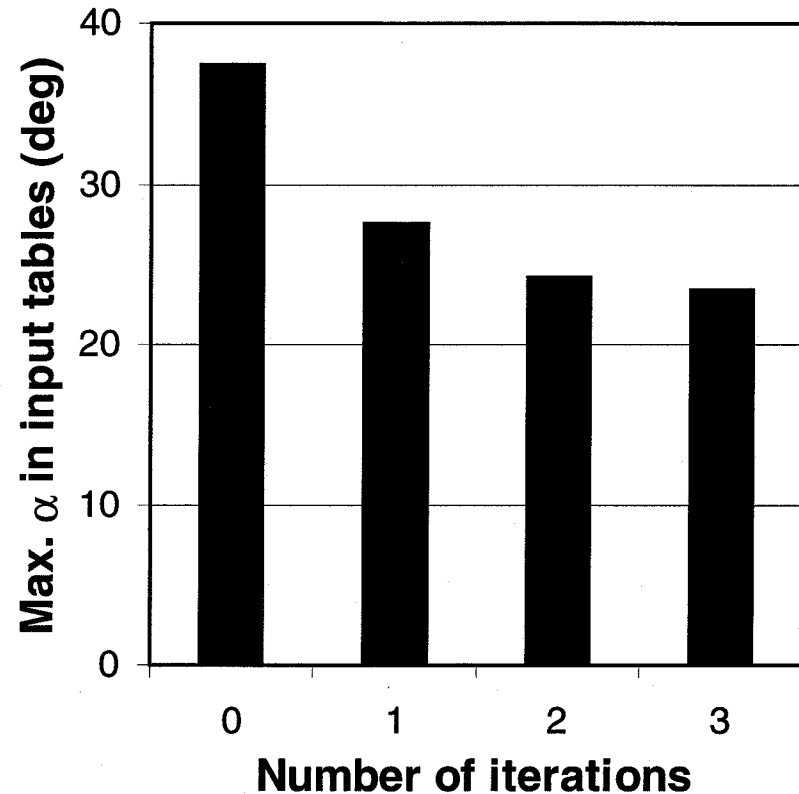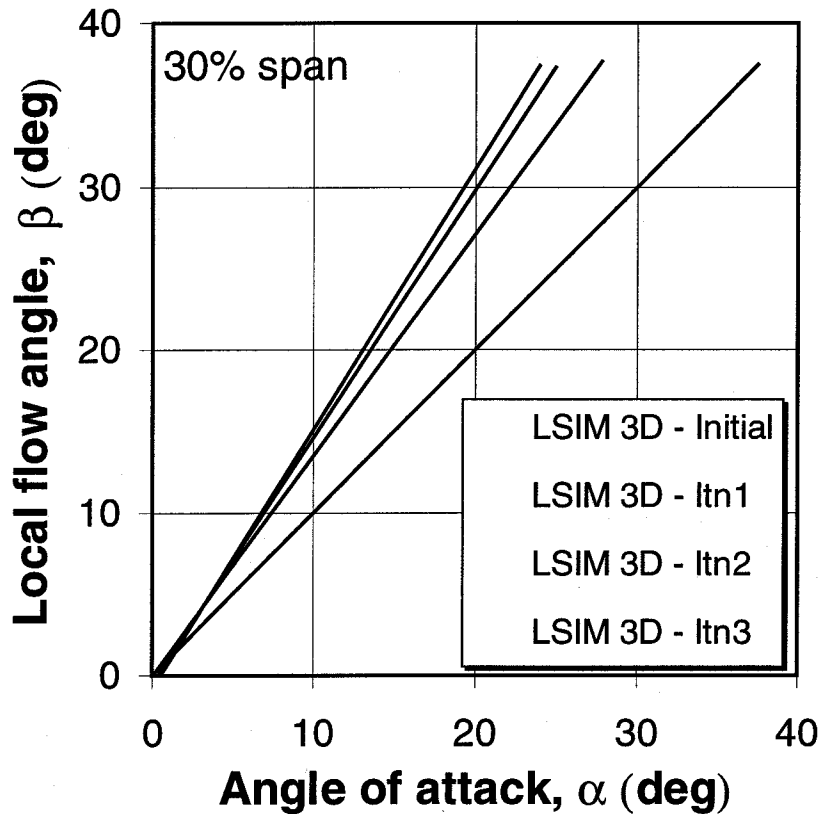
- Nature of β–α: range of known β–α reduces with each iteration leading to use of extrapolation

Conclusions

- LSIM success with hypothetical data

- Identified 30% span as station of interest
  - Significant differences using 3D panel code

- Identified angle-range reduction problem

- Need for additional data for further LSIM tests
  - CER phase III features not fully understood
  - $C_{dp\ 3\text{-}D} > C_{dp\ 2\text{-}D}$?
  - Need data at higher angles of attack
  - NASA Ames wind tunnel tests good opportunity . . .

O-21

Recommendations

- Check previous results
  - ➣ Pre-stall behavior (low c_n at 30%)
  - ➣ Post-stall behavior (63% c_n > 47% c_n)

- 30% station of interest
  - ➣ Concentrate on spanwise locations 25% - 50%
  - ➣ Extra probes between 30% and 47% span ?

- Angle-range reduction
  - ➣ Use controlled environment to collect data over greater range of local flow angles

NREL-NASA Ames Tests Science Panel, Oct. 1998

21

O-22

Future Work

- Apply LSIM to more datasets
  - IEA Annex XIV tests
  - NREL Phase IV data

- Continue Error Analysis
  - Additional data to increase angle-range
  - Sensitivity study - effects of unsteady aerodynamics data?

O-23

Acknowledgment

- ## Forthcoming Paper:

  Whale J., Fisichella, C.J. and Selig, M.S., ''Correcting inflow measurements from HAWTS using a lifting-surface code,'' *Proceedings of the 18th ASME Wind Energy Conference, Reno, NV, January 1999.*

- ## Acknowledgment:

  M.Hand (NREL) for preparing the CER data

O-24

HAWT Post-Stall Performance Prediction

Michael Selig

Associate Professor

Dept of Aeronautical and Astronautical Engineering
University of Illinois at Urbana-Champaign

James Tangler
NREL Technical Monitor

Objectives

- Use analytical methods in an effort to determine the driving mechanisms that cause stall delay (includes identification of key scaling parameters)

- Gather all available experimental data for use in validating approach

- Develop an improved method for correcting field test airfoil aerodynamic data for comparison to 2-D data

- Develop a semi-empirical formulation for modifying the 2-D airfoil characteristics for 3-D post stall effects for use BEMT codes (eg, PROP)

- Implement model in PROPID/WTPREP, ADAMS and YawDyn

O-26

People and Projects

- Experimental data collection
  - Jonathan Whale, Nikhil Raj
- Angle of attack corrections for 3-D field tests
  - Jonathan Whale, Christopher Fisichella
- Analytical studies focused on improving the model
  - Zhaohui Du
- 2-D airfoil post stall performance prediction
  - Renchi Raju
- Model development and implementation into PROPID/WTPREP, ADAMS/YawDyn
  - Zhaohui Du, Nikhil Raj, Craig Hansen

NREL-NASA Ames Tests Science Panel, Oct. 1998
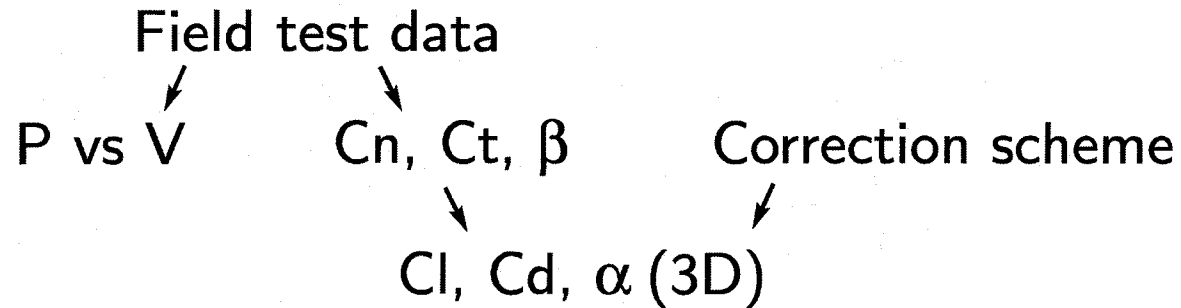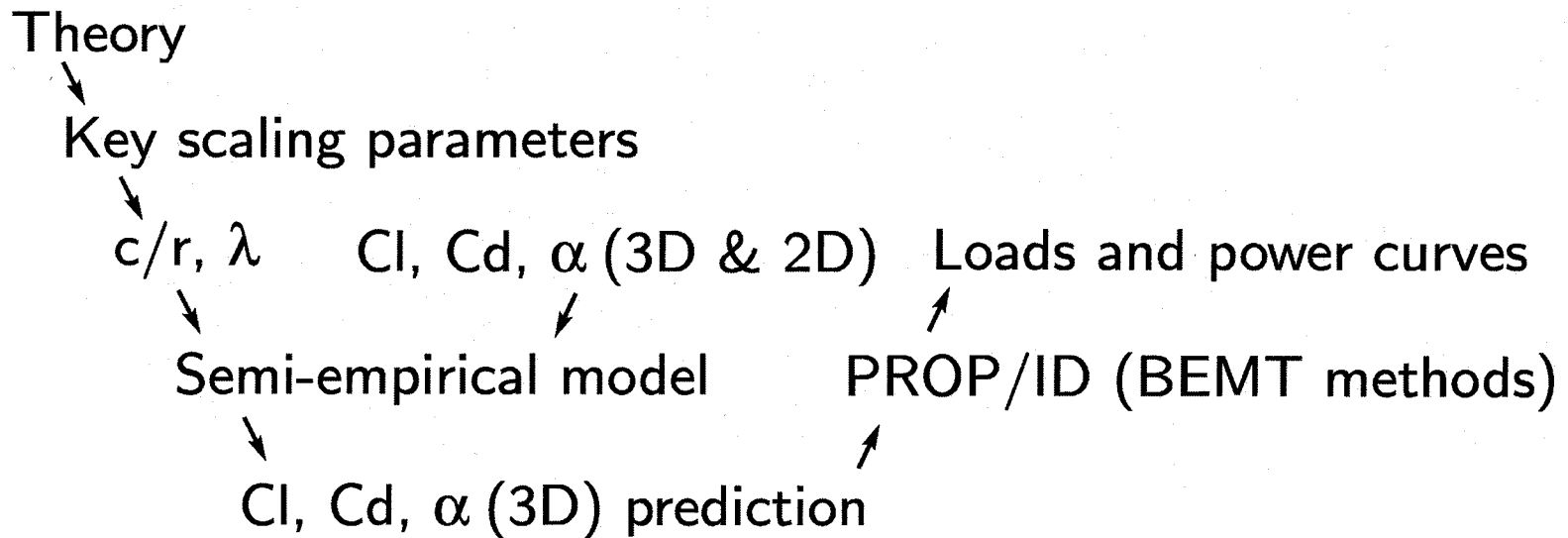
Model Development and Implementation into BEMT Codes

- **CER Phase III results with UIUC and Corrigan models**
- **Model builds off of 2D airfoil data**

30% Span Location

47% Span Location
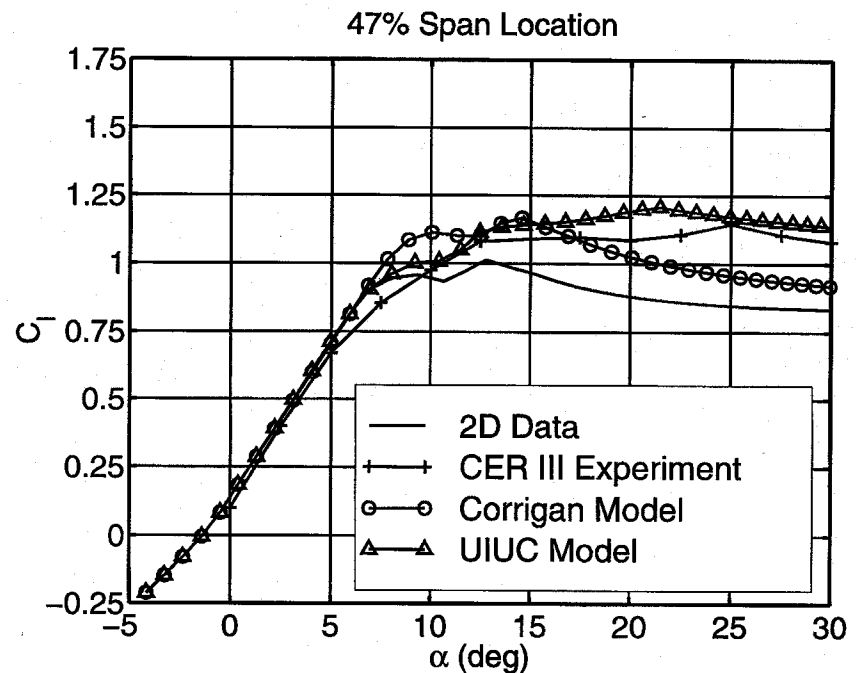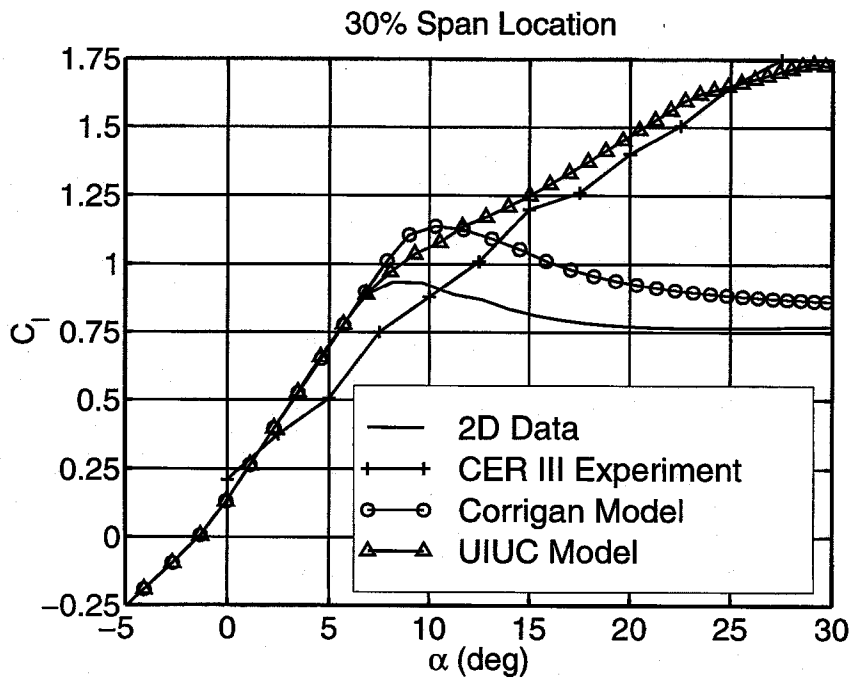
- **NREL data from D. Simms talk (IEA aero meeting #5)**
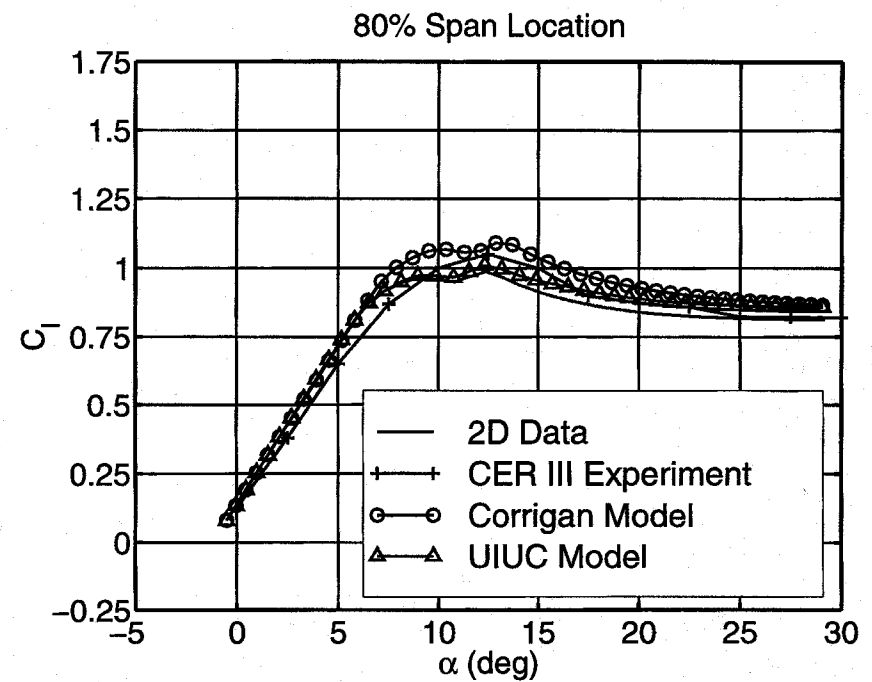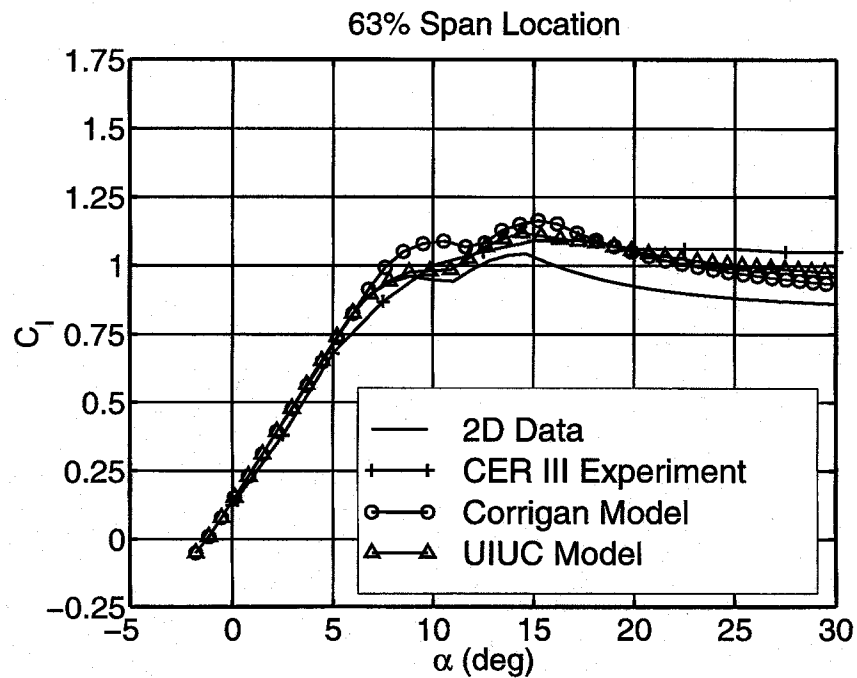
- **Refs: Raj and Selig (1998), Du and Selig (1998a), Du and Selig (1998b)**

O-30

- ## Power curve comparisons.

67% increase in C_d
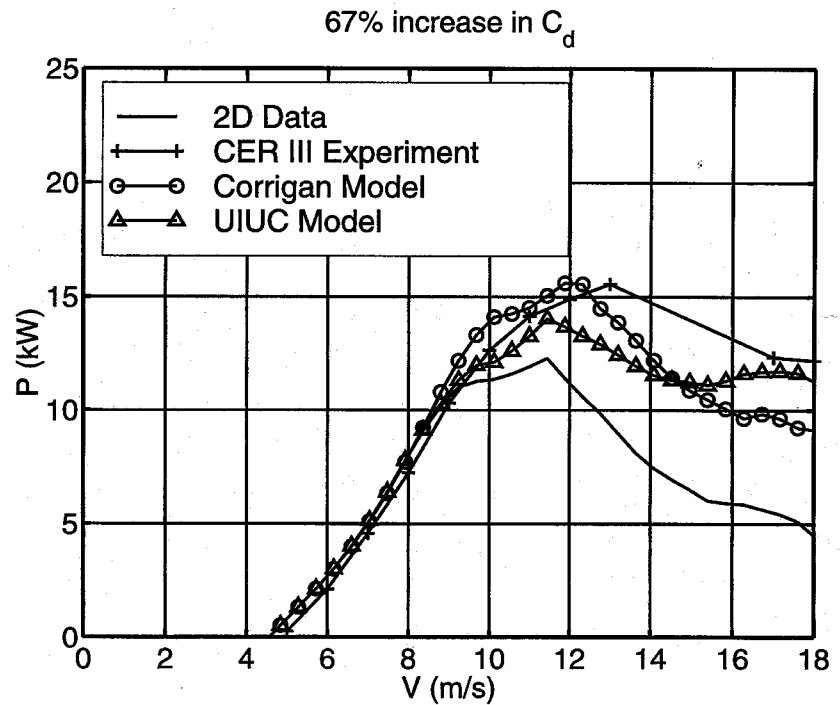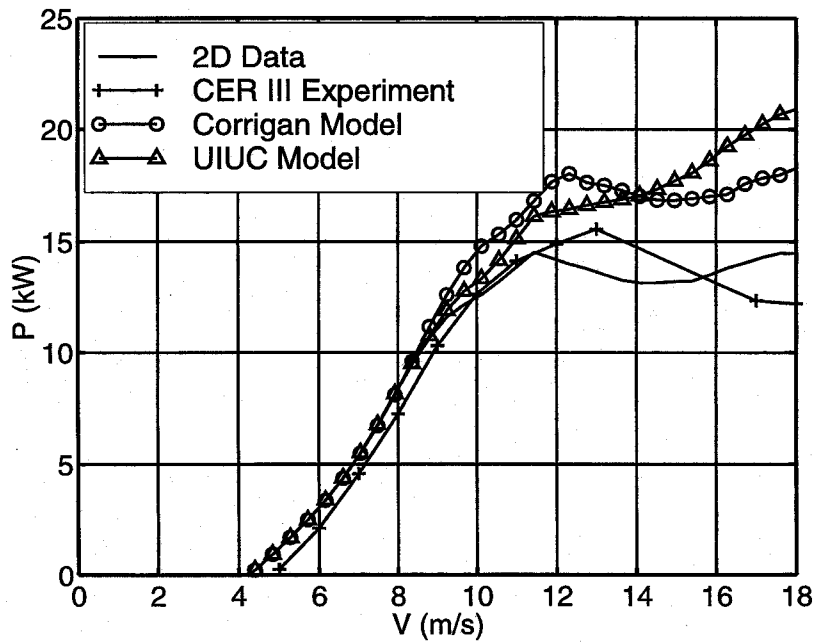
⇨ Drag now becomes a issue(?).

O-31

Future Directions

- Apply correction method to new experimental data to be acquired
- Use updated C_l-α data to refine model
- Continue analytical studies aimed at bringing more physics into the semi-empirical model
- Conclude 2D post-stall airfoil method
- Integrate model in to ADAMS/YawDyn
- Hold aero-design short course before 1999 NREL Subcontractors Review Meeting

---

- Finish tip-loss model and integrate into PROPID

O-32

References

- http://www.uiuc.edu/ph/www/m-selig/wind.html
- Du, Z. and Selig, M.S. (1998a), "A 3-D Stall-Delay Model for Horizontal Axis Wind Turbine Performance Prediction," ASME/AIAA Joint Wind Energy Symposium, AIAA Paper 98-0021, Reno, NV, January 1998.
- Du, Z. and Selig, M.S. (1998b), "The Effect of Rotation on the Boundary Layer of Wind Turbine Blade," AWEA WINDPOWER 1998 Conference, Bakersfield, CA, April 1998.
- Raj, N. and Selig, M.S. (1998), "Capabilities of WTPREP for Blade Airfoil Data for HAWTs," American Wind Energy Association WINDPOWER 1998 Conference, Bakersfield, CA, April 1998.

O-33

Appendix P:

Presentation by J. Tangler, NREL

Shortcomings of Steady-State Performance Prediction

P-2

James Tangler

National Renewable Energy Laboratory

NREL - AMES Science Panel Meeting

October 5-6, 1998

National Wind Technology Center

Issues

P-3

- ■ Accuracy of test data
  - turbulence
- ■ Accuracy of Blade-Element/Momentum
  - delayed root stall
  - delayed tip stall

National Wind Technology Center
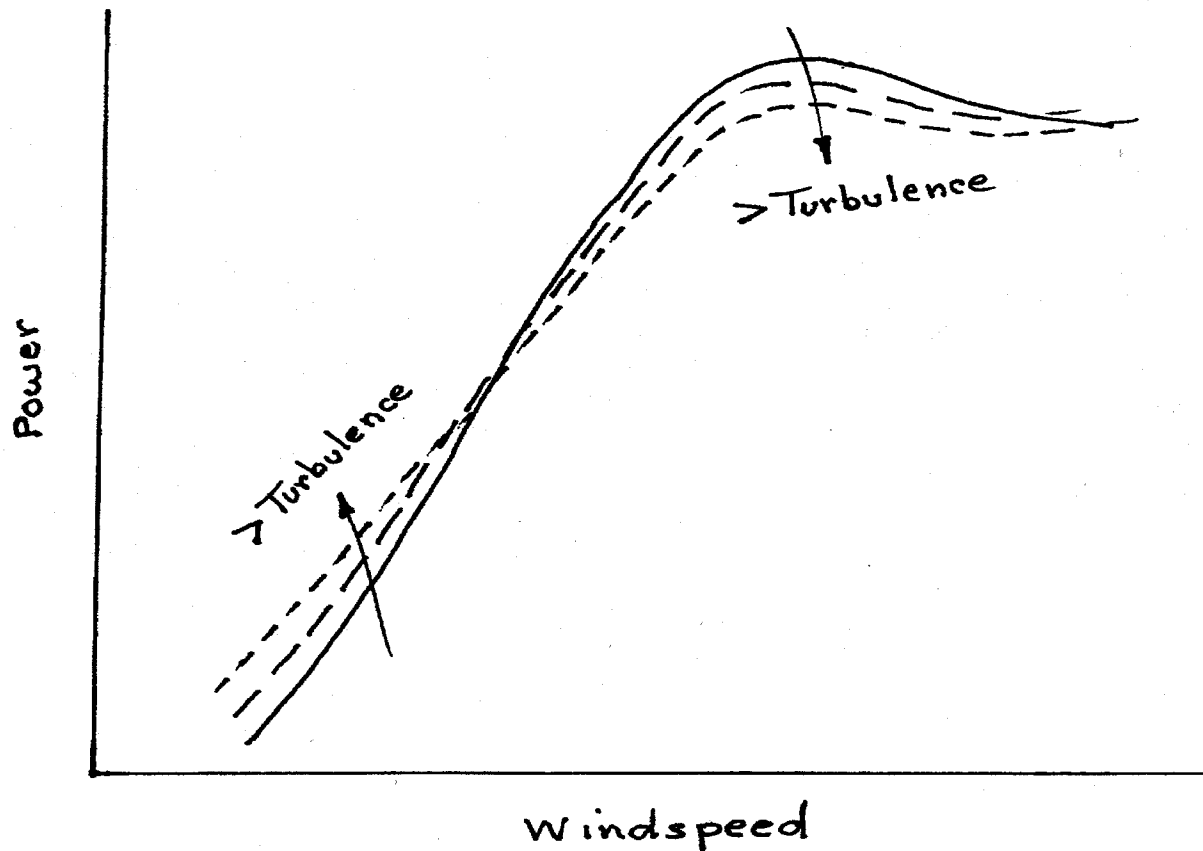
Effect of Delayed Root and Tip Stall on Lift Coefficient

National Wind Technology Center
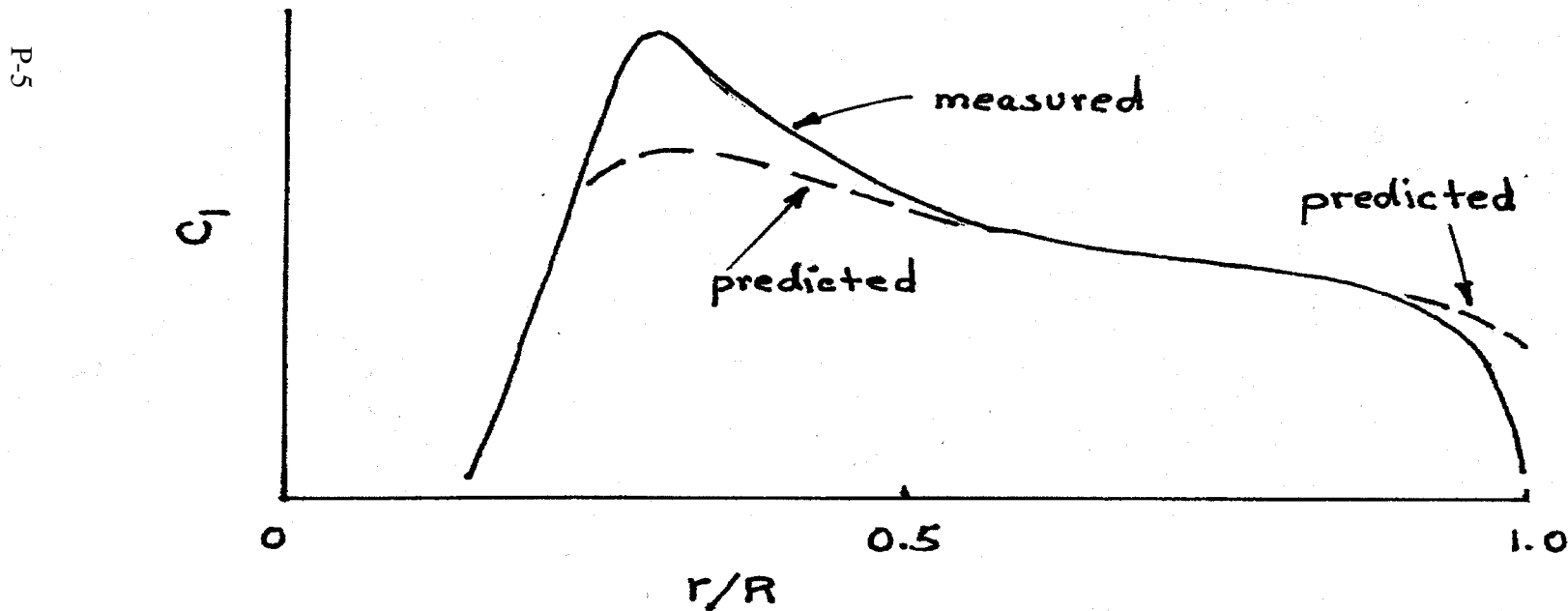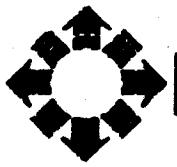
Empirical Stall Delay Model

- Centrifugal spanwise pumping
- Pressure gradient spanwise pumping
- Chordwise Coriolis displacement
- Modification to 2-D wind-tunnel post-stall data

P-6

National Wind Technology Center

Simplified Equations

$$\Delta\alpha = \left(\alpha_{C_{l,max}} - \alpha_{C_{l=0}}\right)\left[\left(\frac{K\theta_{TE}}{0.136}\right)^{n} - 1\right]$$

c/r = 0.1517K^{-1.004}

National Wind Technology Center
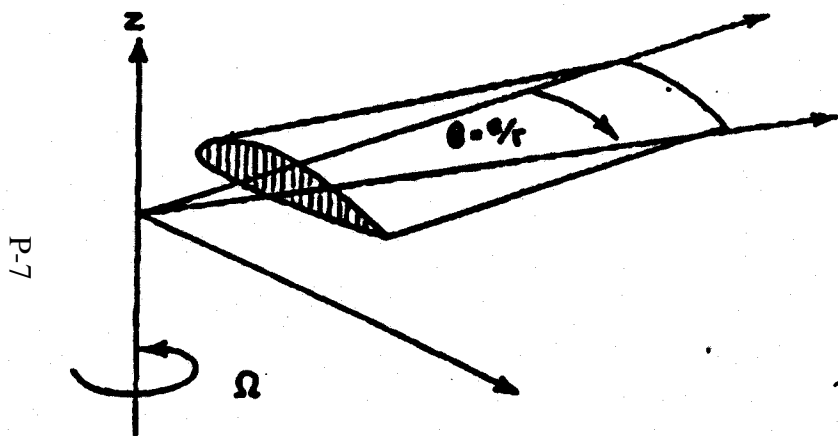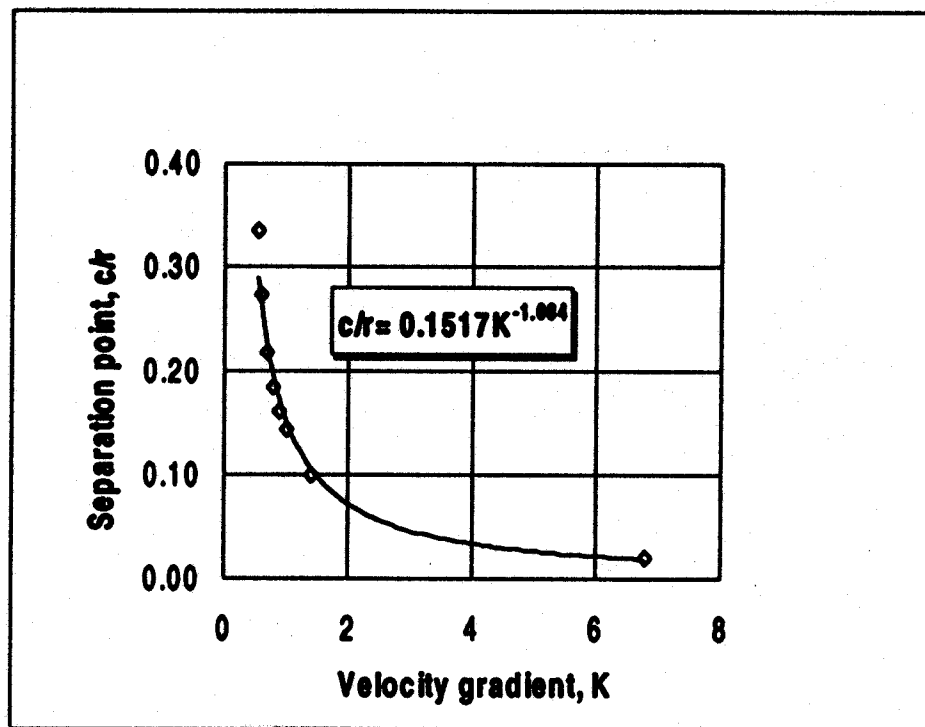
CER Blade Geometry

■ constant-chord blade   ■ tapered-chord blade

National Wind Technology Center
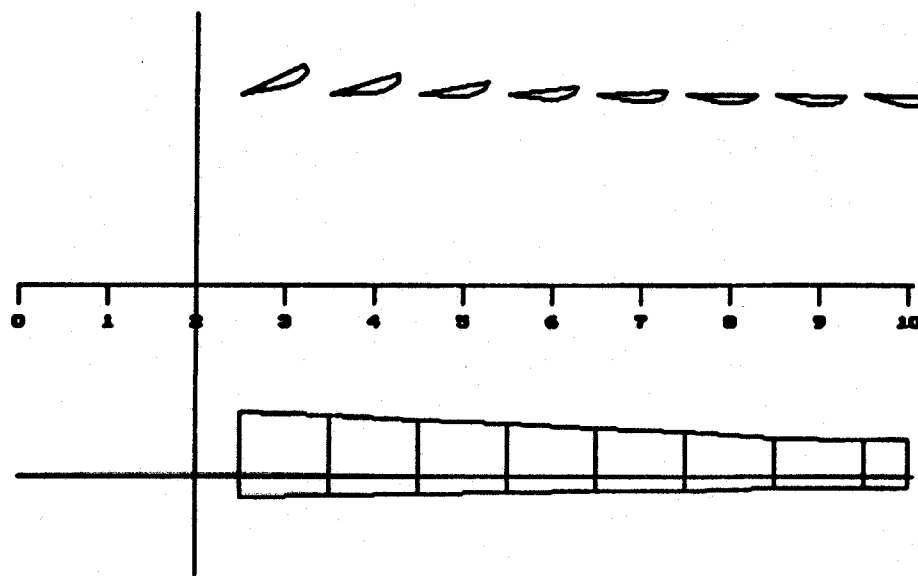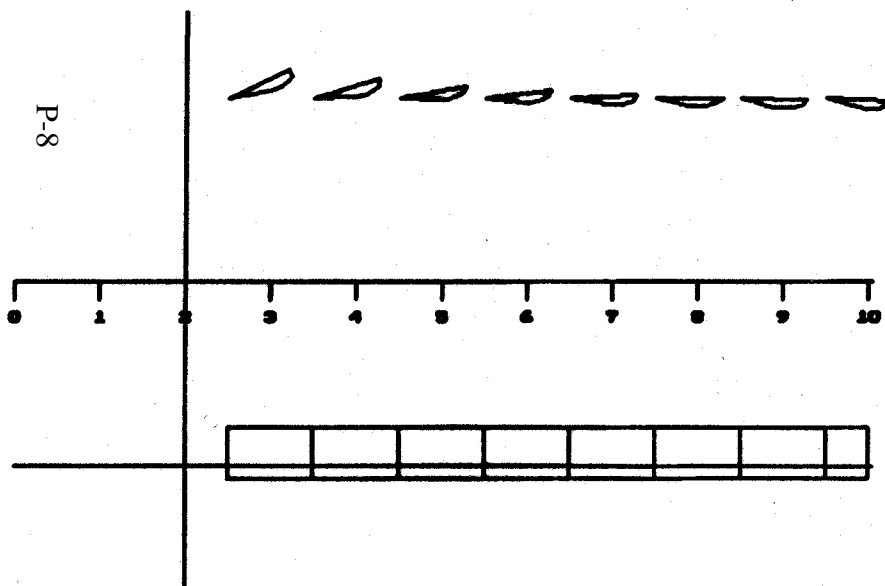
Implementation Procedure

r/R	c/R	c/r	K	alfa clmax	alfa clzero	del theta	K*the/0.136	del alfa(n=1)
0.05	0.05	1	0.1778	9	-1.2	10.2	1.307353	3.135
0.15	0.0911	0.607333	0.280745	9	-1.2	10.2	1.25372	2.567949
0.25	0.0911	0.3644	0.448256	9	-1.2	10.2	1.201062	2.050633
0.35	0.0911	0.260286	0.610069	9	-1.2	10.2	1.167591	1.709426
0.45	0.0911	0.202444	0.76799	9	-1.2	10.2	1.143201	1.460649
0.55	0.0911	0.165636	0.922965	9	-1.2	10.2	1.124092	1.26574
0.65	0.0911	0.140154	1.075577	9	-1.2	10.2	1.108428	1.10597
0.75	0.0911	0.121467	1.226222	9	-1.2	10.2	1.095184	0.970681
0.85	0.0911	0.107176	1.375184	9	-1.2	10.2	1.08373	0.854049
0.95	0.0911	0.095895	1.522677	9	-1.2	10.2	1.073652	0.751252

National Wind Technology Center

Modification of Wind-Tunnel Data
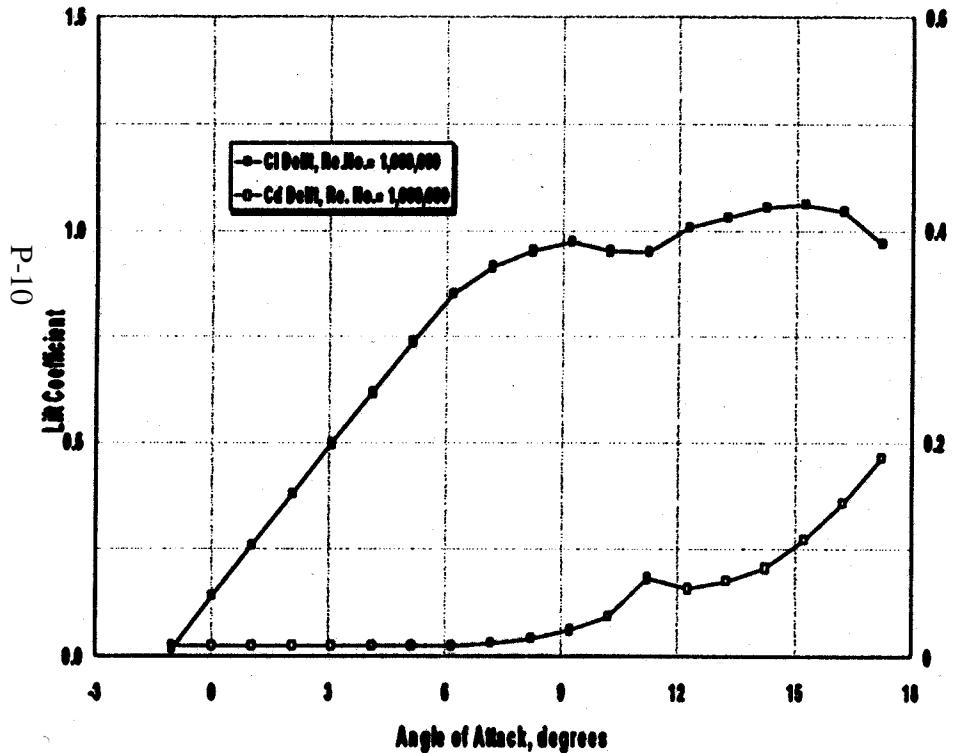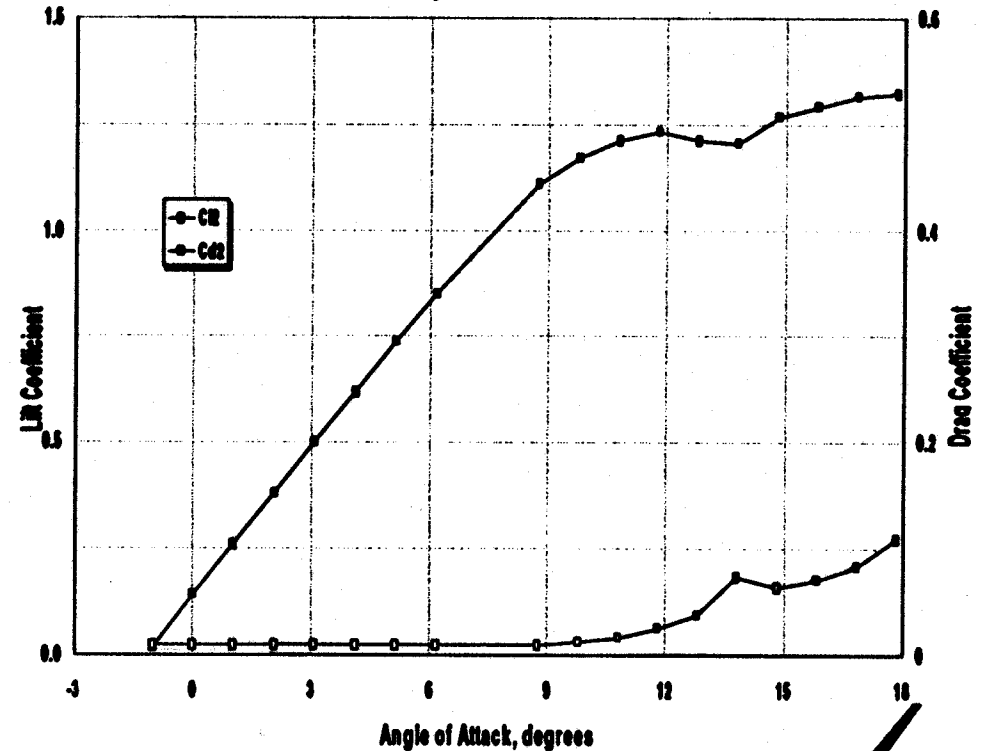
Spanwise Data Tables - CER

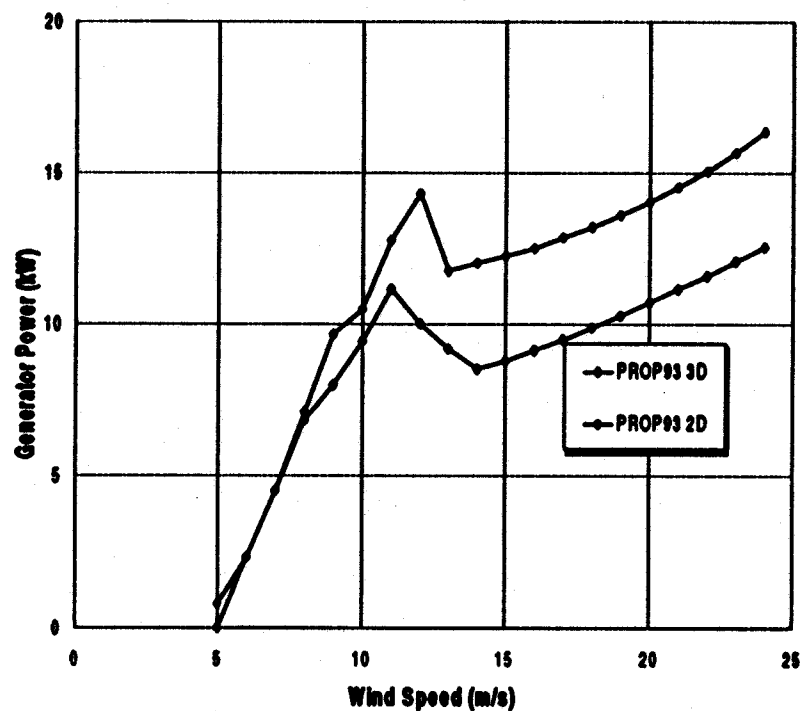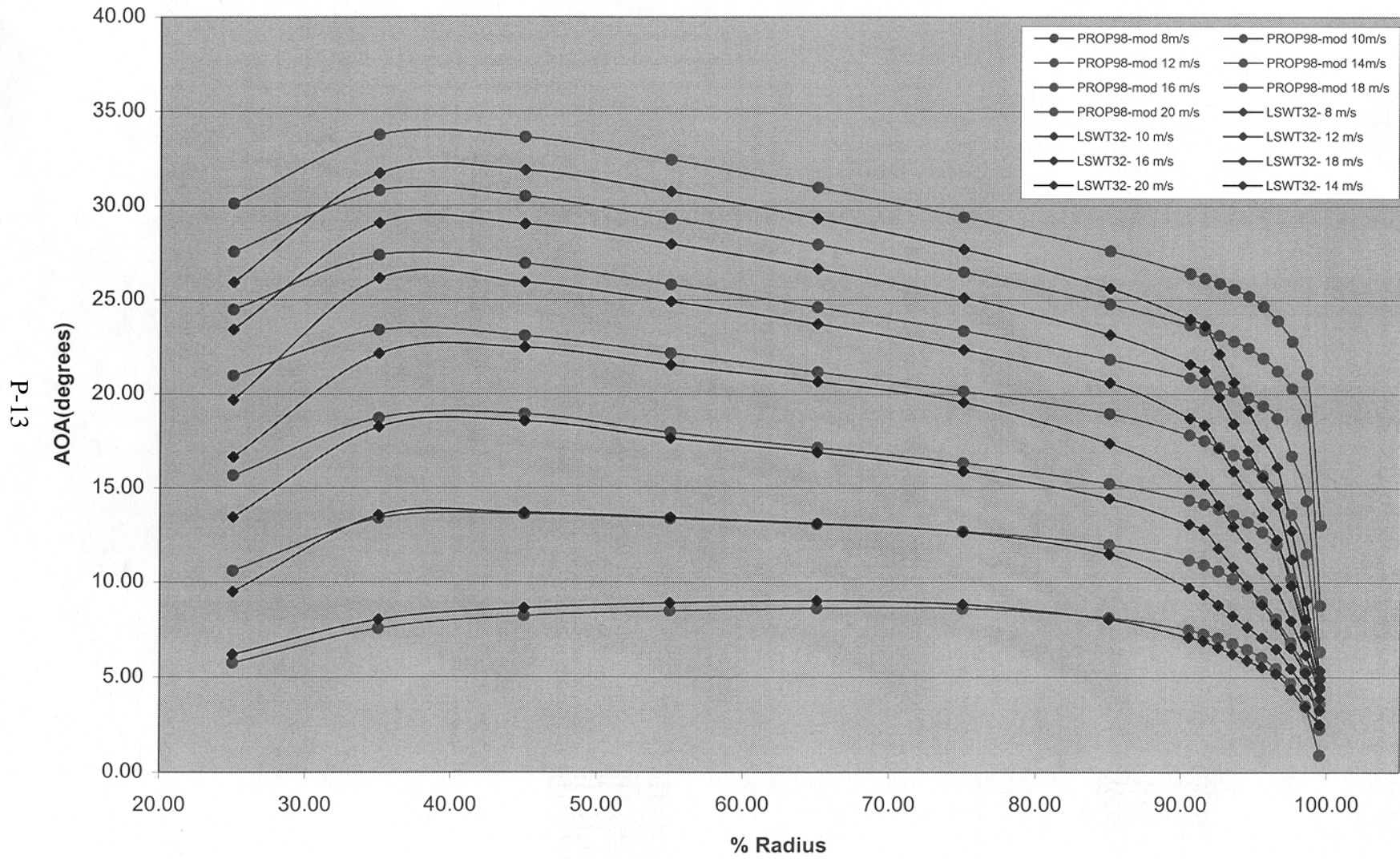
National Wind Technology Center
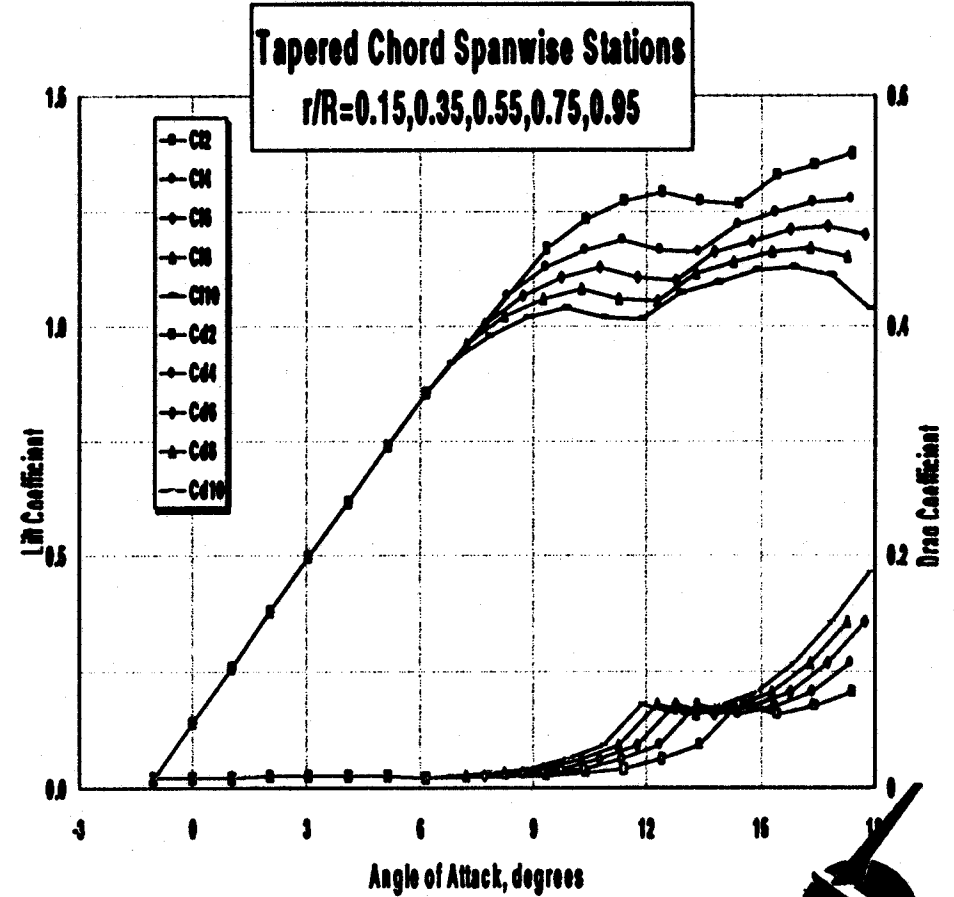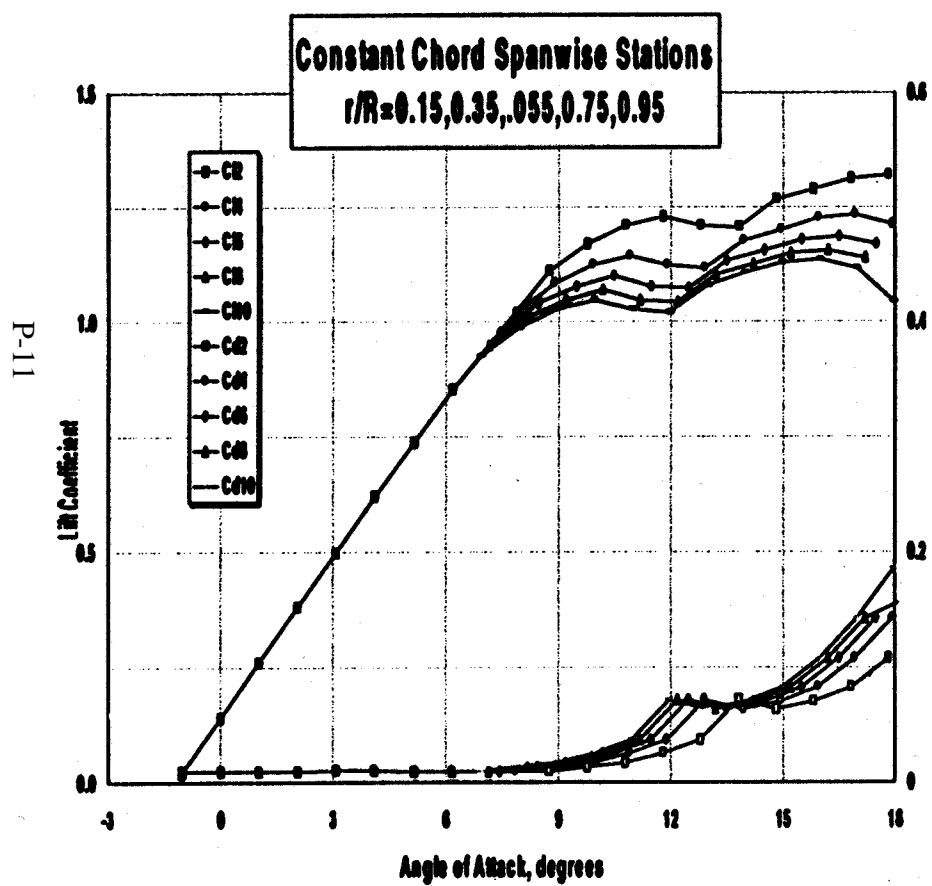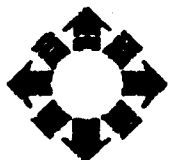
CER Predicted Power Curves, 2D & 3D

Power Curve for +8 Degree Pitch Angle
Twisted Blades
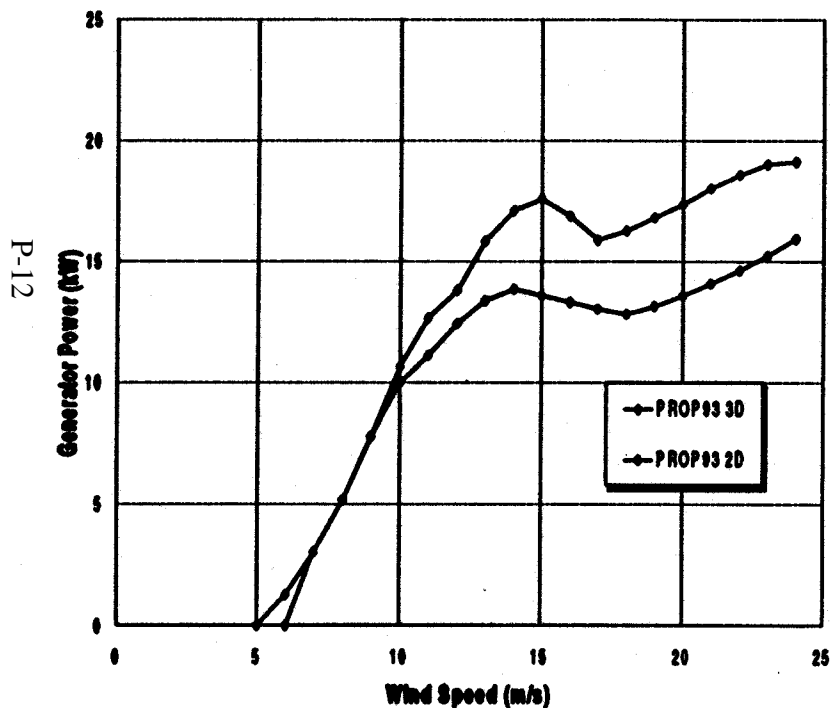
Power Curve for +8 Degree Pitch Angle
Twisted/Tapered Blades

P-12

National Wind Technology Center

AOA of PROP98 Modified Versus LSWT32

P-13

Recommendations

- Steady-state power curve for a couple of blade pitch angles
- Blade tip and root pressure distributions

- Wake geometry from tip smoke
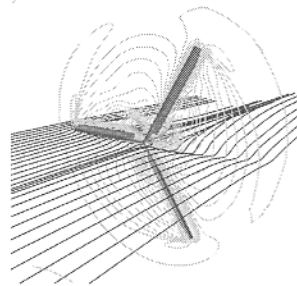- Pressure distributions with tip plates

P-14

National Wind Technology Center

Appendix Q:

Presentation by E. Duque, NASA Ames

**CFD Modeling of
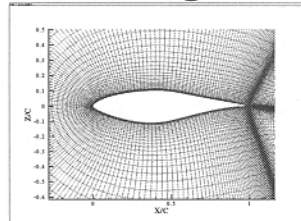Unsteady Wind Turbine Aerodynamics**
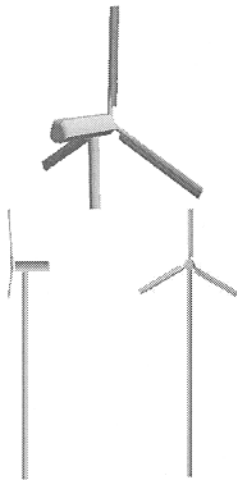
UC**DAVIS**

**Army/NASA/UC Davis
A Joint Research Interchange**

- Background
- Objectives
- Research progress
    - Combined Experiment
    - Airfoils & Cylinders
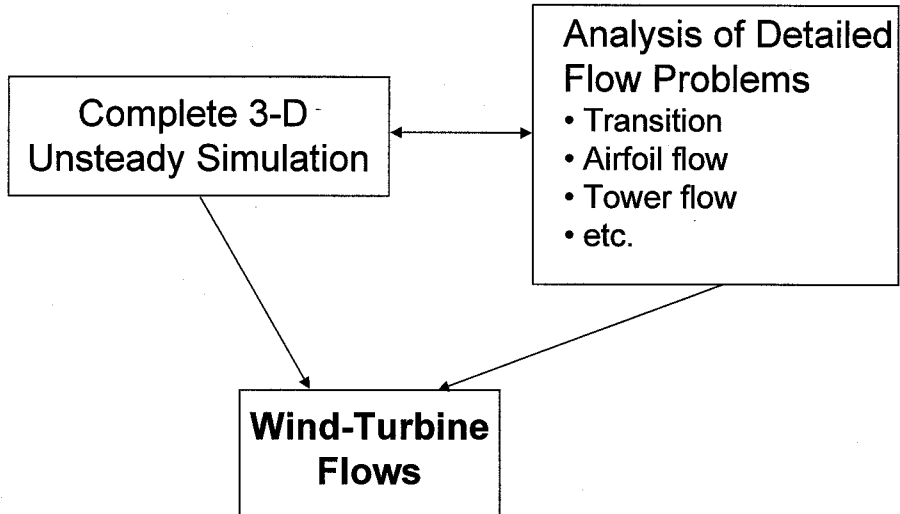   - Boundary Layer Transition
- Concluding remarks
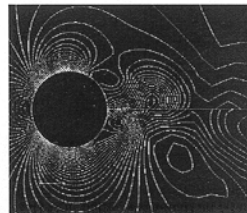
Army/NASA/UC Davis Team

- PI: Earl P.N. Duque (Army/NASA) - 3D RaNS
- Case P. van Dam (Professor UC Davis)
  - David D. Chao (PhD Candidate) - Airfoils, RaNS
  - Robert Brodeur (MS Candidate) - Turbulence Transition
  - Alex Plageman (Aachen) - Turbulence Transition
  - Karen Yee (Undergraduate) - Aero/Yawdyn
- Large Scale computations with smaller scale fundamental studies
- Leverages Army & NASA's CFD investment

Objectives

- Apply/improve computational fluid dynamics techniques to simulate unsteady flows about wind turbines and rotorcraft
- Develop an unsteady Reynolds averaged Navier-Stokes simulation of the NREL Combined Experiment Rotor
- Support 80' x 120' wind tunnel test
- Apply simulation results to aid in development of engineering methods
- Improve fundamental knowledge of wind turbine aerodynamics

Approach

```
                          ┌────────────────────┐
                          │ Analysis of Detailed│
                          │ Flow Problems       │
  ┌──────────────────┐    │ • Transition        │
  │ Complete 3-D     │◄──►│ • Airfoil flow      │
  │ Unsteady Simulation│  │ • Tower flow        │
  └──────────────────┘    │ • etc.              │
                          └────────────────────┘
             │                      │
             └──────┐      ┌────────┘
                    ▼      ▼
                ┌──────────────┐
                │ Wind-Turbine │
                │    Flows     │
                └──────────────┘
```

Technical Challenges

- Inflow not well defined
- Flow unsteadiness
- Boundary-layer transition
- Flow separation (laminar & turbulent)
- Aero-structural interaction
- Acoustics

Flow Solver

- OVERFLOW (Rotor version) by Buning (NASA) with rotor modifications by J. Ahmad (NASA Contractor)
- Developed for helicopter and fixed wing applications
- Hover (isolated rotor) version in development
- Active development for aeroacoustics, aeroelasticity, dynamics and controls, parallel computing
- Compressible Navier-Stokes
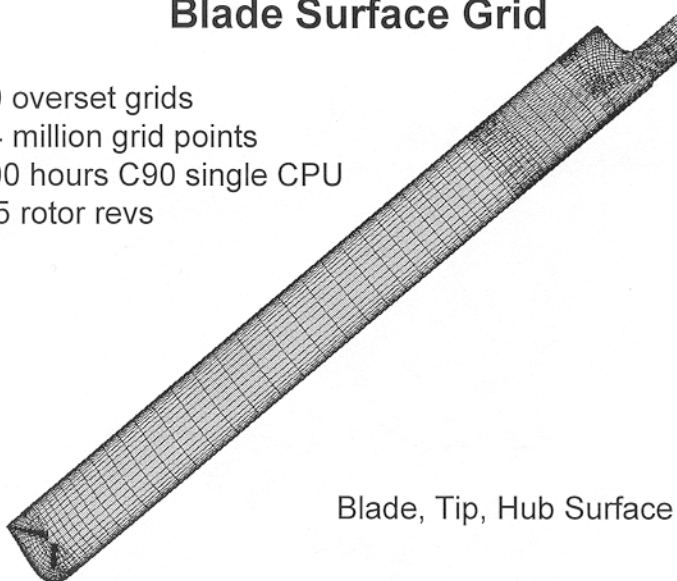- Various Turbulence Models
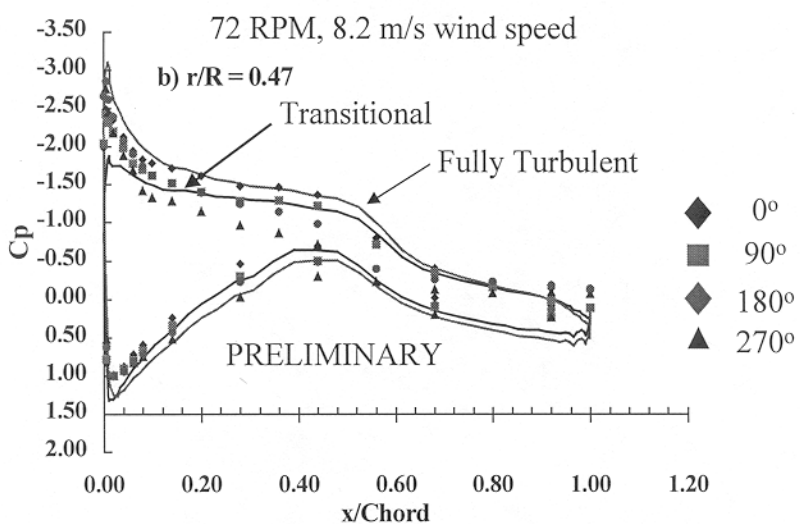- Overset Moving Grids
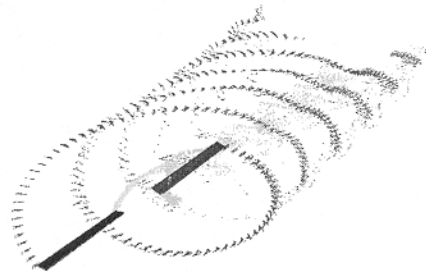
Phase II Rotor Overset Grid System

Blade and Hub
Volume Grids

Tip Cap Surface Detail
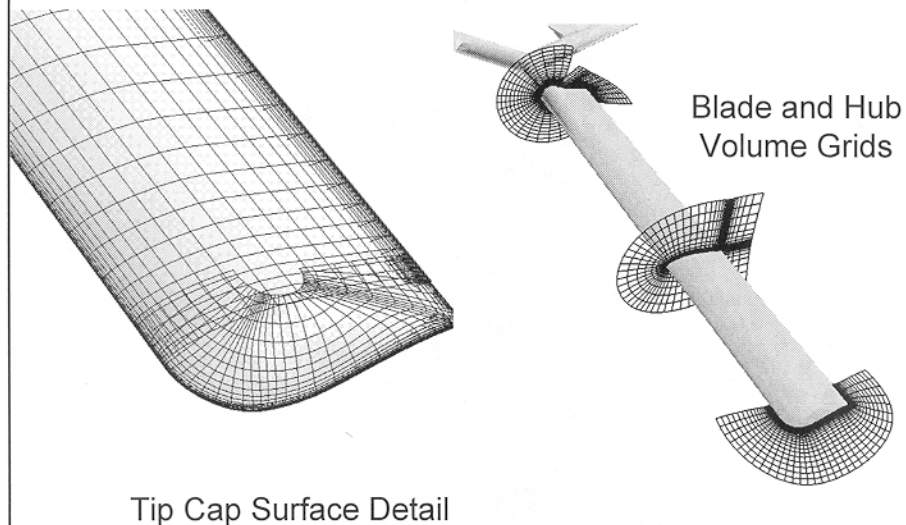
Blade Surface Grid

- 20 overset grids
- ~4 million grid points
- 100 hours C90 single CPU for 5 rotor revs

Blade, Tip, Hub Surface Grids
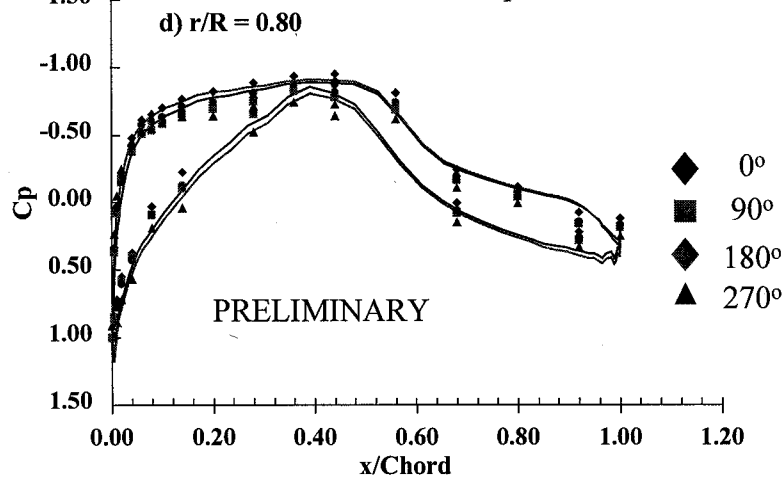

**Pressure Coefficient
Isolated Rotor - r/R = 0.47**

72 RPM, 8.2 m/s wind speed

b) r/R = 0.47

Transitional

Fully Turbulent

PRELIMINARY

♦ 0°
■ 90°
♦ 180°
▲ 270°

Cp

x/Chord

Pressure Coefficient
Isolated Rotor - r/R = 0.53
72 RPM, 8.2 m/s wind speed

c) r/R = 0.63

PRELIMINARY

◆ 0°
■ 90°
◆ 180°
▲ 270°

(Cp vs x/Chord)
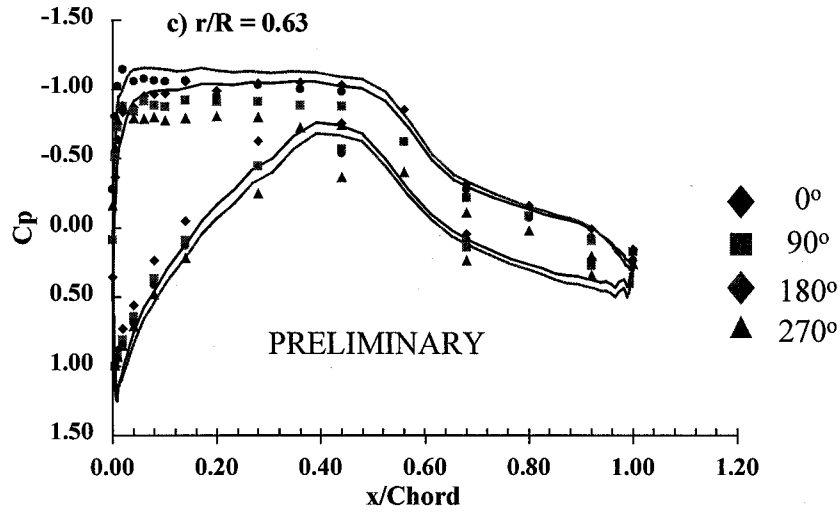
Pressure Coefficient
Isolated Rotor - r/R = 0.80
72 RPM, 8.2 m/s wind speed

d) r/R = 0.80

PRELIMINARY

◆ 0°
■ 90°
◆ 180°
▲ 270°

(Cp vs x/Chord)

Isolated Rotor: Normal Force 63%

72 RPM, 8.2 m/s wind speed
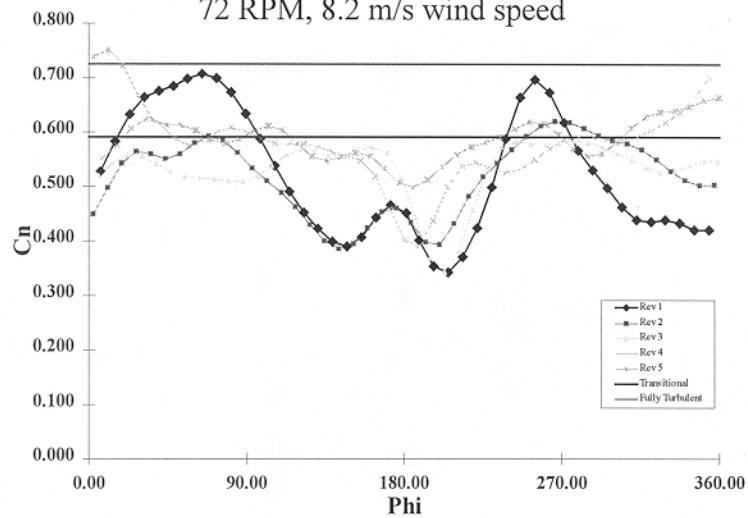
Isolated Rotor - Summary

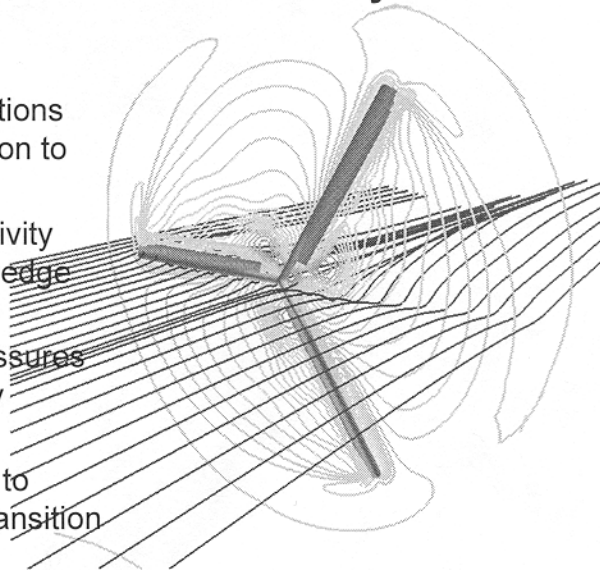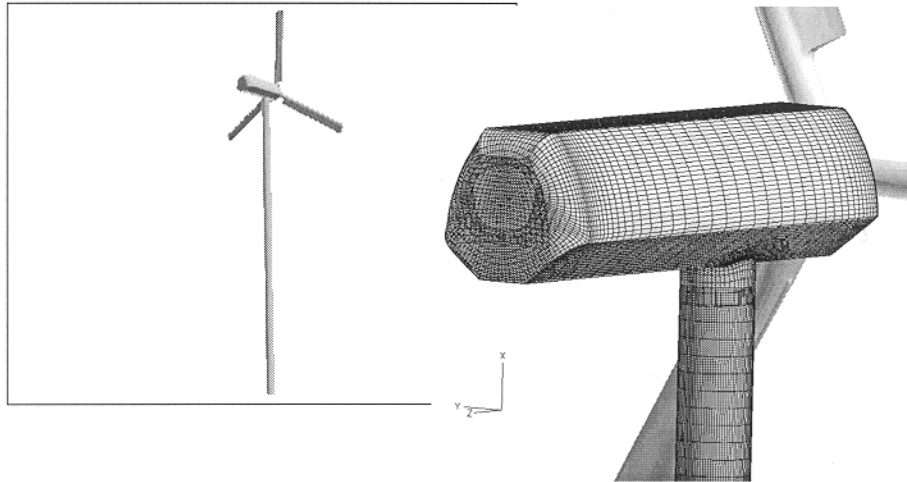- Pressure Distributions have fair correlation to field data
- Low speed sensitivity exhibited leading edge stagnation
- Trailing edge pressures indicate geometry differences
- Inboard sensitive to boundary layer transition

Rotor-Post Flowfield - In Progress

Rotor-Post Calculations

- Improving understanding of cylinder flowfields
- Modified tip grids to improved topology
- Running

0.200
0.000
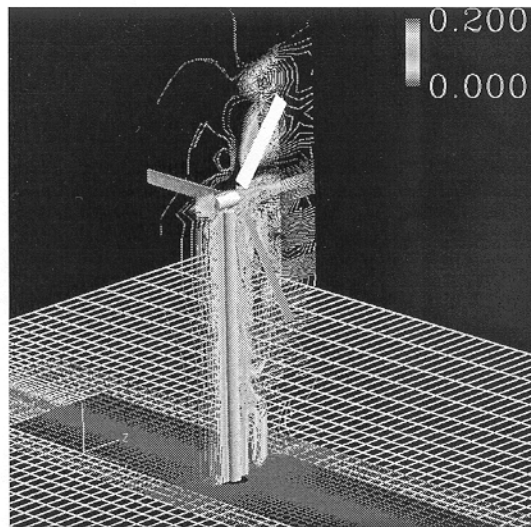
FY 99 Plans

- Implement transition models in rotor-post 3D RaNS
- Investigate feeding CFD airloads to Yawdyn and ADAMS
- Compute select 80'x120' tunnel entry test points
  - Yaw angles
  - 2-Bladed rotor
  - Detailed analysis of unsteady flow field and loads

Appendix R:

Presentation by C. VanDam, University of California, Davis

Presentation not Available

Appendix S:

Presentation by D. Simms and M. Hand, NREL

Overview and Status of the NREL Unsteady Aerodynamics Experiment

NREL- NASA Ames Wind Turbine Tunnel Test

Science Panel Meeting #1
October 5-6, 1998

Experiment Configuration
Phase V

✦ **2-bladed HAWT**
  - Nominal 10 m rotor diameter, 20 kW generator
  - Constant chord (.457 m) twisted blades
  - Downwind or upwind operation
  - Independent blade variable pitch
  - 72 RPM or variable speed

✦ **Instrumented for:**
  - Rotating aerodynamic forces
  - Wind inflow
  - Tower, turbine, blade structural responses
  - Power production
  - Flow visualization
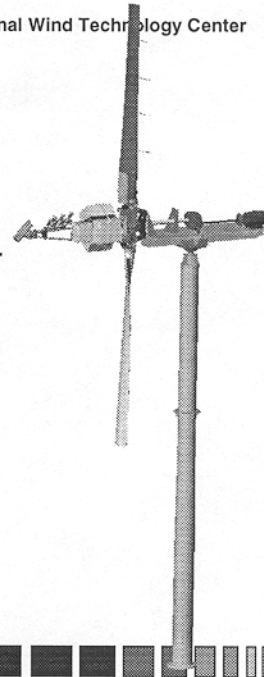
Rotor Instrumentation

NREL National Renewable Energy Laborato   National Wind Technology Center

Pressure taps and 5-hole probes at 5 span stations

Blade camera

Boom lights

Boom camera

Instrumentation boom

Instrumentation packages

Upwind vane with static & dynamic probe (to rotor through rotary pneumatic coupling)
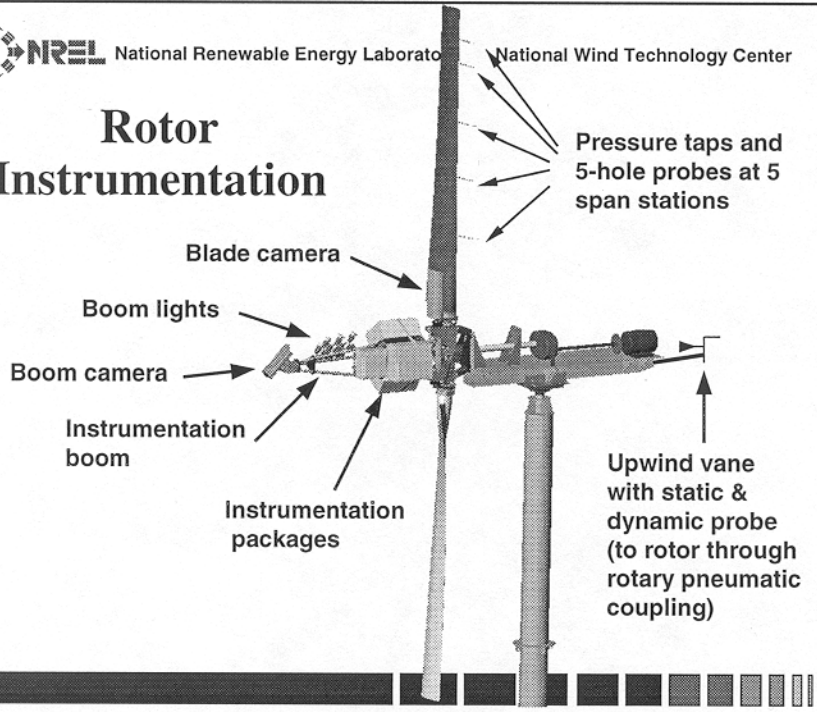
Constant Chord Twisted Blade Set

NREL National Renewable Energy Laboratory   National Wind Technology Center

✦ NREL S809 airfoil

✦ .457 m chord

✦ Optimally-twisted blade

– Constant angle-of-attack across span

– Full-span transition into and out of stall

AOA distribution as predicted by PROP at $V_w = 10$ m/s
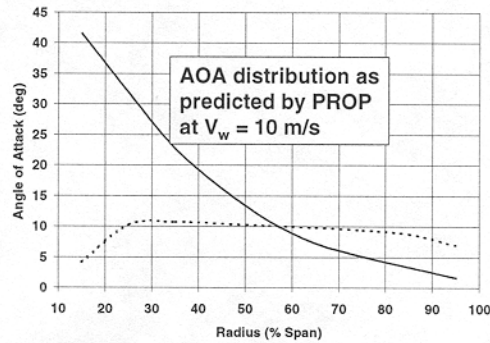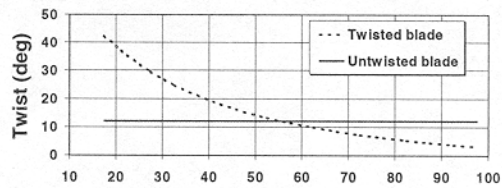
Local Blade Flow Angle Measurements

- ✦ **Local flow angle flags**
  - – Good correlation for steady-state & lower frequency events
  - – Large size may obstruct flowfield downstream
  - – Limited frequency response
- ✦ **5-hole pitot probe**
  - – Increased frequency response
  - – 3D flow data - quantify spanwise flow
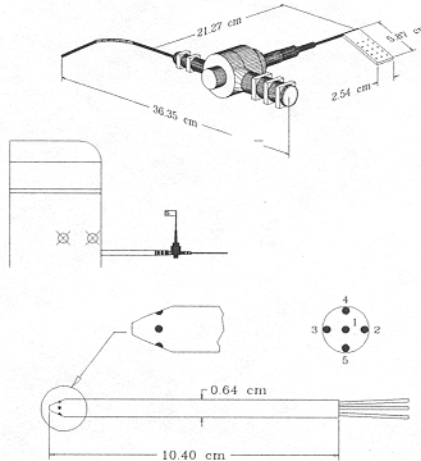
Blade Pressure Measurements

- ✦ 155 instrumented surface pressure taps
- ✦ 5 pressure stations + intermediate tap locations
- ✦ 520.83 Hz sample rate
- ✦ One data snapshot each 0.833 degrees of rotation
- ✦ Automated calibrations maintain required accuracy
- ✦ Dynamic pressure and local flow angles from 5-hole probes

× Pressure Tap

S809 Airfoil

% Chord (0.457m Chord)

—— Full Pressure Tap Distribution

× × Pressure Taps at 4% and 36% Chord Only

% Radius (5.023m Radius)

Pneumatic Outputs:
- ESP-32 Normal Operate Control (80 psi)
- ESP-32 Zero Control (80 psi)
- Purge Valve Normal Operate Control (80 psi)
- Purge Valve Zero Control (80 psi)
- Purge Pressure (5 psi)
- Calibration Pressure (+- 1.0 psi max)
- Ambient Reference Pressure (800-1100 mb)

Control Pressure (80 psi) → **Pressure System Controller**

Electronic Inputs:

124 Analog-Multiplexed Channels from four ESP-32's

Comm out
PCM out
PCM in   DC in

PCM #1
PCM #2

2 Duplex CCITT/V.24 Comm Links

16-bit Digital Pressure Transducer Signals

10 12-bit Digital Channels (2 per connector)

31 Channels from one ESP-32   or

13 Strain Gage Channels (13 per connector)

8 High-Level Analog Channels (13 per connector)

Clock in
PCM out

Rotor-Based PCM Encoder

PCM #3

DC in

31 Channels from one ESP-32   or   18 High-Level and 13 Strain Gage Channels

Power Supply

Rotating Signals
Non-Rotating Signals

Slip Rings

8 12-bit Digital Input Signal Channels (2 per connector)

Clock in   PCM out

PCM #4

30 High-Level Analog Input Signal Channels (12 per connector)

Ground-Based PCM Encoder

DC in

Power Supply

Ground-Station PC

24 Strain Gage Input Signal Channels (12 per connector)

120 VAC

Rotor Loads

- Blade root flap and edge bending moments
- Shaft X-X and Y-Y bending moments
- Shaft torque
- Nacelle pitch, yaw, and fore-aft acceleration
- Blade tip flap and edge acceleration (not shown)

Nacelle Accelerometers

Blade Root Strain Gages

Hub-Shaft Strain Gages

Low-Speed Shaft Strain Gages
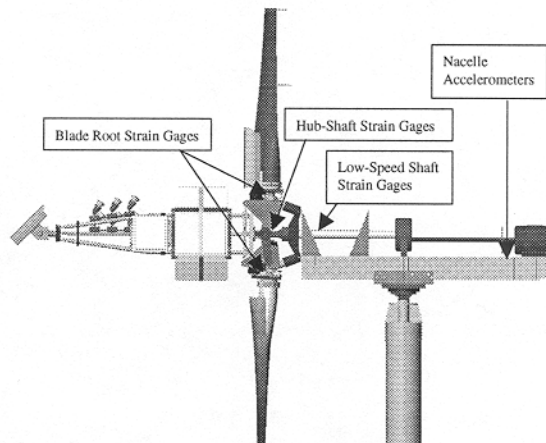
Combined Experiment Phases

	Phase II	Phase III	Phase IV	Phase V
Date collected	5/15 - 7/25/90	3/22 - 3/29/96	4/4 - 5/20/96	3/30/98 -
Blade configuration	3 Untwisted	3 Twisted	3 Twisted	2 Twisted
LFA measurement method	Flags	Flags	5-hole probes	5-hole probes
Span locations instrumented with pressure taps	4	5	5	5
Span locations instrumented with LFA sensors	4	4	5	5
Meteorological configuration	Vertical plane array	Horizontal & vertical shear	Horizontal & vertical shear	Horizontal & vertical shear
Locked yaw data	Yes	No	Yes	Yes
Parked/ slow rotating blade data	No	Yes	Yes	Yes
Pitch angles (tip pitch)	8º, 12º	3º	-3º, +3º +8º	-9, -3º, +3º +8º, +12
Number of available 10-minute data sets	29	20	92	92
Video flow visualization data	Yes	No	Yes	Yes

Number of channels and types of field measurements

Inflow	Phase II	Phase III	Phase IV	Phase V
Wind Speed	16	7	7	7
Wind Direction	7	3	3	3
Wind Elevation	2	2	2	2
Temperature	2	2	2	2
Barometer	1	1	1	1
Blade Flow Angle				
Local flow angle (flag)	4	4	-	-
Local flow angle (5-hole probe)	-	1	5	5
Cross-flow angle (5-hole probe)	-	1	5	5
Pressure				
Blade dynamic pressure	4	5	5	5
Blade 30% span	28	22	22	22
Blade 47% span	28	22	22	22
Blade 63% span	28	22	22	22
Blade 80% span	28	22	22	22
Blade 95% span	-	22	22	22
Blade Intermediate span	14	20	20	20
Nacelle upwind static/ dynamic vane	-	-	-	1
Loads				
Blade strain	13	10	6	6
Blade tip acceleration	-	6	6	6
Low speed shaft strain	4	3	3	7
Teeter link/ damper	-	-	-	3
Tower strain	2	-	-	-
Yaw moment	1	-	1	1
Nacelle acceleration	-	3	3	3
Position/ speed/ power				
Blade pitch	1	3	3	3
Flap angle	-	-	-	2
Rotor azimuth	1	1	1	1
Yaw position	1	1	1	1
RPM	1	1	1	1
Generator Power	1	1	1	1
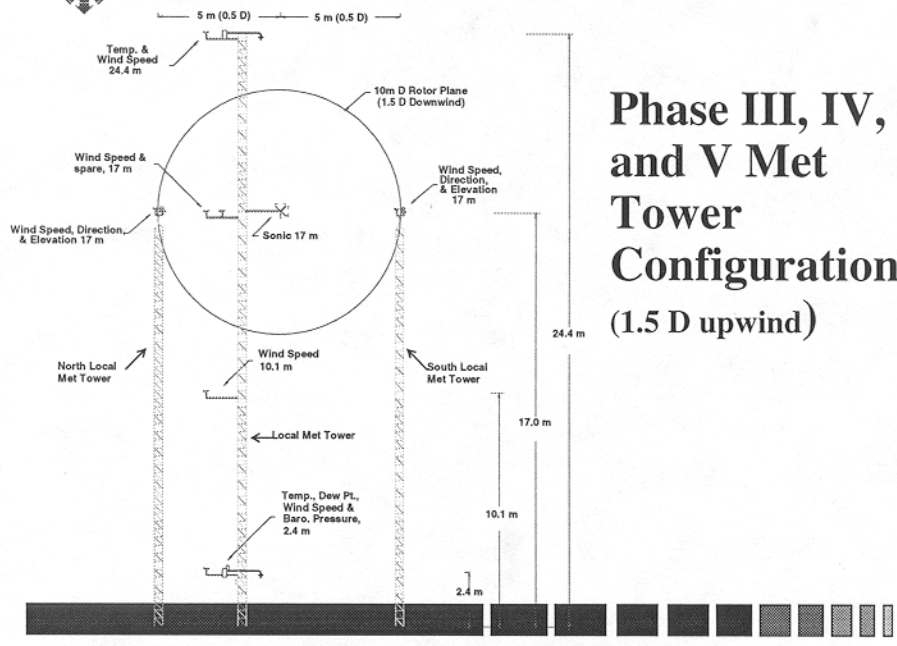
Measured Data Bandwidth & Filtering

- ✦ All measured channels sampled at 520 Hz
- ✦ 1.92 msec (.83 degrees of azimuth) resolution
- ✦ Analog channels anti-alias filtered
  - – Strains gages, accelerometers & generator power were filtered to 100 Hz bandwidth with 8-pole Bessell filters (introduces a 5 ms, 2.5 sample delay)
  - – Inflow channels were filtered to 10 Hz bandwidth with 8-pole Butterworth filters (introduces an 80 ms, 42 sample delay)
  - – No filtering of pressures or digital channels (azimuth angle, yaw angle, RPM, pitch angles)

Calibration Procedures

✦ **Pressures**
  – 5 ESP-32 scanning transducers (155 channels)
    • All calibrated simultaneously
    • Calibration source provides ± 8500 Pa range
    • Linear least-square regression referenced to precision differential transducer
    • Compare pre- and post-calibration each 10-minute campaign to ensure data remain within tolerance

✦ **Strains, inflow, etc.**
    • "End-to-end" calibration (e.g. blade pull)
    • "Shunt" calibration with manufacturer-specified calibration (remove transducer, inject precision voltage) (e.g. anemometers)

New Hub Development


✦ **Versatile 2-bladed rotor**
  – Each blade hinged at center of axis of rotation
  – Flap degree of freedom

✦ **Can be configured as a:**
  – Teetered rotor with teeter motion dampers (as shown)
  – Free-flapping coned rotor with flap motion actuators or dampers
  – Rigid rotor

✦ **Independent blade pitch motion**
  – Electro-mechanical actuators
  – Controlled to maintain accurate constant or variable pitch
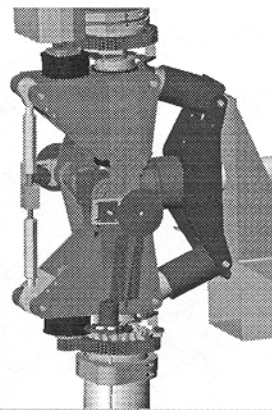
Near-term Plans - FY99

✦ **Further field testing of new hinged hub**
  - Teetered, high wind and extreme yaw tests
  - Rigid
    • Upwind and downwind
    • With and without tufts and cameras
    • With and without 5-hole probes
  - Possibly free-flapping
✦ **Complete construction of tapered and twisted blade set**
✦ **Prepare for wind tunnel test**
✦ **Ongoing model validation**

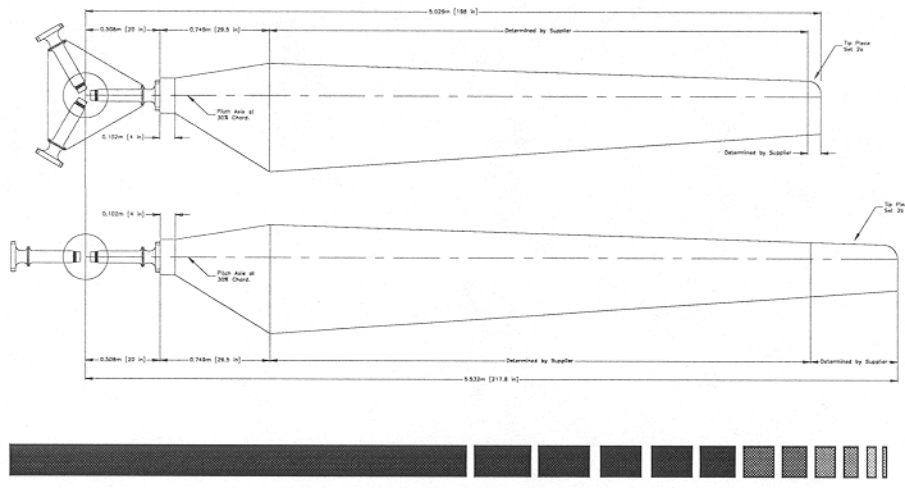# New Blade Development

✦ Tapered and twisted 5 m blade set
✦ Tip pieces to extend diameter to 5.5 m for 2-bladed rotor
✦ S809 along entire span
✦ Maintain .457 m chord at 80% span (5 m)
✦ 22 degrees of twist, taper from .74 to .31 m
✦ Ready late 1998

Twisted and Tapered Blade Set

Centrifugal Force Correction

- For all blade surface pressure measurements, the common reference pressure source was the pressure inside one of the rotating instrumentation boxes on the hub.
- The hub mounted instrumentation box was damped to atmospheric pressure through an orifice which resulted in a time constant of approximately 5-10 seconds.

$$P_{cor} = P_{meas} + P_{cent}$$

$$P_{cent} = \frac{1}{2}\rho(r\omega)^2$$

where

P_{cor} = differential pressure corrected for centrifugal force, Pa
P_{meas} = pressure differential measured at blade-mounted transducer, Pa
P_{cent} = centrifugal force correction, Pa
ρ = air density, kg/m^3
r = radial distance to surface pressure tap, m
ω = rotor speed, rad/s

Twisted and Tapered Blade Set

Centrifugal Force Correction

- For all blade surface pressure measurements, the common reference pressure source was the pressure inside one of the rotating instrumentation boxes on the hub.
- The hub mounted instrumentation box was damped to atmospheric pressure through an orifice which resulted in a time constant of approximately 5-10 seconds.

$$P_{cor} = P_{meas} + P_{cent}$$
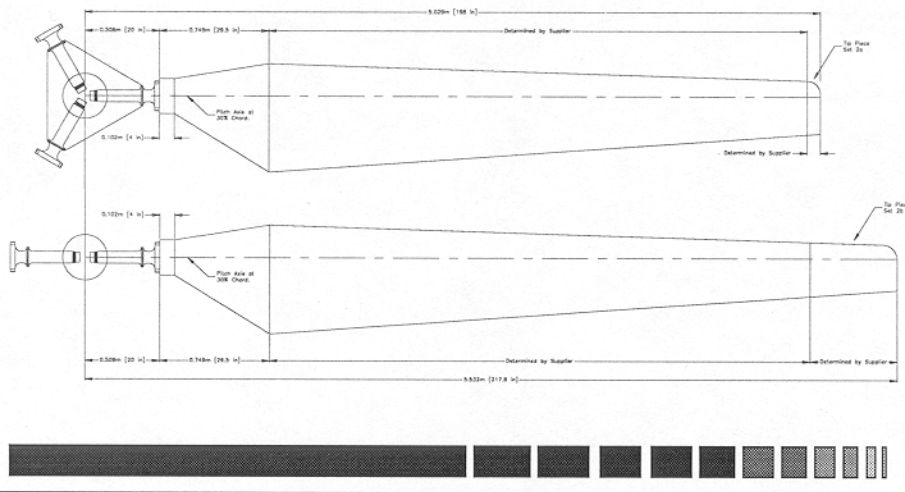
$$P_{cent} = \frac{1}{2}\rho(r\omega)^2$$

where

P_{cor} = differential pressure corrected for centrifugal force, Pa

P_{meas} = pressure differential measured at blade-mounted transducer, Pa

P_{cent} = centrifugal force correction, Pa

ρ = air density, kg/m^3

r = radial distance to surface pressure tap, m

ω = rotor speed, rad/s

Force Coefficient Calculation

$$C_p = \frac{P_{cor}}{Q_{stag}}$$

C_p = normalized pressure coefficient, dimensionless
P_{cor} = differential pressure corrected for centrifugal force, Pa
Q_{stag} = stagnation point dynamic pressure (corrected for centrifugal force), Pa.

$$C_N = \sum_{i=1}^{\#oftaps} \left(\frac{C_{p_i} + C_{p_{i+1}}}{2} \right)(x_{i+1} - x_i)$$

$$C_T = -\sum_{i=1}^{\#oftaps} \left(\frac{C_{p_i} + C_{p_{i+1}}}{2} \right)(y_{i+1} - y_i)$$

x_i = normalized distance along chord line from leading edge to i^{th} pressure tap
y_i = normalized distance from chord line along axis orthogonal to chord to i^{th} pressure tap

---

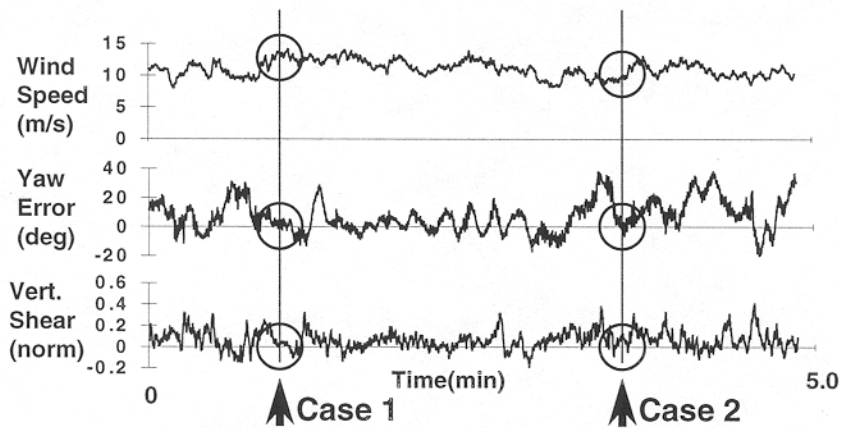# Determining Baseline Performance

+ "Quasi-steady" blade aerodynamic performance
  - Find instances when turbine is operating under relatively steady inflow conditions
  - Look for 3 consecutive steady cycles with:
    • invariant inflow velocity
    • minimal yaw
  - Cycle-averaged value from middle cycle is considered "baseline"
+ Baseline conditions exist in fewer than 1% of all data cycles

National Renewable Energy Laboratory   National Wind Technology Center

Typical 5-Minute Data Set (360 cycles)

National Renewable Energy Laboratory   National Wind Technology Center

Case 1 - Selected Baseline Cycles 74-76
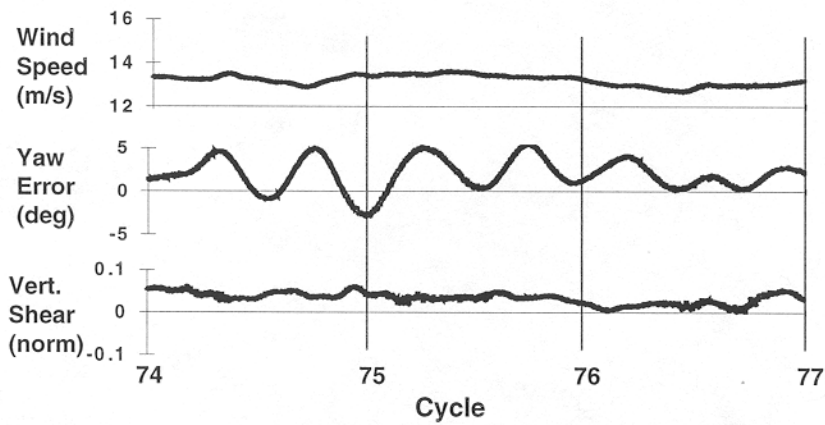
Case 2 - Non-Baseline Cycles 266-268
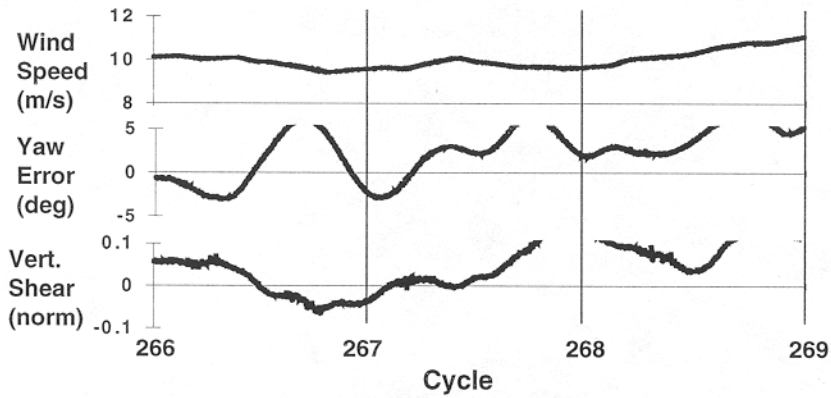
30% Span Baseline Cycles
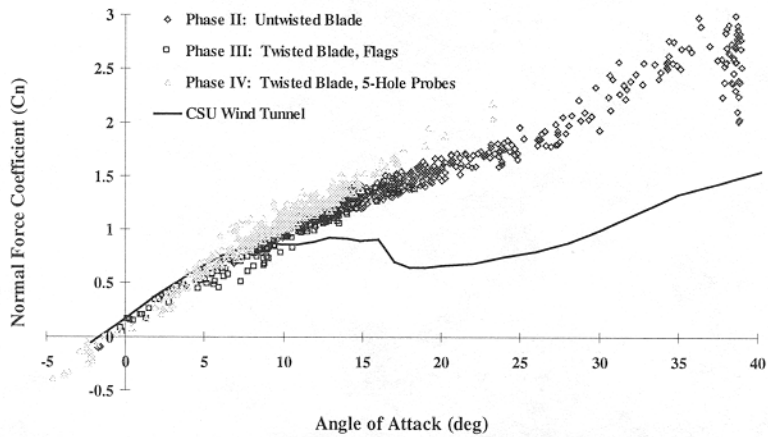
47% Span Baseline Cycles
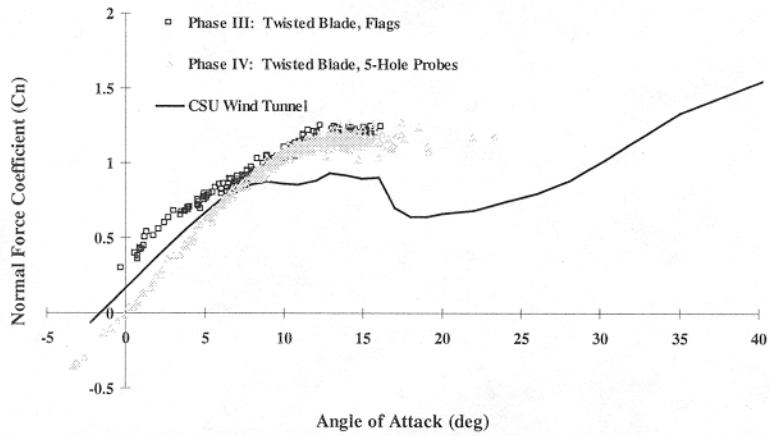
63% Span Baseline Cycles
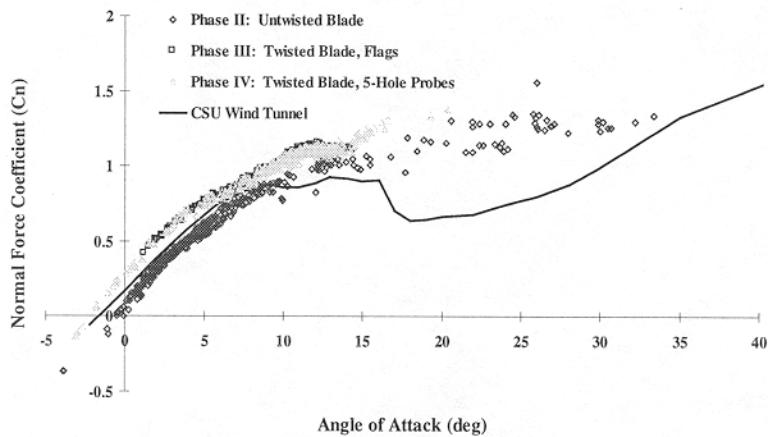
80% Span Baseline Cycles
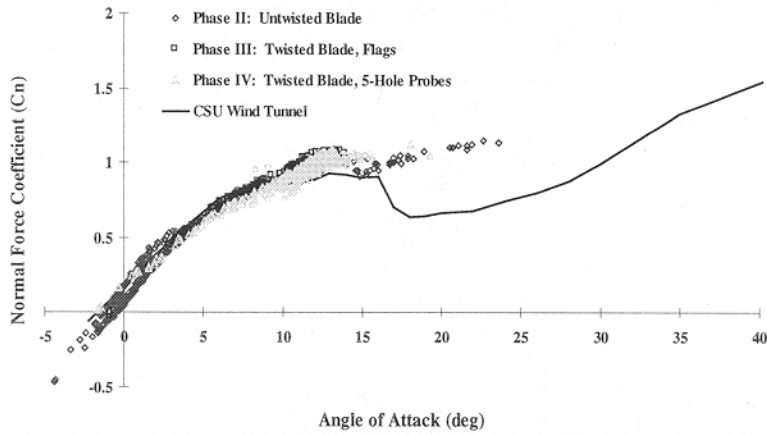
IEA Annex XIV
Database Contributions

		Yaw Error				
		-40 degrees (15 s duration)	-20 degrees (15 s duration)	0 degrees (60 s duration)	20 degrees (15 s duration)	40 degrees (15 s duration)
Wind Speed	7 m/s	P2, P3, P4	P2, P3, P4	P2, P3, P4	P2, P3, P4	P2, P3, P4
	10 m/s		P2, P3, P4	P2, P3, P4	P2, P3, P4	P4
	13 m/s		P2, P3, P4	P2, P3, P4	P2, P3, P4	
	15 m/s			Parked rotor		
	16 m/s			P2, P3, P4		
	19 m/s			P2, P4		

Appendix T:

Presentation by L. Fingersh, NREL

Preparation and Transport

- Remove blades
- Remove nacelle from tower
- Pack blades, nacelle and new tower in cargo container
- Pack ground data system, computers, tools and spare parts in second cargo container
- Ship both containers to NASA

Installation and Calibration

- Set new tower outside the tunnel
- Install nacelle on new tower
- Install blades on hub
- Connect electrical control and data systems
- Perform calibration and checkout outside
- Move whole installation inside the tunnel
- Move control and data systems to control room

Additional Installation

- Install guy cables to tower
- Install sonic anemometer(s) on microphone stands
- Connect to tunnel instrumentation
  - Inflow ring
  - Tunnel pressures
  - Force balance
- ☆ Begin data collection

Appendix U:

Presentation by M. Robinson, NREL

Unsteady Aerodynamics Parameters

Reduced Frequency (wc/2V)

m/sec	Frequency Hz		
	1.2	2.4	3.4
5	0.345	0.689	0.977
10	0.172	0.345	0.488
20	0.086	0.172	0.244
30	0.057	0.115	0.163
40	0.043	0.086	0.122
50	0.034	0.069	0.098

Non-Dimensional Pitch Rate (ac/V)

m/sec	Deg / Sec		
	16.5	33	66
5	0.026	0.053	0.105
10	0.013	0.026	0.053
20	0.007	0.013	0.026
30	0.004	0.009	0.018
40	0.003	0.007	0.013
50	0.003	0.005	0.011

Area Ratio
0.085881

Non-Rotating Blade Tests

Static Angle of attack

Vinf (m/s)	-20	-15	-10	-5	0	5	10	15	20	25	30	35	40	45	50	55	60
20	1	1	1	1	1	1	1	1	1	1	1	1	1	1	1	1	1
40	1	1	1	1	1	1	1	1	1	1	1	1	1	1	1	1	1

Clean
Instrumented w/ probes

Dynamic Angle of Attack (Pitch)
0 + 60 * sin(wt)

Vinf (m/s)	P					
	0.1	0.5	1	1.5	2	
20	1	1	1	1	1	Clean
40	1	1	1	1		Instrumented w/ probes

Dynamic Angle of Attack (Ramp)
0 - (+60, -60); (a+) * (t)

Vinf (m/s)	(deg/sec)				
	0.5	16.5	33	66	
20	1	1	1	1	Clean
40	1	1	1	1	Instrumented w/ probes

BEM Power Prediction

Blade tip pitch angle = 3 degrees

NREL Unsteady Aerodynamics Experiment
YawDyn Predicted Blade Angle of Attack

Pitch = 3.0 degrees, Yaw = 0.0 degrees

**NREL Unsteady Aerodynamics Experiment
YawDyn Predicted Blade Angle of Attack**

Pitch = 3.0 degrees, Yaw = 30.0 degrees

Rotating Blade Baseline Tests

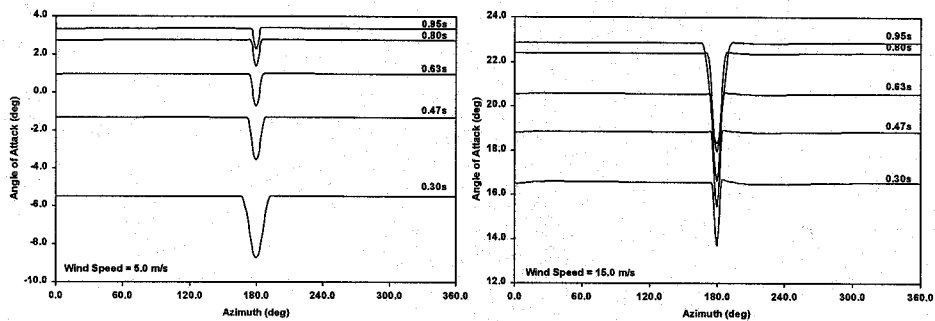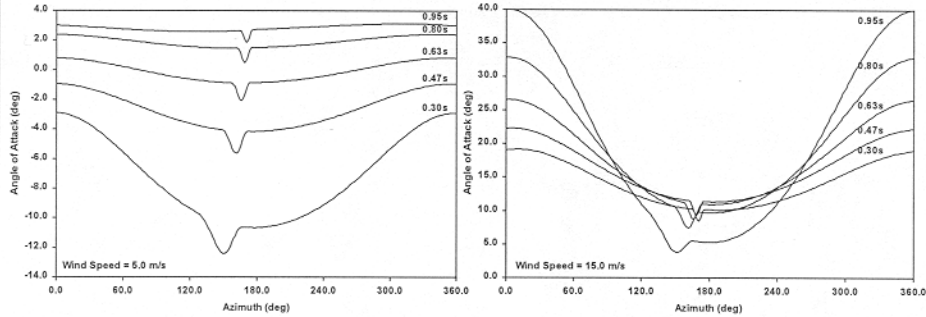| V (m/s)	0	5	10	20	30	45	60	90	135	180	+60R	+30R	-5	-10	-20	-30	-45	-90	-135	-60R	-30R
0	1																				
1	1																				
2	1																				
3	1																				
4	1																				
5	1	1	1	1	1	1	1	1	1	1	1	1	1	1	1	1	1	1	1	1	1
6	1																				
7	1																				
7.5	1	1	1	1	1	1	1	1	1	1	1	1	1	1	1	1	1	1	1	1	1
8	1																				
9	1																				
10	1	1	1	1	1	1	1	1	1	1	1	1	1	1	1	1	1	1	1	1	1
11	1																				
12	1																				
12.5	1	1	1	1	1	1	1	1	1	1	1	1	1	1	1	1	1	1	1	1	1
13	1																				
14	1																				
15	1	1	1	1	1	1	1	1	1	1	1	1	1	1	1	1	1	1	1	1	1
16	1																				
17	1																				
18	1																				
19	1																				
20	1	1	1	1	1	1	1	1	1	1	1	1	1	1	1	1	1	1	1	1	1
21	1																				
22	1																				
23	1																				
24	1																				
25	1	1	1	1	1	1	1	1	1	1	1	1	1	1	1	1	1	1	1	1	1

Blade Pitch Angle   3°
Downwind
Clean & Instrumented w/ probes

⬥NREL Rotating Blade Baseline Tests

V (m/s)	Pitch 3°	(-) 3°	(-) 8°
0	x	1	1
1	x	1	1
2	x	1	1
3	x	1	1
4	x	1	1
5	x	1	1
6	x	1	1
7	x	1	1
7.5	x	1	1
8	x	1	1
9	x	1	1
10	x	1	1
11	x	1	1
12	x	1	1
12.5	x	1	1
13	x	1	1
14	x	1	1
15	x	1	1
16	x	1	1
17	x	1	1
18	x	1	1
19	x	1	1
20	x	1	1
21	x	1	1
22	x	1	1
23	x	1	1
24	x	1	1
25	x	1	1

Yaw   0°
Upwind
Downwind
Clean
Instrumented w/ probes

⬥NREL Free Yaw Release

Vinf (m/s)	Yaw Angle 30	60	90
20	1	1	1
40	1	1	1

Clean
Instrumented w/ probes
Downwind
Pitch angle 3, - 3, - 8 deg

Appendix V:

Selected "Combined Experiment" and "Unsteady Aerodynamics Experiment" Publications

(through January 2000)

1. Journal and Conference Publications

(Authored by NREL Unsteady Aerodynamics project staff, students, and subcontractors)

Schreck, S., Robinson, M. C., Hand, M. M., Simms, D. A., "HAWT Dynamic Stall Response Asymmetries Under Yawed Flow Conditions", AIAA-2000-0040, Prepared for the 38th AIAA Aerospace Sciences Meeting and Exhibit, Reno, NV, January 10-13, 2000, p. 183-196.

Xu, G., Sankar, L. N., "Effects of Transition, Turbulence, and Yaw on the Performance of Horizontal Axis Wind Turbines", AIAA-2000-0048, Prepared for the 38th AIAA Aerospace Sciences Meeting and Exhibit, Reno, NV, January 10-13, 2000, p. 259-265.

Duque, E. P. N.; van Dam, C. P.; Hughes, S. C., "Navier- Stokes Simulations of the NREL Combined Experiment Phase II Rotor", AIAA-99-0037, Prepared for the 37th AIAA Aerospace Sciences Meeting and Exhibit, Reno, NV, January 11-14, 1999, p. 143-153.

Whale, J.; Fisichella, C. J.; Selig, M. S., "Correcting Inflow Measurements from HAWTS Using a Lifting-Surface Code" AIAA-99-0040, Prepared for the 37th AIAA Aerospace Sciences Meeting and Exhibit, Reno, NV, January 11-14, 1999, p. 175-185.

Xu, G.; Sankar, L. N., "Computational Study of Horizontal Axis Wind Turbines", AIAA-99-0042, Prepared for the 37th AIAA Aerospace Sciences Meeting and Exhibit, Reno, NV, January 11-14, 1999, p. 192-199.

Acker, T.; Hand, M., "Aerodynamic Performance of the NREL Unsteady Aerodynamics Experiment (Phase IV) Twisted Rotor", AIAA-99-0045, Prepared for the 37th AIAA Aerospace Sciences Meeting and Exhibit, Reno, NV, January 11-14, 1999, p. 211-221.

Du, Z. and Selig, M. S, "A 3-D Stall-Delay Model for Horizontal Axis Wind Turbine Performance Prediction", Prepared for the 36th AIAA Aerospace Sciences Meeting and Exhibit, Reno, NV, January 12-15, 1998, p. 9-19

Freeman, J. B.; Robinson, M. C., "Algorithm Using Spherical Coordinates to Calculate Dynamic Pressure from 5-Hole Pressure Probe Data", Prepared for the 36th AIAA Aerospace Sciences Meeting and Exhibit, Reno, NV, January 12-15, 1998, p. 70-74.

Tangler, J. T., Selig, M. S., "An Evaluation of an Empirical Model for Stall Delay Due to Rotation for HAWTs", Prepared for the American Wind Energy Association Windpower '97 Conference and Exhibition, June 15-18, 1997, Austin TX, p 87-96.

Huyer, S. A.; Simms, D.; Robinson, M. C., "Unsteady Aerodynamics Associated with a Horizontal-Axis Wind Turbine", AIAA Journal. Vol. 34, Number 7, July 1996, pp. 1410-1419.

Simms, D.A.; Robinson, M. C.; Hand, M.M.; Fingersh, L.J., "Characterization and Comparison of Baseline Aerodynamic Performance of Optimally-Twisted Versus Non-Twisted HAWT Blades", NREL/ TP-442-2028, Prepared for the Fifteenth ASME Wind Energy Symposium, 29 January - 2 February 1996, Houston, TX., p 143-148.

Robinson, M. C., Galbraith, R. A. McD., Shipley, D. E., and Miller, M. S., "Unsteady Aerodynamics of Wind Turbines", AIAA 95-0526, Prepared for the 33rd Aerospace Sciences Meeting and Exhibit, January 9-12, 1995, Reno, NV.

Shipley, D. E.; Miller, M. S.; Robinson, M. C., "Dynamic Stall Occurrence on a Horizontal Axis Wind Turbine Blade", Prepared for the ASME/ ETCE Conference, January 29 - February 1 1995, Houston, TX, p. 167-173.

Simms, D. A., Fingersh, L. J., Butterfield, C. P., "NREL Unsteady Aerodynamics Experiment Phase III Test Objectives and Preliminary Results", Prepared for the ASME/ ETCE Conference, January 29 - February 1 1995, Houston, TX, p. 273-275.

Fingersh, L. J., Simms, D. A.,Butterfield, C. P., Jenks, M. D., "An Overview of the Unsteady Aerodynamics Phase III Data Acquisition System and Instrumentation", Prepared for the ASME/ ETCE Conference, January 29 - February 1 1995, Houston, TX, p. 277-280.

Simms, D. A., "Full-Scale Wind Turbine Rotor Aerodynamics Research at the National Renewable Energy Laboratory, NREL/TP-441-7225, Presented at the European Wind Energy Conference, October 10-14, 1994.

Shipley, D. E.; Miller, M. S.; Robinson, M. C.; Luttges, M. W.; and Simms, D. A.; "Evidence that Aerodynamic Effects, Including Dynamic Stall, Dictate HAWT Structural Loads and Power Generation in Highly Transient Time Frames", NREL/TP-441-7080, Prepared for the Windpower '94 Conference, Minneapolis, MG, May 9-13, 1994.

Robinson, M. C.; Luttges, M. W.; Miller, M. S.; Shipley, D. E.; Young, T. S., and Simms, D. A., "Wind Turbine Blade Aerodynamics: The Analysis of Field Test Data", presented at the 13th ASME/ ETCE Wind Energy Symposium, New Orleans, LA, January 23-26, 1994, NREL/TP-441-7108.

Simms, D. A.;Butterfield, C. P., "International Collaborative Research in Wind Turbine Rotor Aerodynamics", NREL/ TP-441-5810, Prepared for the ASME ETCE Wind Energy Symposium, January 23-26, 1994.
Hansen, A. C.;Butterfield, C. P., "Aerodynamics of Horizontal-Axis Wind Turbines", Annual Review of Fluid Mechanics. Vol. 25, 1993, pp. 115-149.

Robinson, M. C.; Luttges, M. W.; Miller, M. S.; Shipley, D. E.; Young, T. S., and Simms, D. A., "Wind Turbine Blade Aerodynamics: The Combined Experiment", presented at the Windpower '93 Conference, San Francisco, CA, July 12-16, 1993, NREL/TP-441-7107.

Huyer, S. A., Butterfield, C. P., Simms, D. A., "Characterization of Dynamic Stall Phenomena on Wind Turbine Blades Using Surface Pressure Measurements", Prepared for the 11th ASME Wind Energy Symposium, January 26-29, 1992, ASME, p. 45-46.

Huyer, S. A., Simms, D. A., Butterfield, C. P., "Dynamic Stall on Wind Turbine Blades", Prepared for the 11th ASME Wind Energy Symposium, January 26-29, 1992, p. 47-48.

Butterfield, C. P., Huyer, S. A., Simms, D. A., "Recent Results from Data Analysis of Dynamic Stall on Wind Turbine Blades", NREL/TP-257-4654, Prepared for the International Energy Agency Experts Meeting on Wind Turbine Aerodynamics, Stuttgart, Germany, December 3-4, 1991.

Simms, D. A., Butterfield, C. P., "A Comparison of Spanwise Aerodynamic Loads Estimated from Measured Bending Moments Versus Direct Pressure Measurements on Horizontal Axis Wind Turbine Blades", NREL/TP-257-4507, Prepared for the Windpower '91 Conference and Exposition, Palm Springs, California, September 24-27, 1991, pp. 146-154.

Butterfield, C. P., Hansen, A. C., Simms. D. A., Scott, G., "Dynamic Stall on Wind Turbine Blades", Presented at Windpower '91 Conference and Exposition, Palm Springs, California, September 24-27, 1991, pp. 132-138.

Butterfield, C. P.;Nelsen, E. N., "Aerodynamic Testing of a Rotating Wind Turbine Blade", Prepared for Solar '89, NREL/ TP-217-3490, Denver, Colorado, 19-22 June 1989. 7 pp.

Butterfield, C. P., "Aerodynamic Pressure and Flow-Visualization Measurement from a Rotating Wind Turbine Blade", NREL/TP-217-3433, Prepared for the Eighth ASME Wind Energy Symposium, Houston, Texas, 22-25 January 1989, 11 pp.

Butterfield, C. P., "SERI 'Pilot' Aerodynamics Experiment", Prepared for the Seventh ASME Wind Energy Symposium; Eleventh Annual Energy-Sources Technology Conference and Exhibition; New Orleans, Louisiana; January 10-13, 1988. SED-Vol. 5, The American Society of Mechanical Engineers, p. 89.

2. NREL Technical Publications
(Authored by NREL Unsteady Aerodynamics project staff, students, and subcontractors)

Simms, D.A.; Hand, M.M.; Fingersh, L.J., Jager, D. W., "Unsteady Aerodynamics Experiment Phases II-IV Test Configurations and Available Data Campaigns", NREL/ TP-500-25950, July 1999.

Giguere, P. and Selig, M. S., "Design of a Tapered and Twisted Blade for the NREL Combined Experiment Rotor", NREL/SR-500-26173, Department of Aeronautical and Astronautical Engineering, University of Illinois at Urbana-Champaign, Urbana, Illinois, April 1999.

Miller, M. S.; Shipley, D. E.; Young, T. S.; Robinson, M. C.; Luttges, M. W.; and Simms, D. A., "Combined Experiment Phase II Data Characterization", NREL/TP-442-6916, November 1995.

Miller, M. S.; Shipley, D. E.; Young, T. S.; Robinson, M. C.; Luttges, M. W.; and Simms, D. A., "The Baseline Data Sets for Phase II of the Combined Experiment", NREL/TP-442-6915, July 1995.

Miller, M. S.; Shipley, D. E.; Robinson, M. C.; Luttges, M. W.; and Simms, D. A.; "Determination of the Reliability of the Combined Experiment Data", NREL/TP-442-6914.

Shipley, D. E.; Miller, M. S.; Robinson, M. C.; Luttges, M. W.; and Simms, D. A.; "Techniques for the Determination of Local Dynamic Pressure and Angle of Attack on a Horizontal Axis Wind Turbine", NREL/TP-442-7393, May 1995.

Butterfield, C. P., Musial, W. P., Simms, D. A., "Combined Experiment Final Report - Phase I", NREL/TP-257-4655, May 1992

Butterfield, C. P., Musial, W. P., Simms, D. A., "Combined Experiment Final Report - Phase II", NREL/TP-442-4807, May 1992

Huyer, S. A. "Examination of Forced Unsteady Separated Flow Fields on a Rotating Wind Turbine Blade", NREL/TP-442-4864, May 1992

Simms, D. A., "Unsteady Aero Experiment Test Plan", NREL/TP-257-4656, August 1991.

3. Other Selected Publications Utilizing Combined/ Unsteady Aerodynamics Experiment Data

Masson, C., Smaili, A., Ammara, I., Leclerc, C., "Aerodynamic Investigations on Tower-Shadow Impacts for HAWTs", AIAA-2000-0041, Prepared for the 38th AIAA Aerospace Sciences Meeting and Exhibit, Reno, NV, January 10-13, 2000, p. 208-218.

Munduate, X., Coton, F. N., "Identification of Dynamic Stall Regions on Horizontal Axis Wind Turbines", AIAA-2000-0039, Prepared for the 38th AIAA Aerospace Sciences Meeting and Exhibit, Reno, NV, January 10-13, 2000, p. 172-182.

Sorensen, N. N., Michelsen, J. A., "Aerodynamic Predictions for the Unsteady Aerodynamics Experiment Phase II Rotor at the National Renewable Energy Laboratory", AIAA-2000-0037, Prepared for the 38th AIAA Aerospace Sciences Meeting and Exhibit, Reno, NV, January 10-13, 2000, p. 161-171.

Leclerc, C.; Masson, C., "Predictions of Aerodynamic Performance and Loads of HAWTS Operating in Unsteady Conditions", AIAA-99-0066, Prepared for the 37th AIAA Aerospace Sciences Meeting and Exhibit, Reno, NV, January 11-14, 1999, p. 335-345.

Madsen, P. H.; Pierce, K.; Buhl, M., "Predicting Ultimate Loads for Wind Turbines", AIAA-99-0069, Prepared for the 37th AIAA Aerospace Sciences Meeting and Exhibit, Reno, NV, January 11-14, 1999, p. 355-364.

Madsen, H. A.; Petersen, J. T.; Bruining, A.; Brand, A.; Graham, M., "Field Rotor Measurements Data Sets Prepared for Analysis of Stall Hysteresis", Risø-R-1046(EN), Risø National Laboratory, Roskilde, Denmark, May 1998.

Wang, T., Coton, F. N., Galbraith, R. A., "An Examination of Two Tower-Shadow Modelling Strategies for Downwind Wind Turbines", Presented at the 36th AIAA Aerospace Sciences Meeting and Exhibit, Reno, NV, January 12-15, 1998, p. 20-30.

Schepers, J. F.; Brand, A. J.; Bruining, A.; Graham, J. M. R.; Hand, M. M.; Infield, D. G.; Madsen, H. A.; Paynter, R. J.; Simms D. A.; "Final Report of IEA Annex XIV: Field Rotor Aerodynamics", ECN-C-97-027, June 1997, Netherlands Energy Research Foundation, Petten, The Netherlands.

Coton, F. N., Wang, T., Galbraith, R. A., "A Fully Unsteady Prescribed Wake Model For HAWT Performance Prediction in Yawed Flow", Prepared for the American Wind Energy Association Windpower '97 Conference and Exhibition, June 15-18, 1997, Autsin TX, p 55-64.

Hansen, A. C., Laino, D. J., "Validation Study for AERODYN and YAWDYN Using Phase III Combined Experiment Data", AIAA-97-0943, Prepared for the 1997 ASME Wind Energy Symposium 35th Aerospace Sciences Meeting and Exhibit, January 6-9, 1997, Reno NV.

Borg, J. P., Kirchoff, R., "The Effect of Aerodynamic Imbalance on a Horizontal Axis Wind Turbine", Prepared for the Fifteenth ASME Wind Energy Symposium, 29 January - 2 February 1996, Houston, TX., p 143-148.

Slepski, J. E., Kirchoff, R. H., "The Analysis of Unsteady Wind Turbine Data Using Wavelet Techniques", Prepared for the ASME/ ETCE Conference, January 29 - February 1 1995, Houston, TX, p. 227-235.

Slepski, J. E., Kirchoff, R. H. "An Investigation of Stall on a Rotating Wind Turbine Blade", presented at the 13th ASME/ ETCE Wind Energy Symposium, New Orleans, LA, January 23-26, 1994, p. 17-25.

Miller, M. S., Shipley, D. E., "Structural Effects of Unsteady Aerodynamic Forces on Horizontal-Axis Wind Turbines", Prepared for the AIAA Student Conference, St. Louis, MO. April 18, 1992.

Eggers, A. J. Jr. and Digumarthi, R. V., "Approximate Scaling of Rotational Effects on Mean Aerodynamic Moments and Power Generated by the Combined Experiment Rotor Blades Operating in Deep-Stalled Flow", Presented at 11th ASME Wind Energy Symposium, January 26-29, 1992, ASME, p. 33-43.

Schnepp, R. R., Hansen, A. C, and Wright, A. D., "A Method for Determining Aerodynamic Loads on a Wind Turbine From Blade Flap Bending Moments", Presented at 11th ASME Wind Energy Symposium, January 26-29, 1992, ASME, p. 83-88.

REPORT DOCUMENTATION PAGE

Public reporting burden for this collection of information is estimated to average 1 hour per response, including the time for reviewing instructions, searching existing data sources, gathering and maintaining the data needed, and completing and reviewing the collection of information. Send comments regarding this burden estimate or any other aspect of this collection of information, including suggestions for reducing this burden, to Washington Headquarters Services, Directorate for Information Operations and Reports, 1215 Jefferson Davis Highway, Suite 1204, Arlington, VA 22202-4302, and to the Office of Management and Budget, Paperwork Reduction Project (0704-0188), Washington, DC 20503.

1. AGENCY USE ONLY (Leave blank)	2. REPORT DATE October 1999	3. REPORT TYPE AND DATES COVERED Technical Report

4. TITLE AND SUBTITLE

Plans for Testing the NREL Unsteady Aerodynamics Experiment 10-m Diameter HAWT in the NASA Ames Wind Tunnel: Minutes, Conclusions, and Revised Test Matrix Resulting from the First Science Panel Meeting

5. FUNDING NUMBERS

WE90.1110

6. AUTHOR(S)

D. Simms, S. Schreck, M. Hand, L. Fingersh, J. Cotrell, K. Pierce, M. Robinson

7. PERFORMING ORGANIZATION NAME(S) AND ADDRESS(ES)

8. PERFORMING ORGANIZATION REPORT NUMBER

9. SPONSORING/MONITORING AGENCY NAME(S) AND ADDRESS(ES)

National Renewable Energy Laboratory
1617 Cole Blvd.
Golden, CO 80401-3393

10. SPONSORING/MONITORING AGENCY REPORT NUMBER

NREL/ TP-500-27599

11. SUPPLEMENTARY NOTES

NREL Technical Monitor: N/A

12a. DISTRIBUTION/AVAILABILITY STATEMENT

National Technical Information Service
U.S. Department of Commerce
5285 Port Royal Road
Springfield, VA 22161

12b. DISTRIBUTION CODE

13. ABSTRACT *(Maximum 200 words)*

Currently, the NREL Unsteady Aerodynamics Experiment (UAE) research turbine is scheduled to enter the NASA Ames 80' x 120' wind tunnel in early 2000. To prepare for this 3-week test, a Science Panel meeting was convened at the National Wind Technology Center (NWTC) in October 1998. During this meeting, the Science Panel and representatives from the wind energy community provided numerous detailed recommendations regarding test activities and priorities. The Unsteady Aerodynamics team of the NWTC condensed this guidance and drafted a detailed test plan. This test plan represents an attempt to balance diverse recommendations received from the Science Panel meeting, while taking into account multiple constraints imposed by the UAE research turbine, the NASA Ames 80' x 120' wind tunnel, and other sources.

The NREL–NASA Ames wind tunnel tests will primarily be focused on obtaining rotating blade pressure data. NREL has been making these types of measurements since 1987 and has considerable experience in doing so. The purpose of this wind tunnel test is to acquire accurate quantitative aerodynamic and structural measurements, on a wind turbine that is geometrically and dynamically representative of full-scale machines, in an environment free from pronounced inflow anomalies. These data will be exploited to develop and validate enhanced engineering models for designing and analyzing advanced wind energy machines.

14. SUBJECT TERMS

unsteady aerodynamics; wind tunnel testing; NASA Ames; HAWT; Science Panel

15. NUMBER OF PAGES

16. PRICE CODE

17. SECURITY CLASSIFICATION OF REPORT Unclassified	18. SECURITY CLASSIFICATION OF THIS PAGE Unclassified	19. SECURITY CLASSIFICATION OF ABSTRACT Unclassified	20. LIMITATION OF ABSTRACT UL

NSN 7540-01-280-5500

Standard Form 298 (Rev. 2-89)
Prescribed by ANSI Std. Z39-18
298-102